



NAZIOARTEKO
BIKAINASUN
CAMPUSA
CAMPUS DE
EXCELENCIA
INTERNACIONAL

Zoologia eta Animali Zelulen Biologia Saila
Departamento de Zoología y Biología Celular Animal



An integrated study of molecular, cellular, tissue level and transgenerational effects of silver nanoparticles on dietarily exposed mussels at different seasons

International Ph.D. Thesis submitted by

Nerea Duroudier Martínez

for the degree of

Philosophiae Doctor

May, 2019

FUNDING

This work has been funded by:

- .: Spanish Ministry of Economy and Competitiveness through the NanoSilverOmics project "Mechanisms of action and toxicity of silver nanoparticles in model aquatic and terrestrial organisms using omics technologies" (MAT2012-39372). 2013-2015.
- .: Basque Government through a grant to the Consolidated Research Group "Cell Biology in Environmental Toxicology" (GIC IT810-13). 2013-2018.
- .: University of the Basque Country by means of a grant to the Unit of Formation and Research "Ecosystem Health Protection" (UFI 11/37; 2011-2014), a predoctoral fellowship to Nerea Duroudier (PIF//13/273; 2014-2018) and a grant for the stay at the Centre for Marine and Environmental Research (CIMA, Portugal; 2015).

ACKNOWLEDGEMENTS

I wish to thank all the people and institutions that helped me to carry out this Ph.D. research. Without their support and encouragement, none of this would have been possible.

- .: Professor Miren P. Cajaraville and Dr. Eider Bilbao (University of the Basque Country), supervisors of this PhD thesis, for giving me the opportunity to perform this research work within the "Cell Biology in Environmental Toxicology" research group, for their support, encouragement and research guidance during these years.
- .: All members involved in the NanoSilverOmics project: Dr. Amaia Orbea, Prof. Manu Soto, Dr. Alberto Katsumiti, Dr. Alba Jimeno-Romero, Dr. Jose María Lacave and Dr. Nerea García-Velasco. Thank you for the helpful discussions and for your patience sharing all your knowledge.
- .: Professor Maria J. Bebianno (University of Algarve) for giving me the opportunity of training in her laboratory and Câtia Cardoso for introducing me to the broad world of proteomics in the simplest way.
- .: Professor Jörg Schäfer (University of Bordeaux) and Dr. Mathilde Mikolaczyk for their collaboration and support with the chemical analyses.
- .: Professor Laure Giamberini (University of Lorraine), Prof. Arno C. Gutleb (University of Luxembourg) and Dr. Kahina Mehennaoui (University of Lorraine/ University of Luxembourg) for their collaboration with the CytoViva® hyperspectral imaging analyses.
- .: Pablo Markaide (University of the Basque Country) for his help and support as bioinformatician in the microarray analysis.
- .: To all members of the Research Group "Cell Biology in Environmental Toxicology" (University of the Basque Country) for contributing directly or indirectly to carrying out this work.



TABLE OF CONTENTS

I. INTRODUCTION	1
1. The era of Nanotechnology	3
2. Emission, fate and toxicity of engineered nanoparticles in aquatic environments.....	5
2.1. Factors affecting fate and toxicity of engineered nanoparticles in aquatic environments	6
2.2. Uptake and toxicity of engineered nanoparticles in aquatic organisms	10
3. Silver nanoparticles in the environment	13
4. Bivalve molluscs as model species	22
4.1. Bivalves and eco-nanotoxicology	23
4.2. Biomarkers as suitable tools for assessing nanoparticles toxicity in mussels	25
4.3. The omic's approach: discovering new biomarkers	29
4.4. Trophic transfer studies	31
5. References	33
II. STATE OF THE ART, HYPOTHESIS AND OBJECTIVES	49
III. RESULTS AND DISCUSSION	53
∴ CHAPTER 1.	
Dietary exposure to PVP/PEI coated Ag nanoparticles in adult mussels causes Ag accumulation in adults and abnormal embryo development in their offspring	55
∴ CHAPTER 2.	
Cell and tissue level responses in mussels <i>Mytilus galloprovincialis</i> exposed to PVP/PEI coated silver nanoparticles through the diet at different seasons	91
∴ CHAPTER 3.	
Changes in protein expression in mussels <i>Mytilus galloprovincialis</i> dietarily exposed to PVP/PEI coated silver nanoparticles at different seasons	121
∴ CHAPTER 4.	
Season influences the transcriptomic effects of dietary exposure to PVP/PEI coated Ag nanoparticles on mussels <i>Mytilus galloprovincialis</i>	157
IV. GENERAL DISCUSSION	193
V. CONCLUSIONS AND THESIS	213
VI. APPENDIX.....	218
1. Characterization of Ag NPs by manufacturer's	
2. Protocols	



I. INTRODUCTION

1. The era of Nanotechnology

Nanotechnology is considered the major driving force behind the imminent technological revolution in the 21st century (Wennersten et al., 2008). Already in 1974, Norio Taniguchi first used the term nanotechnology for the processes mainly consisting in the separation, consolidation and deformation of materials by one atom or by one molecule. Additionally, he predicted that by the late 1980s, techniques would have evolved to a degree that dimensional accuracies of better than 100 nm would be achievable (Taniguchi, 1974).

Nowadays, according to the Royal Society and the Royal Academy of Engineering (2004), *nanotechnology* is defined as the design, characterization, production and application of structures, devices and systems by controlling shape and size at nanometer scale. From the manipulation of materials at the nanoscale emerge *nanomaterials* (NMs) which are defined as “natural, incidental or manufactured materials containing particles, in an unbound state or as an aggregate or as an agglomerate and where, for 50% or more of the particles in the number size distribution, one or more external dimensions are in the size range 1 nm-100 nm” (EU Commission, 2011). However, a single internationally accepted definition for NMs does not exist although up to 14 definitions have been proposed by different governmental, industrial and standard organizations. For all the definitions, size is the only common element (Boverhof et al., 2015). In fact, due to their small size together with their high surface-area-to-volume ratio, NMs show novel physico-chemical properties related to melting point, wettability, electrical and thermal conductivity, catalytic activity, light absorption and scattering among others. These characteristics result in enhanced performance over their bulk counterparts (Nel et al., 2006; Klaine et al., 2012; Yang and Westerhoff, 2014; Jeevanandam et al., 2018). Thus, an exponential growth in the development of new NMs by nanotechnology industries as well as a wide incorporation of NMs in consumer products occurred over the past decades.

Life on Earth evolved in the presence of naturally occurring NMs in the hydrosphere, atmosphere, lithosphere and even biosphere (Klaine et al., 2012; Sharma et al., 2015). In fact, colloid is the generic term applied to particles in the 1 nm to 1 μm size range in aquatic systems, which comprises macromolecular organic materials such as humic acids, proteins, and peptides, as well as colloidal inorganic species, typically hydrous iron and manganese oxides (Klaine et al., 2008). In soils, natural NMs include clays, organic matter, iron oxides and other minerals that play an important role in biogeochemical processes (Klaine et al., 2008). In general, natural NMs in the environment are generated as by-products of combustion (fuel burning) and minerals, as biogenic products of microbial

activity, as aerosols from atmospheric phytochemistry and due to the activity of volcanoes and hydrothermal vents (Nowack and Bucheli, 2007; Kahru et al., 2008; Sharma et al., 2015).

However, the total concentration of natural NMs is low in comparison to the potential release of anthropogenic NMs. Anthropogenic NMs are either inadvertently formed as by-products mostly during combustion or produced intentionally by mechanical grinding, engine exhaust and smoke, or synthesized by physical, chemical, biological or hybrid methods (Nowack and Buchelli, 2007; Jeevanandam et al., 2018). In the latter case, they are referred to as manufactured or engineered NMs (ENMs) (Nowack and Buchelli, 2007).

Additionally, ENMs can be classified according to their chemical composition (Figure 1) into different groups (Nowack and Buchelli, 2007; Jeevanandam et al., 2018).

1. Carbon-based nanomaterials

Generally, these NMs contain carbon and are found in morphologies such as hollow tubes, ellipsoids or spheres. Fullerenes, carbon nanotubes, carbon nanofibers, carbon dots, carbon black, graphene and graphitic carbon nitride (g-C₃N₄) are included under the carbon-based NMs category (Figure 1).

2. Organic-based nanomaterials

These NMs are made mostly from organic matter, excluding carbon-based NMs. The use of non-covalent interactions for the self-assembly and design of molecules helps to transform the organic NMs into desired structures such as micelles, liposomes, dendrimers and compact polymeric nanospheres or nanocapsules (Figure 1).

3. Inorganic-based nanomaterials

Metal containing NMs and metal oxide *nanoparticles* (NPs) are included in this group. NPs can be defined as "particles with at least two dimensions between approximately 1 and 100 nm" (EPA, 2017) as well as nanostructured materials. These NMs can be synthesized based on pure metals such as Au or Ag NPs or on metal oxides such as TiO₂ and ZnO NPs and semiconductors such as quantum dots (QDs) or metal chalcogenides (Figure 1).

Among inorganic ENMs, metal and metal oxide NPs (e.g.: Ag, Au, Cu, TiO₂, ZnO, CeO₂, CuO and Fe₂O₃) are widely applied in the field of catalysis, environmental remediation, biomedicine, pigments, coatings, cosmetics and electronics (Mudunkotuwa

and Grassian, 2011; Baker et al., 2014). As the use and prevalence of these NPs inevitably increases, so will their release into freshwater and marine environments.

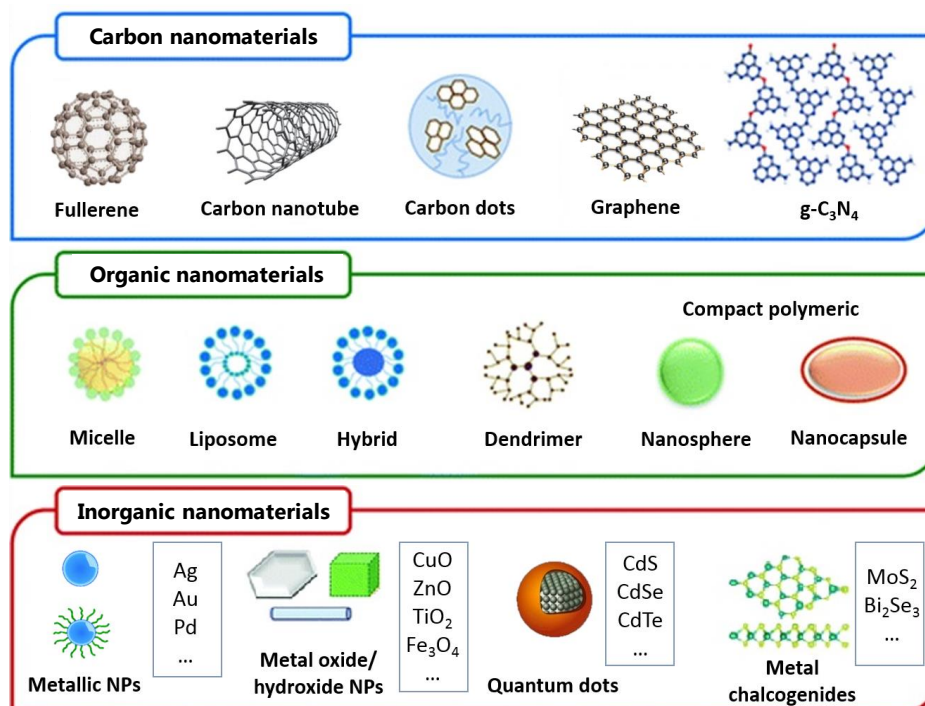


Figure 1: Classification of ENMs based on their chemical composition (Modified from Kumar and Ray, 2018).

2. Emission, fate and toxicity of engineered nanoparticles in aquatic environments

The potential release and entry of ENPs into the environment can occur at any point during ENPs life cycle. In general, NPs can be directly emitted to the environment through aerial deposition, dumping and/or run-offs or indirectly via technical systems, which in general are any human-made sites where ENMs and nanoproducts are stored, used or processed. These technical systems include storage facilities, transport vehicles, wastewater treatment plants (WWTPs) or landfills, among others (Gottschalk and Nowack, 2011; Baker et al., 2014; Caballero-Guzmán and Nowack, 2016; Bundschuh et al., 2018). Thus, three emission scenarios are considered (Figure 2; Caballero-Guzmán and Nowack, 2016; Bundschuh et al., 2018):

- (i) Release during production or transport of raw material and nano-enabled products that may occur during powder handling, storage or transportation.
- (ii) Release during the use of nano-enabled products use, which includes the wearing or washing of textiles, application of cosmetics or sunscreens, weathering or abrasion processes (e.g. painted walls).

- (iii) Release after disposal of NP containing products or waste handling related to any possible waste management activity such as incineration or recycling, application of biosolids to soil, or leachates from landfills.

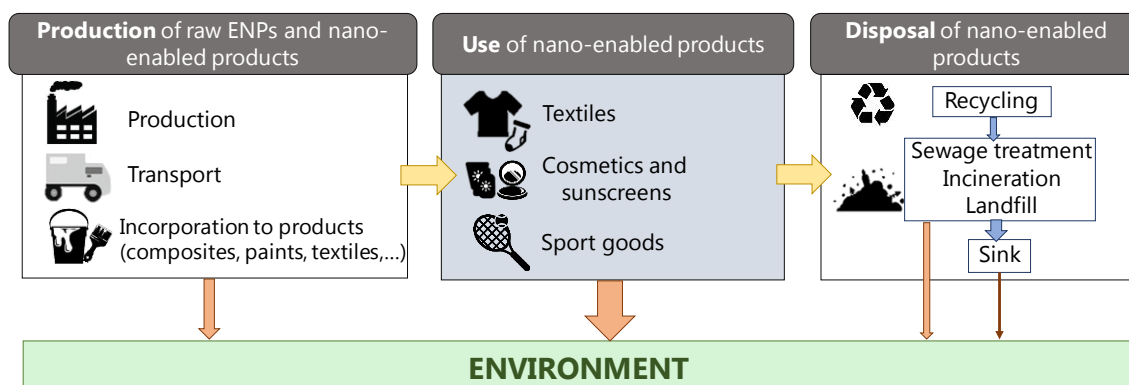


Figure 2: Release of ENMs during their life cycle, from production to nanoproductions disposal. The diagram highlights final transfer of ENMs to the environment (orange arrows). The potential release of ENMs during their use (grey box) may be higher because less control measures are adopted during this phase, which results in a larger final transfer to the environment (as represented by a thick orange arrow). The flow from recycling does not connect to the production box of the left because most likely, ENMs entering the recycling system will either be disposed (landfilled or incinerated), or allocated in material fractions (e.g. plastics) used in the production of other type of applications, instead of ENMs or nano-applications (Modified from Caballero-Guzmán and Nowack, 2016).

2.1. Factors affecting fate and toxicity of engineered nanoparticles in aquatic environments

Once in aquatic environments, NPs can suffer a variety of processes that determine their fate in the abiotic environment and interaction with biota (Figure 3). The intrinsic characteristics of each NP such as chemical composition size, shape and surface structure together with physico-chemical processes such as agglomeration and aggregation, dissolution and transformation into new chemical states determine NPs behavior and toxicity (Nowack and Bucheli, 2007; Klaine et al., 2008; Navarro et al., 2008a; Schirmer et al., 2013; Baker et al., 2014; Sigg et al., 2014).

2.1.1. Intrinsic properties

1. Chemical composition

The elemental composition (organic, inorganic or mixtures) of NPs is essential to understand their biological behavior, biodistribution and toxicity (Harper et al. 2007; Fubini et al., 2011). In fact, toxicity rankings for zebrafish embryos and adults were reported and Ag NPs and Cu NPs were shown to be the most

toxic, followed by other metal containing NPs such as ZnO NPs, CdS QDs, Au NPs, Ni NPs, Co NPs and SiO₂ NPs (Griffith et al., 2008; Lacave et al., 2016). For mussels hemocytes and gill cells, the toxicity ranking based on the results of *in vitro* cell viability assays of metal-bearing NPs was established as Ag NPs > CuO NPs > CdS QDs > ZnO NPs > TiO₂ NPs > Au NPs > SiO₂ NPs (Katsumiti and Cajaraville, 2019).

2. Size and surface area

Particle size and surface area are important characteristics from a toxicological perspective (Nel et al., 2006). As the size of a particle decreases, its surface area as well as NPs surface reactivity increase (Oberdöster et al., 2005; Nel et al., 2006; Sigg et al., 2014). Additionally, particle size determines the uptake of NPs into organisms, tissues or cells (Oberdöster et al., 2005; Baker et al., 2014) as well as the organelle distribution pattern and removal profile of NPs (Sakhtianchi et al., 2013).

3. Shape

Optical, mechanical and electrical properties of NPs have been shown to be affected by their shape (Misra et al., 2013). Additionally, NP shape significantly affects suspension stability and dissolution, which alters physico-chemical behavior of NPs and the biological responses that they may cause. For example, spherical CuO NPs showed higher suspension stability and dissolution compared to rods and spindle shaped-particles (Misra et al. 2013). However, CeO₂ nano rods were reported to be more toxic than spheres due to their faster dissolution, while CeO₂ NPs with sharp edges break cell membranes and cause mechanical damage (Baalousha et al., 2012).

4. Surface structure

Coating agents are organic, inorganic or polymeric substances that are used during the synthesis of NPs to control their size and stabilize the suspension in order to prevent their aggregation through electrostatic repulsion, steric repulsion or both (El Badawy et al., 2010; Schirmer et al., 2013, Sigg et al., 2014; Zhang et al., 2015). However, several studies reported that some coating agents contributed to the overall toxicity caused by NPs. While some coating agents were toxic at certain concentrations to aquatic organisms (Katsumiti et al., 2016; Jimeno-Romero et al., 2016; 2017a; Schiavo et al., 2017; Katsumiti and Cajaraville, 2019), other improved the solubility and

interactions between NPs and biological molecules (Levard et al., 2012; Li et al., 2013) or affected to the formation of reactive oxygen species (ROS) (Li et al., 2013).

2.1.2. Physico-chemical processes

1. Agglomeration or aggregation state

The formation of agglomerates or aggregates and therefore the formation of larger particles in size, may help to remove NPs from the water column due to their settlement into sediments (Nowack and Bucheli, 2007; Sigg et al., 2014). Agglomerates are formed when binding of NPs is weak and the total external surface area of the agglomerated particles is similar to the sum of the surface area of the individual particles. On the other hand, aggregates show a strong binding between particles and the external surface area of aggregated particles is significantly smaller than the sum of the surface area of individual particles (Moreno-Garrido et al., 2015). Among aggregates, two types can be distinguished (Zhang, 2014):

- *Homoaggregates*, which are formed when two particles of the same kind are bound.
- *Heteroaggregates*, formed when aggregation of dissimilar particles (e.g., attachment of NPs to natural organic matter) occurs. Frequently, heteroaggregation is also referred to as sorption or adsorption.

The aggregation or agglomeration rate of ENPs depends on NP concentration, surface area and forces involved in collision, but variations in medium composition such as ionic strength, pH and the concentration of natural organic matter present in fresh- and marine waters influence on these phenomena (Peralta-Videa et al., 2011; Schirmer et al., 2013; Garner and Keller, 2014). Both homo- and heteroaggregation processes increase the bioavailability of ENPs to phytoplankton, filter feeders as well as benthic deposit and detrital feeders (Ward and Kach, 2009; Matranga and Corsi, 2012; Baker et al., 2014).

2. Dissolution rate

Dissolution of inorganic NPs plays an important role in their toxicity, due to the release of ions to the exposure media. The toxicity of such ions to aquatic organisms is well known and strongly depends on their speciation into the exposure media (Schirmer et al., 2013). Dissolution and dissolution rate are

highly dependent on the chemical composition and surface properties of each NP (Odzak et al., 2014), as well as on the particle size (Mudunkotuwa and Grassian, 2011; Odzak et al., 2014). Some other factors such as surface area, surface morphology, crystallinity and crystal structure may also influence NP dissolution (Misra et al., 2012).

Apart from the intrinsic properties of NPs aforementioned, characteristics of the surrounding media (pH, ionic strength, water hardness) and presence of organic components (natural organic matter, polysaccharides, proteins) can also affect suspension stability, leading to NPs agglomeration or aggregation, that may further alter the surface area and dissolution of the NPs (Misra et al., 2012).

3. Transformation

Environmental transformations of NPs will also affect their physical and chemical properties and thus, their fate and toxicity. Significant transformation processes may include oxidation, sulfidation, and reactions with phosphorous. In general, these transformations tend to result in less reactive NPs being less likely to dissolve and less toxic for aquatic organisms (Garner and Keller, 2014; Bundschuh et al., 2018)

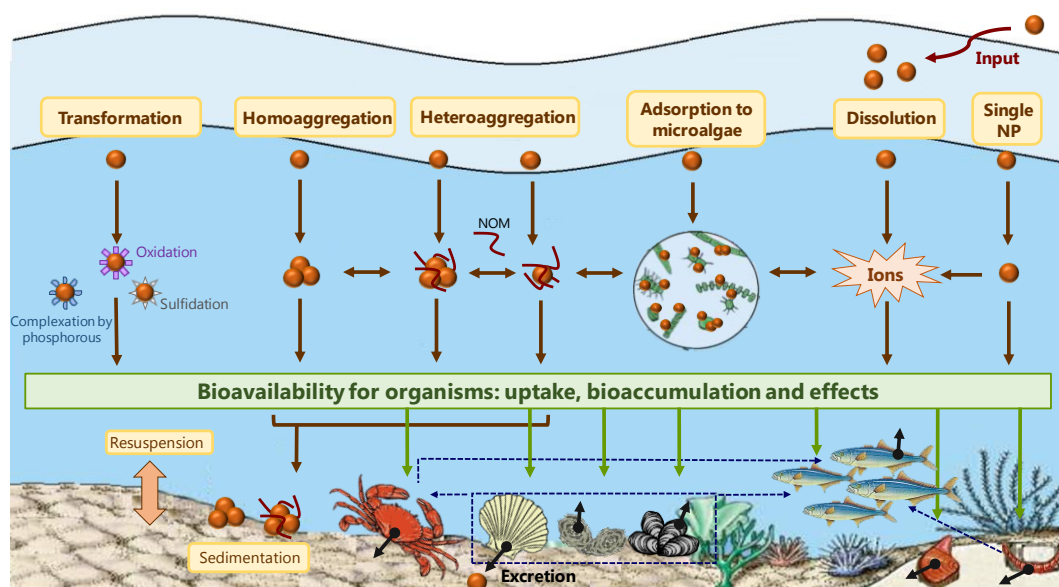


Figure 3: Representation of the potential behavior and fate of ENPs in the marine environment and their interaction with biota. Brown lines represent physico-chemical processes that may affect NPs fate. Potential uptake of NPs is represented by green lines, while potential trophic transfer of NPs is shown by blue dashed arrows. Small black arrows represent elimination of NPs by excretion processes. NOM stands for natural organic matter (Based on Rocha et al., 2015a).

2.2. Uptake and toxicity of engineered nanoparticles in aquatic organisms

Inhalation, ingestion and dermal contact are likely to be the major routes of NPs uptake in terrestrial organisms (Colvin, 2003; Tourinho et al., 2012), while in aquatic organisms, routes of entry may be direct passage across gills, olfactory organs or body wall (Moore, 2006).

At cellular level, when NPs reach the exterior membrane of a cell, they can interact with components of the cell membrane and the extracellular matrix. Interactions of NPs with biomolecules have been described within biological fluids of mammalian models, where plasma proteins form a coating known as protein corona or bio-corona. Proteins in the bio-corona control the interactions between NPs and specific cellular receptors, the internalization pathways and the immune response (Canesi et al., 2017).

In general, NPs may adhere to the cell and block essential pores and membrane functions. Then, internalization of NPs may occur through passive diffusion, via ion transport systems or mainly via endocytic processes (Moore 2006; Baker et al., 2014; Behzadi et al. 2017). Different types of endocytic processes such as clathrin-, caveolae-, RhoA-, CDC42-, ARF6-, and flotilin-mediated endocytosis have been linked to the NP internalization depending on NPs size, cell type and proteins, lipids and the rest of molecules involved in the process (Figure 4; Canton and Battaglia, 2012; Behzadi et al. 2017).

1. Clathrin mediated endocytosis

Clathrin-mediated endocytosis takes place in the cell membrane area which is rich in clathrin protein (about 0.5–2% of the cell surface). This protein is responsible for spontaneous co-assembly into a complex architecture that generates and stabilizes the membrane curvature and then the budding vesicle. Clathrin-mediated endocytosis is the main mechanism by which cells obtain nutrients and plasma membrane components.

2. Caveolae mediated endocytosis

Caveolae are 50-80 nm large flask shaped invaginations in the cell membrane covered by caveolin, which is a dimeric protein involved in the formation of their characteristic flask shape. Caveolae-dependent endocytosis plays an important role in many biological processes, such as cell signaling, transcytosis, regulation of lipids, fatty acids, membrane proteins and membrane tension.

3. RhoA mediated endocytosis

RhoA belongs to the Ras homolog gene family and is a key player in the regulation of actin cytoskeleton dynamics, which has a very important role in most of the endocytic mechanisms.

4. CDC42 mediated endocytosis

Cell division cycle 42 (CDC42) is a member of the Ras superfamily of GTP-binding proteins. This pathway is associated with the formation of tubular invaginations of the cell membrane which can be 200-600 nm long and 30-50 nm wide.

5. ARF6 mediated endocytosis

ADP-ribosylation factor 6 (ARF6) belongs to the ARF family of 6 small GTPases related to the Ras gene and was morphologically associated with tubular rather than vesicular structures in endocytic processes.

6. Flotilin mediated endocytosis

Flotilins are palmitoylated proteins that show a hairpin structure when bound to the cell membrane that is very similar to caveolin. However, flotilins are not related with caveolae biogenesis and they are involved in a specific endocytic pathway independent of clathrin and caveolin.

Moreover, other entry mechanisms such as phagocytosis and macropinocytosis have also been reported (Figure 4; Canton and Battaglia, 2012; Behzadi et al. 2017). Phagocytosis is a type of endocytosis performed only by a few specialized cells such as immune cells. Phagocytosis of NPs is usually initiated by opsonization, in which opsonins (immunoglobulins, complement proteins or other blood proteins) are adsorbed onto the NPs surface. Opsonized NPs are then recognized starting a signaling cascade that can trigger actin assembly, the formation of cell surface extensions and subsequent engulfing and internalization of NPs, forming phagosomes (Canton and Battaglia, 2012; Behzadi et al., 2017). In the macropinocytosis, the formation of waving sheet-like extensions of the plasma membrane engulfs a large quantity of external fluid, thus forming large organelles (>200 nm) called pinosomes (Canton and Battaglia, 2012; Behzadi et al., 2017).

Endocytic vesicles and pinosomes containing NPs are transported to early endosomes, that gradually mature into late endosomes and eventually to lysosomes (Figure 4; Canton and Battaglia, 2012; Sakhtianchi et al., 2013; Kafshgari, et al., 2015;

Behzadi et al., 2017). Some early endosome containing NPs can fuse with endoplasmic reticulum or Golgi and NPs that enter those organelles may leave the cell via vesicles related to the conventional secretion system (Behzadi et al., 2017). In the case of phagosomes, they are directly fused with late endosomes or lysosomes to accelerate the degradative process (Canton and Battaglia, 2012). Additionally, it seems that caveosomes participate in cell transcytosis, a process which involves both endocytosis and exocytosis processes allowing molecules or NPs to cross over the cells (Figure 4; Canton and Battaglia et al., 2012; Sakhtianchi et al., 2013). The organelle distribution pattern and removal of NPs will depend on the physico-chemical characteristics of NPs such as size, shape and surface properties as well as on their uptake pathways (Canton and Battaglia, 2012; Sakhtianchi et al., 2013; Kafshgari, et al., 2015).

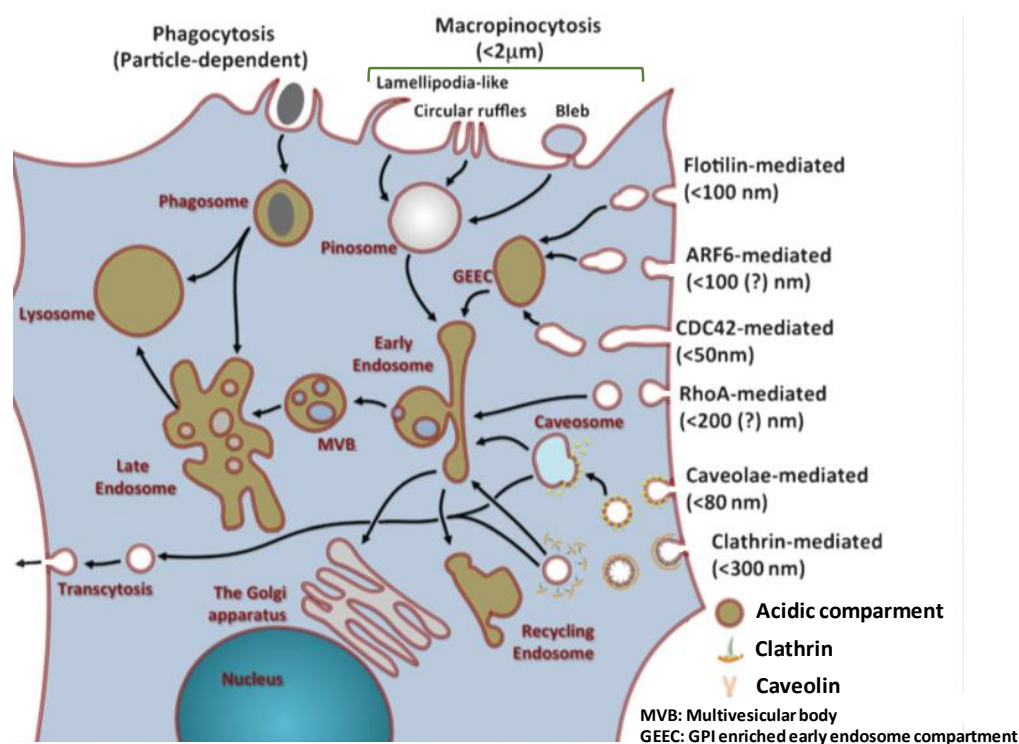


Figure 4: Mechanisms of NPs uptake by endocytosis in a typical eukaryotic cell (Taken from Canton and Battaglia, 2012).

There is not a single mechanism of toxicity that can be considered general for all NPs in all different types of cells, but the most common toxic effects include disruption of membranes or membrane potential, oxidation of proteins, genotoxicity, interruption of energy transduction, oxidative stress and immunomodulation (reviewed in Klaine et al., 2008; Rocha et al., 2015a; Canesi and Corsi, 2016; Bundschuh et al., 2018; Katsumiti and Cajaraville, 2019). Among them, oxidative stress is the most reported phenomenon (Fu et al., 2014; Bundschuh et al., 2018).

3. Silver nanoparticles in the environment

Silver nanoparticles (Ag NPs) have been widely used for more than 100 years in medicine mainly for wound, gonorrhea and conjunctivitis treatments (Figure 5; Nowack et al., 2011).

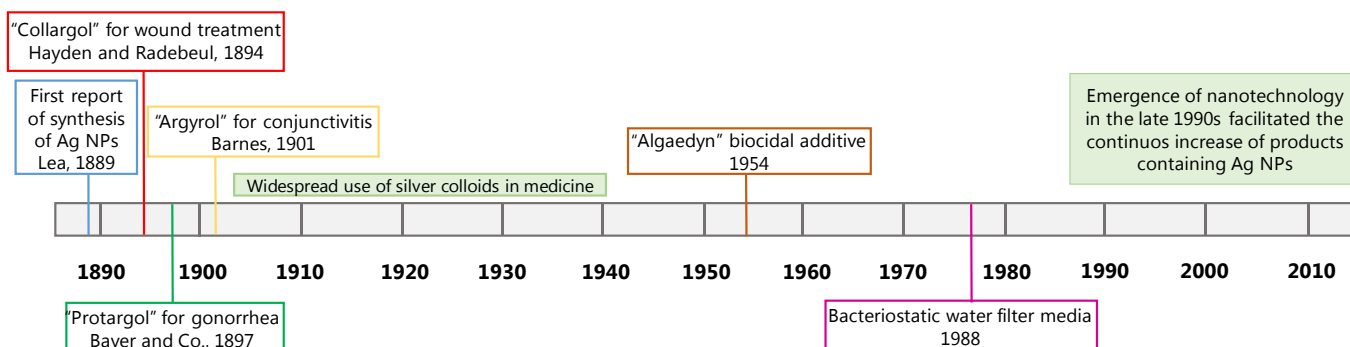


Figure 5: Historical overview of Ag NPs synthesis and use (Modified from Massarsky et al., 2014).

Nowadays, there are several inventories listing consumer products containing NPs that are available in the market. For example, the Nanotechnology Consumer Product Inventory (www.nanotechproject.org/cpi) became one of the most frequently cited resources showing the widespread applications of Nanotechnology in consumer products since 2005 (Vance et al., 2015). According to the database, 443 of the 1814 listed nanomaterial-based consumer products in 32 countries contain Ag NPs in 2016 (Figure 6A). At the same time, the inventory of commercially available products containing ENMs that are available in the European consumer market (The Nanodatabase; <http://nanodb.dk/>; Hansen et al., 2016), lists 378 products containing Ag NPs out of the 3036 registered products. This inventory is updated daily (Figure 6B).

Ag NPs are among the EMNs most often incorporated in nanofunctionalized consumer products mainly due to their antimicrobial properties (Fabrega et al., 2011; Massarsky et al., 2014; Zhang et al., 2016). Compared to their bulk counterpart, Ag NPs present stronger, longer-term and broader spectrum antimicrobial activities mainly because of their high specific surface area and the continued silver ion release (reviewed in Zhang et al., 2016; McGuillicuddy et al., 2017). Additionally, Ag NPs show unique physico-chemical properties, including high electrical and thermal conductivity, making them suitable for their application in microelectronics and medical imaging (reviewed in Fabrega et al., 2011; Zhang et al., 2016). Actually, Ag NPs are widely included in water filters, paints, cosmetics, deodorants, textiles, food packaging, functionalized plastics, wound dressings, electrical appliances such as washing machines and refrigerators,

detergents, biosensors and biomedical products (reviewed in Fabrega et al., 2011; Massarsky et al., 2014; Zhang et al., 2016; McGuillicuddy et al., 2017).

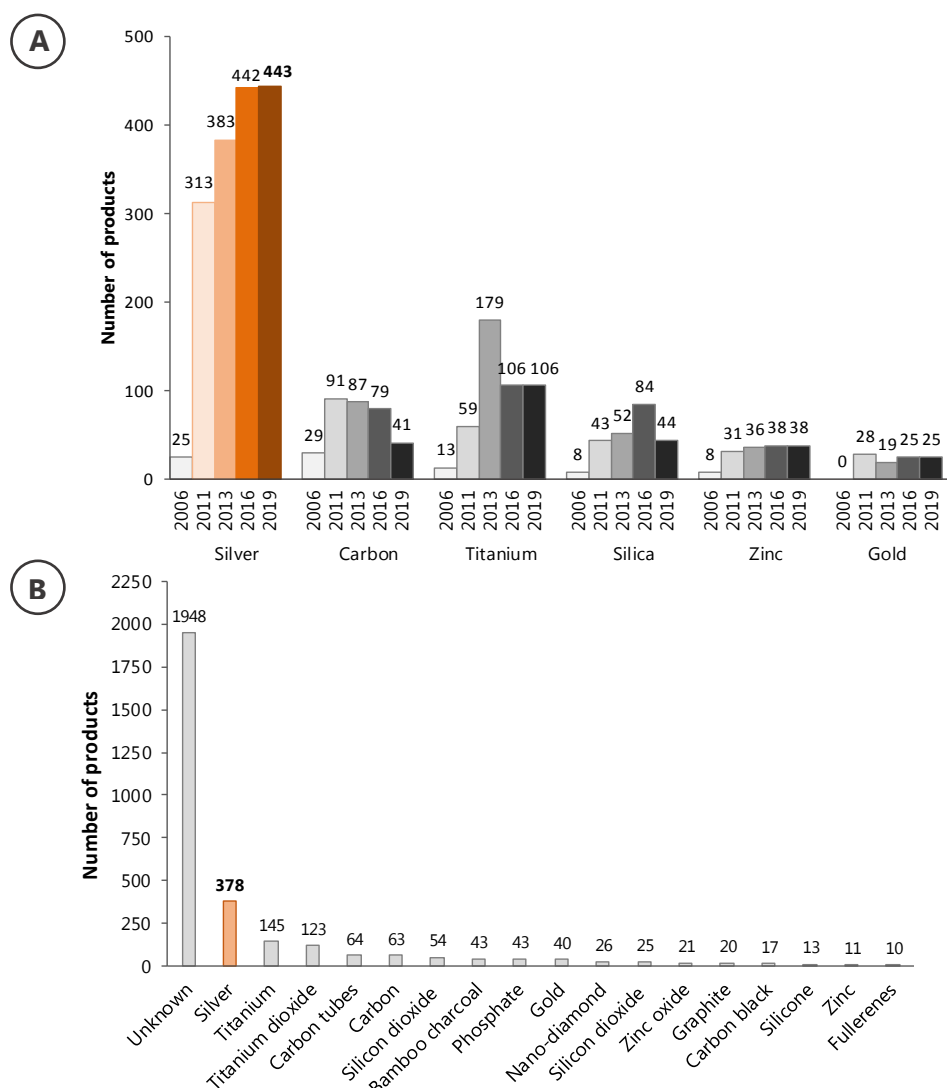


Figure 6: Inventory of number of products containing different types of ENPs. **A)** Number of products containing specific ENPs based on the last update of the Nanotechnology Consumer Product Inventory (www.nanotechproject.org/cpi; last search April 2019). **B)** Number of products containing different types of ENPs based on the Nanodatabase (<http://nanodb.dk/>; last search April 2019). Bars corresponding to Ag NPs are coloured in orange.

The global use and end-of-life phase of Ag NPs containing products may provoke their release into the environment via wastewater streams and effluents (Yu et al., 2013; António et al., 2015; McGuillicuddy et al., 2017; Magesky and Pelletier, 2018). Thus, surface waters receive considerable quantities of waste or released Ag NPs (Moreno-Garrido et al., 2015). Moreover, the major source of Ag NPs in soils is the disposal of wastewater treatment plant sewage sludge or biosolids, after their land application or incineration and posterior deposition (Tourinho et al. 2012).

Several studies have reported that Ag NPs may be released from consumer products into sewage. Benn and Westerhoff (2008) demonstrated that the immersion of commercial socks in shaking water released Ag NPs as well as ionic silver into the media. Some brands of socks could even lose nearly 100% of their total silver content after four consecutive washings (Benn and Westerhoff, 2008). Geranio and colleagues (2009) also simulated the washing of different Ag NPs containing textiles, and reported that at least 50% of the Ag present in the liquid exiting the washing machine was in particle form (>450 nm in size). Another study assessed the release of different species of Ag generated during the household washing process from nano- and conventional Ag textiles, demonstrating that Ag NPs can be formed by washing textiles containing conventional silver (Mitrano et al., 2014).

Actually, concentrations ranging between 0.7 and 11.1 ng/L Ag NPs were measured in effluents of wastewater treatment plants over the seasons in Germany (Li et al., 2016). However, modelling studies have been largely employed in order to estimate environmental concentrations of Ag NPs in different compartments (Blaser et al., 2008; Gottschalk et al., 2009; Tiede et al., 2009; Sun et al., 2014; Dumont et al., 2015; Giese et al., 2018) since NPs detection and quantification in complex natural matrices such as seawater, soils and sediments is still challenging (Von der Kammer et al. 2012; Sikder et al., 2017). These predictions estimated Ag NP concentrations ranging between 0.17 ng/L and 9 µg/L in sewage treatment effluents, 0.002-140 ng/L in surface waters and 0.952 µg/kg and 6 mg/kg in sediments, among others (Table 1; Blaser et al., 2008; Gottschalk et al., 2009; Tiede et al., 2009; Dumont et al., 2015; Giese et al., 2018). Even if predictions for marine waters revealed that concentrations of Ag NPs will reach up to 1 pg/L at the highest extremes in 2050 (Giese et al., 2018), bioturbation and resuspension processes in the sediments could lead to Ag NPs exchange between the sediment and water column, thereby making Ag NPs available to marine organisms (Baker et al., 2014; Rocha et al., 2015a).

Table 1. Predicted environmental concentrations of Ag NPs in different environmental compartments according to different models.

Year	Sewage treatment effluents (ng/L)	Surface waters (ng/L)	Sediments (µg/kg)	Marine waters (ng/L)	Soils (µg/kg)	Reference
2010	9000	140	6000	-	-	Blaser et al., 2008
2012	42.5	0.764	0.952	-	0.0227	Gottschalk et al., 2009
-	-	10	-	-	0.43	Tiede et al., 2009
-	0.17	0.66	2.3	-	0.0012	Sun et al., 2014
-	-	0.002	-	-	-	Dumont et al., 2015
2017	18.890	0.382	1.854	0.0	19.184	Giese et al., 2018
2030	30.608	0.889	3.808	0.0	35.210	
2050	76.391	2.199	8.053	0.0	97.981	

Ag NPs tend to dissolve, and then, released Ag ions may form AgCl NPs and Ag chloride complexes (AgCl^0 , AgCl_2^- , AgCl_3^{2-} or AgCl_4^{3-}) depending on the salinity. Ag ions can also react with negatively charged organic ligands such as thiol groups, which are present on soluble organic matter or living cell surfaces. Additionally, Ag NPs may bind to organic matter producing large aggregates (a few μm) that will precipitate into surface sediments (Magesky and Pelletier, 2018; Zhang et al., 2018).

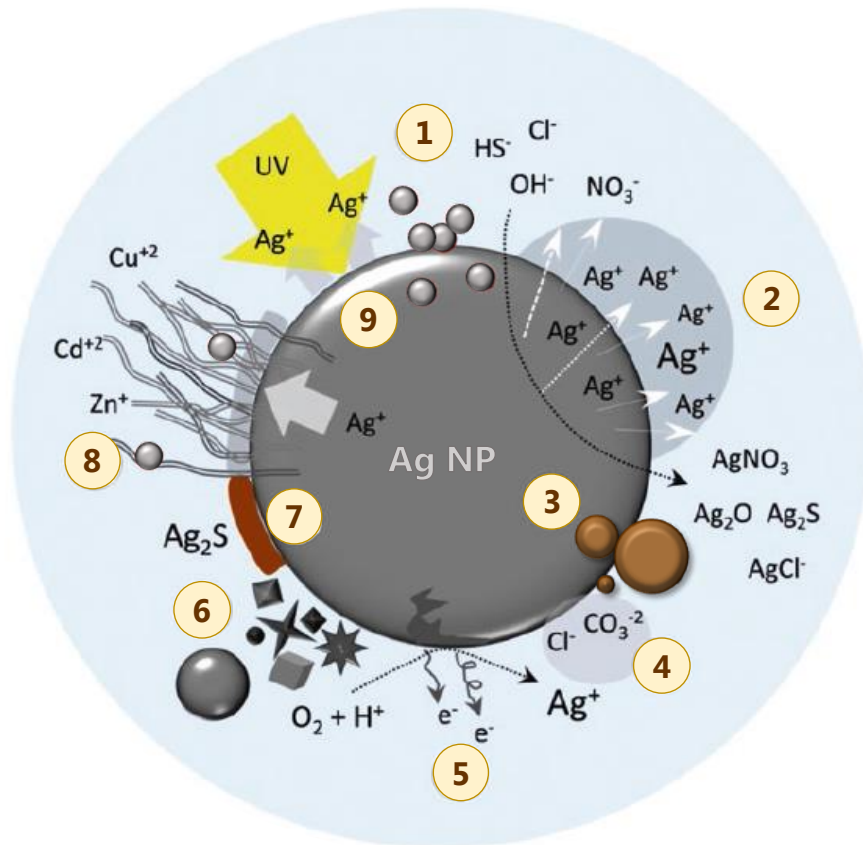


Figure 7: Main physico-chemical processes that may influence the fate and toxicity of Ag NPs in aquatic environments. 1) Aggregation with other Ag NPs (homoaggregation). 2) Dissolution of metal core and release of Ag ions by oxidative processes. 3) Interaction with organic matter (heteroaggregation). 4) Ionic adsorption on the surface of Ag NPs. 5) Oxidation and leaching of Ag ions from the irregular surface of NPs. 6) Different shape may influence internalization of Ag NPs into cells. 7) Sulfidation of Ag NPs (Ag_2S -NPs) can reduce or prevent oxidation and ionic leaching. 8) Coating agents provide stability to Ag NPs, but they also act as ligands for other toxic metals or organic molecules. 9) Photo-oxidation. (Modified from Magesky and Pelletier, 2018).

Toxicity of Ag NPs to different freshwater and marine organisms belonging to different trophic levels has been widely reported and a selection of the results is summarized below:

∴ *Microalgae*

Microalgae are microscopic primary producers that constitute the base of aquatic food chains and are considered the first target for most of the pollutants present in aquatic systems (Baker et al., 2014; Moreno-Garrido et al., 2015). Thus, several studies assessed Ag NPs toxicity to different microalgae species using algal growth inhibition bioassays. For the freshwater *Pseudokirchneriella subcapitata* microalgae, different EC50 values were reported depending on the Ag NP characteristics. Griffitt and colleagues (2009) reported an EC50 value of 190 µg/L for 20-30 nm Ag NPs while the EC50 value increased from 180 to 1140 µg/L Ag NPs as the size of citrate-coated Ag NPs increased from 10 to 80 nm (Ivask et al., 2014). Moreover, the same microalgae showed a higher sensitivity to smaller Ag NPs (3-8 nm) (Ribeiro et al., 2014). In marine species, differences in sensitivity among microalgae species were reported after microalgae exposure to PVP/PEI coated 5 nm Ag NPs. *Tretraselmis suecica* was about 10 times more sensitive (EC50 0.0052 mg Ag/L) than *Isochrysis galbana* (EC50 0.039 mg Ag/L) and *Phaeodactylum tricornutum* (EC50 0.06 mg Ag/L) (Schiavo et al., 2017). However, when the same microalgae species were exposed to uncoated 47 nm Ag NPs (Schiavo et al., 2017), they showed a similar sensitivity compared to *Dunaliella tertiolecta* exposed to uncoated 50 nm Ag NPs (EC50 around 5 mg/L) (Oukarroum et al., 2012). Species differences in sensitivity may be related to differences in cell wall structure and composition, among other factors.

Additionally, other effects such a reduction in the photosynthetic yield of *Chlamydomonas reinhardtii* freshwater microalgae were observed after the exposure to 40 nm Ag NPs, which was attributed to the direct toxic effects caused by the Ag NPs themselves as well as to the Ag ions released from the NPs (Navarro et al., 2008b). Moreover, the exposure to Ag NPs decreased the active chlorophyll levels, the effective quantum yield of PII and cell density and increased cell complexity and ROS production both in *Chlorella autotrophica* and *Dunaliella salina* microalgae (Sendra et al., 2017).

∴ *Invertebrates*

Aquatic invertebrates represent about 95% of animal species and their relevance as test organisms for NP ecotoxicity was highlighted due to their ecological importance and potential role in NPs transfer through food chains (Baun et al., 2008; Canesi and Corsi, 2016). Most investigations assessing toxicity of Ag NPs were focused on marine species, especially on filter-feeding and detritus-feeding bivalves, since their feeding habits leave them vulnerable to ingestion of NPs (Baker et al., 2014).

1. Bivalves

In mussels, waterborne exposure of *Mytilus galloprovincialis* adult organisms to 10 µg/L Ag NPs for 15 days caused Ag accumulation both in digestive gland and gills, induction of metallothionein (MT) protein levels in both tissues as well as lipid peroxidation and induction of the activity of antioxidant enzymes (superoxide dismutase; SOD, catalase; CAT, glutathione peroxidase; GPx) in gills (Gomes et al., 2014a). In addition, the protein expression pattern was different after the exposure to Ag NPs with a higher expression of proteins involved in stress response and cytoskeleton and cell structure both in digestive gland and gills (Gomes et al., 2013a) accompanied by genotoxic effects in hemocytes (Gomes et al., 2013b). Longer exposures (21 days) of mussels to 0.75 µg/L maltose-coated 20 nm Ag NPs destabilized the lysosomal membrane, provoked the loss of digestive cells and digestive gland integrity, as well as edema/hyperplasia in gills and infiltration of hemocytes in connective tissues (Jimeno-Romero et al., 2017b).

In *Crassostrea virginica* oysters, Ringwood and colleagues (2010) reported an increase of *mt* mRNA levels both in embryos and adult organisms after the exposure to 0.16 µg/L of 15 nm Ag NPs for 48 hours. Oysters exposure to 0.2, 2, and 20 µg/L of 20-30 nm Ag NPs for 48 hours provoked a dose-dependent increase in the lysosomal membrane destabilization rate, a significant increase in lipid peroxidation in hepatopancreas and induction of CAT activity in gills (McCarthy et al., 2013).

Comparison of waterborne exposure and dietary exposure to Ag NPs, revealed that even if Ag bioaccumulation was higher in waterborne exposed *Scrobicularia plana* clams than in dietary exposed ones, activity of the antioxidant enzymes (CAT, SOD and glutathione S-transferase; GST) was more affected after dietary than after waterborne exposure to 10 µg/L lactate-stabilized 40 nm Ag NPs

(Buffet et al., 2013). In a mesocosm study, after 21 days of exposure to 10 µg/L of maltose-stabilized 40 nm Ag NPs, clams significantly accumulated Ag in their tissues and induction of antioxidant enzymes (CAT, SOD and GST) and phenoloxidase activities as well as genotoxic effects were reported (Buffet et al., 2014).

2. Echinoderms

Sea urchins are model organisms for developmental biology, but they are also emerging as a valid tool for studies in marine ecotoxicology (Matranga and Corsi, 2012). Gametes, embryos in different developmental stages as well as juveniles of different sea urchin species have been used to assess Ag NPs toxicity.

Spermioxicity test in *Paracentrotus lividus* sea urchins revealed that sperm motility decreased in a dose-dependent manner after the exposure of sperm to a range of concentrations (0.0001, 0.001, 0.01, 0.1 and 1 mg/L) of 10 nm Ag NPs (Gambardella et al., 2015). Moreover, embryos descendant from fertilized eggs with sperm exposed to the same Ag NP type and concentrations, showed developmental abnormalities from the gastrula to pluteus stages, including morphological alterations of the skeletal rods (Gambardella et al., 2013). Similarly, exposure of fertilized eggs of different species of sea urchin (*Arbacia lixula*, *Sphaerechinus granularis* and *P. lividus*) to 1-100 mg/L Ag induced larval deformities and developmental arrest, being *A. lixula* the most sensitive species to Ag NPs toxicity (Burić et al., 2015). Failure of metamorphosis completion, lethargy, oedema, necrosis and immobility in juveniles as well as cellular immune reaction in larvae and juveniles was also reported after the exposure of different larval stages and juveniles of *S. droebachiensis* to 100 µg/L of 15 nm poly-allylamine coated Ag NPs (Magesky et al., 2016).

3. Crustacea

Artemia spp. brine shrimp is used nowadays as a reference biological model in Nanoecotoxicology (Libralato, 2014). Thus, several studies assessing Ag NP toxicity in these organisms are found in the literature. Arulvasu and colleagues (2014) showed that as the concentration of Ag NPs increased, the mortality rate of organisms, aggregation in the gut region, the amount of apoptotic cells and DNA damage increased in brine shrimp nauplii, whereas the percentage of cysts hatching decreased. Brine shrimp larvae also accumulated Ag after 24 hours of

exposure to 100 µg/L of PVP/PEI-coated 5 nm Ag NPs, but they showed low sensitivity with EC50 values of 19.63 mg Ag/L (Lacave et al., 2017).

Exposure of *A. salina* and *A. amphitrite* brine shrimp species to 10 nm Ag NPs significantly altered the swimming speed of the nauplii. In fact, this behavioral endpoint was more sensitive than mortality, independently from the Ag NPs concentration for both species (Gambardella et al., 2015). However, *A. amphitrite* seemed to be more sensitive (LC50 values of 0.55 mg/L after 24 hours and 0.27 mg/L after 48 hours) than *A. salina* nauplii (LC50 values of 9.96 mg/L at 24 hours and 3.79 mg/L at 48 hours) (Gambardella et al., 2015). Similarly, immobilization rate of *A. salina* significantly increased in a concentration-dependent way after 72 hours of exposure to both PVP-coated Ag NPs and Ag nanowires (An et al., 2019). Additionally, ROS production increased after 48 hours of exposure and SOD activity decreased significantly as exposure concentration increased (An et al., 2019).

4. Polychaetes

Agglomeration or aggregation of NPs may help NPs removal from the water column due to their settlement into sediments. Thus, organisms associated with the benthos that are detrital and deposit feeders, such as polychaetes, may become susceptible to their effects (Baker et al., 2014). For example, *Hediste diversicolor* ragworms significantly accumulated Ag after 21 days of exposure to 10 µg/L of maltose-stabilized 40 nm Ag NPs and showed burrowing impairments, induction of CAT, GST, caspase-3 and lysozyme activities in whole organisms and genotoxic effects in coelomocytes (Buffet et al., 2014). Similarly, DNA damage in *Nereis diversicolor* coelomocytes increased as exposure concentrations to ~100 nm Ag NPs increased (Cong et al., 2011). Another study in which eggs, larvae, juveniles and non-mature *Platynereis dumerilii* worms were exposed to citrate-capped 13 nm Ag NPs or humic acid-capped 16 nm Ag NPs revealed that fertilized eggs were the most sensitive life cycle stage while juveniles and adults were more tolerant to Ag NP toxicity (García-Alonso et al., 2014). Moreover, exposure to both types of Ag NPs enhanced the abnormal development of organisms related to morphological malformations and/or differential motility (García-Alonso et al., 2014).

∴ *Fishes*

Toxic effects caused by Ag NPs in fish species have been mainly studied in the model organism zebrafish *Danio rerio*. A variety of effects have been described in this species, depending on the characteristics of the analyzed Ag NPs (Massarsky et al., 2014). For instance, a significant increase of silver burden and transcriptomic alterations were found in gills after acute exposure (48 hours) to 1 mg/L of 26 nm Ag NPs (Griffitt et al., 2009). Similarly, the number of regulated genes in the gills increased in a dose-dependent manner after a 28 days exposure of zebrafish to 5 to 50 µg/L of smaller (~3.1 nm) Ag NPs (Griffitt et al., 2013). Additionally, the exposure of zebrafish to 100 µg/L of PVP-coated Ag NPs for 15 days provoked cell death in fish liver, associated with several indicators of oxidative stress, such as enhancement of nitric oxide production, reduced CAT and SOD activities and increased sulphhydryl groups (Devi et al., 2015). Moreover, zebrafish exposed to 10 µg/L of maltose-coated 20 nm Ag NPs for 21 days, showed Ag accumulation in their soft tissues, histopathological lesions in the gills and alterations in the transcription of genes involved in steroid biosynthesis and glycolysis/gluconeogenesis pathways (Lacave et al., 2018).

Development of early life stages of zebrafish was affected by the exposure to Ag NPs. Ashararani and colleagues (2008) reported spinal cord deformities, cardiac arrhythmia and mortality after the exposure of embryos to concentrations above 50 µg/mL of 10-80 nm Ag NPs. Similarly, the exposure of zebrafish embryos to different concentrations (5, 10, 25, 50 and 100 mg/L) of 10-20 nm Ag NPs, caused dose-dependent deleterious effects in embryonic development, including several deformities, delayed development and even embryos death (Xia et al., 2015). Exposure of zebrafish embryos to low concentrations (0.075 mg/L) of PVP/PEI coated 5 nm Ag NPs or 1 mg/L of maltose-coated 40 nm Ag NPs also led to the appearance of malformations in developing embryos, such as yolk sac, pericardial edema, and tail and spinal cord flexure, among others (Lacave et al., 2016; Orbea et al., 2017).

In marine species, Scown and colleagues (2010) observed that the exposure of rainbow trout to 10 and 100 µg/L of 10 nm Ag NPs for 10 days resulted in Ag accumulation in the gills and liver of fish which affected the oxidative metabolism in gills. However, in the eurihaline Atlantic salmon (*Salmo salar*), 48 hours of exposure to 20 µg/L of ~25 nm Ag NPs was enough to provoke Ag accumulation in gills, induction of genes involved in stress and metal detoxification as well as suppression of Na⁺/K⁺-ATPase mRNA levels (Farmen et al., 2012).

4. Bivalve molluscs as model species

The Bivalvia class is one of the six classes of molluscs and comprises animals enclosed in two shell valves, such as mussels, oysters, scallops and clams (Gosling, 2015). One of the main characteristics of bivalves is their filter-feeding behavior. The ability of these organisms to select among captured particles is well known, but the mechanisms by which particles of poor quality are rejected and those of higher quality are directed toward the mouth and ingested remains unknown (Ward and Shumway, 2004). Microalgae represent one of the most important sources of food for suspension-feeding bivalves, even if some species are known to ingest and digest detritus, bacteria or protozoans (Kreeger and Newell, 2001). The selection of microalgae as main source of food seems to be related to cell size and morphology (Ward and Shumway, 2004) as well as to interactions between microalgae cell surface carbohydrates and lectins present in the mucus covering feeding organs (Pales Espinosa et al., 2009; 2010).

Bivalves shell growth can be continuous even in the absence of feeding, as shell is formed mostly from dissolved calcium present in seawater (Alunno-Bruscia et al., 2001) even if one of the main factors affecting mussel shell shape morphology together with density, age, wave exposure and mussel size is food availability (Seed, 1973; Akester and Martel, 2000; Alunno-Bruscia et al., 2001). Although mussel growth in shell appears to be continuous during the year (Okumuş and Stirling, 1998), the increase in total body weight, also considered a parameter to measure growth, appears to be seasonal, with gross growth concentrated in specific seasons (Seed, 1973). This gross growth is related to the gamete developmental cycle of bivalves, which can exhibit considerable temporal and spatial variations (Seed and Suchanek, 1992) since it can be affected by abiotic factors such as temperature and food availability (Giese and Pearse, 1974; Newell et al., 1989; Gosling, 2015).

Size of bivalves, together with temperature and quantity and quality of food are important factors to initiate the gametogenesis. Development of resting gonads starts during October-November and gonad undergoes continuous development throughout winter until it becomes fully mature or ripe by early spring. During spring months, spawning occurs and under favorable feeding conditions, a second period of gametogenesis takes place until early summer, when gonads are ripe again. By late August or September, most bivalves enter in their gametogenic resting stage (Seed and Suchanek, 1992; Villalba, 1995; Ortiz-Zarragoitia et al., 2011; Gosling, 2015). This seasonal gamete developmental cycle modulates the metabolism and physiology of bivalves (Bayne and Widdows, 1978; Seed and Suchanek, 1992; Sheehan and Power, 1999; Cancio et al., 1999).

The development of bivalves consists of an embryonic phase followed by a larval phase (Figure 8). After spawning, fertilized eggs begin to divide reaching the first larval stage (trochophore; Figure 8.3). The trochophore develops into the veliger larval stage (also known as D-shell larvae due to the characteristic shape of a capital letter D) after 48 hours of fertilization in mussels (Figure 8.4). At this stage, larvae begin to feed and the shell starts to calcify reaching the umbo larvae stage. When larvae reach maturity, gill rudiments become evident and a foot develops to settle on a substrate (Figure 8.5). Finally, larvae suffer metamorphosis, in which the planktonic larvae change to a sedentary benthic living one (His et al., 1999).

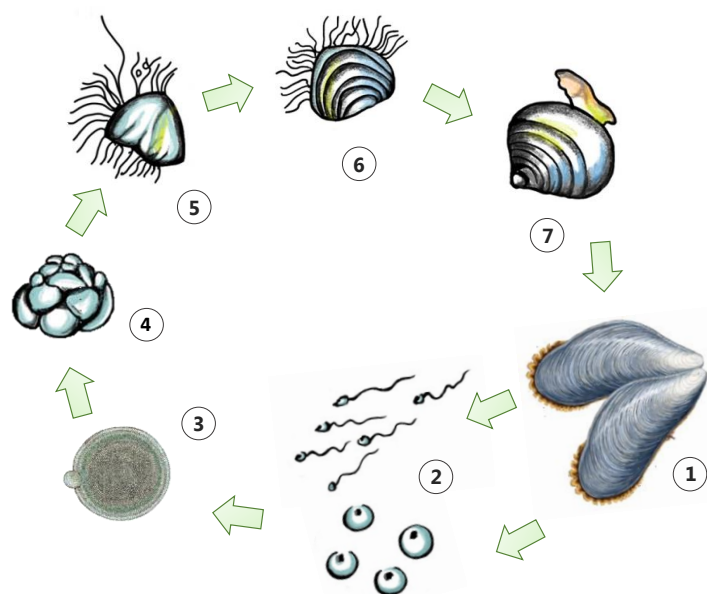


Figure 8: Reproductive cycle of *Mytilus* spp. mussels. **1)** Adult mussels. **2)** Male and female gametes. **3)** Fertilized egg with expelled polar body. **4)** Morula. **5)** Trochophore larva. **6)** Veliger or D-shell larva. **7)** Mature larva with foot. Drawing by J.M. Duroudier.

4.1. Bivalves and eco-nanotoxicology

Marine bivalve molluscs have gained global importance as bioindicators of marine and estuarine pollution since Goldberg (1975) proposed the “Mussel Watch”, a concept that was initially suggested to evaluate the quality of marine waters by using marine bivalves (Goldberg, 1986). Mussels were also proposed as sentinels of pollution in which biological effects caused by pollutants could be measured (Bayne, 1989). Since then, numerous “Mussel Watch” type programs on a local, regional, national and international basis have been carried out successfully in order to assess the pollution status of marine environments (Cajaraville et al., 2000; UNEP, 2004; Farrington et al., 2016; ICES, 2016).

Recently, bivalve molluscs were identified as the main target group to assess NP toxicity in marine environments due to their highly developed processes for cellular internalization of nano and micro-scale particles (Moore, 2006; Canesi et al., 2012; Corsi et al., 2014). In this sense, Moore (2006) proposed the mussel *Mytilus* spp. as a suitable model organism for characterizing the potential impact of NPs and nowadays, mussels are the most utilized bivalve model (Figure 9).

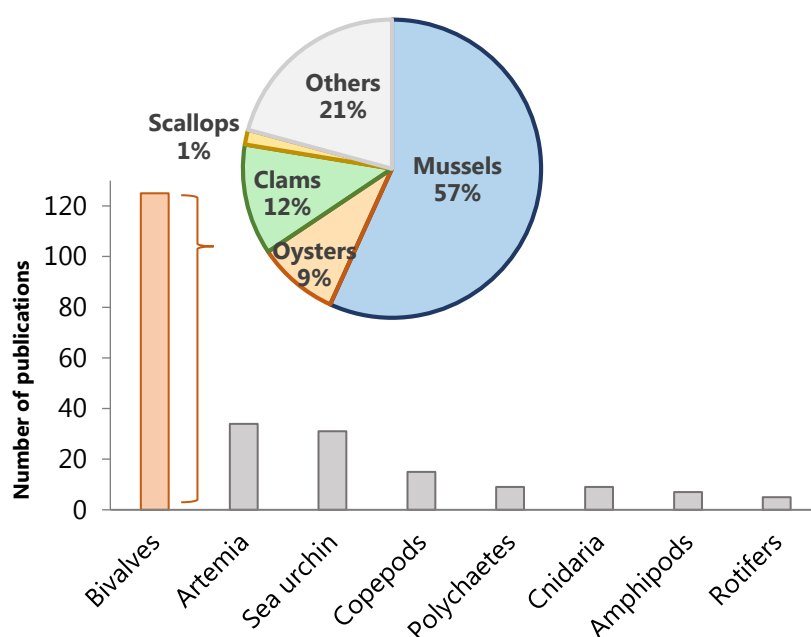


Figure 9: Number of studies assessing the effects of ENPs in different marine invertebrates. Pie chart shows the percentage of studies belonging to different families of bivalves with respect to the total number of investigations published in bivalves. Data were taken from Pubmed (<https://www.ncbi.nlm.nih.gov/pubmed>; April 2019).

In mussels, NPs are trapped by gills which are the first organ/barrier to surrounding water and vulnerable to particle interactions (Corsi et al., 2014; Rocha et al., 2015a). In fact, gill cells are an important target of NP toxicity as shown by *in vitro* studies (Katsumiti et al., 2014; 2015a, 2015b, 2016; 2018). Once in gills, NP are directed to the digestive gland. Mussels digestive gland is considered the main organ for NPs accumulation, where NPs cellular fate and caused effects differ according to the NP type and to experimental conditions (Canesi et al., 2012; Rocha et al., 2015a; Canesi and Corsi, 2016). Digestive cells in digestive gland show a well-developed endo-lysosomal system (Cajaraville et al., 1995; Robledo et al., 1997), due to its role in intracellular digestion of food particles and this system is considered the main subcellular target for metallic NPs in bivalves (Moore, 2006; Canesi et al., 2012; Katsumiti et al., 2014; Rocha et al., 2015a). Internalization of NPs in cells may occur via

endocytosis and then NPs may reach the endosomal and lysosomal compartments (Katsumiti et al., 2014; Jimeno-Romero et al., 2016; 2017b; 2019). Once inside lysosomes, the low pH (≈ 5.0) of lysosomes may favour dissolution of metallic NPs releasing free ions, which together with the remaining NPs, could induce the hypersynthesis of the lysosomal acid phosphatase enzyme and the generation of ROS, finally attacking lysosomal membranes and releasing the lysosomal content into the cytosol and causing DNA damage (Katsumiti et al., 2014).

NPs can be potentially translocated from the digestive system to the hemolymph and to circulating hemocytes (Canesi and Corsi, 2016). Hemocytes are cells responsible for the immune defense due to their specialized systems for endocytosis and phagocytosis of particles of different size (Cajaraville and Pal, 1995). Therefore, these cells are considered also important targets for NPs toxicity (Canesi et al., 2010; Ciacci et al., 2012; Katsumiti et al., 2014; 2015a; 2015b; 2016; 2018; Katsumiti and Cajaraville, 2019).

In this sense, special emphasis has been placed to the effects caused by different types of NPs on the main tissues involved in NPs uptake and accumulation such as gills and digestive gland as well as on the immune system (reviewed in Canesi et al., 2012; 2015; Rocha et al., 2015a; Canesi and Corsi 2016; Katsumiti and Cajaraville, 2019).

4.2. Biomarkers as suitable tools for assessing nanoparticles toxicity in mussels

Over the past decades, the scientific community developed and tested several biochemical, cellular and physiological biomarkers in order to assess the sublethal effects of contaminants in aquatic organisms and therefore, evaluate the impact of environmental pollution (Dagnino et al., 2007). In this line, the biomarker approach together with the traditional chemical analytical approach has been widely used in marine pollution monitoring programs (UNEP, 2004; ICES, 2006; Zorita et al., 2007a; Hylland et al., 2008; Marigómez et al., 2013) and laboratory studies (Zorita et al., 2007b; Canesi et al., 2008; Ruiz et al., 2014; Banni et al., 2017) for the assessment of biological effects caused by different pollutants.

Biomarkers are measurements at the molecular, biochemical or cellular level, which indicate that an organism has been exposed to pollutants (exposure biomarker) and/or the magnitude of the organisms response to pollutants (stress biomarker) (McCarthy and Shugart, 1990). Among biomarkers of exposure, metallothionein levels, cholinesterase activity, peroxisome proliferation and enzymatic activities related to the

cytochrome P450 system can be found (Cajaraville et al., 2000; Viarengo et al., 2007; Hook et al., 2014). While markers of oxidative stress, lysosomal responses, heat shock proteins and DNA damage measurements are considered biomarkers of effect (Viarengo et al., 2007; Hook et al., 2014). Thus, the use of a battery of biomarkers including both exposure and effects biomarkers can describe the physiological status of the organisms (Cajaraville et al., 2000; Marigómez et al., 2004; Dondero et al., 2006; Hook et al., 2014).

However, the interpretation of biomarkers should be addressed carefully since the relationships between tissue body burden of contaminants and biomarker levels can be confounded by age, sex and reproductive status (Hylland et al., 2009). In fact, seasonal variations in biomarker responses such as lysosomal parameters, metallothionein levels, antioxidant enzymes activities and DNA damage have been reported in mussels (Cancio et al., 1999; Orbea et al., 1999; Leiniö and Lehtonen, 2005; Pisanelli et al., 2009; Hagger et al., 2010; Nahrgang et al., 2013; Schmidt et al., 2013; Lekube et al., 2014; González-Fernández et al., 2016; Balbi et al., 2017). These changes are driven by the interaction between abiotic factors in the environment, such as temperature, food availability and oxygen level, and biotic factors, as their physiological state (Bayne and Widdows, 1978; Solé et al., 1995; Cancio et al., 1999; Sheehan and Power, 1999).

In the last years, the biomarker approach has been widely used to evaluate biological responses to different NPs. The application of lysosomal, oxidative stress, immunotoxicity and other biomarkers, together with NP characterization and chemical data, represent a sensitive tool for evaluating the effects and mechanisms of action of different NPs in aquatic invertebrates, especially in marine mussels (Canesi et al., 2012). Some of the results reported in marine mussels are summarized below.

1. Bioaccumulation and subcellular distribution of ENPs

In general, bioaccumulation of different types of metal-containing NPs (CuO NPs, Ag NPs, Au NPs, TiO₂ NPs, CdS QDs and CdTe QDs) has been reported in *Mytilus* spp. mussel soft tissues, as well as in digestive gland and gills separately using different exposure times and concentrations (Tedesco et al., 2010; Gomes et al., 2011; 2012; 2014a; Canesi et al., 2014; Balbi et al., 2014; Rocha et al., 2015b; 2016; Jimeno-Romero et al., 2016; 2017a; 2019). Transmission electron microscope analysis allowed to localize NPs such as TiO₂ NPs, Ag NPs, Au NPs and CdS QDs inside residual bodies of digestive cells (Jimeno-Romero et al., 2016; 2017a; 2017b; 2019) confirming that the endolysosomal system is an important subcellular target for metallic NPs. Moreover, the analysis of metal

distribution in tissues by autometallography showed intralysosomal metal accumulation in the form of black silver deposits in mussel digestive cells exposed to the same NPs (Jimeno-Romero et al., 2016; 2017a; 2017b; 2019). TiO₂ NPs and CdS QDs were localized also in the gills (Jimeno-Romero et al., 2016; 2019). *In vitro* studies showed that 1 hour of incubation was time enough to observe CdS QDs in the endolysosomal system of mussels hemocytes (Katsumiti et al., 2014).

2. Lysosomal responses

The endocytic-lysosomal pathway is the major subcellular entry route for NPs in bivalves. Damage on the lysosomal system may cause disease processes and cell injuries. Destabilization of the lysosomal membrane has been widely reported in digestive cells of *M. galloprovincialis* mussels exposed to metal-containing NPs such as TiO₂ NPs (Barmo et al., 2013; Balbi et al., 2014; Jimeno-Romero et al., 2016), Au NPs (Jimeno-Romero et al., 2017a), CdS QDs (Jimeno-Romero et al., 2019) as well as Ag NPs (Jimeno-Romero et al., 2017b) indicating that NPs provoke a significant general stress in these organisms.

3. Oxidative stress

Oxidative stress refers to a redox imbalance within cells usually related to increased intracellular ROS and decreased antioxidant enzymatic activity which results in damage to cellular macromolecules including DNA, proteins and lipids (Singh et al., 2009). Oxidative damage induced by ENMs in bivalves depends on NP size, composition and concentration, exposure route and time as well as the target organ studied (Rocha et al., 2015a). Regarding NP size, small Au NPs induced higher oxidative stress levels than larger ones after the exposure of *M. edulis* mussels to 750 µg/L of ~5 nm or 13 nm Au NPs, respectively (Tedesco et al., 2008; 2010). When target organs were compared, gills of *M. galloprovincialis* were more susceptible to oxidative stress than digestive gland after the exposure to 10 µg/L CuO NPs for 15 days, even if the antioxidant defense system was overwhelmed in both tissues (Gomes et al., 2011; 2012). Similarly, gills of mussels were more responsive than digestive gland showing a higher induction of antioxidant enzyme activities and lipid peroxidation levels after the exposure to CdTe QDs (Rocha et al., 2015b; 2016) or Ag NPs for 14 days (Gomes et al., 2014a). On the other hand, lipid peroxidation was induced only in mussels digestive gland and no effects were observed in gills or mantle of *M. edulis* after

24 hours of exposure to Au NPs (Tedesco et al., 2010). Mussel hemocytes and gill cells exposed *in vitro* to CdS QDs, Ag NPs or CuO NPs showed an induction in CAT activity, being hemocytes more sensitive than gill cells after the exposure to CdS QDs and CuO NPs (Katsumiti et al., 2014; 2015b; 2018). Additionally, ROS production was induced in both cell types after the *in vitro* exposure to the same metal-containing NPs (Katsumiti et al., 2014; 2015b; 2018).

4. Genotoxicity

DNA is a cellular component highly susceptible to oxidative damage induced by ENMs in bivalve cells that may lead into chromosomal fragmentation, DNA strand breaks, point mutations, oxidative DNA adducts and alterations in gene expression profiles (Singh et al., 2009). In mussels *M. galloprovincialis* hemocytes, genotoxic effects measured as micronuclei and DNA strand breaks were observed after 15 days of exposure to 10 µg/L of CuO NPs, Ag NPs or CdTe QDs, which seemed to be mediated by oxidative stress (Gomes et al., 2013b; Rocha et al., 2014) or due to the direct interaction of QDs with DNA (Rocha et al., 2014). On the other hand, 96 hours of exposure to TiO₂ NPs did not induce genotoxic effects in mussels gills, while enhanced DNA damage was observed in mussels digestive gland (Canesi et al., 2014). In addition, *in vitro* exposure studies of mussel hemocytes and gill cells to CdS QDs, Ag NPs or CuO NPs revealed an increase in DNA strand breaks in both cell types (Katsumiti et al., 2014; 2015b; 2018).

5. Immunotoxicity

As mentioned before, hemocytes are mussels immune cells considered also important targets for NP toxicity. In fact, *in vitro* studies in *M. galloprovincialis* mussels hemocytes showed that after 30 minutes of incubation, different types of NPs (0.7 nm fullerenes, 22 nm TiO₂ and 12 nm SiO₂) were rapidly taken up by the cells and among others, lysosomal function, phagocytic activity, oxyradical production and pro-apoptotic processes are altered (Canesi et al., 2010). Similarly, hemocytes exposure to TiO₂, SiO₂, ZnO or CeO₂ NPs altered their lysosomal membrane stability, phagocytic activity and ROS production depending on the NP (Ciacci et al., 2012). *In vitro* exposures of hemocytes to a wide concentration range of different types of metallic NPs (CdS QDs, TiO₂ NPs, Ag NPs, Au NPs, ZnO NPs, SiO₂ NPs, CuO NPs) for 24 hours showed cytotoxic effects in terms of cell viability (Katsumiti et al., 2014, 2015a; 2015b, 2016; 2018;

reviewed in Katsumiti and Cajaraville, 2019). Main mechanisms of action of CdS QDs, Ag NPs and CuO NPs involved oxidative stress and genotoxicity, activation of lysosomal AcP activity, disruption of actin cytoskeleton and stimulation of phagocytosis, which indicated a NP-specific immunostimulatory effect in mussel hemocytes (Katsumiti et al., 2014, 2015b, 2018; reviewed in Katsumiti and Cajaraville, 2019).

Exposure of adult mussels to TiO₂ NPs for 96 hours, caused alterations in the immune response of hemocytes due to the reduced stability of the lysosomal membrane and phagocytosis and the increased production of nitric oxide and release of lysozymes (Barmo et al., 2013; Balbi et al., 2014).

6. Embryotoxicity

The developmental toxicity caused by ENMs has not been widely investigated yet. Only few studies have assessed the effects during mussels larval development after exposure of sperm or fertilized eggs to different types of metal-bearing NPs (Kadar et al., 2010; 2013; Balbi et al., 2014; Auguste et al., 2018). Abnormalities in D-shell larvae were not observed after the exposure to different TiO₂ NP concentrations (Balbi et al., 2014) neither after the exposure to Fe₂O₃ NPs (Kadar et al., 2010), but the exposure of fertilized eggs to different concentrations of Ag NPs provoked a concentration-dependent increase in malformed D-shell larvae starting at 10 µg/L (Auguste et al., 2018). Similarly, exposure of mussels sperm to zero-valent nano iron (nZVI) caused fertilization impairment and mussel larvae development was stopped mainly at trochophore stage (Kadar et al., 2013).

4.3. The omic's approach: discovering new biomarkers

Due to the high complexity of ecosystems, environmental risk assessment (ERA) is very challenging. Thus, there is a need to develop and validate innovative and reliable tools and integrated approaches for fast detection of changes in population and community structures that can be applied by regulatory agencies (Tarazona, 2013). The application of innovative high-throughput omic's tools (e.g. transcriptomics, genomics, proteomics or metabolomics) to evaluate environmental health status or to early identify hazards using adverse outcome pathways (AOPs) is important and helpful for risk assessment (Tarazona, 2013; Lee et al., 2015).

AOPs were proposed as a paradigm to link direct molecular initiating events (e.g. a molecular interaction between a xenobiotic and a specific biomolecule) and adverse outcomes with biological levels of organization relevant for risk assessment (Figure 10; Ankley et al., 2010). They represent an useful tool for predicting adverse outcomes on the individual, population, community and ecological levels according to biomarker responses (Lee et al., 2015). Thus, the application of omic approaches could help to identify initial molecular markers that may act as key anchors for chemical-biological interactions giving a better understanding of the implications of a specific molecular event in ERA (Hook et al., 2014; Vinken et al., 2014; Lee et al., 2015).

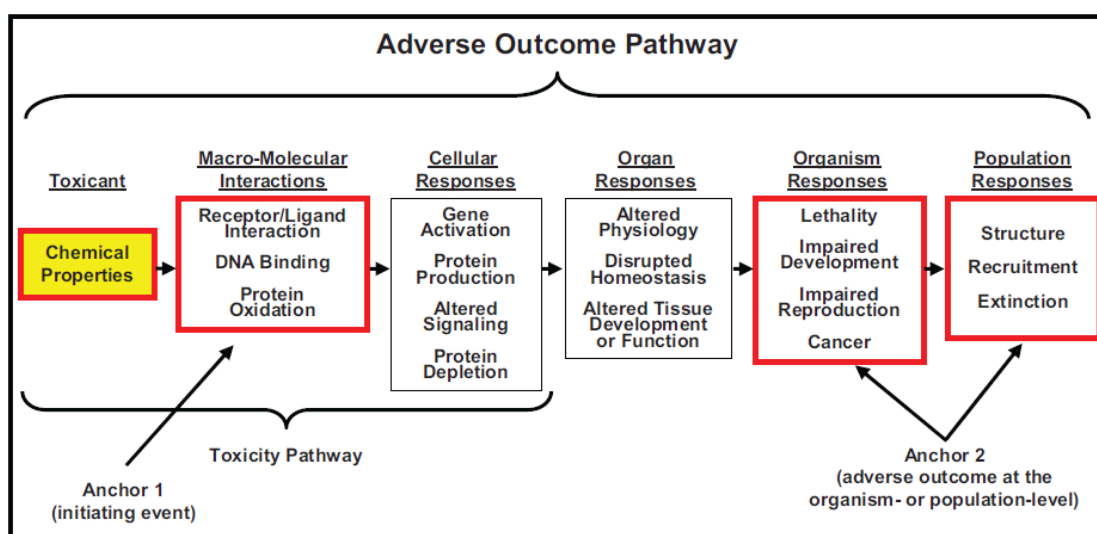


Figure 10: Conceptual diagram of key features of an adverse outcome pathway (AOP). Each AOP begins with a molecular initiating event in which a chemical interacts with a biological target (anchor 1) leading to a sequential series of higher order effects to produce an adverse outcome with direct relevance to a given risk assessment context (e.g., survival, development, reproduction, etc.; anchor 2). The first three boxes are the parameters that define a toxicity pathway (Taken from Ankley et al., 2010).

Moreover, as reviewed in section 4.2., conventional biomarkers have been extensively used to assess ENMs toxicity in bivalve species but many of the toxic responses are common to contaminants in different forms, including NPs, ionic and/or bulk forms in the case of inorganic ones. Therefore, there is a need to develop nano-specific biological measurements to differentiate nano-specific responses and modes of action from their similar ionic/bulk counterparts as well as from other contaminants (Rocha et al., 2015a).

In this sense, omic's technologies have been already applied in the nanotoxicological field in order to identify molecular markers reflecting both exposure and subsequent biological effects of ENMs in mussels. In these studies, it seems that mainly genes and proteins involved in cytoskeleton are affected after exposure of mussels to different types of NPs (Banni et al., 2016; Gomes et al., 2014b; Hu et al., 2014). In a transcriptomic study, genes involved in microtubule-based movement and cellular component organization processes were significantly upregulated after the exposure of mussels to 100 µg/L TiO₂ NPs for 96 hours (Banni et al., 2016). Similarly, proteomics based methods revealed changes in the expression of four cytoskeletal components including *actin* after the exposure of *M. edulis* mussels to three different concentrations of CuO NPs for just 1 hour (Hu et al., 2014) and underexpression of *actin* isoforms in gills and digestive gland of *M. galloprovincialis* mussels exposed to 10 µg/L CuO NPs for 15 days (Gomes et al., 2014b). Additionally, induction of the cytoskeletal protein *paramyosin* was reported in mussels gills after mussels exposure to Ag NPs (Gomes et al., 2013a). The disturbance of these structural proteins of cytoskeleton could be mediated by ROS production and oxidative stress (Gomes et al., 2013a; 2014b; Hu et al., 2014).

4.4. Trophic transfer studies

ENPs may be prone to bioaccumulation and biomagnification along trophic chains potentially affecting marine biological resources and at last instance, impacting on human health due to their transfer through the consumption of contaminated fishery products (Matranga and Corsi, 2012; Baker et al., 2014; Tangaa et al., 2016). Nevertheless, studies assessing the potential trophic transfer of metal, metal oxides and metal mixtures in nano-size in marine organisms remain scarce.

As primary producers that constitute the base of marine aquatic food chains, microalgae could lead to a widespread transfer of ENPs across all trophic levels if ENPs are uptaken and accumulated by microalgae (Matranga and Corsi, 2012; Baker et al., 2014; Moreno-Garrido et al., 2015). In fact, Larginho and colleagues (2014) demonstrated the trophic transfer of Au NPs from *Dunaliella salina* microalgae to *M. galloprovincialis* mussels. Au was accumulated in the digestive gland but the activity of antioxidant enzymes was not altered, neither after the exposure to Au NPs through the water (Larginho et al., 2014). *S. plana* clams exposed to 40 nm lactate Ag NPs for 15 days accumulated higher concentrations of Ag after waterborne exposure in comparison to dietary exposure to Ag NPs, but the response of oxidative stress related

biomarkers was more marked after dietary exposure than after waterborne exposure (Buffet et al., 2013). In another food chain, even if brine shrimps showed to be more selective towards non- or less contaminated microalgae cells, *Artemia salina* fed with *Dunaliella salina* microalgae previously exposed to TiO₂ NPs for 48 hours significantly accumulated Ti in tissues and showed induction of ROS production (Bhuvaneshwari et al., 2018). However, brine shrimps were more sensitive to the waterborne exposure than to the dietary exposure (Bhuvaneshwari et al., 2018). In the food chain consisting of brine shrimps and marine medaka *Oryzias melastigma*, Ag assimilated from brine shrimps exposed to citrate-coated 20 nm Ag NPs inhibited Na⁺/K⁺-ATPase and SOD activities and reduced total body length and water content in marine medaka fed for 28 days (Wang and Wang, 2014).

Assessing the trophic transfer of ENPs is still complex and the need to first understand the uptake and potential toxicity of ENPs along simplified food chains remains, before investigating their effects in mesocosms and complex food webs

References

- ∴ Akester R.J., Martel A.L. 2000. Shell shape, dysodont tooth morphology, and hinge ligament thickness in the bay mussel *Mytilus trossulus* correlate with wave exposure. *Canadian Journal of Zoology* 78: 240-253.
- ∴ Alunno-Bruscia M., Bourget E., Fréchette M., 2001. Shell allometry and length mass density relationship for *Mytilus edulis* in an experimental food-regulated situation. *Marine Ecology. Progress Series* 219: 177-188.
- ∴ An H.J., Sarkheil M., Park H.S., Yu I.J., Johari S.A. 2019. Comparative toxicity of silver nanoparticles (AgNPs) and silver nanowires (AgNWs) on saltwater microcrustacean, *Artemia salina*. *Comparative Biochemistry and Physiology, Part C* 218: 62-69.
- ∴ Ankley G.T., Bennett R.S., Erickson R.J., Hoff D.J., Hornung M.W., Johnson R.D., Mount D.R., Nichols J.W., Russom C.L., Schmieder P.K., Serrano J.A., Tietge J.E., Villeneuve D.L. 2010. Adverse outcome pathways: A conceptual framework to support ecotoxicology research and risk assessment. *Environmental Toxicology and Chemistry* 29: 730-741.
- ∴ António D.C., Cascio C., Jakšić Ž., Jurašin D., Lyons D.M., Nogueira A.J., Rossi F., Calzolari L. 2015. Assessing silver nanoparticles behaviour in artificial seawater by mean of AF4 and spICP-MS. *Marine Environmental Research* 111: 162-169.
- ∴ Arulvasu C., Jennifer S.M., Prabhu D., Chandhirasekar D. 2014. Toxicity effect of silver nanoparticles in brine shrimp *Artemia*. *The Scientific World Journal* ID 256919: doi: 10.1155/2014/256919.
- ∴ Asharani P.V., Wu W.L., Gong Z., Valiyaveetil S. 2008. Toxicity of silver nanoparticles in zebrafish models. *Nanotechnology* 19: 255102-255110.
- ∴ Auguste M., Ciacci C., Balbi T., Brunelli A., Caratto V., Marcomini A., Cuppini R., Canesi L. 2018. Effects of nanosilver on *Mytilus galloprovincialis* hemocytes and early embryo development. *Aquatic Toxicology* 203: 107-116.
- ∴ Baalousha M., Ju-Nam Y., Cole P.A., Hriljac J.A., Jones I.P., Tyler C.R., Stone V., Fernandes T.F., Jepson M.A., Lead J.R. 2012. Characterization of cerium oxide nanoparticles-part 2: nonsize measurements. *Environmental Toxicology and Chemistry* 31: 994-1003.
- ∴ Baker T.J., Tyler C.R., Galloway T.S. 2014. Impacts of metal and metal oxide nanoparticles on marine organisms. *Environmental Pollution* 186: 257-271.
- ∴ Balbi T., Smerilli A., Fabbri E., Ciacci C., Montagna M., Graselli E., Brunelli A., Pojana G., Marcomini A., Gallo G., Canesi L. 2014. Co-exposure to n-TiO₂ and Cd²⁺ results in interactive effects on biomarker responses but not in increased toxicity in the marine bivalve *M. galloprovincialis*. *Science of the Total Environment* 493: 355-364.
- ∴ Balbi T., Fabbri R., Montagna M., Camisassi G., Canesi L. 2017. Seasonal variability of different biomarkers in mussels (*Mytilus galloprovincialis*) farmed at different sites of the Gulf of La Spezia, Ligurian sea, Italy. *Marine Pollution Bulletin* 116: 348-356.
- ∴ Banni M., Sforzini S., Balbi T., Corsi I., Viarengo A., Canesi L. 2016. Combined effects of n-TiO₂ and 2,3,7,8-TCDD in *Mytilus galloprovincialis* digestive gland: A transcriptomic and immunohistochemical study. *Environmental Research* 145: 135-144.

- ∴ Banni M., Sforzini S., Arlt V.M., Barranguer A., Dallas L.J., Oliveri C., Aminot Y., Pacchioni B., Millino C., Lanfranchi G., Readman J.W., Moore M.N., Viarengo A., Jha A.N. 2017. Assessing the impact of benzo[a]pyrene on marine mussels: application of a novel targeted low density microarray complementing classical biomarker responses. *PLoS ONE* 12 (6): e0178460.
- ∴ Barmo C., Ciacci C., Canonico B., Fabbri R., Cortesec K., Balbi T., Marcomini A., Pojana G., Gallo G., Canesi L. 2013. *In vivo* effects of n-TiO₂ on digestive gland and immune function of the marine bivalve *Mytilus galloprovincialis*. *Aquatic Toxicology* 132-133: 9-18.
- ∴ Baun A., Hartmann N.B., Grieger K., Kisk K.O. 2008. Ecotoxicity of engineered nanoparticles to aquatic invertebrates: a brief review and recommendations for future toxicity testing. *Ecotoxicology* 17: 387-395.
- ∴ Bayne B.L., Widdows J. 1978. The physiological ecology of two populations of *Mytilus edulis* L. *Oecologia* 37: 137-162.
- ∴ Bayne B.L. 1989. Measuring the biological effect of pollution: the mussel watch approach. *Water Science Technology* 21: 1089-1100.
- ∴ Behzadi S., Serpooshan V., Tao W., Hamaly M.A., Alkawareek M.Y., Dreaden E.C., Brown D., Alkilany A.M., Farokhzad O.C., Mahmoudi M. 2017. Cellular uptake of nanoparticles: journey inside the cell. *Chemical Society Reviews* 46: 4218-4244.
- ∴ Benn T.M., Westerhoff P. 2008. Nanoparticle silver released into water from commercially available sock fabrics. *Environmental Science and Technology* 42: 4133-4139.
- ∴ Bhuvaneshwari M., Thiagarajan V., Nemade P., Chandrasekaran N., Mukherjee A. 2018. Toxicity and trophic transfer of P25 TiO₂ NPs from *Dunaliella salina* to *Artemia salina*: Effect of dietary and waterborne exposure. *Environmental Research* 160: 39-46.
- ∴ Blaser S.A., Scheringer M., Macleod M., Hungerbühler K. 2008. Estimation of cumulative aquatic exposure and risk due to silver: contribution of nano-functionalized plastics and textiles. *Science of the Total Environment* 390: 396-409.
- ∴ Boverhof D.R., Bramante C.M., Butala J.H., Clancy S.F., Lafranconi M., West J., Gordon S.C. 2015. Comparative assessment of nanomaterial definitions and safety evaluation considerations. *Regulatory Toxicology and Pharmacology* 73: 137-150.
- ∴ Buffet P.E., Pan J.F., Poirier L., Amiard-Triquet C., Amiard J.C., Gaudin P., Risso. De Faverney C., Guibbolini M., Gilliland D., Valsami-Jones E. and Mouneyrac C. 2013. Biochemical and behavioural responses of the endobenthic bivalve *Scrobicularia plana* to silver nanoparticles in seawater and microalgal food. *Ecotoxicology and Environmental Safety* 89: 117-124.
- ∴ Buffet P.E., Zalouk-Vergnoux A., Châtel A., Berthet B., Métails I., Perrein-Ettajani H., Poirier L., Luna-Acosta A., Thomas-Guyon H., Risso-de Faverney C., Guibbolini M., Gilliland D., Valsami-Jones E., Mouneyrac C. 2014. A marine mesocosm study on the environmental fate of silver nanoparticles and toxicity effects on two endobenthic species: The ragworm *Hediste diversicolor* and the bivalve mollusc *Scrobicularia plana*. *Science of the Total Environment* 470-471: 1151-1159.
- ∴ Bundschuh M., Filser J., Lüderwald S., McKee M.S., Metreveli G., Schaumann G.E., Schulz R., Wagner S. 2018. Nanoparticles in the environment: where do we come from, where do we go to? *Environmental Science Europe* 30: 6-22.

- ∴ Burić P., Jakšić Ž., Štajner L., Dutour Sikirić M., Jurašin D., Cascio C3, Calzolari L., Lyons D.M. 2015. Effect of silver nanoparticles on Mediterranean sea urchin embryonal development is species specific and depends on moment of first exposure. *Marine Environmental Research* 111: 50-59.
- ∴ Caballero-Guzmán A., Nowack B. 2016. A critical review of engineered nanomaterial release data: Are current data useful for material flow modeling? *Environmental Pollution* 213: 502-517.
- ∴ Cajaraville M.P., Pal S.G. 1995. Morphofunctional study of the haemocytes of the bivalve mollusc *Mytilus galloprovincialis* with emphasis on the endolysosomal compartment. *Cell Structure and Function* 20: 355-367.
- ∴ Cajaraville M.P., Robledo Y., Etxebarria M., Marigómez I. 1995. Cellular biomarkers as useful tools in the biological monitoring of environmental pollution: molluscan digestive lysosomes. In: *Cell Biology in Environmental Toxicology*. Cajaraville M.P. (Ed.), University of the Basque Country Press Service, Bilbao, pp. 29-55.
- ∴ Cajaraville M.P., Bebianno M.J., Blasco J., Porte C., Sarasquete C., Viarengo A. 2000. The use of biomarkers to assess the impact of pollution in coastal environments of the Iberian Peninsula: a practical approach. *The Science of the Total Environment* 247: 295-311.
- ∴ Cancio I., Ibabe A., Cajaraville M.P. 1999. Seasonal variation of peroxisomal enzyme activities and peroxisomal structure in mussels *Mytilus galloprovincialis* and its relationship with the lipid content. *Comparative Biochemistry and Physiology, Part C* 123: 135-144.
- ∴ Canesi L., Borghi C., Ciacci C., Fabbri R., Lorusso L.C., Vergani L., Marcomini A., Poiana G. 2008. Short-term effects of environmentally relevant concentrations of EDC mixtures on *Mytilus galloprovincialis* digestive gland. *Aquatic Toxicology* 87: 272-279.
- ∴ Canesi L., Barmo C., Fabbri R., Ciacci C., Vergani L., Roch P., Gallo G. 2010. *In vitro* effects of suspensions of selected nanoparticles (C60 fullerene, TiO₂, SiO₂) on *Mytilus* hemocytes. *Aquatic Toxicology* 96: 151-158.
- ∴ Canesi L., Ciacci C., Fabbri R., Marcomini A., Pojana G. and Gallo G. 2012. Bivalve molluscs as a unique target group for nanoparticle toxicity. *Marine Environmental Research* 76: 16-21.
- ∴ Canesi L., Frenzilli G., Balbi T., Bernardeschi M., Ciacci C., Corsolini S., Della Torre C., Fabbri R., Faleri C., Focardi S., Guidi P., Kočan A., Marcomini A., Mariottini M., Nigro M., Pozo-Gallardo K., Rocco L., Scarcelli V., Smerilli A., Corsi I. 2014. Interactive effects of n-TiO₂ and 2,3,7,8-TCDD on the marine bivalve *Mytilus galloprovincialis*. *Aquatic Toxicology* 153: 53-65.
- ∴ Canesi L., Corsi I. 2016. Effects of nanomaterials on marine invertebrates. *Science of the Total Environment* 565: 933-940.
- ∴ Canesi L., Balbi T., Fabbri R., Salis A., Damonte G., Volland M., Blasco J. 2017. Biomolecular coronas in invertebrate species: Implications in the environmental impact of nanoparticles. *NanoImpact* 8: 89-98.
- ∴ Canton I., Battaglia G. 2012. Endocytosis at the nanoscale. *Chemical Society Reviews* 41: 2718-2739.

- ∴ Ciacci C., Canonico B., Bilaničová D., Fabbri R., Cortese K., Gallo G., Marcomini A., Pojana G., Canesi L. 2012. Immunomodulation by different types of N-oxides in the hemocytes of the marine bivalve *Mytilus galloprovincialis*. PLoS ONE 7 (5): e36937. doi:10.1371/journal.pone.0036937
- ∴ Colvin V.L. 2003. The potential environmental impact of engineered nanomaterials. Nature Biotechnology 21: 1166-1170.
- ∴ Cong Y., Banta G.T., Selck H., Berhanu D., Valsami-Jones E., Forbes V.E. 2011. Toxic effects and bioaccumulation of nano-, micron- and ionic-Ag in the polychaete, *Nereis diversicolor*. Aquatic Toxicology 105: 403-411.
- ∴ Corsi I., Cherr G.N., Lenihan H.S., Labille J., Hasselov M., Canesi L., Dondero F., Frenzilli G., Hristozov D., Puntès V., Della Torre C., Pinsino A., Libralato G., Marcomini A., Sabbioni E., Matranga V. 2014. Common strategies and technologies for the ecosafety assessment and design of nanomaterials entering the marine environment. ACS Nano 8: 9694-9709.
- ∴ Dagnino A., Allen J.I., Moore M.N., Broeg K., Canes L., Viarengo A. 2007. Development of an expert system for the integration of biomarker responses in mussels into an animal health index. Biomarkers 12: 155-172.
- ∴ Devi G.P., Ahmed K.B., Varsha M.K., Shrijha B.S., Lal K.K., Anbazhagan V., Thiagarajan R. 2015. Sulfidation of silver nanoparticle reduces its toxicity in zebrafish. Aquatic Toxicology 158: 149-156.
- ∴ Dondero F., Dagnino A., Jonsson H., Capri F., Gastaldi L., Viarengo A. 2006. Assessing the occurrence of a stress syndrome in mussels (*Mytilus edulis*) using a combined biomarker/gene expression approach. Aquatic Toxicology 78: 13-24.
- ∴ Dumont E., Johnson A.C., Keller V.D.J., Williams R.J. 2015. Nano silver and nano zinc-oxide in surface waters-Exposure estimation for Europe at high spatial and temporal resolution. Environmental Pollution 196: 341-349.
- ∴ El Badawy A.M., Luxton T.P., Silva R.G., Scheckel K.G., Suidan M.T., Tolaymat T.M. 2010. Impact of environmental condition (pH, ionic strength and electrolyte type) on the surface charge and aggregation of silver nanoparticles suspensions. Environmental Science and Technology 44: 1260-1266.
- ∴ Environmental Protection Agency (EPA). 2017. Technical Fact Sheet-Nanomaterials. Office of Land and Emergency Management (5106P), EPA 505-F-17-002.
- ∴ European Commission Research. 2011. Communication from the Commission to the European Parliament, the Council and the European Economic and Social Committee. Second Regulatory Review on Nanomaterials COM (2012)572, Brussels.
- ∴ Fabrega J., Luoma S.N., Tyler C.R., Galloway T.S., Lead J.R. 2011. Silver nanoparticles: Behaviour and effects in the aquatic environment. Environment International 37: 517-531.
- ∴ Farmen E., Mikkelsen H.N., Evensen O., Einset J., Heier L.S., Rosseland B.O., Salbu B., Tollefsen K.E., Oughton D.H. 2012. Acute and sub-lethal effects in juvenile Atlantic salmon exposed to low µg/L concentrations of Ag nanoparticles. Aquatic Toxicology 108: 78-84.

- ∴ Farrington J.W., Tripp B.W., Tanabe S., Subramanian A., Sericano J.L., Wade T.L., Knap A.H. 2016. Edward D. Goldberg's proposal of "the Mussel Watch": Reflections after 40 years. *Marine Pollution Bulletin* 110: 501-510.
- ∴ Fu P.P., Xia Q., Hwang H.M., Ray P.C., Yu H. 2014. Mechanisms of nanotoxicity: generation of reactive oxygen species. *Journal of Food and Drug Analysis* 22: 64-75.
- ∴ Fubini B., Fenoglio I., Tomatis M., Turci F. 2011. Effect of chemical composition and state of the surface on the toxic response to high aspect ratio nanomaterials. *Nanomedicine (London, England)* 6: 899-920.
- ∴ Gambardella C., Aluigi M.G., Ferrando S., Gallus L., Ramoino P., Gatti A.M., Rottigni M., Falugi C. 2013. Developmental abnormalities and changes in cholinesterase activity in sea urchin embryos and larvae from sperm exposed to engineered nanoparticles. *Aquatic Toxicology* 130-131: 77-85.
- ∴ Gambardella C., Costa E., Piazza V., Fabbrocini A., Magi E., Faimali M., Garaventa F. 2015. Effect of silver nanoparticles on marine organisms belonging to different trophic levels. *Marine Environmental Research* 111: 41-49.
- ∴ García-Alonso J., Rodríguez-Sánchez N., Misra S.K., Valsami-Jones E., Croteau M.N., Luoma S.N., Rainbow P.S. 2014. Toxicity and accumulation of silver nanoparticles during development of the marine polychaete *Platynereis dumerilii*. *Science of the Total Environment* 476-477: 688-695.
- ∴ Garmendia L., Soto M., Vicario U., Kim Y., Cajaraville M.P., Marigómez I. 2011. Application of a battery of biomarkers in mussel digestive gland to assess long-term effects of the Prestige oil spill in Galicia and Bay of Biscay: tissue-level biomarkers and histopathology. *Journal of Environmental Monitoring* 13: 915-932.
- ∴ Garner K.L., Keller A.A. 2014. Emerging patterns for engineered nanomaterials in the environment: a review of fate and toxicity studies. *Journal of Nanoparticle Research* 16: 2503-2530.
- ∴ Geranio L., Heuberger M., Nowack B., 2009. The behavior of silver nanotextiles during washing. *Environmental Science and Technology* 43: 8113-8118.
- ∴ Giese A.C., Pearse J.S., 1974. *Reproduction of Marine Invertebrates*. Academic Press, New York. pp. 546.
- ∴ Giese B., Klaessig F., Park B., Kaegi R., Steinfeldt M., Wigger H., von Gleich A., Gottschalk F. 2018. Risks, release and concentrations of engineered nanomaterials in the environment. *Scientific Reports* 8: doi: 10.1038/s41598-018-19275-4
- ∴ Goldberg E.D. 1975. The Mussel Watch-A first step in global marine monitoring. *Marine Pollution Bulletin* 6: 111.
- ∴ Goldberg E.D. 1986. The Mussel Watch Concept. *Environmental Monitoring and Assessment* 7: 91-103.
- ∴ Gomes T., Pinheiro J.P., Cancio I., Pereira C.G., Cardos, C., Bebianno M.J. 2011. Effects of copper nanoparticles exposure in the mussel *Mytilus galloprovincialis*. *Environmental Science and Technology* 45: 9356-9362.

- .: Gomes T., Pereira C.G., Cardoso C., Pinheiro J.P., Cancio I., Bebianno M.J. 2012. Accumulation and toxicity of copper oxide nanoparticles in the digestive gland of *Mytilus galloprovincialis*. *Aquatic Toxicology* 118-119: 72-79.
- .: Gomes T., Pereira C.G., Cardoso C., Bebianno M.J. 2013a. Differential protein expression in mussels *Mytilus galloprovincialis* exposed to nano and ionic Ag. *Aquatic Toxicology* 136-137: 79-90.
- .: Gomes T., Araújo O., Pereira R., Almeida A.C., Cravo A., Bebianno M.J. 2013b. Genotoxicity of copper oxide and silver nanoparticles in the mussel *Mytilus galloprovincialis*. *Marine Environmental Research* 84: 51-59.
- .: Gomes T., Pereira C.G., Cardoso C., Sousa V.S., Ribau Teixeira M., Pinheiro J.P., Bebianno M.J. 2014a. Effects of silver nanoparticles exposure in the mussel *Mytilus galloprovincialis*. *Marine Environmental Research* 101: 208-214.
- .: Gomes T., Chora S., Pereira C.G., Cardoso C., Bebianno M.J. 2014b. Proteomic response of mussels *Mytilus galloprovincialis* exposed to CuO NPs and Cu²⁺: An exploratory biomarker discovery. *Aquatic Toxicology* 155: 327-336.
- .: González-Fernández C., Albentosa M., Campillo J.A., Viñas L., Franco A., Beiras J. 2016. Effect of mussel reproductive status on biomarker responses to PAHs: Implications for large-scale monitoring programs. *Aquatic Toxicology* 177: 380-394.
- .: Gosling E. 2015. *Marine Bivalve Molluscs*. 2nd Edition. John Wiley & Sons, West Sussex, UK. pp. 536.
- .: Gottschalk F., Sonderer T., Scholz R.W., Nowack B. 2009. Modeled environmental concentrations of engineered nanomaterials (TiO₂, ZnO, Ag, CNT, fullerenes) for different regions. *Environmental Science and Technology* 43: 9216-9222.
- .: Gottschalk F., Nowack B. 2011. The release of engineered nanomaterials to the environment. *Journal of Environmental Monitoring* 13: 1145-1155.
- .: Griffitt R.J., Luo J., Gao J., Bonzongo J.C., Barber D.S. 2008. Effects of particle composition and species on toxicity of metallic nanomaterials in aquatic organisms. *Environmental Toxicology and Chemistry* 27: 1972-1978.
- .: Griffitt, R.J., Hyndman, K., Denslow, N.D., Barber, D.S., 2009. Comparison of molecular and histological changes in zebrafish gills exposed to metallic nanoparticles. *Toxicological Science* 107: 404-415.
- .: Griffitt R.J., Lavele C.M., Kane A.S., Denslow N.D., Barber D.S. 2013. Chronic nanoparticulate silver exposure results in tissue accumulation and transcriptomic changes in zebrafish. *Aquatic Toxicology* 130-131: 192-200.
- .: Hagger J.A., Lowe D., Dissanayake A., Jones M.B. 2010. The influence of seasonality on biomarker responses in *Mytilus edulis*. *Ecotoxicology* 19: 953-962.
- .: Hansen S.F., Heggelund L.R., Besora P.R., Mackevica A., Boldrin A., Baun A. 2016. Nanoproducts-what is actually available to European consumers? *Environ Science: Nano* 3: 169-180.
- .: Harper S., Maddux B.L.S., Hutchison J.E., Usenko C., Tanguay R. 2007. Biodistribution and toxicity of nanomaterials *in vivo*: effects of composition, size, surface functionalization and

- route of exposure. In: Technical Proceedings of the 2007 NSTI Nanotechnology Conference and Trade Show, vol. 2, pp. 666-669.
- ∴ His E., Beiras R., Seaman M.N.L. 1999. The assessment of marine pollution-bioassays with bivalve embryos and larvae. *Advances in Marine Biology* vol. 37. ISBN 0-12-026137-5.
 - ∴ Hook S.E., Gallagher E.P., Batley G.E. 2014. The Role of Biomarkers in the Assessment of Aquatic Ecosystem Health. *Integrated Environmental Assessment and Management* 10: 327-341.
 - ∴ Hu W., Culloty S., Darmody G., Lynch S., Davenport J., Ramirez-Garcia S., Dawson K.A., Lynch I., Blasco J., Sheehan D. 2014. Toxicity of copper oxide nanoparticles in the blue mussel, *Mytilus edulis*: a redox proteomic investigation. *Chemosphere* 108: 289-299.
 - ∴ Hylland K., Tollefsen K.E., Ruus A., Jonsson G., Sundt R.C., Sanni S., Røe Utvik T.I., Johnsen S., Nilssen I., Pinturier L., Balk L., Barsiene J., Marigómez I., Feist S.W., Børseth J.F. 2008. Water column monitoring near oil installations in the North Sea 2001-2004. *Marine Pollution Bulletin* 56: 414-429.
 - ∴ Hylland K., Ruus A., Grung M., Green N. 2009. Relationships between physiology, tissue contaminants, and biomarker responses in Atlantic cod (*Gadus morhua* L.). *Journal of Toxicology and Environmental Health, A* 72: 226-233.
 - ∴ ICES. 2016. Report of the Working Group on the Biological Effects of Contaminants (WGBEC), 9-13 March 2015, Bergen, Norway. ICES CM 2015/SSGEPI:02. pp. 66.
 - ∴ Ivask A., Kurvet I., Kasemets K., Blinov I., Aruoja V., Suppi, S., Vija H., Käkinen A., Titma T., Heinlaan M., Visnapuu M., Koller D., Kis V., Kahru A. 2014. Size-dependent toxicity of silver nanoparticles to bacteria, yeast, algae, crustaceans and mammalian cells *in vitro*. *PLoS One* 9 (7): e102108. <http://dx.doi.org/10.1371/journal.pone.0102108>.
 - ∴ Jeevanandam J., Barhoum A., Chan Y.S., Dufresne A., Danquah M.K. 2018. Review on nanoparticles and nanostructured materials: history, sources, toxicity and regulations. *Beilstein Journal of Nanotechnology* 9: 1050-1074.
 - ∴ Jimeno-Romero A., Oron M., Cajaraville M.P., Soto M., Marigómez I. 2016. Nanoparticle size and combined toxicity of TiO₂ and DSLS (surfactant) contribute to lysosomal responses in digestive cells of mussels exposed to TiO₂ nanoparticles. *Nanotoxicology* 10: 1168-1176.
 - ∴ Jimeno-Romero A., Izagirre U., Gilliland D., Warley A., Cajaraville M.P., Marigómez I., Soto M. 2017a. Lysosomal responses to different gold forms (nanoparticles, aqueous, bulk) in mussel digestive cells: a trade-off between the toxicity of the capping agent and form, size and exposure concentration. *Nanotoxicology* 11: 658-670.
 - ∴ Jimeno-Romero A., Bilbao E., Izagirre U., Cajaraville M.P., Marigómez I., Soto M. 2017b. Digestive cell lysosomes as main targets for Ag accumulation and toxicity in marine mussels, *Mytilus galloprovincialis*, exposed to maltose-stabilized Ag nanoparticles of different sizes. *Nanotoxicology* 11: 168-183.
 - ∴ Jimeno-Romero A., Bilbao E., Valsami-Jones E., Cajaraville M.P., Soto M., Marigómez I. 2019. Bioaccumulation, tissue and cell distribution, biomarkers and toxicopathic effects of CdS quantum dots in mussels, *Mytilus galloprovincialis*. *Ecotoxicology and Environmental Safety* 167: 288-300.

- ∴ Kadar E., Lowe D.M., Solé M., Fisher A.S., Jha A., Readman J.W., Hutchinson T.H. 2010. Uptake and biological responses to nano-Fe versus soluble Fe-Cl₃ in excised mussel gills. *Analytical and Bioanalytical Chemistry* 396: 657-666.
- ∴ Kadar E., Dyson O., Handy R.D., Al-Subiai S.N. 2013. Are reproduction impairments of free spawning marine invertebrates exposed to zero-valent nano-iron associated with dissolution of nanoparticles? *Nanotoxicology* 7: 135-143.
- ∴ Kafshgari M.H., Harding F.J., Voelcker N.H. 2015. Insights into cellular uptake of nanoparticles. *Current Drug Delivery* 12: 63-77.
- ∴ Kahru A., Dubourguier H.C., Blinova I., Ivask A., Kasemets K. 2008. Biotests and Biosensors for Ecotoxicology of Metal Oxide Nanoparticles: A Minireview. *Sensors* 8: 5153-5170.
- ∴ Katsumiti A., Gilliland D., Arostegui I., Cajaraville M.P. 2014. Cytotoxicity and cellular mechanisms involved in the toxicity of CdS quantum dots in hemocytes and gill cells of the mussel *Mytilus galloprovincialis*. *Aquatic Toxicology* 153: 39-52.
- ∴ Katsumiti A., Berhanu D., Howard K.T., Arostegui I., Oron M., Reip P., Valsami-Jones E., Cajaraville M.P. 2015a. Cytotoxicity of TiO₂ nanoparticles to mussel hemocytes and gill cells *in vitro*: influence of synthesis method, crystalline structure, size and additive. *Nanotoxicology* 9: 543-553.
- ∴ Katsumiti A., Gilliland D., Arostegui I., Cajaraville M.P. 2015b. Mechanisms of toxicity of Ag nanoparticles in comparison to bulk and ionic Ag on mussel hemocytes and gill cells. *PLoS ONE* 10 (6): e0129039. doi:10.1371/journal.pone.0129039.
- ∴ Katsumiti A., Arostegui I., Oron M., Gilliland D., Valsami-Jones E., Cajaraville M.P. 2016. Cytotoxicity of Au, ZnO and SiO₂ NPs using *in vitro* assays with mussels hemocytes and gill cells: Relevance of size, shape and additives. *Nanotoxicology* 10: 185-193.
- ∴ Katsumiti A., Thorley A.J., Arostegui I., Reip P., Valsami-Jones E., Tetley T.D., Cajaraville M.P. 2018. Cytotoxicity and cellular mechanisms of toxicity of CuO NPs in mussel cells *in vitro* and comparative sensitivity with human cells. *Toxicology In Vitro* 48: 146-158.
- ∴ Katsumiti A., Cajaraville M.P. 2019. *In vitro* toxicity testing with bivalve molluscs and fish cells for the risk assessment of nanoparticles in the aquatic environment. In: Corsi I., Blasco J. (Eds.) *Ecotoxicology of nanoparticles in aquatic systems*. CRC Press Taylor & Francis Group. pp. 62-98.
- ∴ Klaine J.K., Alvarez P.J.J., Batley G.E., Fernandes T.F., Handy R.D., Lyon D.Y., Mahendra S., McLaughlin M.J., Lead, J.R. 2008. Nanomaterials in the environment: behaviour, fate, bioavailability and effects. *Environmental Toxicology and Chemistry* 27: 1825-1851.
- ∴ Klaine S.J., Koelmans A.A., Horne N., Carley S., Handy R.D., Kapustka L., Nowack B., Von der Kammer F. 2012. Paradigms to assess the environmental impact of manufactured nanomaterials. *Environmental Toxicology and Chemistry* 31: 3-14.
- ∴ Kreeger D.A., Newell R.I. 2001. Seasonal utilization of different seston carbon sources by the ribbed mussel, *Geukensia demissa* (Dillwyn) in a mid-Atlantic salt marsh. *Journal of Experimental Marine Biology and Ecology* 260: 71-91.

- .: Kumar N., Ray S. S. 2018. Synthesis and Functionalization of Nanomaterials. In: Sinha Ray S. (Eds.) Processing of Polymer-based Nanocomposites. Springer Series in Materials Science, vol 277. Springer, pp. 15-55.
- .: Lacave J.M., Retuerto A., Vicario-Parés U., Gilliland D., Oron M., Cajaraville M.P., Orbea A. 2016. Effects of metal-bearing nanoparticles (Ag, Au, CdS, ZnO, SiO₂) on developing zebrafish embryos. *Nanotechnology* 27: 325102. doi: 10.1088/0957-4484/27/32/325102.
- .: Lacave J.M., Fanjul A., Bilbao E., Gutierrez N., Barrio I., Arostegui I., Cajaraville M.P., Orbea A. 2017. Acute toxicity, bioaccumulation and effects of dietary transfer of silver from brine shrimp exposed to PVP/PEI coated silver nanoparticles to zebrafish. *Comparative Biochemistry and Physiology, Part C* 199: 69-80.
- .: Lacave J.M., Vicario-Parés U., Bilbao E., Gilliland D., Mura F., Dini L., Cajaraville M.P., Orbea A. 2018. Waterborne exposure of adult zebrafish to silver nanoparticles and to ionic silver results in differential silver accumulation and effects at cellular and molecular levels. *Science of the Total Environment* 642: 1209-1220.
- .: Lapresta-Fernández A., Fernández A., Blasco J. 2012. Nanoecotoxicity effects of engineered silver and gold nanoparticles in aquatic organisms. *Trends in Analytical Chemistry* 32: 40-59.
- .: Larginho M., Correia D., Diniz M.S., Baptista P.V. 2014. Evidence of one-way flow bioaccumulation of gold nanoparticles across two trophic levels. *Journal of Nanoparticle Research* 16: 2549-2559.
- .: Lee J.W., Won E.J., Raisuddin S., Lee J.S. 2015. Significance of adverse outcome pathways in biomarker-based environmental risk assessment in aquatic organisms. *Journal of Environmental Science* 35: 115-127.
- .: Lei C., Sun Y., Tsang D.C.W., Lin D. 2018. Environmental transformations and ecological effects of iron-based nanoparticles. *Environmental Pollution* 232: 10-30.
- .: Leiniö S., Lehtonen K. 2005. Seasonal variability in biomarkers in the bivalves *Mytilus edulis* and *Macoma balthica* from the northern Baltic Sea. *Comparative Biochemistry and Physiology, Part C* 140: 408-421.
- .: Lekube X., Izagirre U., Soto M., Marigómez I. 2014. Lysosomal and tissue-level biomarkers in mussels cross-transplanted among four estuaries with different pollution levels. *Science of the Total Environment* 472: 36-48.
- .: Levard C., Hotze E.M., Lowry G.V., Brown Jr. G.E. 2012. Environmental transformations of silver nanoparticles: impact on stability and toxicity. *Environmental Science and Technology* 46: 6900-6914.
- .: Li Y., Zhang W., Niu J., Chen Y. 2013. Surface-coating-dependent dissolution, aggregation, and reactive oxygen species (ROS) generation of silver nanoparticles under different irradiation conditions. *Environmental Science and Technology* 47: 10293-10301.
- .: Li L., Stoiber M., Wimmer A., Xu Z., Lindenblatt C., Helmreich B., Schuster M. 2016. To what extent can full-scale wastewater treatment plant effluent influence the occurrence of silver-based nanoparticles in surface waters? *Environmental Science and Technology* 50: 6327-6333.
- .: Libralato G. 2014. The case of *Artemia* spp. in nanoecotoxicology. *Marine Environmental Research* 101: 38-43.

- ∴ Magesky A., Ribeiro C.A., Pelletier É. 2016. Physiological effects and cellular responses of metamorphic larvae and juveniles of sea urchin exposed to ionic and nanoparticulate silver. *Aquatic Toxicology* 174: 208-227.
- ∴ Magesky A., Pelletier E. 2018. Cytotoxicity and physiological effects of silver nanoparticles on marine invertebrates, In: Saquib Q., Faisal M., Al-Khedhairi A.A., Alatar A.A. (Eds.), *Cellular and Molecular Toxicology of Nanoparticles*. Springer International Publishing, pp. 285-309.
- ∴ Marigómez i., Soto M., Orbea A., Cancio I., Cajaraville M.P., 2004. Chapter 14: Biomonitoring of environmental pollution in the Basque coast using molecular, cellular and tissue-level biomarkers: an integrative approach. In: Borja A., Collins M. (Eds.), *Oceanography and marine environment of the Basque Country*. Elsevier Oceanography Series nº 70, Elsevier, Amsterdam, pp. 335-364.
- ∴ Marigómez I., Garmendia L., Soto M., Orbea A., Izagirre U., Cajaraville M.P. 2013. Marine ecosystem health status assessment through integrative biomarker indices: a comparative study after the Prestige oil spill "Mussel Watch". *Ecotoxicology* 22: 486-505.
- ∴ Massarsky A., Trudeau V.L., Moon T.W. 2014. Predicting the environmental impact of nanosilver. *Environmental Toxicology and Pharmacology* 38: 861-873.
- ∴ Matranga V., Corsi I. 2012. Toxic effects of engineered nanoparticles in the marine environment: Model organisms and molecular approaches. *Marine Environmental Research* 76: 32-40.
- ∴ McCarthy J.F., Shugart L.R. 1990. Biological Markers of Environmental Contamination. In: McCarthy J.F. and Shugart L.R. (Eds.), *Biomarkers of Environmental Contamination*, Lewis Publishers, Boca Raton: 3-14.
- ∴ McCarthy M., Carroll D.L., Ringwood A.H. 2013. Tissue specific response of oysters, *Crassostrea virginica*, to silver nanoparticles. *Aquatic Toxicology* 138-139: 123-128.
- ∴ McGuillicuddy E., Murray I., Kavanagh S., Morrison L., Fogarty A., Cormican M., Dockery P., Prendergast M., Rowan N., Morris D. 2017. Silver nanoparticles in the environment: sources, detection and ecotoxicology. *Science of the Total Environment* 575: 231-246.
- ∴ Misra S.K., Dybowska A., Berhanu D., Luoma S.N., Valasmi-Jones E. 2012. The complexity of nanoparticle dissolution and its importance in nanotoxicological studies. *Science of the Total Environment* 438: 225-232.
- ∴ Misra S.K., Nuseibeh S., Dybowska A., Berhanu D., Tetley T.D., Valsami-Jones E. 2013. The effect of nanoparticle morphology on dispersion stability, dissolution and toxicity: Comparative study using spheres, rods and spindle-shaped nanoplatelets on dispersion stability, dissolution and toxicity of CuO nanomaterials. *Nanotoxicology*: doi:10.3109/17435390.2013.796017.
- ∴ Mitrano D.M., Rimmele E., Wichser A., Erni R., Height M., Nowack B. 2014. Presence of nanoparticles in wash water from conventional silver and nano-silver textiles. *ACS Nano* 8: 7208-7219.
- ∴ Moore M.N. 2006. Do nanoparticles present ecotoxicological risks for the health of the aquatic environment? *Environment International* 32: 967-976.
- ∴ Moreno-Garrido I., Pérez S., Blasco J. 2015. Toxicity of silver and gold nanoparticles on marine microalgae. *Marine Environmental Research* 111: 60-73.

- ∴ Mudunkotuwa I.A., Grassian V.H. 2011. The devil is in the details (or the surface): impact of surface structure and surface energetics on understanding the behaviour of nanomaterials in the environment. *Journal of Environmental Monitoring* 13: 1315-1144.
- ∴ Nahrgang J., Brooks S.J., Evenset A., Camus L., Jonsson M., Smith T.J., Lukina J., Frantzen M., Giarratano E., Renaud P.E. 2013. Seasonal variation in biomarkers in blue mussel (*Mytilus edulis*), Icelandic scallop (*Chlamys islandica*) and Atlantic cod (*Gadus morhua*): implications for environmental monitoring in the Barents Sea. *Aquatic Toxicology* 127: 21-35.
- ∴ Navarro E., Baun A., Behra R., Hartmann N.B., Filser J., Miao A.J., Quigg A., Santschi P.H., Sigg L. 2008a. Environmental behavior and ecotoxicity of engineered nanoparticles to algae, plants, and fungi. *Ecotoxicology* 17: 372-386.
- ∴ Navarro E., Piccapietra F., Wagner B., Marconi F., Kaegi R., Odzak N., Sigg L., Behra R. 2008b. Toxicity of silver nanoparticles to *Chlamydomonas reinhardtii*. *Environmental Science and Technology* 42: 8959-8964.
- ∴ Nel A., Xia T., Mädler L., Li, N. 2006. Toxic Potential of Materials at the Nanolevel. *Science* 311: 622-627.
- ∴ Newell R.I.E. 1989. Species profiles: life histories and environmental requirements of coastal fishes and invertebrates (North and Mid-Atlantic)-blue mussel. US Fish Wildlife Service for Biology and Reproduction 82 (11.102). US Army Corps of Engineers, TR EL 82-4.
- ∴ Nowack B., Bucheli T.D. 2007. Occurrence, behavior and effects of nanoparticles in the environment. *Environmental Pollution* 150: 5-22.
- ∴ Nowack B., Krug H.F., Height M., 2011. 120 years of nanosilver history: implications for policy makers. *Environmental Science and Technology* 45: 1177-1183.
- ∴ Oberdörster G., Oberdörster E., Oberdörster J. 2005. Nanotoxicology: an emerging discipline evolving from studies of ultrafine particles. *Environmental Health Perspectives* 113: 823-839.
- ∴ Odzak N., Kistler D., Behra R., Sigg L. 2014. Dissolution of metal and metal oxide nanoparticles in aqueous media. *Environmental Pollution* 191: 132-138.
- ∴ Okumuş I., Stirling H.P. 1998. Seasonal variations in the meat weight, condition index and biochemical composition of mussels (*Mytilus edulis* L.) in suspended culture in two Scottish sea lochs. *Aquaculture* 159: 249-261.
- ∴ Orbea A., Marigómez I., Fernández C., Tarazona J.V., Cancio I., Cajaraville M.P. 1999. Structure of peroxisomes and activity of the marker enzyme catalase in digestive epithelial cells in relation to PAH content of mussels from two Basque estuaries (Bay of Biscay): seasonal and site-specific variations. *Archives of Environmental Contamination and Toxicology* 36: 158-166.
- ∴ Orbea A., González-Soto N., Lacave J.M., Barrio I., Cajaraville M.P. 2017. Developmental and reproductive toxicity of PVP/PEI-coated silver nanoparticles to zebrafish. *Comparative Biochemistry and Physiology, Part C* 199: 59-68.
- ∴ Ortiz-Zarragoitia M., Garmendia L., Barbero M.C., Serrano T., Marigómez I., Cajaraville M.P. 2011. Effects of the fuel oil spilled by the Prestige tanker on reproduction parameters of wild mussel populations. *Journal of Environmental Monitoring* 13: 84-94.

- ∴ Oukarroum A., Polchtchikov S., Perreault F., Popovic R., 2012. Temperature influence on silver nanoparticles inhibitory effect on photosystem II photochemistry in two green algae, *Chlorella vulgaris* and *Dunaliella tertiolecta*. *Environmental Science Pollution Research* 9: 1755-1762.
- ∴ Pales-Espinosa E., Perrigault M., Ward J.E., Shumway S.E., Allam B. 2009. Lectins associated with the feeding organs of the oyster *Crassostrea virginica* can mediate particle selection. *The Biological Bulletin* 217: 130-141.
- ∴ Pales-Espinosa E., Perrigault M., Ward J.E., Shumway S.E., Allam B. 2010. Microalgal cell surface carbohydrates as recognition sites for particle sorting in suspension-feeding bivalves. *The Biological Bulletin* 218: 75-86.
- ∴ Peralta-Videa J.R., Zhao L., Lopez-Moreno M.L., de la Rosa G., Hong J., Gardea-Torresdey J.L. 2011. Nanomaterials and the environment: a review for the biennium 2008-2010. *Journal for Hazardous Materials* 186: 1-15.
- ∴ Pisanelli B., Benedetti M., Fattorini D., Regoli F. 2009. Seasonal and inter-annual variability of DNA integrity in mussels *Mytilus galloprovincialis*: a possible role for natural fluctuations of trace metal concentrations and oxidative biomarkers. *Chemosphere* 77: 1551-1557.
- ∴ Ribeiro F., Gallego-Urrea J.A., Jurkschat K., Crossley A., Hassellöv M., Taylor C., Soares A.M., Loureiro S. 2014. Silver nanoparticles and silver nitrate induce high toxicity to *Pseudokirchneriella subcapitata*, *Daphnia magna* and *Danio rerio*. *Science of the Total Environment* 466-467: 232-241.
- ∴ Ringwood A.H., McCarthy M., Bates T.C., Carrol D.L. 2010. The effects of silver nanoparticles on oyster embryos. *Marine Environmental Research* 69: S49-S51.
- ∴ Robledo Y., Madrid J.F., Leis O., Cajaraville M.P. 1997. Analysis of the distribution of glycoconjugates in the digestive gland of the bivalve mollusc *Mytilus galloprovincialis* Lmk by conventional and lectin histochemistry. *Cell and Tissue Research* 288: 501-602.
- ∴ Rocha T.L., Gomes T., Cardoso C., Letendre J., Pinheiro J.P., Sousa V.S., Teixeira M.R., Bebianno M.J. 2014. Immunocytotoxicity, cytogenotoxicity and genotoxicity of cadmium-based quantum dots in the marine mussel *Mytilus galloprovincialis*. *Marine Environmental Research* 101: 29-37.
- ∴ Rocha T.L., Gomes T., Sousa V.S., Mestre N.C., Bebianno M.J. 2015a. Ecotoxicological impact of engineered nanomaterials in bivalve molluscs: An overview. *Marine Environmental Research* 111: 74-88.
- ∴ Rocha T.L., Gomes T., Mestre N.C., Cardoso C., Bebianno M.J. 2015b. Tissue specific responses to cadmium-based quantum dots in the marine mussel *Mytilus galloprovincialis*. *Aquatic Toxicology* 69: 10-18.
- ∴ Rocha T.L., Sabóia-Morais S.M., Bebianno M.J. 2016. Histopathological assessment and inflammatory response in the digestive gland of marine mussel *Mytilus galloprovincialis* exposed to cadmium-based quantum dots. *Aquatic Toxicology* 177: 306-315.
- ∴ Royal Society and the Royal Academy of Engineering. 2004. Nanoscience and nanotechnologies: opportunities and uncertainties. Royal Society Publications, London.

- ∴ Ruiz P., Ortiz-Zarragoitia M., Orbea A., Vingen S., Hjelle A., Baussant T., Cajaraville M.P. 2014. Short- and long-term responses and recovery of mussels *Mytilus edulis* exposed to heavy fuel oil no.6 and styrene. *Ecotoxicology* 23: 861-879.
- ∴ Sakhtianchi R., Minchin R.F., Lee K.B., Alkilany A.M., Serpooshan V., Mahmoudi M. 2013. Exocytosis of nanoparticles from cells: role in cellular retention and toxicity. *Advances in Colloid and Interfaces Science* 201-202: 18-29.
- ∴ Schiavo S., Duroudier N., Bilbao E., Mikolaczyk M., Schäfer J., Cajaraville M.P., Manzo S. 2017. Effects of PVP/PEI coated and uncoated silver NPs and PVP/PEI coating agent on three species of marine microalgae. *Science of the Total Environment* 577: 45-53.
- ∴ Schirmer K., Behra R., Sigg L., Suter M.J.F. 2013. Chapter 5: Ecotoxicological aspects of nanomaterials in the aquatic environment. In: Wolfgang Luther and Axel Zweck (Eds.), *Safety Aspects of Engineered Nanomaterials*, Pan Stanford Publishing Pte. Ltd. pp. 141-162.
- ∴ Schmidt W., Power E., Quinn B. 2013. Seasonal variations of biomarker responses in the marine blue mussel (*Mytilus* spp.). *Marine Pollution Bulletin* 74: 50-55.
- ∴ Scown T.M., van Aerle R., Tyler C.R. 2010. Review: Do engineered nanoparticles pose a significant threat to the aquatic environment? *Critical Reviews in Toxicology* 40: 653-670.
- ∴ Seed R., 1973. Absolute and allometric growth in the mussel *Mytilus edulis* L. (Mollusca: Bivalvia). *Proceedings of the Malacological Society of London* 40: 343-357.
- ∴ Seed R., Suchanek T.H. 1992. Chapter 4: Population and community ecology of *Mytilus*. In: The mussel *Mytilus*. ecology, physiology, genetics and culture. Gosling E.M. (Ed.), pp. 87-169
- ∴ Sendra M., Blasco J., Araújo C.V.M. 2017. Is the cell wall of marine phytoplankton a protective barrier or a nanoparticle interaction site? Toxicological responses of *Chlorella autotrophica* and *Dunaliella salina* to Ag and CeO₂ nanoparticles. *Ecological Indicators*. <http://dx.doi.org/10.1016/j.ecolind.2017.08.050>.
- ∴ Sharma V.K., Filip J., Zboril R., Varma R.S. 2015. Natural inorganic nanoparticles-formation, fate, and toxicity in the environment. *Chemical Society Reviews* 44: 8410-8423.
- ∴ Sheehan D., Power A. 1999. Effects of seasonality on xenobiotic and antioxidant defence mechanisms of bivalve molluscs. *Comparative Biochemistry and Physiology, Part C* 123: 193-199.
- ∴ Sigg L., Behra R., Groh K., Isaacson C., Odzak N., Piccapietra F., Röhder L., Schug H., Yue Y., Schirmer K. 2014. Chemical Aspects of Nanoparticle Ecotoxicology. *Chimia* 68: 806-811.
- ∴ Sigmund G., Jiang C., Hofmann T., Chen W. 2018. Environmental transformation of natural and engineered carbon nanoparticles and implications for the fate of organic contaminants. *Environmental Science: Nano* 5: 2500-2518.
- ∴ Sikder M., Lead J.R., Chandler G.T., Baalousha M. 2017. A rapid approach for measuring silver nanoparticle concentration and dissolution in seawater by UV-Vis. *Science of the Total Environment* 618: 597-607.
- ∴ Singh N., Manshian B., Jenkins G.J., Griffiths S.M., Williams P.M., Maffei T.G., Wright C.J., Doak S.H. 2009. NanoGenotoxicology: the DNA damaging potential of engineered nanomaterials. *Biomaterials* 30: 3891-3914.

- ∴ Solé M., Porte C., Albaigés J. 1995. Seasonal variation in the mixed-function oxigenase system and antioxidant enzymes of the mussel *Mytilus galloprovincialis*. *Environmental Toxicology and Chemistry* 14: 157-164.
- ∴ Sun T.Y., Gottschalk F., Hungerbühler K., Nowack B. 2014. Comprehensive probabilistic modelling of environmental emissions of engineered nanomaterials. *Environmental Pollution* 185: 69-76.
- ∴ Tangaa S.R., Selck H., Winther-Nielsen M., Khan F.R. 2016. Trophic transfer of metal-based nanoparticles in aquatic environments: a review and recommendations for future research focus. *Environmental Science: Nano* 3: 966-981.
- ∴ Taniguchi N. 1974. On the Basic Concept of 'Nano-Technology'," Proceedings of the International Conference on Production Engineering, Part II, Tokyo.
- ∴ Tarazona J.V. 2013. Use of New Scientific Developments in Regulatory Risk Assessments: Challenges and Opportunities. *Integrated Environmental Assessment and Management* 9: e85-e91.
- ∴ Tedesco S., Doyle H., Redmond G., Sheehan D. 2008. Gold nanoparticles and oxidative stress in *Mytilus edulis*. *Marine Environmental Research* 66: 131-133
- ∴ Tedesco S., Doyle H., Blasco J., Redmond G., Sheehan D. 2010. Oxidative stress and toxicity of gold nanoparticles in *Mytilus edulis*. *Aquatic Toxicology* 100: 178-186.
- ∴ Tiede K., Hassellöv M., Breitbarth E., Chaudhry Q., Boxall A.B.A. 2009. Considerations for environmental fate and ecotoxicity testing to support environmental risk assessments for engineered nanoparticles. *Journal of Chromatography A* 1216: 503-509.
- ∴ Tourinho P.S., van Gestel C.A., Lofts S., Svendsen C., Soares A.M., Loureiro S. 2012. Metal-based nanoparticles in soil: fate, behavior, and effects on soil invertebrates. *Environmental Toxicology and Chemistry* 31: 1679-1692.
- ∴ UNEP, 2004. UNEP/MAP/MED POL: Guidelines for the development of ecological status and stress reduction indicators for the Mediterranean region. MAP Technical Reports Series No. 154, UNEP/MAP, Athens, pp. 94.
- ∴ Vance M.E., Kuiken T., Vejerano E.P., McGinnis S.P., Hochella M. F. Jr., Rejeski D., Hull M.S. 2015. Nanotechnology in the real world: Redeveloping the nanomaterial consumer products inventory. *Beilstein Journal of Nanotechnology* 6: 1769-1780.
- ∴ Viarengo A., Lowe D., Bolognesi C., Fabbri E., Koehler A. 2007. The use of biomarkers in biomonitoring: a 2-tier approach assessing the level of pollutant-induced stress syndrome in sentinel organisms. *Comparative Biochemistry and Physiology, Part C* 146: 281-300.
- ∴ Villalba A. 1995. Gametogenic cycle of cultured mussel, *Mytilus galloprovincialis*, in the bays of Galicia (N.W. Spain). *Aquaculture* 130: 269-277.
- ∴ Vinken M., Whelan M., Rogiers V. 2014. Adverse outcome pathways: hype or hope? *Archives of Toxicology* 88: 1-2.
- ∴ Von der Kammer F., Ferguson P.L., Holden P.A., Masion A., Rogers K.R., Klaine S.J., Koelmans A.A., Horne N., Unrine J.M. 2012. Analysis of engineered nanomaterials in complex matrices

- (environment and biota): general considerations and conceptual case studies. *Environmental Toxicology and Chemistry* 31: 32-49.
- ∴ Wang J., Wang W.X. 2014. Low bioavailability of silver nanoparticles presents trophic toxicity to marine medaka (*Orzyias melastigma*). *Environmental Science of Technology* 48: 8152-8161.
 - ∴ Ward J.E., Shumway S.E.. 2004. Separating the grain from the chaff: particle selection in suspension-and deposit-feeding bivalves. *Journal of Experimental Marine Biology and Ecology*. 300: 83-130.
 - ∴ Ward J.E., Kach D.J. 2009. Marine aggregates facilitate ingestion Of nanoparticles by suspension-feeding bivalves. *Marine Environmental Research* 68: 137-142.
 - ∴ Wennersten R., Fidler J., Anna S. 2008. Nanotechnology: A New Technological Revolution in the 21st Century. In: *Handbook of Perfomability Engineering*. Misra K.B. (Ed). Springer-Verlag London Limited.
 - ∴ Xia G., Liu T., Wang Z., Hou Y., Dong L., Zhu J., Qi J. 2015. The effect of silver nanoparticles on zebrafish embryonic development and toxicology. *Artificial Cells, Nanomedicine and Biotechnology* 44: 1116-1121.
 - ∴ Yang Y., Westerhoff P. 2014. Presence in, and Release of, Nanomaterials from Consumer Products. In: Capco D.G. and Cheng Y. (Eds.), *Nanomaterial. Impacts on Cell Biology and Medicine*, Springer Science+Business Media.
 - ∴ Yu S.J., Yin Y.G., Liu J.F. 2013. Silver nanoparticles in the environment. *Environmental Science: Processes & Impacts* 15: 78-92.
 - ∴ Zhang W. 2014. Nanoparticle Aggregation: Principles and Modeling. In: Capco D., Chen Y. (Eds) *Nanomaterial. Advances in Experimental Medicine and Biology*, vol 811. Springer, Dordrecht.
 - ∴ Zhang Y., Newton B., Lewis E., Fu P.P., Kafoury R., Ray P.C., Yu H. 2015. Cytotoxicity of organic surface coating agents used for nanoparticles synthesis and stability. *Toxicology In Vitro* 29: 762-768.
 - ∴ Zhang C., Hu Z., Deng B. 2016. Silver nanoparticles in aquatic environments: Physicochemical behavior and antimicrobial mechanisms. *Water Research* 88: 403-427.
 - ∴ Zhang W., Xiao B., Fang T. 2018. Chemical transformation of silver nanoparticles in aquatic environments: mechanism, morphology and toxicity. *Chemosphere* 191: 324-334.
 - ∴ Zorita I., Apraiz I., Ortiz-Zarragoitia M., Orbea A., Cancio I., Soto M., Marigómez I., Cajaraville M.P. 2007a. Assessment of biological effects of environmental pollution along the NW Mediterranean Sea using mussels as sentinel organisms. *Environmental Pollution* 148: 236-250.
 - ∴ Zorita I., Bilbao E., Schad A., Cancio I., Soto M., Cajaraville M.P. 2007b. Tissue- and cell-specific expression of metallothionein genes in cadmium- and copper-exposed mussels analyzed by in situ hybridization and RT-PCR. *Toxicology and Applied Pharmacology* 220: 1



II. STATE OF THE ART, HYPOTHESIS AND OBJECTIVES

STATE OF THE ART

In the last years, engineered nanoparticles (NPs) are being incorporated into many consumer products because they present novel physico-chemical properties in comparison to their bulk counterparts. Metal-bearing NPs are used extensively and, among them, silver NPs (Ag NPs) gained high commercial and scientific interest due to their unique optical, catalytical and antimicrobial properties. Applications for Ag NPs are increasing and thus, concerns about their potential input into aquatic ecosystems and their environmental hazards are also growing. The potential release and entry of NPs into the environment occurs directly or indirectly at any point during NPs life cycle through aerial deposition, dumping and/or run-offs and wastewater treatment plants (WWTPs), among others. In fact, concentrations ranging between 0.7 and 11.1 ng/L Ag NPs were measured in WWTPs effluents, but Ag NPs detection and quantification in complex natural matrices such as seawater, soils and sediments is still challenging. Thus, modelling studies are employed in order to estimate environmental concentrations of Ag NPs in different compartments. In general, these predicted concentrations are notably lower than the concentrations that have been used in toxicological investigations in which toxic effects of Ag NPs have been reported for a variety of organisms living in different compartments.

Mussels *Mytilus* spp. are sentinel species widely used in biomonitoring of environmental pollution programs as well as suitable model organisms for characterizing the potential impact of NPs in marine environments due to their filter-feeding behavior. NPs are trapped by gills, the first organ vulnerable to particle interactions, and then directed to the digestive gland, where NP accumulation, cellular fate and effects depend on their physico-chemical characteristics. Although biomarker responses can be influenced by confounding factors including the gamete developmental stage related to the season, the biomarker approach together with NP characterization and bioaccumulation data, represent a sensitive tool for evaluating effects and mechanisms of action of the different NPs in mussels. In this sense, the application of biomarkers after the waterborne exposure of mussels to Ag NPs revealed adverse effects such as destabilization of the lysosomal membrane in digestive tubules, induction of antioxidant enzyme activities and lipid peroxidation in the digestive gland and gills, genotoxic effects in hemocytes as well as a concentration-dependent increase in malformed D-shell larvae, among others. However, studies assessing the potential trophic transfer of Ag NPs remain scarce even if NPs may be prone to bioaccumulation and biomagnification along trophic chains.

In the last years, the application of omic's tools has arisen for the identification of molecular markers that can help to predict adverse outcome pathways at different biological levels of organization. Among them, transcriptomics and proteomics are being applied to identify molecular markers reflecting both exposure and subsequent biological effects caused by NPs in order to understand their involvement in adverse outcome pathways that are necessary for environmental risk assessment.

HYPOTHESIS

The hypothesis of the present work is that the dietary exposure of marine organisms such as *Mytilus galloprovincialis* mussels to Ag nanoparticles at relatively low concentrations, likely to appear in the environment as a result of the increasing use of this nanomaterial, could cause deleterious effects to mussels at different levels of biological organization including molecular, cellular, tissue level and transgenerational effects, and these effects could be modulated depending on the season.

OBJECTIVES

The **main objective** of the present work is to gain deeper knowledge on the molecular, cellular and tissue level responses as well as transgenerational effects of Ag NPs at doses close to environmentally relevant concentrations in the *Mytilus galloprovincialis* mussel sentinel organisms exposed through the diet at two different seasons.

This general objective has been divided into the four **specific objectives** described below which are addressed in the different chapters of the Results section:

- 1.** To characterize dissolution and aggregation behavior of Ag NPs in the exposure media and to determine Ag bioavailability as well as mussels growth, immune status, gonad condition and transgenerational effects in mussels experimentally exposed to a dose close to environmentally relevant concentrations and a higher dose of Ag NPs through the diet at two different seasons (Chapter 1).
- 2.** To assess Ag accumulation and cellular and tissue level responses using a battery of biomarkers including intralysosomal metal accumulation, lysosomal membrane stability, tissue damage and genotoxicity after the dietary exposure of mussels to a dose close to environmentally relevant concentrations and a higher dose of Ag NPs at two different seasons (Chapter 2).

- 3.** To localize Ag NPs in mussel soft tissues and to determine changes in protein expression profiles associated with the dietary exposure to Ag NPs using proteomic analyses at two different seasons (Chapter 3).
- 4.** To determine changes in gene transcription profiles in mussels dietarily exposed to a dose close to environmentally relevant concentrations and a higher dose of Ag NPs at two different seasons using transcriptomic analysis with microarrays to unveil affected biological pathways that reveal mechanisms of toxicity (Chapter 4).

Finally, all the results obtained are integrated in the General Discussion section of the thesis and an adverse outcome pathway (AOP) is proposed for Ag NPs impact in dietarily exposed mussels at different seasons.



III. RESULTS AND DISCUSSION



CHAPTER 1

Dietary exposure of mussels to PVP/PEI coated Ag nanoparticles causes Ag accumulation in adults and abnormal embryo development in their offspring

This chapter has been published as:

DUROUDIER N., KATSUMITI A., MIKOLACZYK M., SCHÄFER J., BILBAO E., CAJARAVILLE MP. 2019. Dietary exposure of mussels to PVP/PEI coated Ag nanoparticles causes Ag accumulation in adults and abnormal embryo development in their offspring. *Science of the Total Environment* 655: 48-60.

Parts of this chapter have been presented at:

26th ANNUAL MEETING OF THE SOCIETY OF ENVIRONMENTAL TOXICOLOGY AND CHEMISTRY (SETAC)-EUROPE, Nantes, 22-26 May 2016.

DUROUDIER, N; KATSUMITI, A; MIKOLACZYK, M; SCHÄFER, J; BILBAO, E; CAJARAVILLE, M.P. Dietary exposure to PVP/PEI coated Ag nanoparticles in adult mussels causes abnormal embryo development in offspring. Poster presentation.

FINAL CONFERENCE OF THE COST ACTION ES1205 "Engineered Nanomaterial from Wastewater Treatment & Stormwater to Rivers", Aveiro (Portugal), 7-8 February 2017.

DUROUDIER, N; KATSUMITI, A; MIKOLACZYK, M; CARDOSO, C; SCHÄFER, J; BEBIANNO, MJ; BILBAO, E; CAJARAVILLE, MP. Molecular and cellular effects of silver nanoparticles on adult mussels exposed through the diet and on their offspring. Platform presentation.

ABSTRACT

Toxicity of silver nanoparticles (Ag NPs) to aquatic organisms has been widely studied. However, the potential toxic effects of Ag NPs ingested through the food web, especially at environmentally relevant concentrations, as well as the potential effects on the offspring remain unknown. The aims of this work were to screen the cytotoxicity of Poly N-vinyl-2-pyrrolidone/Polyethyleneimine (PVP/PEI) coated 5 nm Ag NPs in hemocytes exposed *in vitro* and to assess the effects of dietary exposure to Ag NPs on mussels growth, immune status, gonad condition, reproductive success and offspring embryo development. For this, mussels *Mytilus galloprovincialis* were fed daily with microalgae *Isochrysis galbana* previously exposed for 24 hours to a dose close to environmentally relevant concentrations (1 µg Ag/L Ag NPs) and to a high dose of 10 µg Ag/L Ag NPs. After 24 hours of *in vitro* exposure, Ag NPs were cytotoxic to mussel hemocytes starting at 1 mgAg/L (LC50: 2.05 mgAg/L). Microalgae significantly accumulated Ag after the exposure to both doses and mussels fed for 21 days with microalgae exposed to 10 µg Ag/L Ag NPs significantly accumulated Ag in the digestive gland and gills. Sperm motility and fertilization success were not affected but exposed females released less eggs than non-exposed ones. The percentage of abnormal embryos was significantly higher than in control individuals after parental exposure to both doses. Overall, results indicate that Ag NPs taken up through the diet can significantly affect ecologically relevant endpoints such as reproduction success and embryo development in marine mussels.

Keywords: silver nanoparticles, dietary exposure, mussels *Mytilus galloprovincialis*, Ag accumulation, reproduction success, embryo development.

RESUMEN

La toxicidad de las nanopartículas de plata (NPs de Ag) ha sido ampliamente estudiada en organismos acuáticos. Sin embargo, aún se desconocen los posibles efectos tóxicos tras la ingestión de NPs de Ag a través de la dieta, especialmente a concentraciones ambientalmente relevantes, así como los posibles efectos en la descendencia. Los objetivos de este trabajo fueron testar la citotoxicidad de NPs de Ag de 5 nm recubiertas de poly N-vinyl-2-pirrolidona/polietilenemina (PVP/PEI) en hemocitos de mejillones usando ensayos *in vitro* y determinar los efectos tóxicos en el crecimiento de los mejillones, en su estado inmune, en la condición gonadal, en el éxito reproductivo y en el desarrollo de la descendencia. Para ello, se alimentaron diariamente mejillones *Mytilus galloprovincialis* con microalgas *Isochrysis galbana* previamente expuestas a una dosis cercana a una concentración ambientalmente relevante (1 µg Ag/L NPs de Ag) y a una dosis mayor de 10 µg Ag/L de NPs de Ag durante 24 horas. Tras 24 horas de exposición *in vitro*, las NPs de Ag resultaron citotóxicas para los hemocitos a partir de 1 mg Ag/L (LC50: 2.05 mg Ag/L). Las microalgas acumularon Ag significativamente tras la exposición a ambas dosis de NPs de Ag mientras que los mejillones alimentados con microalgas expuestas a 10 µg Ag/L de NPs de Ag durante 21 días acumularon Ag en la glándula digestiva y en las branquias. La motilidad de los espermatozoides y el porcentaje de éxito en la fecundación no se vieron afectados, pero las hembras expuestas liberaron menor cantidad de huevos en comparación con las no expuestas. El porcentaje de embriones con desarrollo anómalo tras la exposición de los parentales a ambas concentraciones de NPs de Ag fue significativamente mayor que los embriones descendientes de individuos no expuestos. En general, los resultados indican que la ingestión de NPs de Ag a través de la dieta puede afectar significativamente en aspectos ecológicamente relevantes como el éxito reproductivo y el desarrollo embrionario de los mejillones marinos.

Palabras clave: nanopartículas de plata, exposición vía dieta, mejillones *Mytilus galloprovincialis*, acumulación de Ag, éxito reproductivo, desarrollo embrionario.

1. INTRODUCTION

Silver NPs (Ag NPs) have gained high commercial and scientific interest due to their unique optical, catalytic and antimicrobial properties (Fabrega et al., 2011; Vance et al., 2015; Zhang et al., 2016). Currently, they are incorporated in water filters, paints, cosmetics, detergents, clothing textiles, food packaging, medical devices, and electrical appliances, among others (reviewed in McGuillicuddy et al., 2017). Since applications for Ag NPs are increasing, concerns about their potential input into aquatic ecosystems and their environmental hazards are also growing. Modeling studies estimated the concentrations of Ag NPs in aquatic environments (Blaser et al., 2008; Gottschalk et al., 2009; Tiede et al., 2009; Chio et al., 2012; Dumont et al., 2015), expecting values between 0.002 ng/L Ag NPs in European surface waters (Dumont et al., 2015) and 40 µg/L Ag NPs in effluents of Taiwanese rivers (Chio et al., 2012). Concentrations ranging between 0.7 and 11.1 ng/L Ag NPs were measured in effluents of waste water treatment plants (WWTP) over the seasons in Germany (Li et al., 2016). However, NP detection and quantification in environmental matrices such as seawater is still challenging (Sikder et al., 2017).

Toxicity of Ag NPs to different marine organisms such as microalgae (Schiavo et al., 2017), mussels (Bebiano et al., 2015; Bouallegui et al., 2017; Gomes et al., 2013a; 2013b; 2014; Jimeno-Romero et al., 2017), clams (Buffet et al., 2013; 2014), oysters (McCarthy et al., 2013; Ringwood et al., 2010) and fishes (Wang and Wang, 2014) has been recently investigated. Among these, bivalve molluscs are widely studied since they have been identified as an important target group for NP toxicity in marine environments (Moore, 2006; Canesi et al., 2012; Corsi et al., 2014). In general, most investigations in bivalves focused on understanding the effects of Ag NPs on *in vivo* waterborne exposed adult organisms (Buffet et al., 2013; 2014; Gomes et al., 2013a; 2013b; 2014; Bebianno et al., 2015; Bouallegui et al., 2017; Jimeno-Romero et al., 2017; McCarthy et al., 2013; Ringwood et al., 2010). Effects caused by Ag NPs in bivalve embryos have rarely been studied (Ringwood et al., 2010; Auguste et al., 2018). In mussels in particular, Gomes et al. (2013a) reported genotoxic effects in hemocytes and different protein expression patterns both in digestive gland and gills after the exposure to Ag NPs for 15 days. Bouallegui et al. (2017) analyzed the variations of hemocyte sub-populations after exposure of mussels to Ag NPs and Jimeno-Romero and co-authors (2017) observed that exposure of mussels to Ag NPs for 21 days destabilized the lysosomal membrane, provoked the loss of digestive cells and digestive gland integrity, as well as edema/hyperplasia in gills and hemocyte infiltration of connective tissues. However, higher level effects derived from the exposure to Ag NPs such as effects on growth,

reproduction and embryo development in mussels that could affect mussels population dynamics have not been explored yet.

Very few studies have assessed the potential toxic effects of Ag NPs ingested through the food web, especially in marine environments (Buffet et al., 2013; Wang and Wang, 2014). *Daphnia magna* fed with *Chlamydomonas reinhardtii* microalgae exposed to polymer coated 15 nm Ag NPs and silver nitrate significantly accumulated Ag and grew less than unexposed water fleas (McTeer et al., 2014). In a more complex food chain, Ag nanowires directly inhibited the growth of microalgae, destroyed the digestive organs of water fleas fed with exposed microalgae and finally were accumulated in the body of zebrafish (Chae and An, 2016). Lacave et al. (2017) also observed Ag accumulation in zebrafish after 21 days of exposure to brine shrimps (*Artemia salina*) previously exposed to PVP/PEI coated 5 nm Ag NPs. A three-day feeding exposure was enough to impair fish health as reflected by the significant reduction of lysosomal membrane stability and liver vacuolization and necrosis. In seawater, Buffet et al. (2013) compared the uptake and effects of soluble Ag and 40 nm lactate stabilized Ag NPs in *Scrobicularia plana* clams after 14 days of direct exposure through the water or the diet. Ag bioaccumulation was higher for waterborne than for dietary exposure, but the response of oxidative stress biomarkers was more marked after dietary than after waterborne exposure to both Ag forms. In a food chain consisting of brine shrimps and marine medaka *Oryzias melastigma*, Ag assimilated from brine shrimps exposed to citrate coated 20 nm Ag NPs inhibited Na^+/K^+ -ATPase and superoxide dismutase activities and reduced total body length and water content in marine medaka fed for 28 days (Wang and Wang, 2014).

The *in vivo* studies summarized above have reported several mechanisms of toxicity of Ag NPs in bivalves and other species. Additionally, *in vitro* techniques provide valuable tools to rapidly screen the toxicity of different types of NPs in a wide range of concentrations and to identify additional cellular mechanisms altered by the exposure to Ag NPs (Katsumiti et al., 2015b) or to other metallic NPs (Canesi et al., 2010; 2014; Ciacci et al., 2012; Katsumiti et al., 2014; 2016; Sendra et al., 2018; Volland et al., 2018). In mussels, hemocytes are hemolymph cells responsible for the immune defense (Cheng, 1981; Cajaraville and Pal, 1995) and constitute important targets for NP toxicity (Canesi et al., 2010; Ciacci et al., 2012; Katsumiti et al., 2014; 2015a; 2015b; 2016; 2018). These studies revealed that different NP types (fullerenes and different nanosized metals and metal oxides) are rapidly taken up by hemocytes, affecting different functional parameters, from lysosomal function to phagocytic activity and oxyradical production, and also inducing pro-apoptotic processes (Canesi and Corsi, 2016).

Thus, the aims of this work were to screen the cytotoxicity of Poly N-vinyl-2-pyrrolidone/ Polyethyleneimine (PVP/PEI) coated 5 nm Ag NPs in hemocytes exposed *in vitro* and to assess Ag accumulation pattern and effects on mussels growth, immune status, gonad condition, reproductive success and offspring embryo development after dietary exposure to the same Ag NPs. Based on estimated levels of Ag NPs in the aquatic environment, two different exposure concentrations were selected; one close to environmentally relevant concentrations of Ag NPs (1 µg/L) and a higher dose (10 µg/L). Dissolution and aggregation behavior of PVP/PEI coated Ag NPs in seawater and cell culture medium was also studied.

2. MATERIALS AND METHODS

In the present study we applied both *in vitro* and *in vivo* approaches: the *in vitro* approach to screen the cytotoxicity of PVP/PEI coated 5 nm Ag NPs in mussel hemocytes (detailed in Section 2.2), and the *in vivo* approach to assess Ag accumulation and effects on adult mussels after dietary exposure to the same Ag NPs and embryo development in their offspring (detailed in Section 2.3). The experimental design for all experiments is summarized in Figure 1.

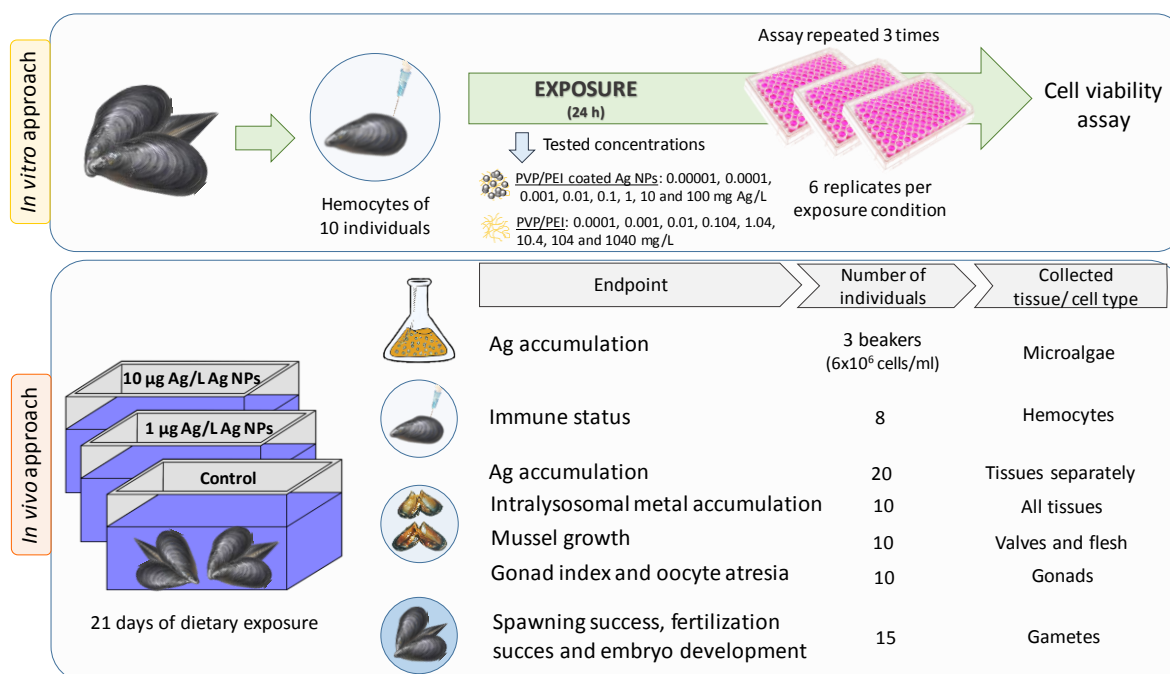


Figure 1. Schematic representation of the *in vitro* and *in vivo* approaches followed in the present study. The different endpoints, number of individuals taken per endpoint as well as the type of cell/ tissue sampled are represented.

2.1. Obtention and characterization of NPs

Stable aqueous suspensions of Ag NPs coated with PVP/PEI (77%:23% at a concentration of 104 g/L in the final dispersion) were purchased from Nanogap (O Milladoiro, Galicia, Spain). According to the manufacturers' information, PVP/PEI coated Ag NPs showed an average size of 5.08 ± 2.03 nm (see Appendix) and a zeta potential of $+18.6 \pm 7.9$ mV in distilled water.

Particle size distribution was analyzed after 24 hours at a concentration of 10 mg/L in seawater (SW) and in Basal Medium Eagle (BME; Sigma B1522; by Dynamic Light Scattering (DLS) using a Zetasizer Nano Z (Malvern Instruments Ltd., Worcestershire, UK). Three replicates of each sample were gently shaken and then measured at 20°C. Dissolution of PVP/PEI coated Ag NPs was assessed in SW after 12, 24, 48 and 72 hours and in BME after 12 and 24 hours, as described by Katsumiti et al. (2015b). Briefly, 10 mL samples of the Ag NP suspensions were prepared at a concentration of 10 mg/L and filled into dialyzer tubes (Spectra/ Por® Float-A-Lyzer; MWCO 0.1-0.5 kDa). The sample-filled dialyzers were then immersed in 1 L SW or BME. Samples (3 replicates of 1 mL) were extracted at 12, 24, 48 and 72 hours from the solution and analyzed for Ag ions using Inductively Coupled Plasma Mass Spectrometry (ICP-MS; Thermo X2 series) after 100-fold dilution using external calibration. Differences obtained for replicate samples were consistently lower than 5 % (Relative Standard Deviation; R.S.D).

2.2. Obtention of hemocytes and *in vitro* toxicity testing

2.2.1. Isolation of hemocytes

Mussels *M. galloprovincialis* (3.5–4.5 cm in shell length) were collected from Plentzia (Bizkaia, Basque Country; 43°24.90"N; 2°56.90"W). Mussels were acclimatized (0.5 l/mussel) for 2 days at 16–18°C, constant aeration and daily food supply before cell isolation. The isolation and culture of mussel hemocytes were performed as reported before (Katsumiti et al., 2018). Briefly, hemolymph from 10 animals was obtained from mussel's posterior adductor muscle under aseptic conditions in a vertical laminar airflow cabinet (Cultair BC100, Cultek S.L., Madrid, Spain) at 18°C. Hemolymph was pooled and diluted (1×10^6 cells/mL, >95 % viable according to trypan blue exclusion assay) in anti-aggregation solution (171 mM NaCl; 0.2 M Tris; 0.15% v/v HCl 1N; 24 mM EDTA). Cell suspension was seeded into 96-well microplates and centrifuged (Beckman Coulter, Palo Alto, USA) at 270 *g* for 10 minutes at 4 °C in order to favour cell attachment. Cells were kept in supplemented BME (1040 mOsm/kg, pH 7.4, 0.001% gentamicine) for 24 hours at

18°C in a Sanyo incubator (Osaka, Japan) to establish the primary cell culture before performing the exposures.

2.2.2. *In vitro* exposure

Mussel hemocytes were exposed for 24 hours to a wide range of concentrations of PVP/PEI coated 5 nm Ag NPs (0.00001, 0.0001, 0.001, 0.01, 0.1, 1, 10 and 100 mg Ag/L) in order to assess cytotoxicity through a cell viability assay. Cytotoxicity of PVP/PEI coating agent alone was also tested at the same concentrations as those present in the Ag NPs dilutions (0.0001, 0.001, 0.01, 0.104, 1.04, 10.4, 104 and 1040 mg/L). The highest concentration tested of Ag NPs (100 mg Ag/L) was directly suspended in cell culture media, vortexed and then successively diluted to obtain the range of tested concentrations. The coating agent PVP/PEI was diluted in phosphate buffered saline solution (PBS) prior to the dilution in cell culture media at tested concentrations. Six replicates of each treatment were used and the experiment was repeated three times.

2.2.3. *Cell viability assay*

The thiazolyl blue tetrazolium bromide (MTT) assay was used following Katsumiti et al. (2018) in order to avoid interference of Ag NPs with the spectrophotometric measurements. The assay relies on the capacity of actively respiring cells to convert the water-soluble MTT into a non-soluble purple formazan. Briefly, after 2.5 hours incubation of the cells with MTT solution (5 mg/mL), resulting product (formazan) was extracted from living cells with dimethyl sulphoxide (DMSO) for 1 hour. To avoid interference of Ag NPs in the assay, samples were transferred to V bottom 96-well microplates and centrifuged at 270 g for 30 min at 4°C. Supernatants were then placed in new flat bottom 96-well microplates and optical density was read at 495 nm in a Biotek EL 312 microplate spectrophotometer reader (Winooski, USA). LC50 values were calculated through Probit analysis.

2.3. Obtention and *in vivo* exposure of mussels

Mussels *M. galloprovincialis* of 3.5-4.5 cm shell length were collected in late April 2015 from Mendexa (Bizkaia, Basque Country; 43°21.39'N; 2°26.90'W). Upon arrival to the laboratory, mussels were placed in an acclimation tank (temperature =15.5°C, salinity =27.5, conductivity =45.6 mS/cm, pH =7.8 at light regime 12 h/12 h L/D) for 5 days without feeding. Then mussels were fed with *Isochrysis galbana* microalgae (20x10⁶ cells/ mussel-day) for 5 days. For that, microalgae were cultured at 20°C under

cool continuous white fluorescent light (GRO-LUX F58W) with constant aeration in reactors at a concentration of 6×10^6 cells/mL. Commercial F2 algae medium (Fritz Aquatics, USA) was supplied according to manufacturer's instructions. Before mussels feeding, concentration of microalgae was checked every day and a volume corresponding to a final dose of 20×10^6 cells/ mussel-day was added to the acclimation tank during 5 days.

After the acclimation period, mussels were distributed in three high density polypropylene containers (100 L), 100 individuals in each tank. Mussels in the control tank were fed for 21 days with the microalgae *I. galbana* (20×10^6 cells/ mussel-day). Mussels in the two treatment tanks were fed for 21 days with the same dose of microalgae *I. galbana* previously exposed for 24 hours to two different doses of PVP/PEI coated 5 nm Ag NPs: a dose of $1 \mu\text{g Ag/L}$, considered close to environmentally relevant concentrations and a higher dose of $10 \mu\text{g Ag/L}$. Water was renewed every day before animal feeding. No mortality occurred along the experimentation time.

After 21 days of exposure, 50 mussels per experimental group were dissected, hemolymph was extracted ($n=8$) and spawning was induced to analyze the different endpoints (Figure 1), as detailed below.

2.4. Bioaccumulation of Ag in algae and mussel soft tissues

2.4.1. Bioaccumulation of Ag in algae

Microalgae (6×10^6 cells/mL) were exposed in triplicate to $1 \mu\text{g Ag/L}$ and $10 \mu\text{g Ag/L}$ Ag NPs for 24 hours in beakers. After 24 hours of exposure, 3 replicates of 12 mL of suspension per beaker were filtered through preweighed poly-L-lysine coated $1.2 \mu\text{m}$ polycarbonated filter membrane (Merck Millipore). Filters were dried in an oven at 130°C for 72 hours, re-weighed and then digested with 4 mL HCl (12M, PlasmaPur) and 2.8 mL HNO_3 (14M, PlasmaPur) in closed 50 mL reactors on a heating block (DigiPREP MS; SCP Science) during 3h at 90°C . After cooling, the digestates were diluted to 30 mL with MilliQ® water, and stored cool and in the dark pending analysis by ICP-MS (Thermo X II series). Blank filters were digested in triplicate, according to the same protocol and blank values were subtracted. Results are expressed as $\mu\text{g Ag/g dw}$. Bioconcentration factor (BCF) of Ag in microalgae was calculated according to Arnot and Gobas (2006):

$$BCF = \frac{\text{Ag concentration in microalgae } (\mu\text{g/kg})}{\text{Total Ag in water } (\mu\text{g/L})} \quad (1)$$

2.4.2. *Bioaccumulation of Ag in mussel soft tissues*

Tissues (gills, digestive gland, gonad and muscle, including foot) of 20 individuals per experimental group were dissected and weighed before being pooled (4 pools of 5 aliquots of each tissue). Pooled samples were then freeze-dried (Telstar Cryodos) for 5 days. Afterwards, subsamples (20–150 mg) of milled material were mineralized using 1.4 mL of HNO₃ (14 M, PlasmaPur) and 2 mL of HCl (12 M, PlasmaPur), according to Daskalakis (1996). Briefly, samples were digested during 3 hours in closed tubes on a hot plate at 90°C (DigiPREP MS; SCP SCIENCE). After cooling, digestates were diluted and analyzed for Ag concentrations by ICP-MS (Thermo, X Series II) using external calibration (made of commercially available standard solutions PLASMACAL, SCP Science). Accuracy and precision were controlled during each analytical session by parallel analyses of international certified reference materials (TORT 2, IAEA 407), and were respectively >90% and <5% (R.S.D.). Results are expressed as µg Ag/g dw shell weight.

Then, bioaccumulation factor (BAF) for each tissue was calculated as follows (Arnot and Gobas, 2006):

$$BAF = \frac{\text{Total Ag concentration in mussel tissues } (\mu\text{g/g})}{\text{Total Ag concentration in microalgae } (\mu\text{g/g})} \quad (2)$$

2.5. **Intralyosomal metal accumulation by autometallography**

Ten mussels per experimental group were dissected, fixed in 10% neutral buffered formalin and routinely processed for paraffin embedding in a Leica Tissue processor ASP 3000 (Leica Instruments, Wetzlar, Germany). Histological cross sections (5 µm in thickness) of all tissues were cut in a Leica RM2255 microtome (Leica Instruments). Slides were then dewaxed in xylene, rehydrated through several baths of ethanol (100%, 96% and 70%) and dried at room temperature. Autometallographical staining was carried out using the BBInternational Silver Enhancing Kit for Light and Electron Microscopy (Agar Scientific Ltd., Stansted, UK) following manufacturer's recommendations. Briefly, sections were covered with the emulsion (initiator and enhancer, 1:1) and incubated in a moisture chamber for 22 minutes in darkness. Then, the reaction was stopped washing immediately the slides in tap water for 2 minutes. Slides were mounted with Kaiser's glycerin and observed under the light microscope to determine the presence of black silver deposits (BSDs) in all tissues. BSDs were quantified in digestive cells under the light microscope (x100 magnification) using the BMS software (Sevisan, Leioa, Spain) as described in Soto et al. (2002). Five measurements were performed in each section of 10 mussel digestive

glands in order to calculate the volume density of BSDs ($V_{V_{\text{BSD}}}$) as volume occupied by BSDs with respect to the volume of digestive tissue ($\mu\text{m}^3/\mu\text{m}^3$).

2.5. Mussel growth

After 21 days of exposure, length (L, maximum measure along the anterior-posterior axis), height (H, maximum dorsoventral axis) and width (W, maximum lateral axis) of 10 mussels per experimental group were measured. Wet flesh and valves were weighed and after 48 hours in an oven at 120°C, dry flesh and valves were weighed. Further, the ratios of shell width/shell height, shell width/shell length and shell length/shell height were calculated (Lobel and Wright, 1982). Finally, flesh condition index (FC) was determined according to Lobel and Wright (1982) as dry flesh weight (mg)/dry shell weight (g).

2.6. Mussel immune status

Immune status of mussels was assessed through the phagocytic activity of hemocytes based on the ability of the cells to phagocytose Neutral Red (NR) stained zymosan particles (Pipe et al., 1995). Hemolymph was extracted from 8 animals per experimental group and diluted at 10^6 cells/mL. Hemolymph suspension then was seeded into a 96 well microplate (6 wells per animal) and allowed to attach to the microplate surface for 30 minutes. After incubation of cells with NR stained zymosan particles for 30 minutes at 18°C, cells were fixed with methanol for 20 minutes. Then, NR was extracted from cells with an acetic acid-ethanol solution and absorbance was read at 550 nm in a microplate reader (Biotek EL 312, Winooski, USA).

2.7. Mussel gonad index and oocyte atresia

For gonad index calculation and oocyte atresia analysis, mantle-gonads of 10 female mussels per experimental group were identified by froth and then dissected out, fixed in 10% neutral buffered formalin and routinely processed for paraffin embedding in a Leica Tissue processor ASP 3000 (Leica Instruments, Wetzlar, Germany). Histological sections (5 μm in thickness) were cut in a Leica RM2255 microtome (Leica Instruments) and stained with hematoxylin/ eosin (Gamble and Wilson, 2002). Gonad sections were examined under the light microscope (Nikon Eclipse Ni; Nikon Instruments, Tokyo, Japan) and female gender was confirmed for all samples. Gonad index (GI) value was assigned to each individual gonad as described by Kim et al. (2006) and a mean GI was then calculated for each studied group.

Prevalence of atretic oocytes was estimated as percentage of area occupied by atretic oocytes with respect to total area after estimating randomly five areas ($\times 10$ magnification) in one section per individual in the 10 individuals per experimental group.

2.8. Spawning, fertilization success and embryo development

After 21 days of exposure, mussels were induced to spawn according to the procedure described by His et al. (1997) with modifications described below. Parameters checked were spawning success, egg morphology, sperm motility, fertilization success and embryo development.

Fifteen mussels per experimental group were induced to spawn by thermal stimulation. To get a greater thermal shock and facilitate the spawning, mussels were kept for 2 hours at 4°C and then they were immersed in SW at 18°C and 28°C until they started to spawn. Spawners were individually transferred to beakers with 100 mL of sterilized SW. Male spawners produced a dense milky sperm solution which was sieved through a 30 μm mesh to remove debris. Sperm motility was checked visually and sperm of 4 males per experimental group was pooled. Similarly, eggs from 4 female spawners per group were sieved through a 100 μm sieve to remove tissue debris and the number of eggs was counted under the light microscope. A 5 mL volume of the pooled sperm solution was added to each beaker containing all the eggs from each individual female. After 30 minutes, fertilization success (number of fertilized eggs/number of total eggs $\times 100$) was calculated for each female after microscopic examination. Round eggs with expelled polar bodies were considered as fertilized (His et al., 1999).

After fertilization, volumes corresponding to 600 fertilized eggs per female were transferred to sterile Falcons containing 25 mL of sterilized SW (3 replicates per female) and fertilized eggs were incubated at 18°C for 48 hours in a shaker (lowest speed). After the incubation period, 100 μL of 4% buffered formalin was added to each Falcon. The percentage of abnormal embryos was determined under the light microscope (Nikon Eclipse *Ni*; Nikon Instruments, Tokyo, Japan) for randomly selected 100 out of the 600 embryos in each of the 3 replicates per female. The categories of abnormalities included: (a) segmented eggs, normal or malformed embryos that did not reach the D-larval stage, grouped as abnormal embryos; and (b) D-larvae, with either convex hinge, indented shell margins, incomplete shell or protruded mantle, grouped as abnormal larvae (His et al., 1997).

2.9. Statistical analyses

Statistical analyses were conducted using the statistical package SPSS v.22 (SPSS Inc., IBM Company, Chicago, USA). Prior to statistical analysis, results represented as percentage (prevalence of atretic oocytes, fertilization success and development of abnormal embryos) were set to arcsine transformation (Sokal and Rohlf, 1969). Bootstrap resampling techniques (Efron and Tibshirani, 1993) were used to set significant differences with respect to controls (N=2000 repetitions) in all studied endpoints followed by Bonferroni's correction for multiple comparisons. Significance level was globally stated at 5% ($p < 0.05$).

3. RESULTS

3.1. Characterization of Ag NPs in SW and BME

After dispersion in SW, PVP/ PEI coated 5 nm Ag NPs immediately reached a mean size of roughly 97 nm according to DLS measurements (Table 1). After 24 hours, particle size remained stable around 94 nm (Table 1). In BME, aggregation behavior of PVP/PEI coated 5 nm Ag NPs after 24 hours was similar to the one observed in SW, reaching a final size of approximately 94 nm (Table 1).

Dissolution of Ag NPs in SW was detected along the 72 hours of experimentation (Table 1). After 12 hours, Ag NPs released around 4% of Ag ions increasing the dissolution to around 14% at 24 hours. After 48 hours ~17% of Ag ions were released from Ag NPs and at 72 hours, dissolution increased to 20%. In BME, after 12 hours about 14% of Ag ions were released into the media and this value increased up to 18% after 24 hours (Table 1).

Table 1. Size distribution (nm) and released Ag⁺ (%) from total starting material of PVP/PEI coated 5 nm Ag NPs (10 mg Ag/L) in seawater for 72 hours and Basal Eagle Medium along 24 hours. Values are given as mean \pm S.D. (n.m. = not measured data).

Time (h)	Seawater		Basal Medium Eagle	
	Size (nm)	Dissolution rate (%)	Size (nm)	Dissolution rate (%)
0	97.91 \pm 2.64	0	n.m.	0
12	n.m.	4.59	n.m.	14.38
24	94.09 \pm 1.53	14.02	94.28 \pm 2.34	18.21
48	n.m.	17.35	n.m.	n.m.
72	n.m.	20.34	n.m.	n.m.

3.2. *In vitro* toxicity

PVP/PEI coated 5 nm Ag NPs significantly decreased hemocytes viability starting at 1 mg Ag/L (Figure 2). At exposure levels of 10 and 100 mg Ag/L, cell viability dropped to 2.73 and 3.39% with respect to control cells, respectively, indicating a strong cytotoxicity (Figure 2). The coating agent PVP/PEI alone was also cytotoxic to mussel hemocytes at the two highest concentrations tested: 104 and 1040 mg/L (equivalent to PVP/PEI concentrations present in 10 and 100 mg Ag/L Ag NPs suspensions, respectively) (Figure 2). At these concentrations, hemocyte viability decreased significantly to 86.9 and 64.2% of control, respectively, indicating a slight effect on cell viability (Figure 2). LC50 value calculated for PVP/PEI coated 5 nm Ag NPs was 2.05 mg Ag/L, while in the case of PVP/PEI, the LC50 value exceeded the maximum concentration tested (>1040 mg/L).

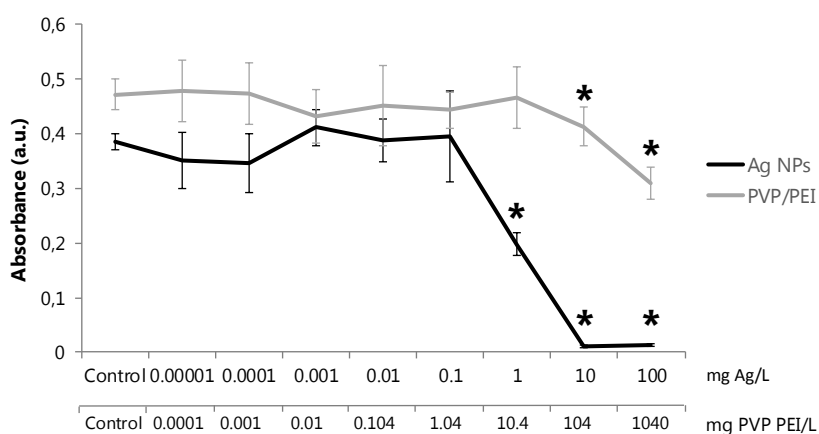


Figure 2. MTT cell viability assay in mussel hemocytes exposed to 5 nm PVP/ PEI coated Ag NPs and to PVP/ PEI alone (at the same concentrations present in Ag NP suspensions) for 24 hours. Data are given as absorbance values in arbitrary units (a.u.) (means \pm 95% confidence intervals). Black and grey asterisks indicate significant differences ($p < 0.05$) in treated cells with respect to controls after the exposure to Ag NPs and PVP/PEI alone, respectively, according to the bootstrap analysis followed by Bonferroni's correction. $n = 6$ replicates per treatment.

3.3. Bioaccumulation of Ag in algae and mussel soft tissues

Ag was significantly accumulated in microalgae exposed to Ag NPs at 10 μg Ag/L for 24 hours (Figure 3A), reaching a mean value of 21.3 ± 2.1 μg Ag/g d.w. The increased Ag concentration in microalgae exposed to 1 μg Ag/L for 24 hours was not significantly different from controls. However, BCF calculations revealed similar values

for both exposure conditions: 2.49 after the exposure to 1 $\mu\text{g Ag/L}$ Ag NPs and 2.12 after the exposure to 10 $\mu\text{g Ag/L}$ Ag NPs.

Mussels fed for 21 days with microalgae exposed daily to 10 $\mu\text{g Ag/L}$ Ag NPs significantly accumulated Ag in the digestive gland (1.52 ± 0.35 $\mu\text{g Ag/g}$ d.w. shell weight) and gills (1.25 ± 0.10 $\mu\text{g Ag/g}$ d.w. shell weight, Figure 3B) in comparison to controls. Accumulation of Ag was also significantly higher in digestive gland and gills of mussels exposed to 10 $\mu\text{g Ag/L}$ Ag NPs in comparison to muscle (0.50 ± 0.10 $\mu\text{g Ag/g}$ dw shell weight) and gonad (0.22 ± 0.06 $\mu\text{g Ag/g}$ d.w. shell weight, Figure 3B). After 21 days of dietary exposure to 1 $\mu\text{g Ag/L}$ Ag NPs, Ag was mainly accumulated in the digestive gland and gills of mussels, although a slight accumulation was also observed in muscle and gonad in comparison to the same tissues in controls (Figure 3B).

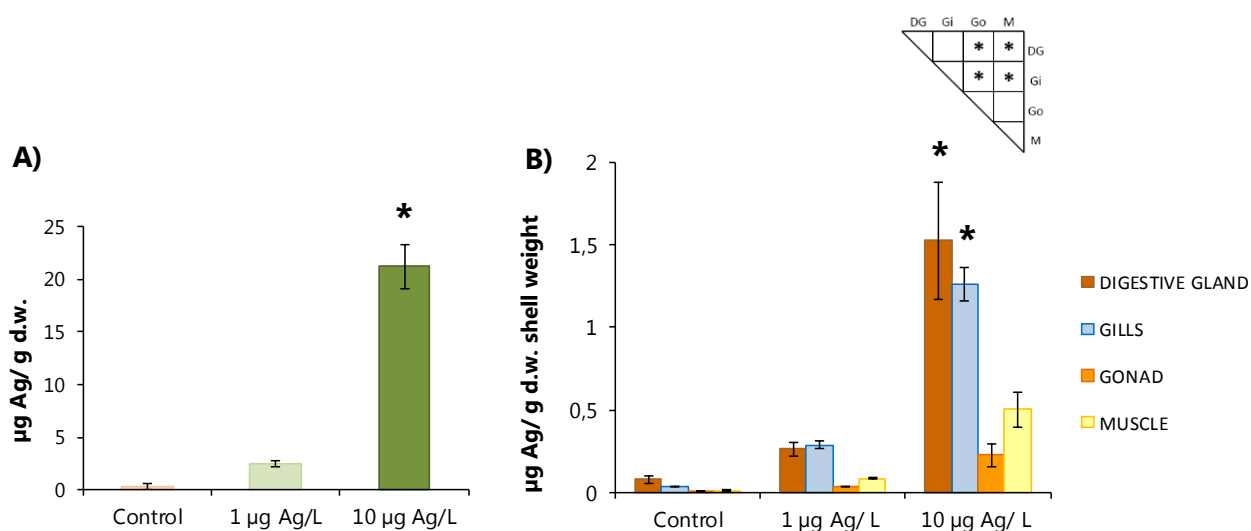


Figure 3. Bioaccumulation of Ag in **A)** microalgae ($\mu\text{g Ag/g}$ d.w.) after 24 hours of exposure to 1 $\mu\text{g Ag/L}$ or to 10 $\mu\text{g Ag/L}$ of Ag NPs and **B)** different tissues of mussels ($\mu\text{g Ag/g}$ d.w. shell weight) exposed through diet for 21 days to 1 $\mu\text{g Ag/L}$ or to 10 $\mu\text{g Ag/L}$ of Ag NPs. Significant differences with respect to controls based on the bootstrap analysis ($p < 0.05$) followed by Bonferroni's correction are shown by asterisks. Asterisks in the upper triangular matrix show significant differences among tissues based on bootstrap analysis ($p < 0.05$) followed by Bonferroni's correction where DG stands for digestive gland, Gi for gills, Go for gonad and M for muscle. Values are given as means \pm S.D. Mean values for microalgae results correspond to 3 filters per beaker of exposure condition (3 replicates) and for mussels results to 4 pools of 5 individuals each per exposure group.

Nevertheless, values were not significantly different from controls. BAF for mussels dietarily exposed to 1 $\mu\text{g Ag/L}$ Ag NPs was nearly two times higher (0.65) than the value for mussels exposed to the high dose (0.39) (Table 2). In both treatments, BAF was similar in digestive gland and gills and higher than BAF observed in gonads and muscle (Table 2).

Table 2. Bioaccumulation factor (BAF) for each tissue separately (digestive gland, gills, gonad and muscle) and total BAF in mussels after 21 days of dietary exposure to 1 $\mu\text{g Ag/L}$ or to 10 $\mu\text{g Ag/L}$ of Ag NPs.

	BAF	
	1 $\mu\text{g Ag/L}$	10 $\mu\text{g Ag/L}$
Digestive gland	0.2597	0.1697
Gills	0.2848	0.1419
Gonad	0.0331	0.0250
Muscle	0.0822	0.0555
Total	0.6598	0.3921

3.4. Intralysosomal metal accumulation by autometallography

The presence of metals was observed as black silver deposits (BSDs) mainly in the digestive gland and gills of mussels exposed to both 1 and 10 $\mu\text{g Ag/L}$ Ag NPs through the diet (Figure 4). Even if Ag was accumulated in gonads, BSDs were not found in this tissue. In gills, BSDs were located in epithelial cells of both frontal (especially in the postlateral region) and abfrontal parts of the gill filaments (Figure 4B). In the digestive gland, BSDs were specially located in the basal lamina of digestive tubules as well as in the lysosomes of the digestive cells (Figure 4E). The quantification of BSDs present in digestive cell lysosomes revealed that intralysosomal metal accumulation increased significantly in a dose-dependent manner after dietary exposure to 1 or 10 $\mu\text{g Ag/L}$ Ag NPs with respect to controls (Figure 4F).

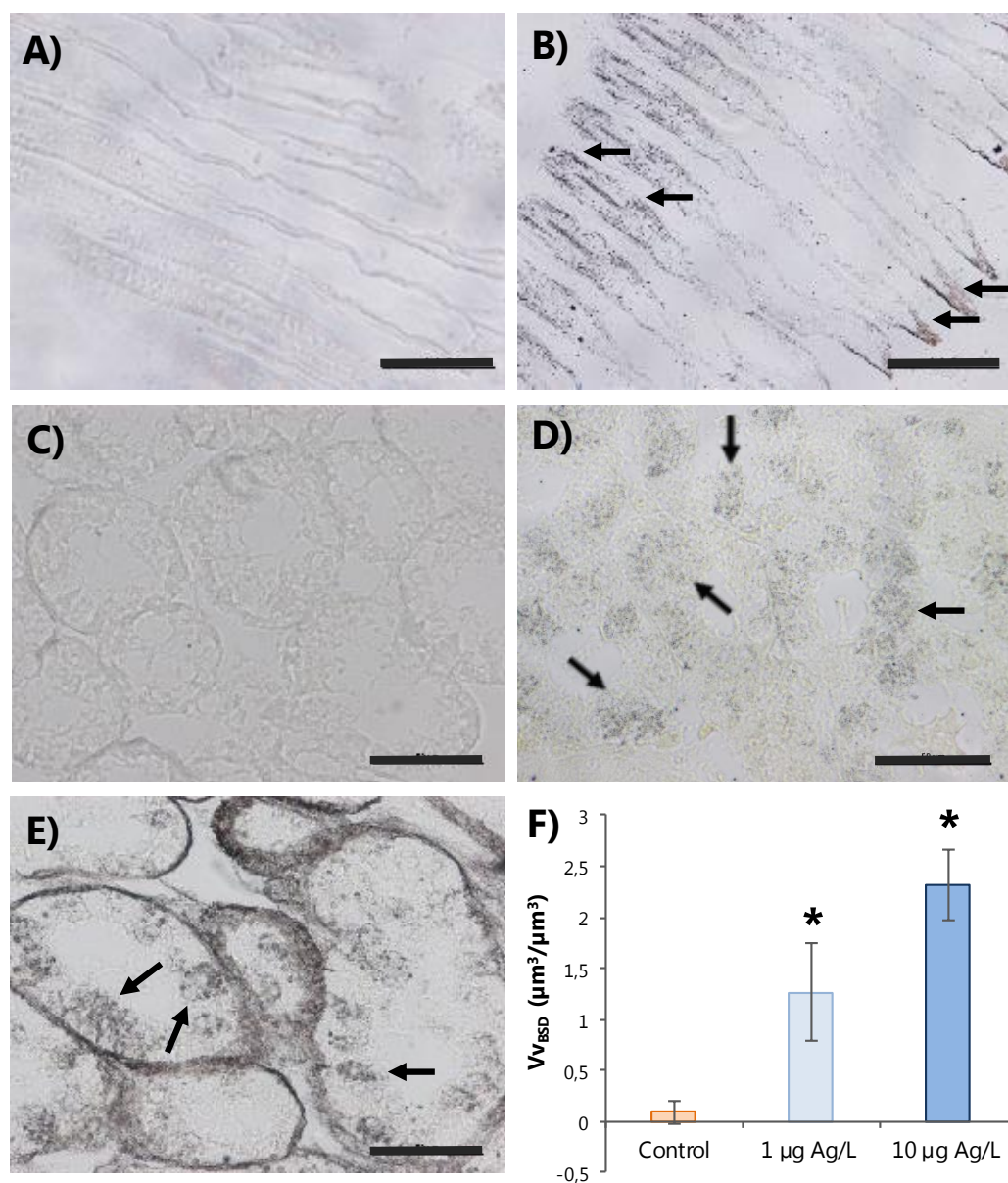


Figure 4. Autometallographic localization of metals in **A, C**) gills and digestive gland of control mussels, **B**) gills of mussels dietarily exposed to 10 µg Ag/L of Ag NPs and **D, E**) digestive gland of mussels dietarily exposed to 1 and 10 µg Ag/L of Ag NPs, respectively. Black arrows indicate black silver deposits (BSDs) in **B**) gills and **D, E**) lysosomes of digestive tubules. Scale bars 50 µm. **F**) Intralysosomal metal accumulation as volume density of BSDs (Vv_{BSD} ; $\mu\text{m}^3/\mu\text{m}^3$), in mussel digestive tubules after 21 days of dietary exposure to 1 µg Ag/L or to 10 µg Ag/L of Ag NPs. Values are given as means \pm S.D. Significant differences with respect to controls based on the bootstrap analysis ($p < 0.05$) followed by Bonferroni's correction are shown by asterisks. $n = 9$ individuals per group.

3.5. Mussel growth

No significant differences between control and treated groups were observed nor in the measured ratios W/H, W/L and L/H neither in the FC of mussels after 21 days of dietary exposure (Table 3).

Table 3. Biometric parameters (cm) and flesh condition index (mg/g) in control mussels and in mussels after 21 days of dietary exposure to 1 μg Ag/L or to 10 μg Ag/L of Ag NPs. Values are given as mean \pm S.D. No significant differences between control and exposed organisms were found ($p > 0.05$) according to the bootstrap analysis followed by Bonferroni's correction. $n = 10$ individuals per group.

	LENGTH (L; cm)	WIDTH (W; cm)	HEIGHT (H; cm)	W/H (cm/cm)	W/L (cm/cm)	L/H (cm/cm)	FLESH CONDITION INDEX (mg/g)
Control	4.23 \pm 0.17	2.43 \pm 0.17	1.51 \pm 0.17	0.57 \pm 0.15	0.57 \pm 0.03	2.82 \pm 0.45	125.29 \pm 21.42
1 μg Ag/L	4.23 \pm 0.29	2.41 \pm 0.12	1.44 \pm 0.09	0.57 \pm 0.08	0.57 \pm 0.02	2.94 \pm 0.24	135.58 \pm 21.13
10 μg Ag/L	4.23 \pm 0.45	2.35 \pm 0.24	1.42 \pm 0.12	0.55 \pm 0.15	0.55 \pm 0.03	2.98 \pm 0.12	124.13 \pm 27.04

3.6. Mussel immune status

After 21 days of dietary exposure of mussels, no significant differences between control and treated groups were observed in the phagocytic activity of hemocytes, although a reduction trend was appreciated at both doses with respect to controls (Figure 5).

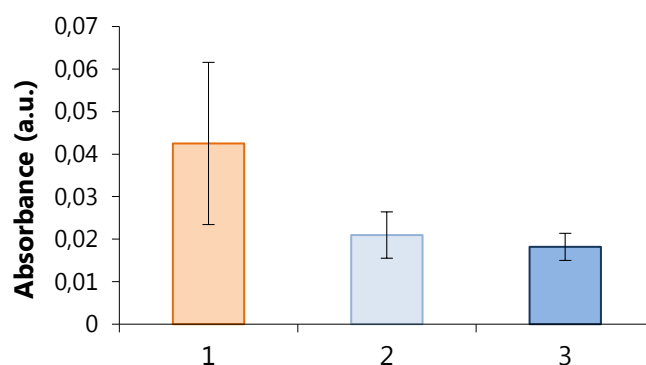


Figure 5. Phagocytic activity in hemocytes (absorbance in a.u.) of control mussels and of mussels exposed through the diet for 21 days to 1 μg Ag/L or to 10 μg Ag/L of Ag NPs. Data are given as mean \pm S.E. for $n = 8$ individuals per group. No significant differences were observed by the bootstrap analysis ($p > 0.05$) followed by Bonferroni's correction.

3.7. Gonad index and oocyte atresia

Gonads of all female mussels were in an advanced gametogenic stage or in a mature stage. Mean value for GI was 4.4 ± 0.77 for control mussels and 4.16 ± 0.79 and 4.4 ± 0.77 for mussels dietarily exposed to 1 or 10 $\mu\text{g Ag/L Ag NPs}$, respectively. Non-exposed females showed around 8.72% of atretic oocytes. Prevalence of atretic oocytes was 9.78% for mussels dietarily exposed to 1 $\mu\text{g Ag/L Ag NPs}$ and 8.19% for mussels exposed to 10 $\mu\text{g Ag/L Ag NPs}$. No significant differences between control and treated groups were observed in gonad index or in prevalence of atretic oocytes.

3.8. Spawning success, fertilization success and embryo development

As to spawning success, females dietarily exposed to 1 or 10 $\mu\text{g Ag/L Ag NPs}$ released significantly less eggs than non-exposed ones (Figure 6). In all the cases, eggs were round and malformations were not detected. Similarly, sperm motility was not altered. Fertilization success was similar for all the groups: $90.6 \pm 0.59\%$ for control mussels and $89.6 \pm 0.52\%$ and $90 \pm 0.64\%$ for females dietarily exposed to 1 or 10 $\mu\text{g Ag/L Ag NPs}$, respectively.

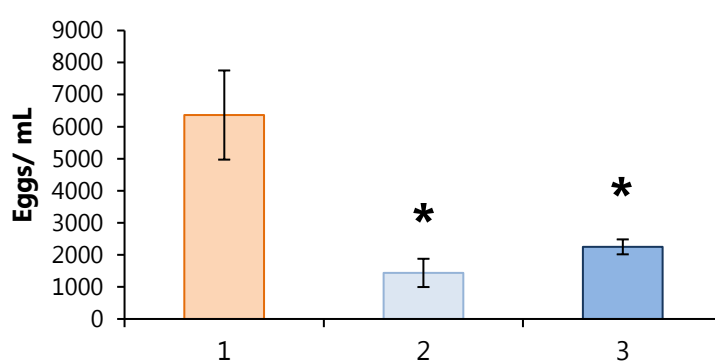


Figure 6. Number of eggs per mL released by spawner females ($n=4$) in control mussels and in mussels after 21 days of dietary exposure to 1 $\mu\text{g Ag/L}$ or to 10 $\mu\text{g Ag/L}$ of Ag NPs. Values are given as mean \pm S.E. Significant differences with respect to controls based on the bootstrap analysis ($p < 0.05$) followed by Bonferroni's correction are shown by asterisks.

At 48 hours after fertilization, a significantly higher number of abnormal larvae was observed among descendants of parents exposed to 1 or to 10 $\mu\text{g Ag/L Ag NPs}$ in comparison to controls (Figures 7 and 8). Around 14.5% of embryos descendant from adults dietarily exposed to 1 $\mu\text{g Ag/L Ag NPs}$ were abnormal, while a higher number of abnormal embryos (20.8%) was recorded after the dietary exposure to 10 $\mu\text{g Ag/L Ag NPs}$ (Figure 8). Observed abnormalities included a) segmented eggs,

normal or malformed embryos that had not reached the D-larval stage (pre-veliger larvae), grouped as abnormal embryos and b) D-larvae with indented shell margins, incomplete shell or protruded mantle, grouped as abnormal larvae (Figures 7 and 8). Out of the 14.5% of abnormalities observed after the dietary exposure of parentals to $1 \mu\text{g Ag/L}$ Ag NPs, 8.0% were abnormal larvae and 6.5% abnormal embryos (Figure 8). After the dietary exposure of adults to $10 \mu\text{g Ag/L}$ Ag NPs, abnormal larvae comprised the largest group (18.3%) and only around 2.6% of abnormal embryos occurred (Figure 8).

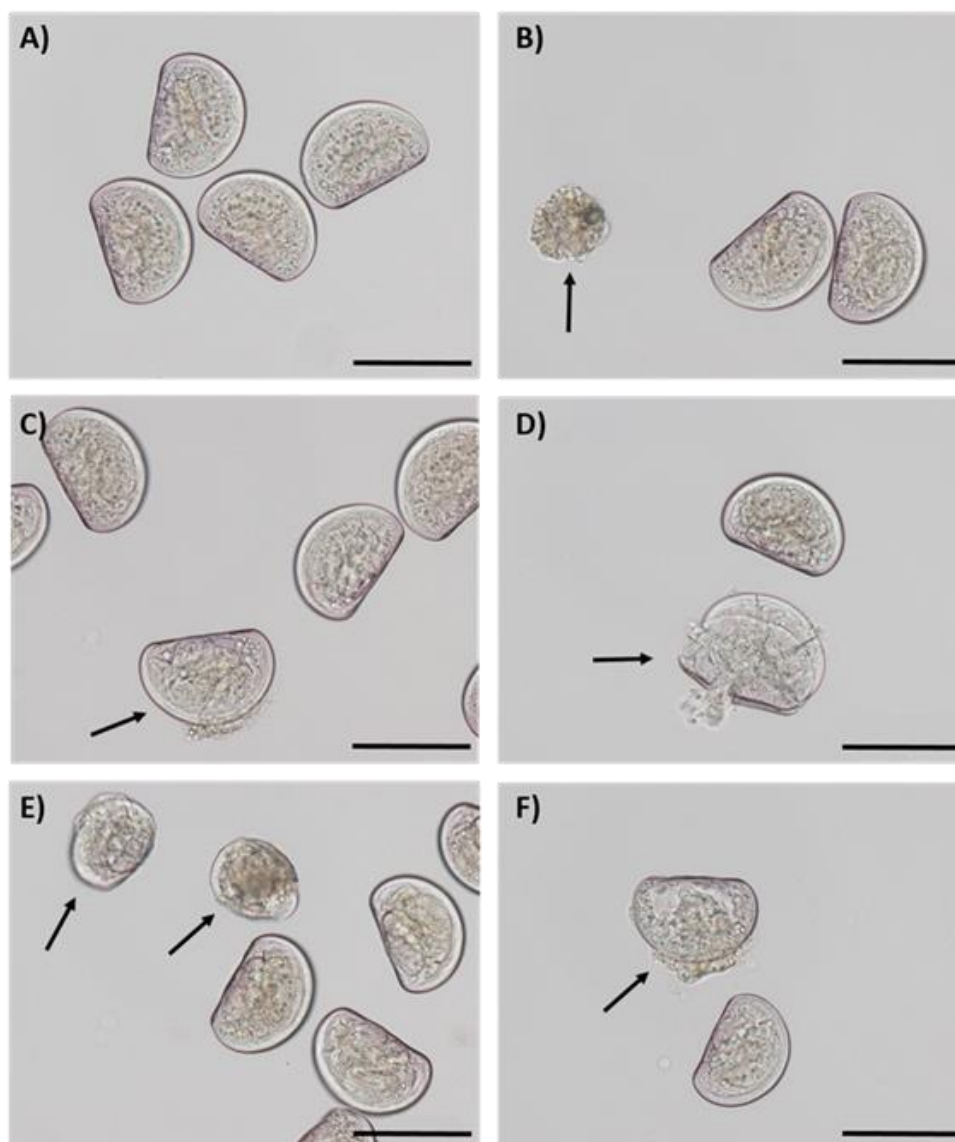


Figure 7. Micrographs of normal D-shell larvae and different abnormal embryos (black arrows) observed after 48 hours post-fertilization. **A)** Normal D-shell larvae descendant from a non-exposed mussel. **B, C, D)** Abnormal embryos descendant from mussels dietarily exposed to $1 \mu\text{g Ag/L}$ of Ag NPs for 21 days: **B)** embryo whose development was stopped at trochophore stage, **C)** pre-veliger larvae and **D)** larvae with damaged shell. **E, F)** Abnormal embryos descendant from mussels dietarily exposed to $10 \mu\text{g Ag/L}$ of Ag NPs for 21 days: **E)** deformed D-shell larvae and **F)** D-shell larvae with protruding mantle. Scale bars $100 \mu\text{m}$.

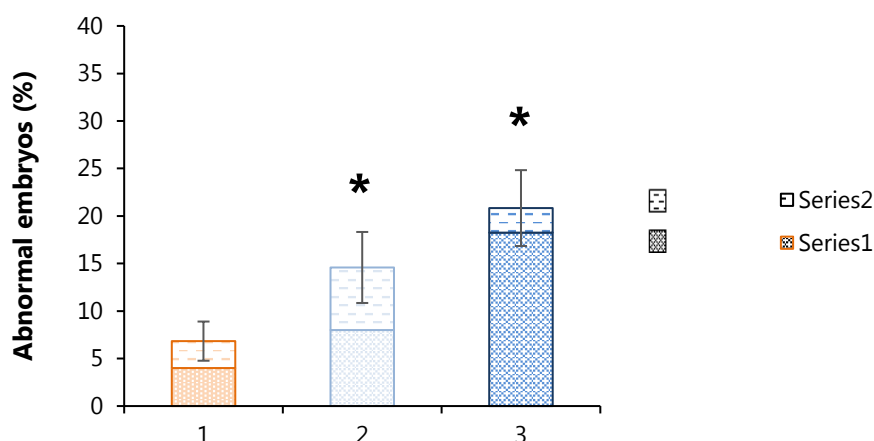


Figure 8. Percentage of abnormal embryos descendant of mussels (n=4) and type of abnormalities observed in control mussels and in mussels after 21 days of dietary exposure to 1 µg Ag/L or to 10 µg Ag/L of Ag NPs. Values are given as means ± S.D. Significant differences with respect to controls based on the bootstrap analysis ($p < 0.05$) followed by Bonferroni's correction are shown by asterisks.

4. DISCUSSION

Coating agents are chemicals (i.e. polymers and surfactants) used in the synthesis of Ag NPs to prevent or reduce their aggregation and/or dissolution (El Badawy et al., 2010). In the present work PVP/PEI coated 5 nm Ag NPs aggregated and released Ag ions both in SW and in BME culture media. Particle size for PVP/PEI coated 5 nm Ag NPs aggregates was similar for both exposure media, while dissolution was higher in BME than in SW after 12 or 24 hours. Stability of Ag NP suspensions is influenced by different environmental factors such as pH, ionic strength, salinity and dissolved organic matter, among others (El Badawy et al., 2010; Fabrega et al., 2011; Zhang et al., 2016). High ionic strength and saline media, such as SW and artificial SW (ASW) facilitate the aggregation (El Badawy et al., 2010; Chambers et al., 2014; Levard et al., 2012; Wang et al., 2014) and dissolution of Ag NPs (Sikder et al., 2017). In this sense, dissolution of Ag NPs with different coating agents has been reported in SW and ASW (Angel et al., 2013; Buffet et al., 2014; Katsumiti et al., 2015b; Odzak et al., 2014; Schiavo et al., 2017; Sendra et al., 2017; Sikder et al., 2017). Dissolution of maltose coated Ag NPs reached 34.6% after 7 days in ASW (Buffet et al., 2014) and citrate coated Ag NPs showed a faster dissolution rate than PVP coated particles in both freshwater and SW (Angel et al., 2013). After 48 hours, a dissolution rate of 20% for 17 nm uncoated Ag NPs was reported (Sendra et al., 2017) and Schiavo et al. (2017) observed a similar dissolution rate for PVP/PEI coated 5

nm Ag NPs after 24 hours in ASW. In the case of BME culture media, dissolution of Ag NPs was higher than in SW, in line with previous results with CuO NPs (Volland et al., 2018). The high Ag ion release in cell culture media in comparison to other exposure media has been related to interactions of the dissolved ions with free cysteine and cysteine groups of proteins present in cell culture media (Hansen and Thünemann, 2015). These amino acids are known to remove free Ag ions from solution and shift the equilibrium toward the release of more silver ions (Zook et al., 2011). The implication of a higher release of Ag ions in BME medium compared to seawater is that hemocytes were exposed to a higher percentage of the dissociated Ag ions (18%) compared to algae (14%). Overall, as a consequence of aggregation and dissolution behavior of studied Ag NPs, in the present work mussel hemocytes *in vitro* and algae were exposed to 94-97 nm aggregates of Ag NPs (>80% of the nominal Ag concentration) and also to dissolved Ag (14-18% of the nominal Ag concentration).

Cytotoxicity of different metal bearing NPs has been assessed in mussel hemocytes *in vitro* (Ciacci et al., 2012; Katsumiti et al., 2014; 2015a; 2015b; 2016; 2018), including maltose stabilized Ag NPs of 20, 40 and 100 nm (Katsumiti et al., 2015b). In the present study, PVP/PEI coated 5 nm Ag NPs were cytotoxic to mussel hemocytes, significantly decreasing hemocytes viability from 1 mg Ag/L up to 100 mg Ag/L (LC50 = 2.05 mg Ag/L). In comparison, maltose 20 nm Ag NPs were less toxic for mussel hemocytes, cell viability decreasing at 10 to 100 mg Ag/L (LC50 = 5.8 mg Ag/L) (Katsumiti et al., 2015b). Comparing solubility of maltose 20 nm Ag NPs (Katsumiti et al., 2015b) with PVP/PEI coated 5 nm Ag NPs in the present work, PVP/PEI coated 5 nm Ag NPs showed a slightly higher dissolution rate in seawater after 24 hours (11.7% versus 14%, respectively), in agreement with the generally accepted idea that solubility of Ag NPs may be an important driver of their toxicity (Navarro et al., 2008; Behra et al., 2013; Katsumiti et al., 2015b; Zhang et al., 2018). Differences in size, coating agent and other physico-chemical characteristics between the two nanoparticles may also explain differences in cytotoxicity to mussel hemocytes.

In the present work Ag accumulation occurred in microalgae *I. galbana* exposed to PVP/PEI coated 5 nm Ag NPs for 24 hours, although it remains unclear whether Ag NPs were internalized in the microalgae or not. In different freshwater microalgae species that show cell wall such as *Raphidocelis subcapitata* (Ribeiro et al., 2015) and *Chlamydomonas reinhardtii* (Piccapietra et al., 2012) Ag NPs were not internalized and Ag levels measured in the microalgae were derived from ionic or dissolved Ag complexes. In contrast, other studies showed that <20 nm Ag NPs can be adsorbed onto the cell surface of *Euglena gracilis* microalgae (Yue et al., 2017) or internalized in the periplasmic space

of the *C. reinhardtii* microalgae (Wang et al., 2016) as well as within vacuole-like structures of the freshwater *Ochromonas danica* species (Miao et al., 2010). These findings emphasize the role of the algal cell wall as a potential barrier against NP entry into the cells, only NPs smaller than the diameter of cell wall pores (5-20 nm) being internalized (Navarro et al., 2008; Yue et al., 2017). *I. galbana* microalgae presents a soft cell coating composed of coalesced carbohydrates scales (Zhu and Lee., 1997; Bendif et al., 2013). In a previous study we observed by light and focused ion beam microscopy that aggregates of the same PVP/PEI coated 5 nm Ag NPs used in the present work interacted with *I. galbana* microalgae by entrapping them in a network of heteroaggregates and by covering their surface (Schiavo et al., 2017). According to these findings and the observed aggregation and dissolution behavior of studied Ag NPs in SW, Ag significantly accumulated in microalgae exposed to PVP/PEI coated 5 nm Ag NPs for 24 hours could derive partly from dissolved Ag and single Ag particles internalized through the spaces between the oval scales (scale size 0.42x0.31-0.36 μm , Seoane et al., 2009), and partly from 94-97 nm Ag NP aggregates attached to the microalgae cell surface (Schiavo et al., 2017).

Whether internalized or attached to the surface of microalgae, accumulated Ag was successfully transferred to mussels exposed for 21 days to contaminated algae, Ag being accumulated mainly in the digestive gland and gills. The slight accumulation of Ag in gonads is of special interest as it could suggest direct effects on the gametes. In agreement, accumulation of Ag after 15 days of waterborne exposure to Ag NPs (<100 nm) has been already reported in mussels gills and digestive gland, being the accumulation higher in the latter (Gomes et al., 2013b; Bebianno et al., 2015). Similarly, highest radioactivity levels were found in the digestive system of Iceland scallops after waterborne exposure to small (10-20 nm) and large (70-80 nm) $^{110\text{m}}\text{Ag}$ labeled Ag NPs, whereas much lower levels were observed in all other tissues (gills, gonads, kidney and muscle tissues) (Al-Sid-Cheikh et al., 2013). Although gills are the first vulnerable barrier to particle interactions (Canesi et al., 2012; Canesi and Corsi, 2016), the digestive gland of bivalves is considered the main organ for accumulation of NPs, where their cellular fate and effects differ according to the NP type and experimental conditions, including exposure route (Canesi and Corsi, 2016; Faggio et al., 2018).

The BCF values in the present work were 2.49 and 2.12 after the exposure of microalgae to 1 and 10 $\mu\text{g Ag/L}$ Ag NPs, respectively. For mussels, BAF values were 0.65 and 0.39 after the dietary exposure to 1 and 10 $\mu\text{g Ag/L}$ Ag NPs, respectively. Similarly, after 24 hours of exposure to 5 and 10 $\mu\text{g Ag/L}$ Ag NPs, *R. subcapitata* showed BCF values of 4 and 3, respectively (Ribeiro et al., 2017). The cladoceran *Daphnia magna* fed with

those microalgae showed a BAF of 0.5 (Ribeiro et al., 2017). In a mesocosm study, the trophic transfer of Ag NPs was assessed through the *Chlorella* sp. microalgae, *Moina macrocopa* water flea, *Chironomus* spp. blood worm and *Barbonymus gonionotus* silver barb species (Yoo-Iam et al., 2014). After the exposure to 3.68 mg/L Ag NPs for 24 hours, BCF ranged from 1.89 for silver barb fish to 52.32 for the water flea (Yoo-Iam et al., 2014). However, authors considered that trophic transfer of Ag NPs from food sources to consumers occurred only from *Chlorella* sp. to the water flea (BAF= 1.41) since BAF for the rest of the food chain was less than 1 (Yoo-Iam et al., 2014). It has been reported that biomagnification of silver in algal feeders such as filter feeding organisms is unlikely since desorption and the combination of intracellular and extracellular digestion can affect Ag assimilation in marine bivalves (Connell et al., 1991; Ratte, 1999).

In agreement with Ag bioaccumulation results, autometallographic BSDs were mainly located in gills and digestive gland of mussels dietarily exposed to both doses of Ag NPs, with the highest values of intralysosomal metal accumulation occurring in digestive cells of mussels exposed to 10 µg Ag/L Ag NPs. This observation is consistent with the dose-dependent increase in intralysosomal metal accumulation reported in mussels digestive gland waterborne exposed to different sized Ag NPs-(Jimeno-Romero et al., 2017) and in intestine and liver of zebrafish dietarily exposed to the same PVP/PEI coated 5 nm Ag NPs studied in the present work (Lacave et al., 2017). BSDs do not reflect only Ag levels since autometallography is not metal-specific (Danscher, 1981; Marigómez et al., 2002) but, in the present study, scarce BSDs were observed in control samples. Thus, the significantly higher volume density of BSDs measured in the digestive tubules of exposed mussels together with results obtained by ICP-MS, suggest that observed BSDs corresponded to the presence of Ag, in either dissolved or particulate form. As in the present work, accumulation of Ag has been already reported in the basal lamina of digestive tubules of oysters (Amiard-Triquet et al., 1991; Rementería et al., 2016) and *M. edulis* mussels (George et al., 1986). The accumulation of metals in the basal lamina of the digestive tubules or wandering hemocytes in the connective tissue has been associated to the impairment of the excretory function (Marigómez et al., 2002). BSDs were not found in the gonad tissue although Ag was accumulated in gonads according to chemical analysis. Ag was probably sequestered by Ag-binding proteins or sulphhydryl and sulphate groups of glycoproteins and proteoglycans or precipitated as Ag sulphide (George et al., 1986; Martoja et al., 1988) in this tissue, hindering the reaction that allows the formation of BSDs.

In spite of significant Ag accumulation, mussels growth was not affected by the exposure to Ag NPs through the diet, probably because the 21 day exposure period at

the selected concentrations was not long enough to produce significant effects on growth. In fact, previous long term studies revealed that exposure to ionic Ag had no effect on laboratory-reared mussels nor in wild mussels after 12 months of exposure to 5, 10 or 25 µg Ag/L, whereas copper inhibited mussels growth after 4 months of exposure to 10 µg Cu/L (Calabrese et al., 1984). Similarly, the growth of *Lymnaea stagnalis* freshwater snails was not altered after dietary exposure to Ag⁺ or humic acid capped Ag NPs, although they did not grow after dietary exposure to citrate capped Ag NPs due to damaged digestion (Croteau et al., 2011). Additionally, it should be considered that usually a rapid addition of tissue mass is most common in young organisms and occurs only during certain seasons (Luoma and Rainbow, 2005).

Increasing evidence supports the hypothesis that in marine invertebrates the immune system represents an important target for the effects of NPs (Canesi and Corsi, 2016; Manzo et al., 2017). In the present study, hemocytes phagocytic activity was not significantly affected in mussels dietarily exposed to Ag NPs, although a reduction trend was appreciated with respect to controls. This reduction trend is contrary to previous reports that described an immunostimulatory effect of Ag NPs (Katsumiti et al., 2015b) as well as of other metallic NPs (Ciacci et al., 2012; Katsumiti et al., 2014; 2018) after *in vitro* exposure of hemocytes. This different response could be a consequence of the higher exposure doses used for *in vitro* assays compared to *in vivo* experiments or due to a direct interaction of NPs with hemocytes surface in *in vitro* exposures, since a decrease in the phagocytic activity caused by metallic NPs on mussel hemocytes has been reported in other *in vivo* studies (Gagné et al., 2008; Couleau et al., 2012; Barmo et al., 2013; Balbi et al., 2014).

As to the gonad condition, all female mussels were in an advanced gametogenic stage or in a mature stage, as observed in previous years in different sites of the SE Bay of Biscay (Azpeitia et al., 2017), and prevalence of atretic oocytes was low in all groups. An increased prevalence of atretic oocytes has been linked to the impairment of reproduction ability of female mussels and a possible decrease in gamete quality (Ortiz-Zarragoitia and Cajaraville, 2010; Ortiz-Zarragoitia et al., 2011). Although no differences in prevalence of atretic oocytes occurred among groups after the dietary exposure to Ag NPs, spawning success in females was significantly reduced indicating that the reproduction ability of female mussels at the two doses tested was affected. Resorption of degenerate or atretic gametes has been described as a common process in mussel gonad (Pipe, 1987; Newell, 1989) and, as proposed by Baussant et al. (2011), atretic oocytes could have been resorbed during the experimental time, thus giving rise to a lower number of eggs being spawned at the end of the 21 day experimental period in

exposed mussels. The net result of oocyte degeneration and resorption is a recycling of nutrients to meet the energy requirements of basal metabolism, a phenomenon known to occur under stress or as a result of exposure to pollutants (Lowe and Pipe, 1986).

From an ecotoxicological perspective, data on embryo development are important to establish the sensitivity of the species to different types of pollutants and to address the consequences for the early life stages of the organisms (Balbi et al., 2014). Different studies have assessed the effects on mussels larval development after the exposure of sperm or fertilized eggs to different types of metallic NPs (Kadar et al., 2010; 2013; Libralato et al., 2013; Balbi et al., 2014; Auguste et al., 2018). Abnormalities in D-shell larvae were not observed after the exposure to the studied TiO₂ NP concentrations (Libralato et al., 2013; Balbi et al., 2014) neither after the exposure to Fe₂O₃ NPs (Kadar et al., 2010). However, the exposure of fertilized eggs to different concentrations of Ag NPs provoked a concentration-dependent increase in malformed D-shell larvae starting at 10 µg/L (Auguste et al., 2018). In agreement, in the present work a higher prevalence of malformed embryos was found in descendants of adults exposed to PVP/PEI coated 5 nm Ag NPs, even for the dose close to environmentally relevant concentrations (1 µg Ag/L Ag NPs). To the best of our knowledge, this is the first work that assessed the effects on mussels embryos after the exposure of parentals to Ag NPs. Parental exposure of bivalve molluscs to different toxicants such as TBT, benzo(a)pyrene or North Sea crude oil has been shown to affect early life stages (Inoue et al., 2004; 2006; Choy et al., 2007; Baussant et al., 2011).

5. CONCLUSIONS

Overall, results showed a successful transfer of incorporated PVP/PEI coated 5 nm Ag NPs from microalgae to mussels. Ag accumulation was highest in the digestive gland and gills, and accumulation also occurred in the gonad. Ag NPs were cytotoxic to mussel hemocytes exposed *in vitro*, whereas hemocytes phagocytic activity was slightly reduced after *in vivo* dietary exposure of mussels. Sperm motility and fertilization success were not altered, but exposed females released less eggs than exposed ones. Further, a significantly higher percentage of abnormal embryos was observed after parental exposure to both doses of Ag NPs. These observations suggest that low doses of Ag NPs in aquatic environments could have an impact on the health of individuals as well as on population fitness of mussels and other sensitive organisms. Future studies should address mechanisms and consequences of NP exposure for the early life stages of mussels and other marine organisms.

ACKNOWLEDGEMENTS

This work has been funded by the Spanish Ministry of Economy and Competitiveness (NanoSilverOmics project MAT2012-39372), Basque Government (SAIOTEK project S-PE13UN142 and Consolidated Research Group GIC IT810-13), University of the Basque Country UPV/EHU (UFI 11/37 and PhD fellowship to N.D.) and French Ministry of Higher Education and Research (PhD fellowship to M.M.)

REFERENCES

- ∴ Al-Sid-Cheikh M., Rouleau C., Pelletier E. 2013. Tissue distribution and kinetics of dissolved and nanoparticulate silver in Icelan scallop (*Chlamys islandica*). *Marine Environmental Research* 86: 21-28.
- ∴ Amiard-Triquet C., Berthet B., Martoja R. 1991. Influence of salinity on trace metal (Cu, Zn, Ag) accumulation at the molecular, cellular and organism level in the oyster *Crassostrea gigas* Thunberg. *Biology of Metals* 4: 144-151.
- ∴ Angel B.M., Batley G.E., Jarolimek C.V., Rogers N.J. 2013. The impact of size on the fate of nanoparticulate silver in aquatic systems. *Chemosphere* 93: 359-365.
- ∴ Arnot J.A., Gobas F.A.P.C. 2006. A review of bioconcentration factor (BCF) and bioaccumulation factor (BAF) assessments for organic chemicals in aquatic organisms. *Environmental Reviews* 14: 257-297.
- ∴ Auguste M., Ciacci C., Balbi T., Brunelli A., Caratto V., Marcomini A., Cuppini R., Canesi L. 2018. Effects of nanosilver on *Mytilus galloprovincialis* hemocytes and early embryo development. *Aquatic Toxicology* 203: 107-116.
- ∴ Azpeitia K., Ortiz-Zarragoitia M., Revilla M., Mendiola D. 2017. Variability of the reproductive cycle on the estuarine and coastal populations of the mussel *Mytilus galloprovincialis* Lmk. from the SE Bay of Biscay (Basque Country). *International Aquatic Research*: DOI 10.1007/s40071-017-0180-3.
- ∴ Balbi T., Smerilli A., Fabbri E., Ciacci C., Montagna M., Graselli E., Brunelli A., Pojana G., Marcomini A., Gallo G., Canesi L. 2014. Co-exposure to n-TiO₂ and Cd²⁺ results in interactive effects on biomarker responses but not in increased toxicity in the marine bivalve *M. galloprovincialis*. *Science of the Total Environment* 493: 355-364.
- ∴ Barmo C., Ciacci C., Canonico B., Fabbri R., Cortesec K., Balbi T., Marcomini A., Pojana G., Gallo G., Canesi L. 2013. *In vivo* effects of n-TiO₂ on digestive gland and immune function of the marine bivalve *Mytilus galloprovincialis*. *Aquatic Toxicology* 132-133: 9-18.
- ∴ Baussant T., Ortiz-Zarragoitia M., Cajaraville M.P., Benchman R.K., Taban I.C., Sanni S. 2011. Effects of chronic exposure to dispersed oil on selected reproductive processes in adult blue mussel (*Mytilus edulis*) and the consequences for the early life stages of their larvae. *Marine Pollution Bulletin* 62: 1437-1445.
- ∴ Bebianno M.J., Gonzalez-Rey M., Gomes T., Mattos J.J., Flores-Nunes F., Bainy A.C.D. 2015. Is gene transcription in mussel gills altered after exposure to Ag nanoparticles? *Environmental Science and Pollution Research* 22: 17425-17433.
- ∴ Behra R., Sigg L., Clift M.J.D., Herzog F., Minghetti M., Johnston B., Petri-Fink A., Rothen-Rutishauser B. 2013. Bioavailability of silver nanoparticles and ions: from a chemical and biochemical perspective. *Journal of the Royal Society Interface* 10: 20130396.
- ∴ Bendif E.M., Porbert I., Schroeder D.C., Vargas C. 2013. On the description of *Tisochrysis lutea* gen. nov. sp. nov. and *Isochrysis nuda* sp. nov. in the Isochrysidales, and the transfer of *Dicrateria* to the Prymnesiales (Haptophyta). *Journal of Applied Phycology* 25: 1763-1776.

- ∴ Blaser S.A., Scheringer M., Macleod M., Hungerbühler K. (2008). Estimation of cumulative aquatic exposure and risk due to silver: contribution of nano-functionalized plastics and textiles. *Science of the Total Environment* 390: 396-409.
- ∴ Bouallegui Y., Younes R.B., Turki F., Oueslati R. 2017. Impact of exposure time, particle size and uptake pathway on silver nanoparticle effects on circulating immune cells in *Mytilus galloprovincialis*. *Journal of Immunotoxicology* 14: 116- 124.
- ∴ Buffet P.E., Pan J.F., Poirier L., Amiard-Triquet C., Amiard J.C., Gaudin P., Risso. De Faverney C., Guibbolini M., Gilliland D., Valsami-Jones E. and Mouneyrac C. 2013. Biochemical and behavioural responses of the endobenthic bivalve *Scrobicularia plana* to silver nanoparticles in seawater and microalgal food. *Ecotoxicology and Environmental Safety* 89: 117-124.
- ∴ Buffet P.E., Zalouk-Vergnoux A., Châtel A., Berthet B., Métais I., Perrein-Ettajani H., Poirier L., Luna-Acosta A., Thomas-Guyon H., Risso-de Faverney C., Guibbolini M., Gilliland D., Valsami-Jones E., Mouneyrac C. 2014. A marine mesocosm study on the environmental fate of silver nanoparticles and toxicity effects on two endobenthic species: The ragworm *Hediste diversicolor* and the bivalve mollusc *Scrobicularia plana*. *Science of the Total Environment* 470-471: 1151-1159.
- ∴ Calabrese A., MacInnes J.R., Nelson D.A., Greig R.A., Yevich P.P. 1984. Effects of long-term exposure to silver or copper on growth, bioaccumulation and histopathology in the blue mussel *Mytilus edulis*. *Marine Environmental Research* 11: 253-274.
- ∴ Cajaraville M.P., Pal S.G. 1995. Morphofunctional study of the haemocytes of the bivalve mollusc *Mytilus galloprovincialis* with emphasis on the endolysosomal compartment. *Cell Structure and Function* 20: 355- 367.
- ∴ Canesi L., Barmo C., Fabbri R., Ciacci C., Vergani L., Roch P., Gallo G. 2010. *In vitro* effects of suspensions of selected nanoparticles (C60 fullerene, TiO₂, SiO₂) on *Mytilus* hemocytes. *Aquatic Toxicology* 96: 151-158.
- ∴ Canesi L., Ciacci C., Fabbri R., Marcomini A., Pojana G. and Gallo G. 2012. Bivalve molluscs as a unique target group for nanoparticle toxicity. *Marine Environmental Research* 76: 16- 21.
- ∴ Canesi L., Frenzilli G., Balbi T., Bernardeschi M., Ciacci C., Corsolini S., Della Torre C., Fabbri R., Faleri C., Focardi S., Guidi P., Kočan A., Marcomini A., Mariottini M., Nigro M., Pozo-Gallardo K., Rocco L., Scarcelli V., Smerilli A., Corsi I. 2014. Interactive effects of n-TiO₂ and 2,3,7,8-TCDD on the marine bivalve *Mytilus galloprovincialis*. *Aquatic Toxicology* 153: 53-65.
- ∴ Canesi L., Corsi I. 2016. Effects of nanomaterials on marine invertebrates. *Science of the Total Environment* 565: 933-940.
- ∴ Chae Y., An Y.J. 2016. Toxicity and transfer of polyvinylpyrrolidone-coated silver nanowires in an aquatic food chain consisting of algae, water fleas and zebrafish. *Aquatic Toxicology* 173: 94-104.
- ∴ Chambers B.A., Afrooz A.R.N.M., Bae S., Aich N., Katz L., Saleh N.B., Kirisits M.J. 2014. Effects of chloride and ionic strength on physical morphology, dissolution and bacterial toxicity of silver nanoparticles. *Environmental Science and Technology* 48: 761-769.

- ∴ Chio C.P., Chen W.Y., Chou W.W., Hsieh N.H., Ling M.P., Liao C.M. 2012. Assessing the potential risks to zebrafish posed by environmentally relevant copper and silver nanoparticles. *Science of the Total Environment* 420: 111-118.
- ∴ Cheng T.C. 1981. Bivalves. In: Ratcliffe NA, Rowley AF, editors. *Invertebrate blood cells*. London: Academic Press. pp. 233–300.
- ∴ Choy E.J., Jo Q., Moon H.B., Kang C.K., Kang J.C. 2007. Time-course uptake and elimination of benzo(a)pyrene and its damage to reproduction and ensuing reproductive outputs of Pacific oyster *Crassostrea gigas*. *Marine Biology* 151: 157-165.
- ∴ Ciacci C., Canonico B., Bilaničová D., Fabbri R., Cortese K., Gallo G., Marcomini A., Pojana G., Canesi L. 2012. Immunomodulation by different types of N-oxides in the hemocytes of the marine bivalve *Mytilus galloprovincialis*. *PloS ONE* 7 (5): e36937. doi:10.1371/journal.pone.0036937
- ∴ Connell D.B., Sanders J.G., Riedel G.F., Abbe G.R. 1991. Pathways of silver uptake and trophic transfer in estuarine organisms. *Environ Science and Technology* 25: 921–924.
- ∴ Corsi I., Cherr G.N., Lenihan H.S., Labille J., Hasselov M., Canesi L., Dondero F., Frenzilli G., Hristozov D., Punes V., Della Torre C., Pinsino A., Libralato G., Marcomini A., Sabbioni E., Matranga V. 2014. Common strategies and technologies for the ecosafety assessment and design of nanomaterials entering the marine environment. *ACS Nano* 8: 9694-9709.
- ∴ Couleau N., Techer D., Pagnout C., Jomini S., Foucaud L., Laval-Gilly P., Falla J., Bennasroune A. 2012. Hemocyte responses of *Dreissena polymorpha* following a short-term *in vivo* exposure to titanium dioxide nanoparticles: preliminary investigations. *Science of the Total Environment* 438: 490-497.
- ∴ Croteau M.N., Misra S.K., Luoma S.N., Valsami-Jones E. 2011. Silver bioaccumulation dynamics in a freshwater invertebrate after aqueous and dietary exposures to nanosized and ionic Ag. *Environmental Science and Technology* 45: 6600-6607.
- ∴ Danscher G. 1981. Light and electron microscopic localization of silver in biological tissue. *Histochemistry* 71: 177-186.
- ∴ Daskalakis K.D. 1996. Variability of metal concentrations in oyster tissue and implications to biomonitoring. *Marine Pollution Bulletin* 32: 794-801.
- ∴ Dumont E., Johnson A.C., Keller V.D.J., Williams R.J. 2015. Nano silver and nano zinc-oxide in surface waters- exposure estimation for Europe at high spatial and temporal resolution. *Environmental Pollution* 196: 341- 349.
- ∴ El Badawy A.M., Luxton T.P., Silva R.G., Scheckel K.G., Suidan M.T., Tolaymat T.M. 2010. Impact of environmental condition (pH, ionic strength and electrolyte type) on the surface charge and aggregation of silver nanoparticles suspensions. *Environmental Science and Technology* 44: 1260-1266.
- ∴ Efron B., Tibshirani R.J. 1993. *An Introduction to the Bootstrap*. London: Chapman & Hall.
- ∴ Fabrega J., Luoma S.N., Tyler C.R., Galloway T.S., Lead J.R. 2011. Silver nanoparticles: behaviour and effects in the aquatic environment. *Environmental International* 37: 517-531.

- ∴ Faggio C., Tsarpali V., Dailianis S. 2018. Mussel digestive gland as a model for assessing xenobiotics: an overview. *Science of the Total Environment* 613: 220-229.
- ∴ Gagné F., Auclair J., Turcotte P., Fournier M., Gagnon C., Sauvé S., Blaise C. 2008. Ecotoxicity of CdTe quantum dots to freshwater mussels: impacts on immune system, oxidative stress and genotoxicity. *Aquatic Toxicology* 86: 333-340.
- ∴ Gamble M., Wilson I. 2002. The hematoxylin and eosin. In: Brancfort J.D., Gamble M. (Eds.), *Theory and Practice of Histological Techniques*. Churchill Livingstone- Elsevier Science Ltd., London, UK, pp. 125
- ∴ George S.G., Pirie B.J.S., Calabrese A., Nelson D.A. 1986. Biochemical and ultrastructural observations of long-term silver accumulation in the mussel, *Mytilus edulis*. *Marine Environmental Research* 18: 255-265.
- ∴ Gomes T., Araújo O., Pereira R., Almeida A.C., Cravo A., Bebianno M.J. 2013a. Genotoxicity of copper oxide and silver nanoparticles in the mussel *Mytilus galloprovincialis*. *Marine Environmental Research* 84: 51-59.
- ∴ Gomes T., Pereira C.G., Cardoso C., Bebianno M.J. 2013b. Differential protein expression in mussels *Mytilus galloprovincialis* exposed to nano and ionic Ag. *Aquatic Toxicology* 136- 137: 79-90.
- ∴ Gomes T., Pereira C.G., Cardoso C., Sousa V.S., Ribau Teixeira M., Pinheiro J.P., Bebianno M.J. 2014. Effects of silver nanoparticles exposure in the mussel *Mytilus galloprovincialis*. *Marine Environmental Research* 101: 208-214.
- ∴ Gottschalk F., Sonderer T., Scholz R.W., Nowack B. 2009. Modeled environmental concentrations of engineered nanomaterials (TiO₂, ZnO, Ag, CNT, fullerenes) for different regions. *Environmental Science and Technology* 43: 9216- 9222.
- ∴ Hansen U., Thünemann A.F. 2015. Characterization of silver nanoparticles in cell culture medium containing fetal bovine serum. *Langmuir* 31: 6842- 6852.
- ∴ His E., Seaman M. N. L., Beiras R. 1997. A simplification the bivalve embryogenesis and larval development bioassay method for water quality assessment. *Water Research* 31: 351-355.
- ∴ His E., Beiras R., Seaman M.N.L. 1999. The assessment of marine pollution-bioassays with bivalve embryos and larvae. *Advances in Marine Biology* vol. 37. ISBN 0-12-026137-5.
- ∴ Inoue S., Oshima Y., Nagai K., Yamamoto T., Go J., Kai N., Honjo T. 2004. Effect of maternal exposure to tributyltin on reproduction of the pearl oyster (*Pinctada fucata martensii*). *Environmental Toxicology and Chemistry* 23: 1276-1281.
- ∴ Inoue S., Oshima Y., Usuki H., Hamaguchi M., Hanamura Y., Kai N., Shimasaki Y., Honjo T. 2006. Effects of tributyltin maternal and/or waterborne exposure on the embryonic development of the Manila clam, *Ruditapes philippinarum*. *Chemosphere* 63: 881-888.
- ∴ Jimeno-Romero A., Bilbao E., Izagirre U., Cajaraville M.P., Marigómez I., Soto M. 2017. Digestive cell lysosomes as main targets for Ag accumulation and toxicity in marine mussels, *Mytilus galloprovincialis*, exposed to maltose-stabilized Ag nanoparticles of different sizes. *Nanotoxicology* 11: 168-183.

- ∴ Kadar E., Lowe D.M., Solé M., Fisher A.S., Jha A., Readman J.W., Hutchinson T.H. 2010. Uptake and biological responses to nano-Fe versus soluble Fe-Cl₃ in excised mussel gills. *Analytical and Bioanalytical Chemistry* 396: 657-666.
- ∴ Kadar E., Dyson O., Handy R.D., Al-Subiai S.N. 2013. Are reproduction impairments of free spawning marine invertebrates exposed to zero-valent nano-iron associated with dissolution of nanoparticles? *Nanotoxicology* 7: 135-143.
- ∴ Katsumiti A., Gilliland D., Arostegui I., Cajaraville M.P. 2014. Cytotoxicity and cellular mechanisms involved in the toxicity of CdS quantum dots in hemocytes and gill cells of the mussel *Mytilus galloprovincialis*. *Aquatic Toxicology* 153: 39-52.
- ∴ Katsumiti A., Berhanu D., Howard K.T., Arostegui I., Oron M., Reip P., Valsami-Jones E., Cajaraville M.P. 2015a. Cytotoxicity of TiO₂ nanoparticles to mussel hemocytes and gill cells *in vitro*: influence of synthesis method, crystalline structure, size and additive. *Nanotoxicology* 9: 543-553.
- ∴ Katsumiti A., Gilliland D., Arostegui I., Cajaraville M.P. 2015b. Mechanisms of toxicity of Ag nanoparticles in comparison to bulk and ionic Ag on mussel hemocytes and gill cells. *PLoS ONE* 10 (6): e0129039. doi:10.1371/journal.pone.0129039
- ∴ Katsumiti A., Arostegui I., Oron M., Gilliland D., Valsami-Jones E., Cajaraville M.P. 2016. Cytotoxicity of Au, ZnO and SiO₂ NPs using *in vitro* assays with mussels hemocytes and gill cells: Relevance of size, shape and additives. *Nanotoxicology* 10: 185-193.
- ∴ Katsumiti A., Thorley A.J., Arostegui I., Reip P., Valsami-Jones E., Tetley T.D., Cajaraville M.P. 2018. Cytotoxicity and cellular mechanisms of toxicity of CuO NPs in mussel cells *in vitro* and comparative sensitivity with human cells. *Toxicology In Vitro* 48: 146-158.
- ∴ Kim Y., Ashton-Alcox K.A., Powell E.N. 2006. Gonadal analysis. NOAA histological techniques for marine bivalve mollusks: update. NOAA Technical Memories NOS NCCOS 27, Silver Spring (USA): 1-18.
- ∴ Lacave J.M., Fanjul A., Bilbao E., Gutierrez N., Barrio I., Arostegui I., Cajaraville M.P., Orbea A. 2017. Acute toxicity, bioaccumulation and effects of dietary transfer of silver from brine shrimp exposed to PVP/PEI coated silver nanoparticles to zebrafish. *Comparative Biochemistry and Physiology, Part C* 199: 69-80.
- ∴ Levard C., Hotze E.M., Lowry G.V., Brown Jr. G.E. 2012. Environmental transformations of silver nanoparticles: impact on stability and toxicity. *Environmental Science and Technology* 46: 6900-6914.
- ∴ Li L., Stoiber M., Wimmer A., Xu Z., Lindenblatt C., Helmreich B., Schuster M. 2016. To what extent can full-scale wastewater treatment plant effluent influence the occurrence of silver-based nanoparticles in surface waters? *Environmental Science and Technology* 50: 6327-6333.
- ∴ Libralato G., Minetto D., Totaro S., Micetic I., Pigozzo A., Sabbioni E., Marcomini A., Ghirardini A.V. 2013. Embryotoxicity of TiO₂ nanoparticles to *Mytilus galloprovincialis* (Lmk). *Marine Environmental Research* 92: 71-78.
- ∴ Lowe D.M., Pipe R.K. 1986. Hydrocarbon exposure in mussels: a quantitative study of the responses in the reproductive and nutrient storage cell systems. *Aquatic Toxicology* 8: 265-272.

- .: Lobel P.B., Wright D.A. 1982. Relationship between body zinc concentration and allometric growth measurements in the mussel *Mytilus edulis*. *Marine Biology* 66: 145-150.
- .: Luoma S.N., Rainbow P.S. 2005. Why is metal bioaccumulation so variable? *Biodynamics as a unifying concept*. *Environmental Science and Technology* 39: 1921-1931.
- .: Manzo S., Schiavo S., Oliviero M., Toscano A., Ciaravolo M., Cirino P. 2017. Immune and reproductive system impairment in adult sea urchin exposed to nanosized ZnO via food. *Science of the Total Environment* 599-600: 9-13.
- .: Marigómez I., Soto M., Cajaraville M.P., Angulo E., Giamberini L. 2002. Cellular and subcellular distribution of metals in molluscs. *Microscopy Research and Technique* 56: 358-392.
- .: Martoja R., Ballan-Dufrançais C., Jeantet A.Y., Gouzerh P., Amiard J.C., Amiard-Triquet C., Berthet B., Baud J.P. 1988. Effets chimiques et cytologiques de la contamination expérimentale de l'huitre *Crassostrea gigas* Thunberg par l'argent administré sous forme dissoute et par voie alimentaire. *Canadian Journal of Fisheries and Aquatic Sciences* 45: 1827-1844.
- .: McCarthy M., Carroll D.L., Ringwood A.H. 2013. Tissue specific response of oysters, *Crassostrea virginica*, to silver nanoparticles. *Aquatic Toxicology* 138-139: 123-128.
- .: McGuillicuddy E., Murray I., Kavanagh S., Morrison L., Fogarty A., Cormican M., Dockery P., Prendergast M., Rowan N., Morris D. 2017. Silver nanoparticles in the environment: sources, detection and ecotoxicology. *Science of the Total Environment* 575: 231-246.
- .: McTeer J., Dean A.P., White K.N., Pittman J.K. 2014. Bioaccumulation of silver nanoparticles into *Daphnia magna* from a freshwater algal diet and the impact of phosphate availability. *Nanotoxicology* 8: 305-316.
- .: Miao A.J., Luo Z., Chen C.S., Chin W.C., Santschi P.H., Quigg A. 2010. Intracellular uptake: a possible mechanism for silver engineered nanoparticle toxicity to a freshwater alga *Ochromonas danica*. *PLoS ONE* 5: e15196.
- .: Moore M.N. 2006. Do nanoparticles present ecotoxicological risks for the health of the aquatic environment? *Environment International* 32: 967-976.
- .: Navarro E., Piccapietra F., Wagner B., Marconi F., Kaegi R., Odzak N., Sigg L., Behra R. 2008. Toxicity of silver nanoparticles to *Chlamydomonas reinhardtii*. *Environmental Science and Technology* 42: 8959-8964.
- .: Newell R.I.E. 1989. Species profiles: life histories and environmental requirements of coastal fishes and invertebrates (North and Mid-Atlantic)-blue mussel. *US Fish Wildlife Service for Biology and Reproduction* 82 (11.102). US Army Corps of Engineers, TR EL 82-4.
- .: Odzak N., Kistler D., Behra R., Sigg L. 2014. Dissolution of metal and metal oxide nanoparticles in aqueous media. *Environmental Pollution* 191: 132-138.
- .: Ortiz-Zarragoitia M., Cajaraville M.P. 2010. Intersex and oocyte atresia in a mussel population from the Biosphere's Reserve of Urdaibai (Bay of Biscay). *Ecotoxicology and Environmental Safety* 73: 693-701.
- .: Ortiz-Zarragoitia M., Garmendia L., Barbero M.C., Serrano T., Marigómez I., Cajaraville M.P. 2011. Effects of the fuel oil spilled by the *Prestige* tanker on reproduction parameters of wild mussel populations. *Journal of Environmental Monitoring* 13: 84-94.

- ∴ Piccapietra F., Gil Allué C., Sigg L., Behra R. 2012. Intracellular silver accumulation in *Chlamydomonas reinhardtii* upon exposure to carbonate coated silver nanoparticles and silver nitrate. *Environmental Science and Technology* 46: 7390-7397.
- ∴ Pipe R.K. 1987. Oogenesis in the marine mussel *Mytilus edulis*: an ultrastructural study. *Marine Biology* 95: 405-414.
- ∴ Pipe R.K., Coles J.A., Farley S.R. 1995. Assays for measuring immune response in the mussel *Mytilus edulis*. *Techniques in Fish Immunology* 4: 93-100.
- ∴ Ratte T.H. 1999. Bioaccumulation and toxicity of silver compounds: a review. *Environmental Toxicology and Chemistry* 18: 89-108.
- ∴ Rementería A., Mikolaczyk M., Lanceleur L., Blanc G., Soto M., Schäfer J., Zaldibar B. 2016. Assessment of the effects of Cu and Ag in oyster *Crassostrea gigas* (Thunberg, 1793) using a battery of cell and tissue level biomarkers. *Marine Environmental Research* 122: 11-22.
- ∴ Ribeiro F., Gallego-Urrea J.A., Goodhead R.M., Van Gestel C.A., Moger J., Soares A.M., Loureiro S. 2015. Uptake and elimination kinetics of silver nanoparticles and silver nitrate by *Raphidocelis subcapitata*. The influence of silver behaviour in solution. *Nanotoxicology* 9: 686-695.
- ∴ Ribeiro F., Van Gestel C.A.M., Pavlaki M.D., Azevedo S., Soares A.M.V.M., Loureiro S. 2017. Bioaccumulation of silver in *Daphnia magna*: waterborne and dietary exposure to nanoparticles and dissolved silver. *Science of the Total Environment* 574: 1633- 1639.
- ∴ Ringwood A.H., McCarthy M., Bates T.C., Carrol D.L. 2010. The effects of silver nanoparticles on oyster embryos. *Marine Environmental Research* 69: S49-S51.
- ∴ Schiavo S., Duroudier N., Bilbao E., Mikolaczyk M., Schäfer J., Cajaraville M.P., Manzo S. 2017. Effects of PVP/PEI coated and uncoated silver NPs and PVP/PEI coating agent on three species of marine microalgae. *Science of the Total Environment* 577: 45-53.
- ∴ Sendra M., Blasco J., Araújo C.V.M. 2017. Is the cell wall of marine phytoplankton a protective barrier or a nanoparticle interaction site? Toxicological responses of *Chlorella autotrophica* and *Dunaliella salina* to Ag and CeO₂ nanoparticles. *Ecological Indicators*. <http://dx.doi.org/10.1016/j.ecolind.2017.08.050>.
- ∴ Sendra M., Volland M., Balbi T., Fabbri R., Yeste M.P., Gatica J.M., Canesi L., Blasco J. 2018. Cytotoxicity of CeO₂ nanoparticles using *in vitro* assay with *Mytilus galloprovincialis* hemocytes: relevance of zeta potential, shape and biocorona formation. *Aquatic Toxicology* 200: 13-20.
- ∴ Seoane S., Eikrem W., Arluzea J., Orive E. 2009. Haptophytes of the Nervión River estuary, northern Spain. *Botanica Marina* 52: 47-59.
- ∴ Sikder M., Lead J.R., Chandler G.T., Baalousha M. 2017. A rapid approach for measuring silver nanoparticle concentration and dissolution in seawater by UV-Vis. *Science of the Total Environment* 618: 597-607.
- ∴ Sokal R.R., Rohlf F.J. 1969. *Introduction to Biostatistics*, 2nd Edition. Dover Publications Inc. Mineola, New York.

- ∴ Soto M., Zaldibar B., Cancio I., Taylor M.G., Turner M., Morgan A.J., Marigómez I. 2002. Subcellular distribution of cadmium and its cellular ligands in mussel digestive gland cells as revealed by combined autometallography and X-ray microprobe analysis. *The Histochemical Journal* 34: 273-280.
- ∴ Tiede K., Hassellöv M., Breitbarth E., Chaudhry Q., Boxall A.B.A. 2009. Considerations for environmental fate and ecotoxicity testing to support environmental risk assessments for engineered nanoparticles. *Journal of Chromatography A* 1216: 503-509.
- ∴ Vance M.E., Kuiken T., Vejerano E.P., McGinnis S.P., Hochella M.F. Jr., Rejeski D., Hull M.S. 2015. Nanotechnology in the real world: redeveloping the nanomaterial consumer products inventory. *Beilstein Journal of Nanotechnology* 6: 1769-1780.
- ∴ Volland M., Hampel M., Katsumiti A., Yeste M.P., Gatica J.M., Cajaraville M.P., Blasco J. 2018. Synthesis methods influence characteristics, behaviour and toxicity of bare CuO NPs compared to bulk CuO and ionic Cu after *in vitro* exposure of *Ruditapes philippinarum* hemocytes. *Aquatic Toxicology* 199: 285-295.
- ∴ Wang H., Burgess R.M., Cantwell M.G., Portis L.M., Perron M.M., Wu F., Ho K.T. 2014. Stability and aggregation of silver and titanium dioxide nanoparticles in seawater: role of salinity and dissolved organic carbon. *Environmental Toxicology and Chemistry* 33: 1023-1029.
- ∴ Wang J., Wang W.X. 2014. Low bioavailability of silver nanoparticles presents trophic toxicity to marine medaka (*Orzias melastigma*). *Environmental Science and Technology* 48: 8152-8161.
- ∴ Wang S., Lv J., Ma J., Zhang S. 2016. Cellular internalization and intracellular biotransformation of silver nanoparticles in *Chlamydomonas reinhardtii*. *Nanotoxicology* 10: 1129-1135.
- ∴ Yoo-Iam M., Chaichana R., Satapanajarua T. 2014. Toxicity, bioaccumulation and biomagnification of silver nanoparticles in green algae (*Chlorella* sp.), water flea (*Moina macrocopa*), blood worm (*Chironomus* spp.) and silver barb (*Barbonymus gonionotus*). *Chemical Speciation and Bioavailability* 26: 257-265.
- ∴ Yue Y., Li X., Sigg L., Suter M.J.F., Pillai S., Behra R., Schirmer K. 2017. Interaction of silver nanoparticles with algae and fish cells: a side-by-side comparison. *Journal of Nanobiotechnology* 15: 16-26.
- ∴ Zhang C., Hu Z., Deng B. 2016. Silver nanoparticles in aquatic environments: physicochemical behavior and antimicrobial mechanisms. *Water Research* 88: 403-427.
- ∴ Zhang W., Xiao B., Fang T. 2018. Chemical transformation of silver nanoparticles in aquatic environments: mechanism, morphology and toxicity. *Chemosphere* 191: 324-334.
- ∴ Zhu C.J., Lee Y.K. 1997. Determination of biomass dry weight of marine microalgae. *Journal of Applied Phycology* 9: 189-194.
- ∴ Zook J.M., Long S.E., Cleveland D., Geronimo C.L.A., MacCuspie R.I. 2011. Measuring silver nanoparticle dissolution in complex biological and environmental matrices using UV-visible absorbance. *Analytical and Bioanalytical Chemistry* 401: 1993-2002.



CHAPTER 2

Cell and tissue level responses in mussels *Mytilus galloprovincialis* exposed to PVP/PEI coated silver nanoparticles through the diet at different seasons

This chapter is being prepared for submission to:

DUROUDIER N., KATSUMITI A., MIKOLACZYK M., SCHÄFER J., BILBAO E., CAJARAVILLE MP. Cell and tissue level responses in mussels *Mytilus galloprovincialis* exposed to PVP/PEI coated silver nanoparticles through the diet at different seasons. Nanotoxicology.

Parts of this chapter have been presented at:

NANOSPAIN-TOXICOLOGY CONFERENCE 2015, IMAGINENANO, Bilbao, 10-13 March 2015

DUROUDIER, N; KATSUMITI, A; JIMENO-ROMERO, A; MIKOLACZYK, M; SCHÄFER, J; BILBAO, E; CAJARAVILLE, MP. Molecular and cellular responses of mussels *Mytilus galloprovincialis* fed with the microalgae *Isochrysis galbana* exposed to PVP/PEI-coated silver nanoparticles at different seasons. Platform and poster presentation.

25th ANNUAL MEETING OF THE SOCIETY OF ENVIRONMENTAL TOXICOLOGY AND CHEMISTRY (SETAC)-EUROPE, Barcelona, 3-7 May 2015.

DUROUDIER, N; KATSUMITI, A; JIMENO-ROMERO, A; MIKOLACZYK, M; J SCHÄFER, G; BILBAO, E; CAJARAVILLE, MP. Bioaccumulation of silver and genotoxic effects in mussels *Mytilus galloprovincialis* exposed to PVP/PEI-coated silver nanoparticles through the diet at different seasons. Platform presentation.

10th IBERIAN and 7th IBERO-AMERICAN CONGRESS ON ENVIRONMENTAL CONTAMINATION AND TOXICOLOGY, Vila Real (Portugal), 14-17 July 2015.

CAJARAVILLE, MP; DUROUDIER, N; GARCÍA-VELASCO, N; LACAVE, JM; FANJUL, A; MIKOLACZYK, M; JIMENO-ROMERO, A; KATSUMITI, A; SCHÄFER, J; BILBAO, E; SOTO, M; ORBEA, A. Mechanisms of action and toxicity of silver nanoparticles in model aquatic and terrestrial organisms. Platform presentation.

FINAL CONFERENCE OF THE COST ACTION ES1205 "Engineered Nanomaterial from Wastewater Treatment & Stormwater to Rivers", Aveiro (Portugal), 7-8 February 2017.

DUROUDIER, N; KATSUMITI, A; MIKOLACZYK, M; CARDOSO, C; SCHÄFER, J; BEBIANNO, MJ; BILBAO, E; CAJARAVILLE, MP. Molecular and cellular effects of silver nanoparticles on adult mussels exposed through the diet and on their offspring. Platform presentation.

ABSTRACT

Silver nanoparticles (Ag NPs) are present in numerous consumer products due to their antimicrobial and other unique properties, thus concerns about their potential input into aquatic ecosystems are increasing. Toxicity of Ag NPs in waterborne exposed aquatic organisms has been widely investigated, but studies assessing the potential toxic effects caused after ingestion through the food web, especially at environmentally relevant concentrations, remain scarce. Further, the possibility that effects may differ depending on the season is still unexplored. Thus, the aim of this work was to assess cell and tissue level responses in mussels *Mytilus galloprovincialis* dietarily exposed to poly N-vinyl-2-pyrrolidone/polyethyleneimine (PVP/PEI) coated 5 nm Ag NPs for 1, 7 and 21 days both in autumn and in spring. For this, mussels were fed daily with microalgae *Isochrysis galbana* previously exposed for 24 hours to a dose close to environmentally relevant concentrations (1 µg Ag/L Ag NPs) in spring and to a higher dose (10 µg Ag/L Ag NPs) both in autumn and in spring. Mussels fed with microalgae exposed to the high dose significantly accumulated Ag after 21 days in both seasons, higher levels being measured in autumn compared to spring. Intralysosomal metal accumulation measured in digestive gland of mussels and time- and dose-dependent reduction of mussels health status was similar in both seasons. DNA strand breaks increased significantly in hemocytes at both exposure doses along the 21 days in spring and micronuclei frequency showed an increasing trend after 1 and 7 days of exposure to 1 µg Ag/L Ag NPs in spring and to 10 µg Ag/L in both seasons. Values decreased after 21 days of exposure in all the cases. In conclusion, PVP/PEI coated 5 nm Ag NPs ingested through the food web were significantly accumulated in mussel tissues and caused adverse cellular effects both in autumn and in spring.

Keywords: silver nanoparticles, dietary exposure, mussels *Mytilus galloprovincialis*, Ag accumulation, cell and tissue level responses, genotoxicity.

RESUMEN

Las nanopartículas de plata (NPs de Ag) se encuentran en numerosos productos de consumo debido a sus propiedades antimicrobianas y otras propiedades únicas. Por ello, la preocupación acerca de su entrada en los ecosistemas acuáticos está creciendo. La toxicidad de las NPs de Ag en organismos acuáticos expuestos a través del agua se ha estudiado ampliamente sin embargo, apenas hay estudios que evalúen su posible toxicidad tras la ingestión a través de la dieta, especialmente a concentraciones ambientalmente relevantes. Además, la posibilidad de que estos efectos difieran dependiendo de la estación del año sigue siendo desconocida. Por todo ello, el objetivo de este trabajo fue evaluar las respuestas a nivel celular y tisular en mejillones *Mytilus galloprovincialis* expuestos a NPs de Ag de 5 nm recubiertas de N-vinyl-2-pirrolidona/polietilenamina (PVP/PEI) a través de la dieta durante 1, 7 y 21 días tanto en otoño como en primavera. Para ello, los mejillones se alimentaron diariamente con microalgas *Isochrysis galabana* previamente expuestas durante 24 horas a una dosis cercana a las concentraciones ambientalmente relevantes (1 µg Ag/L NPs de Ag) en primavera y a una concentración mayor de 10 µg Ag/L NPs de Ag tanto en otoño como en primavera. Los mejillones alimentados con algas expuestas a la dosis alta acumularon Ag significativamente tras 21 días de exposición en las dos estaciones, midiéndose mayores concentraciones en otoño que en primavera. La acumulación intralisosómica de metal medida en la glándula digestiva, así como la reducción en el estado general de los mejillones fueron dependientes del tiempo y la dosis, siendo la respuesta similar en ambas estaciones. La rotura de hebras del DNA en los hemocitos aumentó significativamente tras la exposición a las dos concentraciones durante 21 días y la frecuencia de micronúcleos mostró una tendencia creciente tras 1 y 7 días de exposición a 1 µg Ag/L NPs de Ag en primavera y a 10 µg Ag/L NPs de Ag en ambas estaciones. Los valores decrecieron tras 21 días de exposición en todos los casos. En conclusión, las NPs de Ag de 5 nm recubiertas de PVP/PEI ingeridas a través de la dieta se acumularon significativamente en los tejidos de los mejillones y provocaron efectos adversos a nivel celular tanto en otoño como en primavera.

Palabras clave: nanopartículas de plata, exposición vía dieta, mejillones *Mytilus galloprovincialis*, acumulación de Ag, respuestas a nivel celular y tisular, genotoxicidad.

1. INTRODUCTION

The input of anthropogenic contaminants to natural water systems has the potential to affect the health status of aquatic organisms altering ecosystem structure and function (De los Ríos et al., 2016). In this sense, biomarkers were proposed as sensitive early warning tools to assess the quality of aquatic environments (Cajaraville et al., 2000; Viarengo et al., 2007). Biomarkers are measurements at the molecular, biochemical or cellular level, which indicate that the organism has been exposed to pollutants (exposure biomarkers) and/or the magnitude of the organisms response to the pollutants (effect biomarkers) (McCarthy and Shugart, 1990). The integrated assessment of biomarkers of exposure (e.g. metallothionein levels, intralysosomal metal accumulation or peroxisome proliferation) together with effect biomarkers (e.g. genotoxicity, lysosomal membrane stability and tissue damage) has been widely applied in sentinel mussels for marine pollution monitoring (UNEP, 2004; Zorita et al., 2007a; Hylland et al., 2008; Garmendia et al., 2011; Marigómez et al., 2013; ICES, 2016; Dallarés et al., 2018) and in laboratory exposure scenarios for the assessment of biological effects caused by different pollutants (Orbea et al., 2002; Zorita et al., 2007b; Canesi et al., 2008; Ruiz et al., 2014; Banni et al., 2017). In the case of novel emerging pollutants, biomarkers have been successfully applied as a sensitive tool for evaluating the effects and mechanisms of action of different nanomaterials in aquatic invertebrates, especially in mussels (Canesi et al., 2014; Rocha et al., 2016; Jimeno-Romero et al., 2017a; 2017b; 2019).

Different nanomaterials, such as carbon nanotubes and silver nanoparticles (Ag NPs), have been identified as potentially present in waste (Marcoux et al., 2013). In fact, the release of Ag NPs into the aquatic environment is expected to rise (Giese et al., 2018) due to their increasing commercial and scientific applications related to their unique optical, catalytic and antimicrobial properties (Fabrega et al., 2011; Vance et al., 2015; Zhang et al., 2016; McGuillicuddy et al., 2017). The availability of methods for the proper detection and measurement of engineered NPs is a key aspect for understanding NPs fate and behaviour in the environment (António et al., 2015), but their quantification in complex natural matrices such as seawater, soils, sediments or tissues is still challenging (Von der Kammer et al. 2012; Sikder et al., 2017). In this sense, little is known about the potential adverse effects of Ag NPs in aquatic organisms at environmentally relevant concentrations. Concentrations ranging between 0.7 and 11.1 ng/L Ag NPs have been measured in effluents of waste water treatment plants over the seasons in Germany (Li et al., 2016). Nevertheless, predictions for aquatic environments based on modelling studies estimated Ag NP concentrations of up to 140 ng/L in European rivers (Blaser et

al., 2008; Gottschalk et al., 2009; Tiede et al., 2009; Dumont et al., 2015; Giese et al., 2018) and up to 40 µg/L in Taiwanese waters (Chio et al., 2012).

Bivalve molluscs are widely studied since they were identified as an important target group to assess NPs toxicity in marine environments (Moore, 2006; Canesi et al., 2012; Corsi et al., 2014). Mussels digestive gland is considered the main organ for NP accumulation, NPs cellular fate and effects differing according to the NP type and to experimental conditions (Canesi et al., 2012; Rocha et al., 2015; Canesi and Corsi, 2016). The digestive tubules of the digestive gland of mussels are composed of digestive and basophilic cells and under normal physiological conditions, the digestive cells outnumber basophilic cells (Cajaraville et al., 1990; Garmendia et al., 2011). However, under different stress situations, including exposure to pollutants such as metal-bearing NPs, the relative occurrence of basophilic cells increases (Rocha et al., 2016; Jimeno-Romero et al., 2017a; 2019). The endolysosomal system of digestive cells, due to its role in intracellular digestion of food particles, represents the main subcellular target for metallic NPs in bivalves (Moore, 2006; Canesi et al., 2012; Katsumiti et al., 2014; Rocha et al., 2015). The low pH (≈ 5.0) in lysosomes may favour the dissolution of metallic NPs and released free ions, together with the remaining NPs, could induce the hypersynthesis of lysosomal acid phosphatase enzyme and the generation of reactive oxygen species (ROS), finally attacking lysosomal membranes (Katsumiti et al., 2014). In fact, lysosomal membrane destabilization has been already measured in the digestive gland of mussels waterborne exposed to Ag NPs (Jimeno-Romero et al., 2017a) as well as to other metallic NPs (Balbi et al., 2014; Jimeno-Romero et al., 2016; 2017b; 2019).

Moreover, NPs can be potentially translocated from the digestive system to the hemolymph and to circulating hemocytes (Canesi and Corsi, 2016). Hemocytes are cells responsible for the immune defense (Cajaraville and Pal, 1995) and are considered important targets for metal-bearing NP toxicity (Canesi et al., 2010; Ciacci et al., 2012; Katsumiti et al., 2014; 2015a; 2015b; 2016; 2018). In fact, alterations in the phagocytic activity, reduction of cell viability, stimulation of lysosomal enzyme release, increase of ROS production as well as induction of lysosomal membrane destabilization and DNA damage have been widely reported in bivalve hemocytes after *in vitro* exposure to different metallic NPs (Canesi et al., 2010; Ciacci et al., 2012; Katsumiti et al., 2014; 2015a; 2015b; 2016; 2018). DNA damage is a stress index usually considered of great importance to define the physiological status of organisms (Cajaraville et al., 2000). DNA damage in mussel hemocytes exposed to metallic NPs is frequently assessed by the comet assay (Gomes et al., 2013; Katsumiti et al., 2014; 2015b; 2018). However, the combination of the comet assay and cytogenotoxic assays such as the micronuclei test is considered a more

realistic approach to assess the nano-genotoxic effects in bivalves (Canesi et al., 2014; Rocha et al., 2014) since the comet assay enables identification of reversible DNA strand breaks while the micronuclei test determines chromosomal damage induced by clastogenic (DNA breakage) or aneugenic (abnormal segregation) effects (Bolognesi and Fenech, 2012).

The application of a battery of biomarkers has helped to understand the effects of Ag NPs on *in vivo* waterborne exposed marine bivalves (Ringwood et al., 2010; Buffet et al., 2013; 2014; Gomes et al., 2013; 2014; McCarthy et al., 2013; Bebianno et al., 2015; Jimeno-Romero et al., 2017a), but there is scarce information about the transfer of engineered NPs through the food web (Tangaa et al., 2016). In fact, few works have assessed potential toxic effects of Ag NPs ingested through the food web in marine bivalves (Buffet et al., 2013). In *Scrobicularia plana* clams, even if Ag bioaccumulation was higher in waterborne exposed clams than in dietary exposed ones, activity of the antioxidant enzymes (catalase, glutathione S-transferase and superoxide dismutase) was more affected compared to controls after dietary than after waterborne exposure to lactate stabilized 40 nm Ag NPs. The dietary exposure of *Mytilus galloprovincialis* mussels to PVP/PEI coated 5 nm Ag NPs caused Ag accumulation in adults, affected spawning success in females and induced abnormal embryo development in their offspring (see Chapter 1). Further, the dietary exposure to the same Ag NPs altered the transcriptome and proteome of mussels digestive gland both in autumn and in spring (see Chapter 2 and Chapter 3).

In general, season is not considered in ecotoxicological studies even if seasonal variations in biomarker responses such as lysosomal parameters and DNA damage have been reported in mussels (Pisanelli et al., 2009; Hagger et al., 2010; Nahrgang et al., 2013; Schmidt et al., 2013; Balbi et al., 2017). These changes are driven by the interaction between abiotic factors in the environment, such as temperature, food availability and oxygen levels, and to biotic factors, as their reproductive and physiological state (Bayne and Widdows, 1978; Solé et al., 1995; Cancio et al., 1999; Sheehan and Power, 1999).

Thus, the aim of the present work was to assess Ag accumulation and cell and tissue level biomarkers in mussels exposed to Ag NPs through the diet using a dose close to environmentally relevant concentrations (1 µg Ag/L Ag NPs) and a higher dose of 10 µg Ag/L Ag NPs in two different seasons, autumn and spring.

2. MATERIALS AND METHODS

2.1. Obtention and characterization of Ag NPs

Ag NPs coated with poly N-vinyl-2-pyrrolidone/polyethyleneimine (PVP/PEI; 77%:23% at a concentration of 104 g/L in the final dispersion) were purchased as a stable aqueous suspension from Nanogap (O Milladoiro, Galicia, Spain). According to the manufacturers' information, PVP/PEI coated Ag NPs showed an average size of 5.08 ± 2.03 nm (see Appendix) and a zeta potential of $+18.6 \pm 7.9$ mV in distilled water.

Particle size distribution and dissolution of PVP/PEI coated 5 nm Ag NPs in seawater (SW) were reported in Chapter 1. Briefly, PVP/PEI coated 5 nm Ag NPs dispersed in SW immediately reached a mean size of roughly 97 nm according to Dynamic Light Scattering measurements using a Zetasizer Nano Z (Malvern Instruments Ltd., Worcestershire, UK). After 24 hours, particle size remained stable around 94-96 nm. Dissolution of Ag NPs in SW was detected along the 72 hours of experimentation. After 12 hours, Ag NPs released around 4% of Ag ions increasing the dissolution to around 14% at 24 hours. After 48 hours ~17% of Ag ions were released from Ag NPs and at 72 hours, dissolution increased to 20% (see Chapter 1).

2.2. Experimental design

Mussels *Mytilus galloprovincialis* 3.5-4.5 cm in shell length were collected in autumn (November 2013) and spring (March 2014) from San Felipe, Galicia (43° 27.599'N, 8° 17.904'W). Upon arrival to the laboratory, mussels were placed in an acclimation tank with natural filtered SW (temperature =15.6°C, salinity =28.7‰, conductivity =36.4 mS/cm, pH =7.7) at light regime 12 h/12 h L/D for 10 days. Mussels were maintained 5 days without feeding and then mussels were fed with *Isochrysis galbana* microalgae (20×10^6 cells/ mussel-day) for other 5 days. For that, microalgae were cultured with natural filtered (0.2 μ m) and sterilized SW at 20°C under cool continuous white fluorescent light (GRO-LUX F58W) with constant aeration in reactors at a concentration of 6×10^6 cells/mL. Commercial F2 algae medium (Fritz Aquatics, USA) was supplied according to the manufacturer's instructions. Concentration of microalgae was checked every day before feeding mussels.

After the acclimation period, mussels were distributed in different high density polypropylene containers (250 L) containing 240 mussels per tank. Mussels in the control tank were fed for 21 days with the microalgae *Isochrysis galbana* (20×10^6 cells/mussel-day) and mussels in the treatment tanks were fed for 21 days with the

same ration of microalgae (20×10^6 cells/mussel-day) previously exposed for 24 hours to $1 \mu\text{g Ag/L Ag NPs}$ in spring or to $10 \mu\text{g Ag/L Ag NPs}$ in autumn and in spring. The comparison between seasons only at the higher exposure dose was considered sufficient to study season-dependent cell and tissue level responses. Water was renewed every day before animal feeding. No mortality was recorded along the experimentation time.

After 1, 7 and 21 days of exposure, whole soft tissues of 20 mussels per experimental group were collected for chemical analysis. Hemolymph of 10 mussels per experimental group was extracted for genotoxicity assays and then, digestive glands were dissected out, and stored at -80°C until processing for lysosomal membrane stability test. Finally, whole soft tissues of 10 mussels per experimental group were fixed in 10% neutral buffered formalin in order to assess the intralysosomal metal accumulation in mussels digestive gland by autometallography as well as to quantify the volume density of basophilic cells. All samples were analyzed using blind codes.

2.3. Accumulation of Ag in mussel soft tissues

Soft tissues of 20 individuals per treatment and exposure time (1, 7 or 21 days) were pooled in 4 groups (4 pools of 5 individuals each) and lyophilized by a freeze-dryer (Telstar Cryodos) for 5 days. Afterwards, samples (20–150 mg) were mineralized using 1.4 mL of HNO_3 (14 M, PlasmaPur) and 2 mL of HCl (12 M, PlasmaPur), according to Daskalakis (1996). Briefly, closed tubes were digested for 3 hours on a hot plate at 90°C (DigiPREP MS; SCP SCIENCE). After cooling, digestates were diluted and Ag concentration was measured by ICP-MS (Thermo, X Series II) using external calibration (made of commercially available standard solutions PLASMACAL, SCP Science). Accuracy ($>90\%$) and precision ($<5\%$, Relative Standard Deviation) were controlled during each analytical session by parallel analysis of international referenced certified materials (TORT 2, IAEA 407). Results are expressed as $\mu\text{g Ag/g dry weight (d.w.)}$.

2.4. Intralysosomal metal accumulation by autometallography

Whole soft tissues of 10 mussels per treatment and exposure time (1, 7 or 21 days) were fixed in 10% neutral buffered formalin for 24 hours and then were routinely processed for paraffin embedding using a Leica Tissue processor ASP 3000 (Leica Instruments, Wetzlar, Germany). Then, histological cross sections ($5 \mu\text{m}$ in thickness) of all tissues were cut in a Leica RM2255 microtome (Leica Instruments). Intralysosomal metal accumulation was determined on histological sections of

mussels dietarily exposed to Ag NPs for 21 days. Slides containing the histological sections were dewaxed in xylene, rehydrated through several baths of ethanol (100%, 96% and 70%) and dried at room temperature. Autometallographical staining was carried out using the BBIInternational Silver Enhancing Kit for Light and Electron Microscopy (Agar Scientific Ltd., Stansted, UK) following manufacturer's recommendations. Briefly, sections were covered with the emulsion (initiator and enhancer, 1:1) and incubated in a moisture chamber for 22 minutes in darkness. Then, the reaction was stopped washing immediately the slides in tap water for 2 minutes. Slides were mounted with Kaiser's glycerin and observed under the light microscope to determine the presence of black silver deposits (BSDs) in all tissues. BSDs were quantified in digestive cells under the light microscope (x100 magnification) using the BMS software (Sevisan, Leioa, Spain) as described in Soto et al. (2002). Five areas were randomly measured in each section of each digestive gland in order to calculate the volume density of BSDs ($V_{V_{\text{BSD}}}$) as the volume occupied by BSDs with respect to the volume of digestive cells ($\mu\text{m}^3/\mu\text{m}^3$).

2.5. Lysosomal membrane stability

Digestive glands of 5 mussels per treatment and exposure time (1, 7 or 21 days) were dissected out, snap frozen in liquid nitrogen and stored at -80°C . Eight serial sections (10 μm thick) of each frozen digestive gland were cut in a Leica CM 3000 cryotome (Leica Instruments, Wetzlar, Germany) onto successive serial slides and stored at -40°C until processing. The stability of the lysosomal membrane was based on the time of acid labilization required to produce the maximum staining intensity in digestive cell lysosomes after the detection of N-acetylhexosaminidase activity according to UNEP/RAMOGÉ (1999). Results are expressed as time in minutes (min).

2.6. Cell type composition of the digestive tubules

Histological sections obtained from the same paraffin embedded samples processed in section 2.4. were stained with hematoxylin-eosin (Gamble and Wilson, 2002). Digestive and basophilic cells were counted in three randomly selected areas with a drawing tube attached to a Leitz Laborlux S (Wetzlar, Germany) light microscope at 40x magnification. Then, changes in the cell-type composition of the digestive tubule epithelium were determined as volume density of basophilic cells ($V_{V_{\text{BAS}}}$) after applying a stereological point counting procedure (Soto et al., 2002): $V_{V_{\text{BAS}}} = V_{\text{BAS}} / (V_{\text{BAS}} + V_{\text{DC}})$; where V_{BAS} is the volume of basophilic cells and V_{DC} is the volume of digestive cells. $V_{V_{\text{BAS}}}$ is expressed as $\mu\text{m}^3/\mu\text{m}^3$.

2.7. Genotoxicity in hemocytes

Hemolymph of 10 mussels per treatment and exposure time (1, 7 or 21 days) was extracted and transferred to a Falcon tube containing 2 mL of 10 mM EDTA/SW for the micronuclei test in both seasons and the comet assay in spring.

2.7.1. *Micronuclei test*

Hemolymph solution (200 μ L) of 8 mussels was cytocentrifuged at 700 rpm for 2 min using a cytocentrifuge (Cytopro® Cytocentrifuge Series 2, ELITechGroup, Utah, United States). Slides were air dried for 20 min and then hemocytes were stained using the Hemacolor® Kit (Merck, Darmstadt, Germany) following manufacturer's instructions. Slides were air dried overnight and then mounted with DPX mounting medium. 1000 randomly selected agranular hemocytes per mussel were examined under the light microscope (Nikon Eclipse Ni microscope, Nikon Instruments, Tokyo, Japan) at 100x magnification. Micronucleated cells were classified following the accepted criteria for mussels: well-preserved cell cytoplasm, micronuclei (MN) not touching the main nucleus, similar or weaker staining than the main nucleus and size of MN \leq 1/3 in comparison to the main nucleus (Venier et al., 1997). Results are reported in % frequencies.

2.7.2. *Comet assay*

Comet assay was performed in mussel hemocytes according to Raisuddin and Jha (2004) with some modifications reported by Katsumiti et al. (2014). Samples obtained in autumn were accidentally lost and thus only samples obtained in spring were analyzed. Briefly, 100 μ L of hemolymph of 10 mussels per experimental group were centrifuged (300 g x 10 mins at 4°C) and supernatant was removed. The pellet containing hemocytes was resuspended with 200 μ L of 0.5% low melting point agarose. Two drops (100 μ L each) of hemocytes suspension were placed on the frosted ends of slides coated with normal melting point agarose (1% in phosphate buffered saline solution). Slides were chilled for 10 min on ice and then immersed in chilled lysis solution (2.5 M NaCl, 100 mM EDTA, 10 mM Tris base, 1% N-lauroyl-sarcosine sodium salt, 1% Triton X-100, and 10% DMSO; adjusted to pH 10) for 1 hour in darkness. Then, slides were washed twice with distilled water and transferred to an electrophoresis tank containing electrophoresis buffer (150 mM NaOH and 300 mM EDTA; pH 13). After 20 min of incubation, electrophoresis was carried out for 30 min (300 mA, 25 V). Finally, samples were immersed in neutralization buffer (0.4 M Tris-HCl buffer; pH 7.5) for 10 minutes, fixed with

methanol (-20°C) for 3 min and stored at 4°C until image analysis. For that, samples were stained with 20 µL of ethidium bromide (2 µg/mL in distilled water) and directly observed under an Olympus BX61 fluorescence microscope (Olympus optical Co., Hamburg, Germany). Quality of samples obtained in autumn was not good enough, thus, only samples belonging to spring were measured. 100 randomly selected cells were analyzed from each slide (50 in each gel from duplicate slides) and scored using the Komet 5.5 image analysis software (Andor Imaging, Liverpool, UK). Results are expressed as percentage (%) of tail DNA.

2.8. Statistical analysis

Statistical analyses were conducted using the statistical package SPSS v.22 (SPSS Inc., IBM Company, Chicago, USA). Prior to statistical analysis, results represented as percentages were subjected to arcsine transformation (Sokal and Rohlf, 1969). The Mann-Whitney's U test for pairwise comparisons in autumn and the Kruskal-Wallis test followed by the Dunn's test for multiple comparisons in spring were used to set significant differences with respect to controls. Season-dependent differences were established only at the higher exposure dose within each exposure time based on the Kruskal-Wallis test followed by the Dunn's test in all studied endpoints. Significance level was globally set at 5% ($p < 0.05$).

3. RESULTS

3.1. Accumulation of Ag in mussel soft tissues

Ag was not accumulated after 1 day of dietary exposure to 1 or 10 µg Ag/L Ag NPs in autumn nor in spring (Figure 1 A,B). After 7 days of dietary exposure to 10 µg Ag/L Ag NPs, Ag was significantly accumulated in spring (Figure 1B) and Ag accumulation was significantly higher in spring in comparison to autumn (Figure 1 A,B). Ag was significantly accumulated after 21 days of dietary exposure to 10 µg Ag/L Ag NPs both in autumn (Figure 1 A) and in spring (Figure 1B). Ag accumulation in mussel soft tissues after 21 days of exposure to 10 µg Ag/L Ag NPs was significantly higher in autumn (0.73 µg Ag/g d.w.) than in spring (0.35 µg Ag/g d.w.) (Figure 1 A,B).

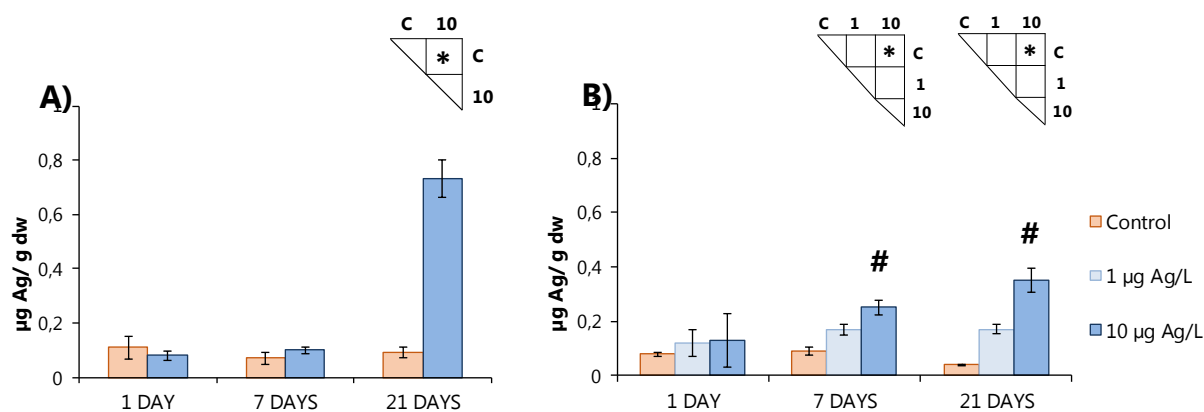


Figure 1. Bioaccumulation of Ag in mussels ($\mu\text{g Ag/g d.w.}$) exposed through the diet for 1, 7 and 21 days to **A)** $10 \mu\text{g Ag/L}$ Ag NPs in autumn and to **B)** $1 \mu\text{g Ag/L}$ or $10 \mu\text{g Ag/L}$ of Ag NPs in spring. Values are given as means \pm S.D. Mean values belong to 4 pools of 5 individuals per exposure group. Significant differences with respect to controls based on the Mann-Whitney's U test in autumn and the Dunn's test in spring are shown in the upper triangular matrices ($p < 0.05$). Significant differences ($p < 0.05$) between seasons within the same day are indicated with #.

3.2. Intralysosomal metal accumulation by autometallography

The volume density of BSDs present in digestive cell lysosomes revealed that in both seasons intralysosomal metal accumulation was significantly higher after the dietary exposure to $10 \mu\text{g Ag/L}$ Ag NPs in comparison to non-exposed mussels (Figure 2 A,B). No significant differences in intralysosomal metal accumulation were observed between seasons (Figure 2 A,B).

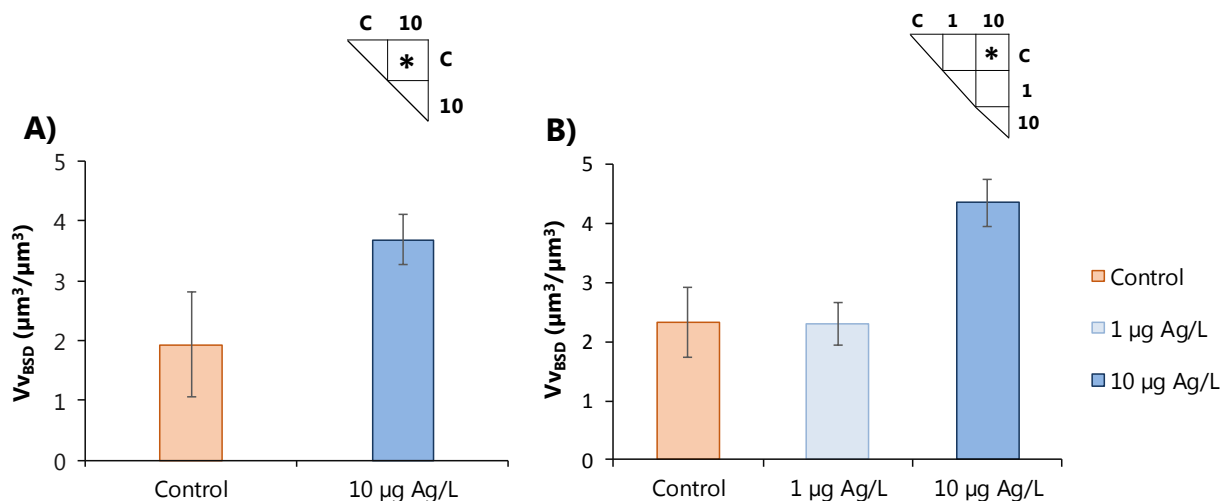


Figure 2. Intralysosomal metal accumulation as volume density of BSDs ($Vv_{\text{BSD}}; \mu\text{m}^3/\mu\text{m}^3$) in mussel digestive cells after 21 days of dietary exposure to **A)** $10 \mu\text{g Ag/L}$ of Ag NPs in autumn and to **B)** $1 \mu\text{g Ag/L}$ or to $10 \mu\text{g Ag/L}$ of Ag NPs in spring. Values are given as means \pm S.D. Significant differences with respect to controls based on the Mann-Whitney's U test in autumn and the Dunn's test in spring are shown by asterisks ($p < 0.05$).

3.3. Alterations in lysosomal membrane stability

A significant reduction of lysosomal membrane stability was measured in both seasons after the dietary exposure of mussels to 10 $\mu\text{g Ag/L}$ Ag NPs (Figure 3 A,B). Both in autumn and in spring, lysosomal membrane stability was significantly reduced in exposed mussels compared to non-exposed ones at all exposure times (Figure 3 A,B). A dose-dependent response was observed in spring, although differences with respect to controls at 1 $\mu\text{g Ag/L}$ Ag NPs were not significant (Figure 3B). Mussels lysosomal membrane stability was similarly affected in both seasons (Figure 3 A,B).

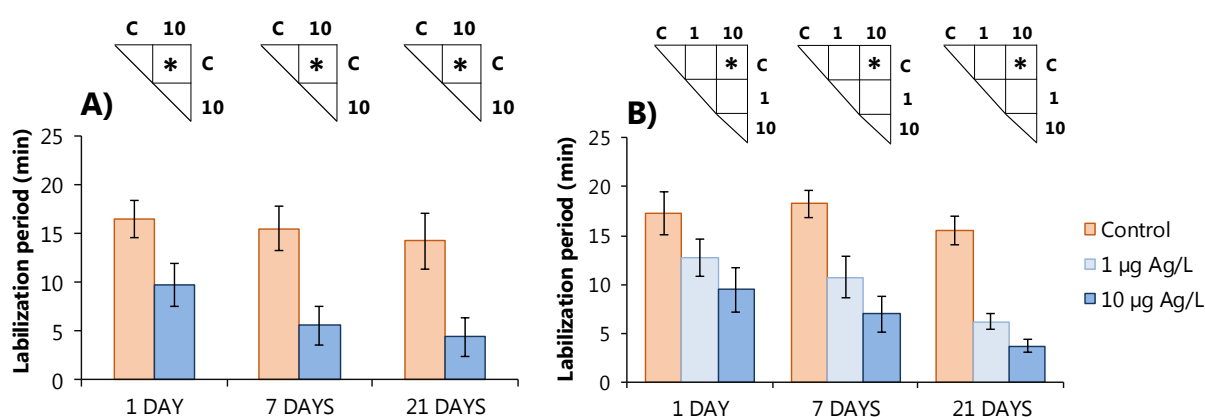


Figure 3. Labilization period (min) of lysosomal membrane in mussels digestive cells after 1, 7 and 21 days of dietary exposure to **A)** 10 $\mu\text{g Ag/L}$ Ag NPs in autumn and to **B)** 1 $\mu\text{g Ag/L}$ or 10 $\mu\text{g Ag/L}$ of Ag NPs in spring. Values are given as means \pm S.D. Significant differences with respect to controls based on the Mann-Whitney's U test in autumn and the Dunn's test in spring are shown by asterisks ($p < 0.05$).

3.4. Cell type composition of the digestive tubules

The volume density of basophilic cells of mussels digestive gland epithelium was not altered after the dietary exposure to 10 $\mu\text{g Ag/L}$ Ag NPs in autumn (Figure 4A) and 1 $\mu\text{g Ag/L}$ or 10 $\mu\text{g Ag/L}$ Ag NPs in spring (Figure 4B) for 1, 7 and 21 days. In non-exposed mussels, the volume density of basophilic cells was significantly higher in spring compared to autumn at day 1 (Figure 4 A,B).

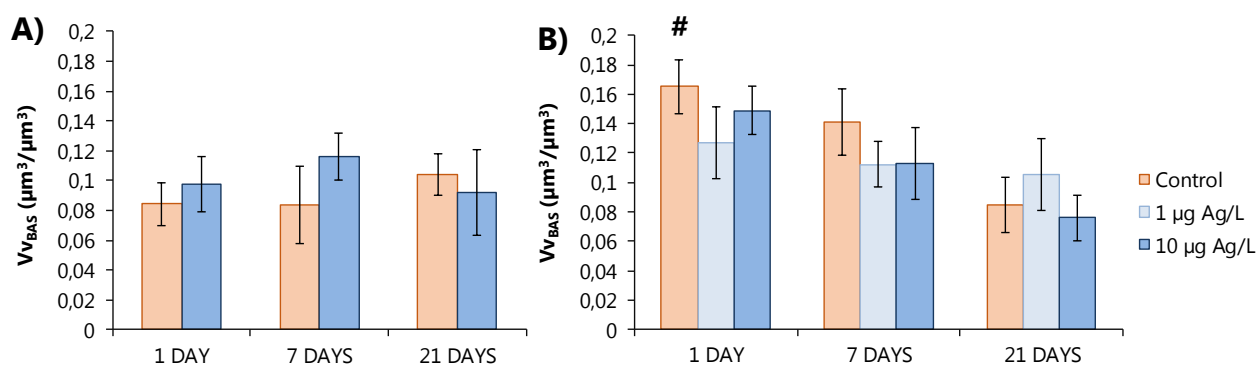


Figure 4. Volume density of basophilic cells (Vv_{BAS} ; $\mu\text{m}^3/\mu\text{m}^3$) in the digestive tubules of mussels exposed through the diet to **A)** 10 μg Ag/L Ag NPs in autumn and to **B)** 1 μg Ag/L or 10 μg Ag/L of Ag NPs in spring for 1, 7 and 21 days. Values are given as means \pm S.E. No significant differences with respect to controls were observed. Significant differences ($p < 0.05$) between seasons within the same day are indicated with #.

3.5. Genotoxicity in hemocytes

3.5.1. Micronuclei test

In autumn, micronuclei frequency increased after 1, 7 and 21 days of dietary exposure to 10 μg Ag/L Ag NPs but differences with respect to controls were significant only at day 1 (Table 1). In spring, the increase in micronuclei frequency was dose-dependent after 1 and 7 days of dietary exposure being this increase significant with respect to controls after the dietary exposure to 10 μg Ag/L Ag NPs for 7 days (Table 1). The response to 10 μg Ag/L Ag NPs was similar in both seasons showing an increasing trend in micronuclei frequency along the 21 days of exposure with respect to controls, but a decrease in micronuclei levels at day 21 compared to days 1 and 7 (Table 1). Season-dependent differences were not observed in the micronuclei frequency within the same exposure time.

Table 1. Micronuclei frequency (‰) in hemocytes of mussels exposed through the diet to 10 μg Ag/L Ag NPs in autumn and to 1 μg Ag/L or 10 μg Ag/L of Ag NPs in spring. Values are given as means \pm S.E. Significant differences with respect to controls based on the Mann-Whitney's U test in autumn and the Dunn's test in spring are shown by asterisks ($p < 0.05$).

	AUTUMN			SPRING		
	1 DAY	7 DAYS	21 DAYS	1 DAY	7 DAYS	21 DAYS
Control	0.125 \pm 0.125	0.75 \pm 0.313	0.25 \pm 0.164	0.75 \pm 0.366	0.375 \pm 0.183	0.875 \pm 0.398
1 μg Ag/L Ag NPs	-	-	-	1.85 \pm 0.852	1 \pm 0.267	1.28 \pm 0.443
10 μg Ag/L Ag NPs	1.625 \pm 0.420	1.75 \pm 0.701	0.75 \pm 0.365	2 \pm 0.707	2.5 \pm 0.5	1.25 \pm 0.366

3.5.2. Comet assay

The nuclei of hemocyte cells showed strand breaks in DNA after dietary exposure of mussels both to 1 and 10 μg Ag/L of Ag NPs at all exposure times in spring (Figure 5). The quantification of these strand breaks in DNA revealed a significant increase of DNA damage with respect to controls after the dietary exposure to 1 or 10 μg Ag/L Ag NPs at all exposure times (Figure 6). DNA strand breaks were also significantly higher after the dietary exposure to 10 μg Ag/L Ag NPs compared to 1 μg Ag/L Ag NPs at all exposure times (Figure 6).

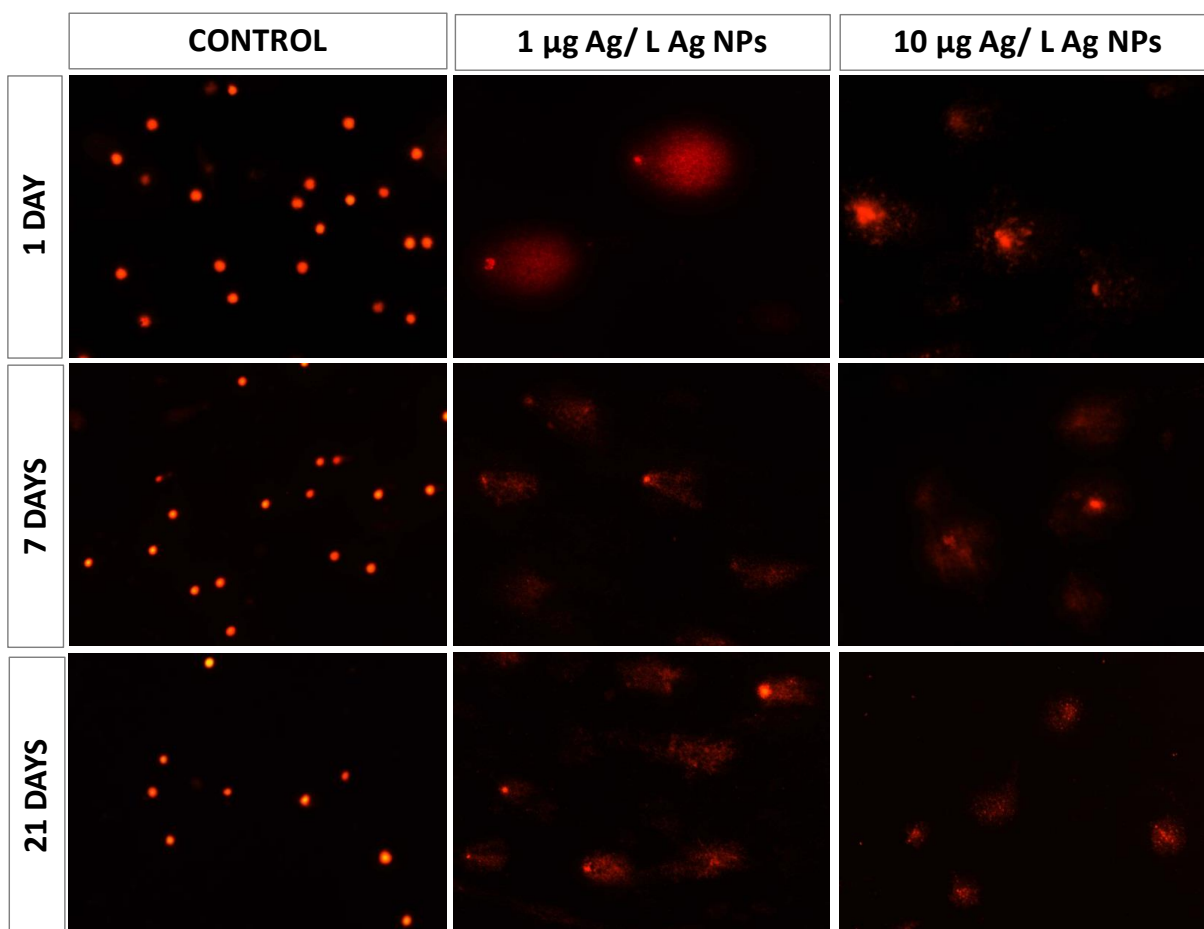


Figure 5. Micrographs showing strand breaks observed in hemocytes of mussels exposed to 1 μg Ag/L or 10 μg Ag/L Ag NPs for 1, 7 and 21 days in spring.

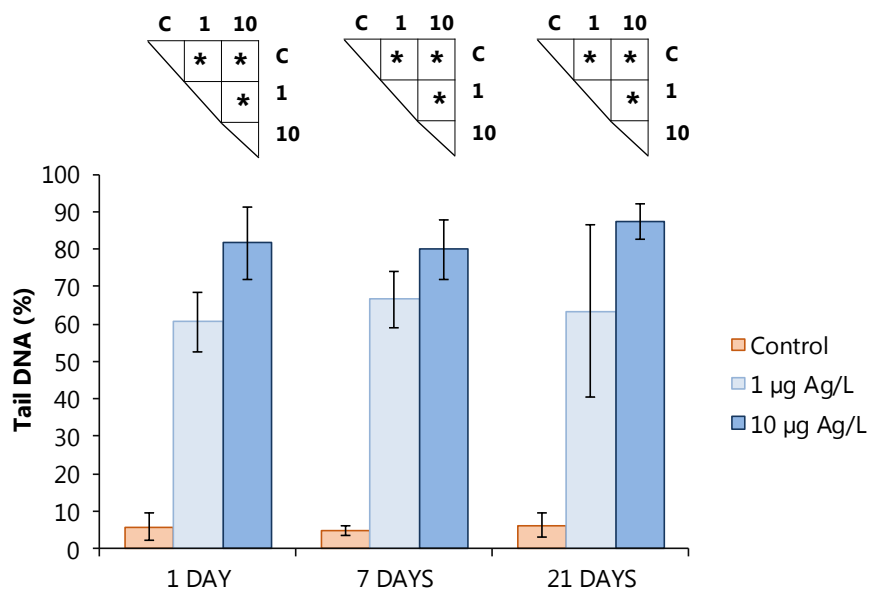


Figure 6. DNA damage (% tail DNA) in hemocytes of mussels exposed through the diet to 1 µg Ag/L or 10 µg Ag/L Ag NPs in spring according to the comet assay. Values are given as means \pm S.D. Significant differences between pairs of means are shown in the upper triangular matrices based on the Dunn's test ($p < 0.05$).

4. DISCUSSION

Marine environments are likely to be the ultimate sink for any NP (Klaine et al., 2008), where organisms can be exposed through water, diet or both. It has been widely reported that waterborne Ag NPs affect to cellular mechanisms involved in nano-internalization, induce DNA damage and alter the protein expression, the antioxidant cellular defence as well as the immune response in marine invertebrates (reviewed in Magesky and Pelletier, 2018). In the present study, cell and tissue level responses in mussels *M. galloprovincialis* exposed to PVP/PEI coated 5 nm Ag NPs through the diet at a dose approaching environmentally relevant concentrations and at a higher dose were assessed in two different seasons (autumn and spring).

Marine bivalves exposed to different types of Ag NPs usually accumulate low concentrations of Ag in their tissues (Buffet et al., 2013; 2014; Jimeno-Romero et al., 2017a) as observed in the present study. Although an increasing trend of Ag accumulation was observed after the dietary exposure to 1 µg Ag/L Ag NPs in spring, this accumulation was not statistically significant. On the other hand, Ag was significantly accumulated after 7 days of dietary exposure to 10 µg Ag/L Ag NPs in spring, being Ag

accumulation higher in spring compared to autumn. In both seasons, mussel soft tissues significantly accumulated Ag after 21 days of dietary exposure to 10 µg Ag/L Ag NPs, being higher levels (around 2-fold) of Ag accumulated in autumn than in spring. Differences in metal concentration in mussels can result from changes in the physiology of animals related to the season, rather than from changes in metal exposure conditions (Mubiana et al., 2005) since exposure conditions including food ration, salinity and temperature were similar in the two seasons in the present work. The effect of seasonal development of gonadic tissues on whole body weight in bivalves has been shown to biologically dilute the total burden of different metals such as Cu, Zn, Ag, Cd, Cu and Pb, thus resulting in lower concentrations of metals during the gametogenesis period (Regoli and Orlando, 1994; Paéz-Osuna et al., 1995; Fattorini et al., 2008; Lanceleur et al., 2011). Thus, the lower concentration of Ag measured in mussel soft tissues in spring could be related to the increase of body weight caused by the development of gametes, observed in spring (see Chapter 3). For future studies, the use of the metal/shell-weight index could be useful as it avoids variability in metal accumulation due to variations in soft-body weight related to the season (Fischer, 1983; Soto et al., 1995).

The digestive gland of bivalves is considered the main organ for accumulation of NPs (Canesi and Corsi, 2016). In fact, after dietary exposure of mussels to Ag NPs both in autumn and in spring, Ag NPs were located in the digestive gland of mussels in both seasons, indicating a successful transfer of Ag NPs from microalgae to mussels (see Chapter 3). Thus, intralysosomal metal accumulation was measured in this organ. Several studies have already reported a significant intralysosomal metal accumulation in digestive cells of mussels waterborne exposed to different types of metal-containing NPs such as TiO₂, Au, CdS and Ag, among others (Jimeno-Romero et al., 2016; 2017a; 2017b; 2019). Waterborne exposure of mussels to different sized Ag NPs provoked a dose-dependent increase in intralysosomal metal accumulation (Jimeno-Romero et al., 2017a). Mussels and zebrafish dietarily exposed to the same PVP/PEI coated 5 nm Ag NPs studied in the present work, showed a dose-dependent increase in intralysosomal metal accumulation in mussels digestive cells in spring (see Chapter 1) and in intestine and liver of zebrafish (Lacave et al., 2017). In the present work, a significant intralysosomal metal accumulation occurred in digestive cells of mussels dietarily exposed to 10 µg Ag/L Ag NPs for 21 days in both seasons, but not for the 1 µg Ag/L Ag NPs dose, close to environmentally relevant concentrations, suggesting that the exposure concentration or time were not high or long enough to cause a significant response, as seen for ICP-MS results. Additionally, the few BSDs quantified in control digestive cell lysosomes could be due to the high levels of Cu measured in wild mussels inhabiting the same estuary (Besada et al., 2011) as BSDs do not reflect only Ag levels since autometallography is not

metal-specific (Danscher, 1981; Marigómez et al., 2002). However, the significantly higher volume density of BSDs measured in the digestive tubules of mussels exposed to 10 µg Ag/L Ag NPs, together with results obtained by ICP-MS, suggest that observed BSDs corresponded to the presence of Ag, in either dissolved or particulate form.

In mussels, lysosomal perturbations such as the destabilization of the lysosomal membrane are considered early indicators of adverse effects provoked by an array of different factors, including exposure to pollutants (Lowe et al., 1995; Cajaraville et al., 2000; Moore et al., 2006). Damage to lysosomal membranes can cause the release of acid hydrolases into the cytosol, possibly leading to a more severe damage and to cell death (Viarengo et al., 2007). Destabilization of the lysosomal membrane has been widely reported in digestive cells of mussels exposed to metal-containing NPs such as TiO₂ NPs (Barmo et al., 2013; Balbi et al., 2014; Jimeno-Romero et al., 2016), Au NPs (Jimeno-Romero et al., 2017b), CdS QDs (Jimeno-Romero et al., 2019) as well as Ag NPs (Jimeno-Romero et al., 2017a). In accordance with the reported studies, in the present work the dietary exposure of mussels to the high dose of PVP/PEI coated 5 nm Ag NPs for 1, 7 and 21 days provoked a time-dependent decrease in lysosomal membrane stability in both seasons, suggesting a general stress response in dietarily exposed mussels that could be also related to the measured intralysosomal metal accumulation in digestive tubules. Even if not statistically significant, a decreasing trend in lysosomal membrane stability was also observed after the dietary exposure of mussels to the dose close to environmentally relevant concentrations, indicating that low concentrations of Ag NPs could also affect mussel general health status.

Further, the cell type composition of the digestive gland epithelium in molluscs can be altered due to environmental factors or to the exposure to pollutants (Cajaraville et al., 1990; Zaldibar et al., 2007; Garmendia et al., 2011; Bignell et al., 2012). Thus, the increase in the relative proportion of basophilic cells in mussel digestive tubules as a result of digestive cell loss and basophilic cell hypertrophy is also considered a general stress condition (Cajaraville et al., 1990; Garmendia et al., 2011). According to previous studies, waterborne exposure of mussels to different types of metal-containing NPs affected the cell type composition of the digestive gland epithelium increasing the proportion of basophilic cells (Rocha et al., 2016; Jimeno-Romero et al., 2017a; 2019). After 1 and 21 days of exposure, a higher basophilic cell volume density was measured in mussels waterborne exposed to two differently sized Ag NPs, as well as to ionic Ag and bulk Ag (Jimeno-Romero et al., 2017a). However, in the present study, cell type composition in the digestive gland of mussels exposed to Ag NPs through the diet was not altered along the exposure period nor in autumn nor in spring. This disagreement

could be related to differences in the exposure route, exposure concentrations and/or NP characteristics such as surface coating and size.

NPs can induce indirectly DNA damage by oxidative stress or can directly interact with DNA due to their small size and high surface area (Singh et al., 2009). Among the methods developed for detecting DNA damage, the measurement of DNA strand breaks by the comet assay and the chromosomal DNA damage by the micronucleus test are the most used techniques in bivalves (Mitchellmore and Chipman, 1998; Lee and Steinert, 2003; Bolognesi and Hayashi, 2011). In this sense, the application of the comet assay in several *in vitro* (Katsumiti et al., 2014; 2015b; 2018; Volland et al., 2018) and *in vivo* investigations (Gomes et al., 2013; Buffet et al., 2014; Mouneyrac et al., 2014, Rocha et al., 2014) revealed that exposure to different types of metallic NPs, including Ag NPs, induced DNA damage in bivalves. Maltose stabilized Ag NPs produced DNA damage at 1.25 and 2.5 mg Ag/L in mussel hemocytes according to *in vitro* studies (Katsumiti et al., 2015b). Waterborne exposure to 10 µg /L Ag NPs increased the percentage of tail DNA with the exposure time in mussel hemocytes (Gomes et al., 2013) and induced a higher genotoxicity in the digestive gland of *S. plana* clams than soluble Ag after 21 days of exposure (Buffet et al., 2014). In agreement with these waterborne exposure studies, in the present work the dietary exposure of mussels to Ag NPs in spring provoked a significant dose-dependent increase of DNA damage in exposed mussels, even at the dose close to environmentally relevant concentrations at all exposure times.

Additionally, an increasing trend in micronuclei frequency was also observed after 1 and 7 days of dietary exposure to 10 µg Ag/L Ag NPs both in autumn and in spring, similar to that reported after 4 days of exposure to TiO₂ NPs (Rocco et al., 2015) or 21 days of exposure to CuO NPs (Ruiz et al., 2015). However, after 21 days of dietary exposure to the same dose, micronuclei frequency values decreased with respect to levels recorded at days 1 and 7 in both seasons. Micronuclei are formed when the levels of double strand breaks in DNA exceed the repair capacity of dividing cells (Luzhna et al., 2013) and chromosomal DNA damage occurs as a result of either chromosome breakage or chromosome mis-segregation during mitosis (Bolognesi and Fenech, 2012). Thus, the decrease of micronuclei frequencies could suggest the elimination of damaged cells by apoptosis (Luzhna et al., 2013) or the activation of DNA repair mechanisms. The activation of the p53 tumor suppressor gene has been described as responsible for arresting the cell cycle and activating transcription of genes that mediate DNA repair, thus preventing the conversion of damage to mutation (Singh et al., 2009). In fact, mussels exposed to 0.01 mg/L ZnO NPs for 28 days showed an up-regulation of p53 already after 72 hours of exposure (Li et al., 2018). Additionally, the exposure of mussels to C60 fullerenes,

benzo(α)pyrene or a combination of both pollutants for 3 days caused a significant increase in DNA strand break levels together with an induction of p53, which was linked with the recovery of genotoxic effects observed after 3 days post-exposure (Di et al., 2017).

In the present work, genotoxicity assessed by the comet assay was the most sensitive biomarker of those tested. In fact, this assay is considered more sensitive than other available methods for the assessment of genotoxic effects since DNA strand breaks form very quickly and allow the detection of early genotoxic responses (Mitchelmore and Chipman, 1998; Frenzilli et al., 2009). But, interestingly, the comet assay and the micronuclei test give complementary information that is crucial to understand the time course of genotoxic effects caused by pollutants (Frenzilli et al., 2009) such as NPs. Even if several works have reported seasonal variations in genotoxic biomarkers (Pisanelli et al., 2009; Almeida et al., 2013; Schmidt et al., 2013) as well as in effect biomarkers such as lysosomal parameters (Hagger et al., 2010; Nahrgang et al., 2013; Balbi et al., 2017), in the present study, season did not influence on the selected cellular biomarkers after the dietary exposure to Ag NPs. Changes in water temperature and salinity related to season have been described as natural environmental factors responsible for alterations in lysosomal membrane stability and baseline micronuclei frequency values in mussels (Regoli et al., 1992; Domouhtsidou and Dimitriadis, 2001; Bolognesi and Hayashi, 2011). The seasonal gamete developmental cycle is also known to affect biomarker responses (Bayne and Widdows, 1978; Solé et al., 1995; Cancio et al., 1999; Sheehan and Power, 1999). In this work exposure conditions including food ration, salinity and temperature were similar in the two seasons whereas gamete developmental stage differed (early gametogenesis in autumn versus advanced gametogenesis in spring) (see Chapter 4). In spite of this, selected cellular biomarkers responded similarly to the dietary Ag NP exposure in the two studied seasons, underlining their reliability as effect assessment tools in nanotoxicology.

5. CONCLUSIONS

The transfer of PVP/PEI coated 5 nm Ag NPs from microalgae to mussels caused significant cellular responses in mussels which were comparable to those reported in waterborne exposure studies to Ag NPs. Ag was significantly accumulated in mussels after 21 days of exposure to the high dose of PVP/PEI coated 5 nm Ag NPs through the diet both in autumn and in spring. Although higher levels of Ag were accumulated in autumn in comparison to spring, intralysosomal metal accumulation in digestive cells in

comparison to controls was similar in both seasons. Lysosomal membrane stability decreased in a dose- and time-dependent manner showing a general stress response in mussels, even if cell type composition of the digestive tubules was not altered. Additionally, Ag NPs ingested through the diet caused genotoxic effects in mussel hemocytes even at the dose close to environmentally relevant concentrations. On the other hand, the increase in micronuclei frequency was transitory in both seasons, suggesting the activation of DNA repair mechanisms. Overall, PVP/PEI coated 5 nm Ag NPs ingested through the food web caused similar cellular effects in mussels both in autumn and in spring, suggesting that selected cellular biomarkers are stable enough to be applied in sentinel mussels at different seasons.

ACKNOWLEDGEMENTS

This work has been funded by the Spanish Ministry of Economy and Competitiveness (NanoSilverOmics project MAT2012-39372), Basque Government (SAIOTEK project S-PE13UN142 and Consolidated Research Group GIC IT810-13), the University of the Basque Country UPV/EHU (UFI 11/37 and PhD fellowship to N.D.) and French Ministry of Higher Education and Research (PhD fellowship to M.M.).

REFERENCES

- ∴ António D.C., Cascio C., Jakšić Ž., Jurašin D., Lyons D.M., Nogueira A.J., Rossi F., Calzolari L. 2015. Assessing silver nanoparticles behaviour in artificial seawater by mean of AF4 and spICP-MS. *Marine Environmental Research* 111: 162-169.
- ∴ Balbi T., Smerilli A., Fabbri E., Ciacci C., Montagna M., Graselli E., Brunelli A., Pojana G., Marcomimi A., Gallo G., Canesi L. 2014. Co-exposure to n-TiO₂ and Cd²⁺ results in interactive effects on biomarker responses but not in increased toxicity in the marine bivalve *M. galloprovincialis*. *Science of the Total Environment* 493: 355- 364.
- ∴ Balbi T., Fabbri R., Montagna M., Camisassi G., Canesi L. 2017. Seasonal variability of different biomarkers in mussels (*Mytilus galloprovincialis*) farmed at different sites of the Gulf of La Spezia, Ligurian sea, Italy. *Marine Pollution Bulletin* 116: 348-356.
- ∴ Banni M., Sforzini S., Arlt V.M., Barranguer A., Dallas L.J., Oliveri C., Aminot Y., Pacchioni B., Millino C., Lanfranchi G., Readman J.W., Moore M.N., Viarengo A., Jha A.N. 2017. Assessing the impact of benzo[a]pyrene on marine musels: application of a novel targeted low density microarray complementing classical biomarker responses. *PLoS ONE* 12 (6): e0178460.
- ∴ Barmo C., Ciacci C., Canonico B., Fabbri R., Cortesec K., Balbi T., Marcomini A., Pojana G., Gallo G., Canesi L. 2013. *In vivo* effects of n-TiO₂ on digestive gland and immune function of the marine bivalve *Mytilus galloprovincialis*. *Aquatic Toxicology* 132-133: 9-18.
- ∴ Bayne B.L., Widdows J. 1978. The physiological ecology of two populations of *Mytilus edulis* L. *Oecologia* 37: 137-162.
- ∴ Bebianno M.J., Gonzalez-Rey M., Gomes T., Mattos J.J., Flores-Nunes F., Bairy A.C.D. 2015. Is gene transcription in mussel gills altered after exposure to Ag nanoparticles? *Environmental Science and Pollution Research* 22: 17425-17433.
- ∴ Besada V., Andrade J.M., Schultze S., González J.J. 2011. Monitoring of heavy metals in wild mussels (*Mytilus galloprovincialis*) from the Spanish North-Atlantic coast. *Continental Shelf Research* 31: 457-465.
- ∴ Bignell J, Cajaraville M.P., Marigómez I. 2012. Chapter 15: Background document: histopathology of mussels (*Mytilus* spp.) for health assessment in biological effects monitoring. Integrated monitoring of chemicals and their effects. In: Davies I.M., Vethaak A.D. (Eds.). ICES Cooperative Research Report N. 315, Copenhagen, Denmark: pp. 111-120.
- ∴ Blaser S.A., Scheringer M., Macleod M., Hungerbühler K. 2008. Estimation of cumulative aquatic exposure and risk due to silver: contribution of nano-functionalized plastics and textiles. *Science of the Total Environment* 390: 396-409.
- ∴ Bolognesi C., Hayashi M. 2011. Micronucleus assay in aquatic animals. *Mutagenesis* 26: 205-213.
- ∴ Bolognesi C., Fenech M. 2012. Mussel micronucleus cytome assay. *Nature Protocols* 7: 1125-1137.
- ∴ Buffet P.E., Pan J.F., Poirier L., Amiard- Triquet C., Amiard J.C., Gaudin P., Risso. De Faverney C., Guibbolini M., Gilliland D., Valsami-Jones E. and Mouneyrac C. 2013. Biochemical and behavioural responses of the endobenthic bivalve *Scrobicularia plana* to silver nanoparticles in seawater and microalgal food. *Ecotoxicology and Environmental Safety* 89: 117-124.

- ∴ Buffet P.E., Zalouk-Vergnoux A., Châtel A., Berthet B., Métais I., Perrein-Ettajani H., Poirier L., Luna-Acosta A., Thomas-Guyon H., Risso-de Faverney C., Guibbolini M., Gilliland D., Valsami-Jones E., Mouneyrac C. 2014. A marine mesocosm study on the environmental fate of silver nanoparticles and toxicity effects on two endobenthic species: The ragworm *Hediste diversicolor* and the bivalve mollusc *Scrobicularia plana*. *Science of the Total Environment* 470-471: 1151-1159.
- ∴ Cajaraville M.P., Díez G., Marigómez I.A., Angulo E. 1990. Responses of basophilic cells of the digestive gland of mussels to petroleum hydrocarbon exposure. *Diseases of Aquatic Organisms* 9: 221-228.
- ∴ Cajaraville M.P., Pal S.G. 1995. Morphofunctional study of the haemocytes of the bivalve mollusc *Mytilus galloprovincialis* with emphasis on the endolysosomal compartment. *Cell Structure and Function* 20: 355-367.
- ∴ Cajaraville M.P., Bebianno M.J., Blasco J., Porte C., Sarasquete C., Viarengo A. 2000. The use of biomarkers to assess the impact of pollution in coastal environments of the Iberian Peninsula: a practical approach. *The Science of the Total Environment* 247: 295-311.
- ∴ Cancio I., Ibabe A., Cajaraville M.P. 1999. Seasonal variation of peroxisomal enzyme activities and peroxisomal structure in mussels *Mytilus galloprovincialis* and its relationship with the lipid content. *Comparative Biochemistry and Physiology, Part C* 123: 135-144.
- ∴ Canesi L., Borghi C., Ciacci C., Fabbri R., Lorusso L.C., Vergani L., Marcomini A., Poiana G. 2008. Short-term effects of environmentally relevant concentrations of EDC mixtures on *Mytilus galloprovincialis* digestive gland. *Aquatic Toxicology* 87: 272-279.
- ∴ Canesi L., Barmo C., Fabbri R., Ciacci C., Vergani L., Roch P., Gallo G. 2010. *In vitro* effects of suspensions of selected nanoparticles (C60 fullerene, TiO₂, SiO₂) on *Mytilus* hemocytes. *Aquatic Toxicology* 96: 151-158.
- ∴ Canesi L., Ciacci C., Fabbri R., Marcomini A., Pojana G. and Gallo G. 2012. Bivalve molluscs as a unique target group for nanoparticle toxicity. *Marine Environmental Research* 76: 16-21.
- ∴ Canesi L., Frenzilli G., Balbi T., Bernardeschi M., Ciacci C., Corsolini S., Della Torre C., Fabbri R., Faleri C., Focardi S., Guidi P., Kočan A., Marcomini A., Mariottini M., Nigro M., Pozo-Gallardo K., Rocco L., Scarcelli V., Smerilli A., Corsi I. 2014. Interactive effects of n-TiO₂ and 2,3,7,8-TCDD on the marine bivalve *Mytilus galloprovincialis*. *Aquatic Toxicology* 153: 53-65.
- ∴ Canesi L., Corsi I. 2016. Effects of nanomaterials on marine invertebrates. *Science of the Total Environment* 565: 933-940.
- ∴ Chio C.P., Chen W.Y., Chou W.W., Hsieh N.H., Ling M.P., Liao C.M. 2012. Assessing the potential risks to zebrafish posed by environmentally relevant copper and silver nanoparticles. *Science of the Total Environment* 420: 111-118.
- ∴ Ciacci C., Canonico B., Bilaničová D., Fabbri R., Cortese K., Gallo G., Marcomini A., Pojana G., Canesi L. 2012. Immunomodulation by different types of N-oxides in the hemocytes of the marine bivalve *Mytilus galloprovincialis*. *PLoS ONE* 7 (5): e36937. doi:10.1371/journal.pone.0036937
- ∴ Corsi I., Cherr G.N., Lenihan H.S., Labille J., Hasselov M., Canesi L., Dondero F., Frenzilli G., Hristozov D., Puntès V., Della Torre C., Pinsino A., Libralato G., Marcomini A., Sabbioni E.,

- Matranga V. 2014. Common strategies and technologies for the ecosafety assessment and design of nanomaterials entering the marine environment. *ACS Nano* 8: 9694-9709.
- ∴ Danscher G. 1981. Light and electron microscopic localization of silver in biological tissue. *Histochemistry* 71: 177-186.
- ∴ Daskalakis K.D. 1996. Variability of metal concentrations in oyster tissue and implications to biomonitoring. *Marine Pollution Bulletin* 32: 794-801.
- ∴ De Los Ríos A., Echavarri-Erasun B., Lacorte S., Sánchez-Ávila J., De Jonge M., Blust R., Orbea A., Juanes J.A., Cajaraville M.P. 2016. Relationships between lines of evidence of pollution in estuarine areas: Linking contaminant levels with biomarker responses in mussels and with structure of macroinvertebrate benthic communities. *Marine Environmental Research* 121: 49-63.
- ∴ Di Y., Aminot Y., Schroeder D.C., Readman J.W., Jha A.N. 2017. Integrated biological responses and tissue-specific expression of p53 and ras genes in marine mussels following exposure to benzo(α)pyrene and C60 fullerenes, either alone or in combination. *Mutagenesis* 32: 77-90.
- ∴ Domouhtsidou G.P., Dimitriadis V.K. 2001. Lysosomal and lipid alterations in the digestive gland of mussels, *Mytilus galloprovincialis* (L.) as biomarkers of environmental stress. *Environmental Pollution* 115: 123-137.
- ∴ Dumont E., Johnson A.C., Keller V.D.J., Williams R.J. 2015. Nano silver and nano zinc-oxide in surface waters-Exposure estimation for Europe at high spatial and temporal resolution. *Environmental Pollution* 196: 341- 349.
- ∴ Fabrega J., Luoma S.N., Tyler C.R., Galloway T.S., Lead J.R. 2011. Silver nanoparticles: Behaviour and effects in the aquatic environment. *Environment International* 37: 517-531.
- ∴ Fattorini D., Notti A., Di Mento R., Cicero A.M., Gabellini M., Russo A., Regoli F. 2008. Seasonal, spatial and inter-annual variations of trace metals in mussels from the Adriatic sea: a regional gradient for arsenic and implications for monitoring the impact of off-shore activities. *Chemosphere* 72: 1524-1533.
- ∴ Fischer H. 1983. Shell weight as an independent variable in relation to cadmium content of molluscs. *Marine Ecology Progress Series* 12: 59-75.
- ∴ Frenzilli G., Nigro M., Lyons B.P. 2009. The Comet assay for the evaluation of genotoxic impact in aquatic environments. *Mutation Research* 681: 80-92.
- ∴ Gamble M. and Wilson I. 2002. The hematoxylin and eosin. In: Brancfort J.D., Gamble M. (Eds.), *Theory and Practice of Histological Techniques*. Churchill Livingstone- Elsevier Science Ltd., London, UK. pp. 125.
- ∴ Garmendia L., Soto M., Vicario U., Kim Y., Cajaraville M.P., Marigómez I. 2011. Application of a battery of biomarkers in mussel digestive gland to assess long-term effects of the Prestige oil spill in Galicia and Bay of Biscay: tissue-level biomarkers and histopathology. *Journal of Environmental Monitoring* 13: 915-932.
- ∴ Giese B., Klaessig F., Park B., Kaegi R., Steinfeldt M., Wigger H., von Gleich A., Gottschalk F. 2018. Risks, release and concentrations of engineered nanomaterial in the environment. *Scientific Reports* 8: doi: 10.1038/s41598-018-19275-4.

- .: Gomes T., Araújo O., Pereira R., Almeida A.C., Cravo A., Bebianno M.J. 2013. Genotoxicity of copper oxide and silver nanoparticles in the mussel *Mytilus galloprovincialis*. *Marine Environmental Research* 84: 51-59.
- .: Gomes T., Pereira C.G., Cardoso C., Sousa V.S., Ribau Teixeira M., Pinheiro J.P., Bebianno M.J. 2014. Effects of silver nanoparticles exposure in the mussel *Mytilus galloprovincialis*. *Marine Environmental Research* 101: 208-214.
- .: Gottschalk F., Sonderer T., Scholz R.W., Nowack B. 2009. Modeled environmental concentrations of engineered nanomaterials (TiO₂, ZnO, Ag, CNT, fullerenes) for different regions. *Environmental Science and Technology* 43: 9216-9222.
- .: Hagger J.A., Lowe D., Dissanayake A., Jones M.B. 2010. The influence of seasonality on biomarker responses in *Mytilus edulis*. *Ecotoxicology* 19: 953-962.
- .: Hook S.E., Gallagher E.P., Batley G.E. 2014. The role of biomarkers in the assessment of aquatic ecosystem health. *Integrated Environmental Assessment and Management* 10: 327-341.
- .: Hylland K., Tollefsen K.E., Ruus A., Jonsson G., Sundt R.C., Sanni S., Røe Utvik T.I., Johnsen S., Nilssen I., Pinturier L., Balk L., Barsiene J., Marigómez I., Feist S.W., Børseth J.F. 2008. Water column monitoring near oil installations in the North Sea 2001-2004. *Marine Pollution Bulletin* 56: 414-429.
- .: ICES. 2016. Report of the Working Group on the Biological Effects of Contaminants (WGBEC), 9-13 March 2015, Bergen, Norway. ICES CM 2015/SSGEPI:02. 66 pp.
- .: Jimeno-Romero A., Oron M., Cajaraville M.P., Soto M., Marigómez I. 2016. Nanoparticle size and combined toxicity of TiO₂ and DSLS (surfactant) contribute to lysosomal responses in digestive cells of mussels exposed to TiO₂ nanoparticles. *Nanotoxicology* 10: 1168-1176.
- .: Jimeno-Romero A., Bilbao E., Izagirre U., Cajaraville M.P., Marigómez I., Soto M. 2017a. Digestive cell lysosomes as main targets for Ag accumulation and toxicity in marine mussels, *Mytilus galloprovincialis*, exposed to maltose-stabilized Ag nanoparticles of different sizes. *Nanotoxicology* 11: 168-183.
- .: Jimeno-Romero A., Izagirre U., Gilliland D., Warley A., Cajaraville M.P., Marigómez I., Soto M. 2017b. Lysosomal responses to different gold forms (nanoparticles, aqueous, bulk) in mussel digestive cells: a trade-off between the toxicity of the capping agent and form, size and exposure concentration. *Nanotoxicology* 11: 658-670.
- .: Jimeno-Romero A., Bilbao E., Valsami-Jones E., Cajaraville M.P., Soto M., Marigómez I. 2019. Bioaccumulation, tissue and cell distribution, biomarkers and toxicopathic effects of CdS quantum dots in mussels, *Mytilus galloprovincialis*. *Ecotoxicology and Environmental Safety* 167: 288-300.
- .: Katsumiti A., Gilliland D., Arostegui I., Cajaraville M.P. 2014. Cytotoxicity and cellular mechanisms involved in the toxicity of CdS quantum dots in hemocytes and gill cells of the mussel *Mytilus galloprovincialis*. *Aquatic Toxicology* 153: 39-52.
- .: Katsumiti A., Berhanu D., Howard K.T., Arostegui I., Oron M., Reip P., Valsami-Jones E., Cajaraville M.P. 2015a. Cytotoxicity of TiO₂ nanoparticles to mussel hemocytes and gill cells *in vitro*: influence of synthesis method, crystalline structure, size and additive. *Nanotoxicology* 9: 543-553.

- ∴ Katsumiti A., Gilliland D., Arostegui I., Cajaraville M.P. 2015b. Mechanisms of toxicity of Ag nanoparticles in comparison to bulk and ionic Ag on mussel hemocytes and gill cells. *PLoS ONE* 10 (6): e0129039. doi:10.1371/journal.pone.0129039.
- ∴ Katsumiti A., Arostegui I., Oron M., Gilliland D., Valsami-Jones E., Cajaraville M.P. 2016. Cytotoxicity of Au, ZnO and SiO₂ NPs using *in vitro* assays with mussels hemocytes and gill cells: Relevance of size, shape and additives. *Nanotoxicology* 10: 185-193.
- ∴ Katsumiti A., Thorley A.J., Arostegui I., Reip P., Valsami-Jones E., Tetley T.D., Cajaraville M.P. 2018. Cytotoxicity and cellular mechanisms of toxicity of CuO NPs in mussel cells *in vitro* and comparative sensitivity with human cells. *Toxicology In Vitro* 48: 146-158.
- ∴ Lacave J.M., Fanjul A., Bilbao E., Gutierrez N., Barrio I., Arostegui I., Cajaraville M.P., Orbea A. 2017. Acute toxicity, bioaccumulation and effects of dietary transfer of silver from brine shrimp exposed to PVP/PEI coated silver nanoparticles to zebrafish. *Comparative Biochemistry and Physiology, Part C* 199: 69-80.
- ∴ Lancelleur L., Schäfer J., Chiffoleau J.F., Blanc G., Auger D., Renault S., Baudrimont M., Audry S. 2011. Long-term records of cadmium and silver contamination in sediments and oysters from the Gironde fluvial-estuarine continuum-Evidence of changing silver sources. *Chemosphere* 85: 1299-1305.
- ∴ Lee R.F., Steinert S. 2003. Use of the single cell gel electrophoresis/comet assay for detecting DNA damage in aquatic (marine and freshwater) animals. *Mutation Research* 544: 43-64.
- ∴ Li L., Stoiber M., Wimmer A., Xu Z., Lindenblatt C., Helmreich B., Schuster M. 2016. To what extent can full-scale wastewater treatment plant effluent influence the occurrence of silver-based nanoparticles in surface waters? *Environmental Science and Technology* 50: 6327-6333.
- ∴ Li J., Schiavo S., Xiangli D., Rametta G., Miglietta M.L., Oliviero M., Changwen W., Manzo S. 2018. Early ecotoxic effects of ZnO nanoparticle chronic exposure in *Mytilus galloprovincialis* revealed by transcription of apoptosis and antioxidant-related genes. *Ecotoxicology* 27: 369-384.
- ∴ Lowe D.M., Soverchia C., Moore M.N. 1995. Lysosomal membrane responses in the blood and digestive cells of mussels experimentally exposed to fluoranthene. *Aquatic Toxicology* 33: 105-112.
- ∴ Luzhna L., Kathiria P., Kovalchuk O. 2013. Micronuclei in genotoxicity assessment: from genetics to epigenetics and beyond. *Frontiers in Genetics* 4: 131-147.
- ∴ Magesky A., Pelletier E. 2018. Cytotoxicity and physiological effects of silver nanoparticles on marine invertebrates, In: Saquib Q., Faisal M., Al-Khedhairy A.A., Alatar A.A. (Eds.), *Cellular and Molecular Toxicology of Nanoparticles*. Springer International Publishing, pp. 285-309.
- ∴ Marcoux M.A., Matias M., Olivier F., Keck G. 2013. Review and prospect of emerging contaminants in waste -Key issues and challenges linked to their presence in waste treatment schemes: General aspects and focus on nanoparticles. *Waste Management* 33: 2147-2156.
- ∴ Marigómez I., Soto M., Cajaraville M.P., Angulo E., Giamberini L. 2002. Cellular and subcellular distribution of metals in molluscs. *Microscopy Research and Technique* 56: 358-392.
- ∴ Marigómez I., Soto M., Orbea A., Cancio I., Cajaraville M.P. 2004. Chapter 14: Biomonitoring of environmental pollution in the Basque coast using molecular, cellular and tissue-level

- biomarkers: an integrative approach. In: Borja A., Collins M. (Eds.), Oceanography and marine environment of the Basque Country. Elsevier Oceanography Series n° 70, Elsevier, Amsterdam, pp. 335-364.
- ∴ Marigómez I., Garmendia L., Soto M., Orbea A., Izagirre U., Cajaraville M.P. 2013. Marine ecosystem health status assessment through integrative biomarker indices: a comparative study after the Prestige oil spill "Mussel Watch". *Ecotoxicology* 22: 486-505.
 - ∴ McCarthy J.F., Shugart L.R. 1990. Biological markers of environmental contamination. In: McCarthy J.F. and Shugart L.R. Eds., Biomarkers of environmental contamination, Lewis Publishers, Boca Raton: 3-14.
 - ∴ McCarthy M., Carroll D.L., Ringwood A.H. 2013. Tissue specific response of oysters, *Crassostrea virginica*, to silver nanoparticles. *Aquatic Toxicology* 138-139: 123-128.
 - ∴ McGuillicuddy E., Murray I., Kavanagh S., Morrison L., Fogarty A., Cormican M., Dockery P., Prendergast M., Rowan N., Morris D. 2017. Silver nanoparticles in the environment: Sources, detection and ecotoxicology. *Science of the Total Environment* 575: 231-246.
 - ∴ Mitchelmore C.L., Chipman J.K. 1998. DNA strand breakage in aquatic organisms and the potential value of the comet assay in environmental monitoring. *Mutation Research* 399: 135-147.
 - ∴ Moore M.N. 2006. Do nanoparticles present ecotoxicological risks for the health of the aquatic environment? *Environment International* 32: 967-976.
 - ∴ Moore M.N., Allen J.I., McVeigh A. 2006. Environmental prognostics: An integrated model supporting lysosomal stress responses as predictive biomarkers of animal health status. *Marine Environmental Research* 61: 278-304.
 - ∴ Mouneyrac C., Buffet P.E., Poirier L., Zalouk-Vergnoux A., Guibbolini M., Faverney C.R., Gilliland D., Berhanu D., Dybowska A., Châtel A., Perrein-Ettajni H., Pan J.F., Thomas-Guyon H., Reip P., Valsami-Jones E. 2014. Fate and effects of metal-based nanoparticles in two marine invertebrates, the bivalve mollusc *Scrobicularia plana* and the annelid polychaete *Hediste diversicolor*. *Environmental Science and Pollution Research International* 21: 7899-7912.
 - ∴ Mubiana V.K., Qadah D., Meys J., Blust R. 2005. Temporal and spatial trends in heavy metal concentrations in the marine mussel *Mytilus edulis* from the Western Scheldt estuary (The Netherlands). *Hydrobiologia* 540: 169-180.
 - ∴ Nahrgang J., Brooks S.J., Evenset A., Camus L., Jonsson M., Smith T.J., Lukina J., Frantzen M., Giarratano E., Renaud P.E. 2013. Seasonal variation in biomarkers in blue mussel (*Mytilus edulis*), Icelandic scallop (*Chlamys islandica*) and Atlantic cod (*Gadus morhua*): implications for environmental monitoring in the Barents Sea. *Aquatic Toxicology* 127: 21-35.
 - ∴ Orbea A., Ortiz-Zarragoitia M., Cajaraville M.P. 2002. Interactive effects of benzo(a)pyrene and cadmium and effects of di(2-ethylhexyl) phthalate on antioxidant and peroxisomal enzymes and peroxisomal volume density in the digestive gland of mussel *Mytilus galloprovincialis* Lmk. *Biomarkers* 7: 33-48.
 - ∴ Páez-Osuna F., Frías-Espéricueta M.G., Osuna-López J.I. 1995. Trace metal concentrations in relation to season and gonadal maturation in the oyster *Crassostrea iridescens*. *Marine Environmental Research* 40: 19-31.

- ∴ Pisanelli B., Benedetti M., Fattorini D., Regoli F. 2009. Seasonal and inter-annual variability of DNA integrity in mussels *Mytilus galloprovincialis*: a possible role for natural fluctuations of trace metal concentrations and oxidative biomarkers. *Chemosphere* 77: 1551-1557.
- ∴ Raisuddin S., Jha A.N. 2004. Relative sensitivity of fish and mammalian cells to sodium arsenate and arsenite as determined by alkaline single-cell gel electrophoresis and cytokinesis-block micronucleus assay. *Environmental Molecular Mutagenesis* 44: 83-89.
- ∴ Regoli F. 1992. Lysosomal responses as a sensitive stress index in biomonitoring heavy metal pollution. *Marine Ecology Progress Series* 84: 63-69.
- ∴ Regoli F., Orlando E. 1994. Seasonal variation of trace metal concentrations in the digestive gland of the mediterranean mussel *Mytilus galloprovincialis*. Comparison between a polluted and a non-polluted site. *Archives of Environmental Contamination and Toxicology* 27: 36-43.
- ∴ Ringwood A.H., McCarthy M., Bates T.C., Carroll D.L. 2010. The effects of silver nanoparticles on oyster embryos. *Marine Environmental Research* 69: S49-S51.
- ∴ Rocco L., Santonastaso M., Nigro M., Mottola F., Costagliola D., Bernardeschi M., Guidi P., Lucchesi P., Scarcelli V., Corsi I., Stingo V., Frenzilli G. 2015. Genomic and chromosomal damage in the marine mussel *Mytilus galloprovincialis*: Effects of the combined exposure to titanium dioxide nanoparticles and cadmium chloride. *Marine Environmental Research* 111: 144-148.
- ∴ Rocha T.L., Gomes T., Cardoso C., Letendre J., Pinheiro J.P., Sousa V.S., Teixeira M.R., Bebianno M.J. 2014. Immunocytotoxicity, cytogenotoxicity and genotoxicity of cadmium-based quantum dots in the marine mussel *Mytilus galloprovincialis*. *Marine Environmental Research* 101: 29-37.
- ∴ Rocha T.L., Gomes T., Sousa V.S., Mestre N.C., Bebianno M.J. 2015. Ecotoxicological impact of engineered nanomaterials in bivalve molluscs: An overview. *Marine Environmental Research* 111: 74-88.
- ∴ Rocha T.L., Sabóia-Morais S.M., Bebianno M.J. 2016. Histopathological assessment and inflammatory response in the digestive gland of marine mussel *Mytilus galloprovincialis* exposed to cadmium-based quantum dots. *Aquatic Toxicology* 177: 306-315.
- ∴ Ruiz P., Ortiz-Zarragoitia M., Orbea A., Vingen S., Hjelle A., Baussant T., Cajaraville M.P. 2014. Short- and long-term responses and recovery of mussels *Mytilus edulis* exposed to heavy fuel oil no.6 and styrene. *Ecotoxicology* 23: 861-879.
- ∴ Ruiz P., Katsumiti A., Nieto J.A., Bori J., Reip P., Orbea A., Cajaraville M.P. 2015. Short-term effects on antioxidant enzymes and long-term genotoxic and carcinogenic potential of CuO nanoparticles in mussels. *Marine Environmental Research* 111: 107-120.
- ∴ Schmidt W., Power E., Quinn B. 2013. Seasonal variations of biomarker responses in the marine blue mussel (*Mytilus* spp.). *Marine Pollution Bulletin* 74: 50-55.
- ∴ Sheehan D., Power A. 1999. Effects of seasonality on xenobiotic and antioxidant defence mechanisms of bivalve molluscs. *Comparative Biochemistry and Physiology, Part C* 123: 193-199.
- ∴ Sikder M., Lead J.R., Chandler G.T., Baalousha M. 2017. A rapid approach for measuring silver nanoparticle concentration and dissolution in seawater by UV-Vis. *Science of the Total Environment* 618: 597-607.

- ∴ Singh N., Manshian B., Jenkins G.J., Griffiths S.M., Williams P.M., Maffei T.G., Wright C.J., Doak S.H. 2009. NanoGenotoxicology: the DNA damaging potential of engineered nanomaterials. *Biomaterials* 30: 3891-3914.
- ∴ Sokal R.R., Rohlf F.J. 1969. *Introduction to Biostatistics*, 2nd Edition. Dover Publications Inc. Mineola, New York.
- ∴ Solé M., Porte C., Albaigés J. 1995. Seasonal variation in the mixed-function oxygenase system and antioxidant enzymes of the mussel *Mytilus galloprovincialis*. *Environmental Toxicology and Chemistry* 14: 157-164.
- ∴ Soto M., Kortabitarte M., Marigómez I. 1995. Bioavailable heavy metals in estuarine waters as assessed by metal/shell-weight indices in sentinel mussels *Mytilus galloprovincialis*. *Marine Ecology Progress Series* 125: 127-136.
- ∴ Soto M., Bignell B., Cancio I., Taylor M.G., Turner M., Morgan A.J., Marigómez I. 2002. Subcellular distribution of cadmium and its cellular ligands in mussel digestive gland cells as revealed by combined autometallography and X-ray microprobe analysis. *The Histochemical Journal* 34: 273-280.
- ∴ Tangaa S.R., Selck H., Winther-Nielsen M., Khan F.R. 2016. Trophic transfer of metal-based nanoparticles in aquatic environments: a review and recommendations for future research focus. *Environmental Science: Nano* 3: 966-981.
- ∴ Tiede K., Hassellöv M., Breitbarth E., Chaudhry Q., Boxall A.B.A. 2009. Considerations for environmental fate and ecotoxicity testing to support environmental risk assessments for engineered nanoparticles. *Journal of Chromatography A* 1216: 503-509.
- ∴ UNEP-RAMOGÉ. 1999. *Manual on the biomarkers recommended for the MED POL Biomonitoring Programme*. UNEP, Athens.
- ∴ UNEP, 2004. *UNEP/MAP/MED POL: Guidelines for the development of ecological status and stress reduction indicators for the Mediterranean region*. MAP Technical Reports Series No. 154, UNEP/MAP, Athens, pp. 94.
- ∴ Vance M.E., Kuiken T., Vejerano E.P., McGinnis S.P., Hochella M. F. Jr., Rejeski D., Hull M.S. 2015. Nanotechnology in the real world: Redeveloping the nanomaterial consumer products inventory. *Beilstein Journal of Nanotechnology* 6: 1769-1780.
- ∴ Venier P., Maron S., Canova S. 1997. Detection of micronuclei in gill cells and haemocytes of mussels exposed to benzo[a]pyrene. *Mutation Research-Genetic Toxicology and Environmental Mutagenesis* 390: 33-44.
- ∴ Viarengo A., Lowe D., Bolognesi C., Fabbri E., Koehler A. 2007. The use of biomarkers in biomonitoring: a 2-tier approach assessing the level of pollutant-induced stress syndrome in sentinel organisms. *Comparative Biochemistry and Physiology, Part C* 146: 281-300.
- ∴ Volland M., Hampel M., Katsumiti A., Yeste M.P., Gatica J.M., Cajaraville M.P., Blasco J. 2018. Synthesis methods influence characteristics, behaviour and toxicity of bare CuO NPs compared to bulk CuO and ionic Cu after *in vitro* exposure of *Ruditapes philippinarum* hemocytes. *Aquatic Toxicology* 199: 285-295.
- ∴ Von der Kammer F., Ferguson P.L., Holden P.A., Masion A., Rogers K.R., Klaine S.J., Koelmans A.A., Horne N., Unrine J.M. 2012. Analysis of engineered nanomaterials in complex matrices

(environment and biota): general considerations and conceptual case studies. *Environmental Toxicology and Chemistry* 31: 32-49.

- ∴ Zaldibar B., Cancio I., Marigómez I. 2007. Reversible alterations in epithelial cell turnover in digestive gland of winkles (*fabbr*) exposed to cadmium and their implications for biomarker measurements. *Aquatic Toxicology* 81: 183-196.
- ∴ Zhang C., Hu Z., Deng B. 2016. Silver nanoparticles in aquatic environments: Physicochemical behavior and antimicrobial mechanisms. *Water Research* 88: 403-427.
- ∴ Zorita I., Apraiz I., Ortiz-Zarragoitia M., Orbea A., Cancio I., Soto M., Marigómez I., Cajaraville M.P. 2007a. Assessment of biological effects of environmental pollution along the NW Mediterranean Sea using mussels as sentinel organisms. *Environmental Pollution* 148: 236-250.
- ∴ Zorita I., Bilbao E., Schad A., Cancio I., Soto M., Cajaraville M.P. 2007b. Tissue- and cell-specific expression of metallothionein genes in cadmium- and copper-exposed mussels analyzed by in situ hybridization and RT-PCR. *Toxicology and Applied Pharmacology* 220: 186-196.



CHAPTER 3

Changes in protein expression in mussels *Mytilus galloprovincialis* dietarily exposed to PVP/PEI coated silver nanoparticles at different seasons

This chapter has been published as:

DUROUDIER N., CARDOSO C., MEHENNAOUI K., MIKOLACZYK M., SCHÄFER J., GUTLEB A.C., GIAMBERINI L., BEBIANNO M.J., BILBAO E., CAJARAVILLE M.P. 2019. Changes in protein expression of mussels *Mytilus galloprovincialis* dietarily exposed to PVP/PEI coated silver nanoparticles at different seasons. *Aquatic Toxicology* 210: 56-68.

Parts of this chapter have been presented at:

30th CONGRESS OF THE NEW EUROPEAN SOCIETY FOR COMPARATIVE PHYSIOLOGY AND BIOCHEMISTRY ESCPB, Barcelona, 1-4 September 2016.

DUROUDIER, N; CARDOSO, C; BEBIANNO, MJ; BILBAO, E; CAJARAVILLE, MP. Changes in protein expression of mussels *Mytilus galloprovincialis* dietarily exposed to PVP/PEI coated silver nanoparticles at different seasons. Platform presentation.

FINAL CONFERENCE OF THE COST ACTION ES1205 "Engineered Nanomaterial from Wastewater Treatment & Stormwater to Rivers", Aveiro (Portugal), 7-8 February 2017.

DUROUDIER, N; KATSUMITI, A; MIKOLACZYK, M; CARDOSO, C; SCHÄFER, J; BEBIANNO, MJ; BILBAO, E; CAJARAVILLE, MP. Molecular and cellular effects of silver nanoparticles on adult mussels exposed through the diet and on their offspring. Platform presentation.

ABSTRACT

Potential toxic effects of Ag NPs ingested through the food web and depending on the season have not been addressed in marine bivalves. This work aimed to assess differences in protein expression in the digestive gland of female mussels after dietary exposure to Ag NPs in autumn and spring. Mussels were fed daily with microalgae previously exposed for 24 hours to 10 µg/L of PVP/PEI coated 5 nm Ag NPs. After 21 days, mussels significantly accumulated Ag in both seasons and Ag NPs were found within digestive gland cells and gills. Two-dimensional electrophoresis distinguished 104 differentially expressed protein spots in autumn and 142 in spring. Among them, *chitinase like protein-3*, *partial* and *glyceraldehyde-3-phosphate dehydrogenase*, that are involved in amino sugar and nucleotide sugar metabolism, carbon metabolism, glycolysis/gluconeogenesis and the biosynthesis of amino acids KEGG pathways, were overexpressed in autumn but underexpressed in spring. In autumn, pyruvate metabolism, citrate cycle, cysteine and methionine metabolism and glyoxylate and dicarboxylate metabolism were altered, while in spring, proteins related to the formation of phagosomes and hydrogen peroxide metabolism were differentially expressed. Overall, protein expression signatures depended on season and Ag NPs exposure, suggesting that season significantly influences responses of mussels to NP exposure.

Keywords: silver nanoparticles, dietary exposure, mussels *Mytilus galloprovincialis*, seasons, proteomic analysis.

RESUMEN

Los posibles efectos tóxicos de las NPs de Ag ingeridas a través de la dieta y dependiendo de la estación del año no han sido evaluados en bivalvos marinos. En este trabajo se trató de determinar diferencias en la expresión proteica en la glándula digestiva de mejillones hembra tras su exposición a través de la dieta a NPs de Ag en otoño y primavera. Los mejillones se alimentaron diariamente con microalgas previamente expuestas durante 24 horas a 10 µg/L de NPs de Ag de 5 nm recubiertas con PVP/PEI. Tras 21 días, los mejillones acumularon Ag significativamente en ambas estaciones del año y se encontraron NPs de Ag entre las células de la glándula digestiva y las branquias. La electroforesis bidimensional permitió distinguir 104 proteínas significativamente expresadas en otoño y 142 en primavera. Entre ellas, las proteínas *chitinase like protein-3*, *partial* y *glyceraldehyde-3-phosphate dehydrogenase*, que forman parte de las diferentes rutas KEGG como el metabolismo de los amino-azúcares y nucleótido-azúcares, del metabolismo del carbono, de la glicólisis/gluconeogénesis y la biosíntesis de aminoácidos, se expresaron significativamente más en otoño pero significativamente menos en primavera. En otoño, se alteraron el metabolismo del piruvato, el ciclo del citrato, el metabolismo de la cisteína y metionina y el metabolismo del glioxilato y dicarboxilato, mientras que en primavera las proteínas diferencialmente expresadas estaban relacionadas con la formación de fagosomas y el metabolismo del peróxido de hidrógeno. En general, los diferentes patrones de expresión proteica dependieron de la estación del año y de la exposición a las NPs de Ag, sugiriendo que la estación influye significativamente en las respuestas de los mejillones tras la exposición a NPs.

Palabras clave: nanopartículas de plata, exposición vía dieta, mejillones *Mytilus galloprovincialis*, estación del año, análisis proteómicos.

1. INTRODUCTION

The rapid development of nanoscience and nanotechnology has led to the increasing incorporation of nanoparticles (NPs) into consumer products (Baker et al., 2014; Corsi et al., 2014; Vance et al., 2015). Due to their unique optical, catalytic and antimicrobial properties, silver NPs (Ag NPs) have gained high commercial and scientific interest (Fabrega et al., 2011; Vance et al., 2015; Zhang et al., 2016; McGuillicuddy et al., 2017). The production, use and degradation of products containing Ag NPs can provoke the potential release and input of Ag NPs into freshwater and marine environments (Baker et al., 2014; Corsi et al., 2014). Once in the environment, Ag NPs may interact with aquatic organisms and may induce toxic effects at different levels of biological organization (Rocha et al., 2015a).

Toxic effects caused by the exposure to Ag NPs through the water have been widely investigated in different freshwater organisms such as microalgae (Navarro et al., 2008; Ribeiro et al., 2014; Sendra et al., 2017a), daphnids (Ribeiro et al., 2014; Khan et al., 2015; Pakrashi et al., 2017) and zebrafish (Griffith et al., 2009; 2013; Ribeiro et al., 2014; Lacave et al., 2017; 2018; Orbea et al., 2017). In seawater, studies based on waterborne exposure to Ag NPs have mainly been focused on microalgae (Gambardella et al., 2015; Schiavo et al., 2017; Sendra et al., 2017b) and bivalves (Ringwood et al., 2010; Buffet et al., 2013; 2014; Gomes et al., 2013a; 2013b; McCarthy et al., 2013; Bebianno et al., 2015; Katsumiti et al., 2015; Jimeno-Romero et al., 2017). However, studies on the potential trophic transfer of metals, metal oxides and metal mixtures in nano-size are scarce but increasingly necessary due to their potential incidence in human and other species health (Tangaa et al., 2016). In fact, few works have assessed the potential toxic effects of metallic NPs ingested through the food web in marine organisms (Larguinho et al., 2014; Wang et al., 2016; Manzo et al., 2017; Bhuvaneshwari et al., 2018), including Ag NPs (Buffet et al., 2013; Wang and Wang 2014).

In general, bivalve molluscs form the most studied invertebrate group since they have been identified as an important target group for NP toxicity in the marine environment (Moore et al., 2006; Canesi et al., 2012; Corsi et al., 2014; Canesi and Corsi, 2016). Most research in bivalves has been focused on understanding the effects of Ag NPs on *in vivo* waterborne exposed organisms using conventional biomarkers (Ringwood et al., 2010; Buffet et al., 2013; 2014; Gomes et al., 2013a; 2014b; McCarthy et al., 2013; Bebianno et al., 2015; Jimeno-Romero et al., 2017), but few studies based on other methods (e. g. transcriptomics, proteomics, metabolomics) have assessed the potential effects caused by Ag NPs (Rocha et al., 2015a). Proteomics-based methods, among others, have been applied to complement the information given by conventional

biomarkers and to identify new protein pathways affected by the exposure to NPs (Dowling and Sheehan, 2006; Rocha et al., 2015a).

Tedesco et al. (2008) first reported the use of redox proteomics in *Mytilus edulis* tissues exposed to 750 µg/L of gold-citrate-NPs (13 nm) for 24 hours. Authors observed high carbonylation and ubiquitination of proteins in mussels gills and digestive gland, respectively (Tedesco et al., 2008). The same Au-citrate-NPs (13 nm) as well as 5 nm Au NPs both provoked a reduction in the amount of thiol-containing proteins in the digestive gland of *M. edulis* mussels (Tedesco et al., 2010a; 2010b), suggesting that Au NPs caused oxidative stress. Similarly, Hu and colleagues (2014) observed a reduction in thiol groups as well as an increase in carbonylated proteins in gills of mussels *M. edulis* exposed to three different concentrations of CuO NPs for just 1 hour. Additionally, some proteins were identified as indicators of oxidation of cytoskeleton proteins and two other as specific enzymes after CuO NPs exposure (Hu et al., 2014). Short exposures (3h, 6h and 12h) to two sizes of Ag NPs (<50 and < 100 nm) also provoked protein thiol oxidation and/or protein carbonylation in mussels gills and digestive gland (Bouallegui et al., 2017). Alterations in the proteome of mussels *M. galloprovincialis* were also assessed after the exposure to CuO NPs or Ag NPs and to their ionic form (Gomes et al., 2013b; Gomes et al., 2014a). In these works, NP and ionic form-dependent protein expression signatures were reported (Gomes et al., 2013b; 2014a). In fact, *major vault protein*, *paramyosin* and *ras (partial)* were overexpressed protein spots in mussels exposed to 10 µg/L Ag NPs for 15 days (Gomes et al., 2013b) and *caspase 3/7-1*, *cathepsin L* and *Zn-finger protein* in mussels exposed to 10 µg/L CuO NPs for 15 days (Gomes et al., 2014a). Thus, such proteins were proposed as putative molecular biomarkers to assess toxicity of Ag NPs and CuO NPs, respectively.

In studies reported above, gender of mussels and developmental stage of gametes were not considered although mussels are intertidal organisms that show seasonal metabolic and enzymatic variations related both to abiotic changes in the environment, such as temperature, food availability and oxygen levels, and to biotic factors such as gender, gamete developmental stage and physiological state (Bayne and Widdows, 1978; Solé et al., 1995; Cancio et al., 1999). Some studies have identified gender-specific natural variations in gene expression patterns (Banni et al., 2011) as well as gender-specific differences in the response to contaminants (Livingstone and Farrar, 1984; Brown et al., 2006; Riva et al., 2011; Ji et al., 2016; Banni et al., 2017) suggesting that gender of mussels should be considered in ecotoxicological studies. In fact, in many works the potential effects of different pollutants have been studied only in female mussels (Dondero et al., 2011; Negri et al., 2013; Banni et al., 2014; 2016; 2017). Thus, in the present study

differences in protein expression profiles were only assessed in female organisms in order to avoid biological variability related to gender. Further, mussels sensitivity towards chemical insults may vary in some stages of their reproductive cycle such as the reproduction period (Leiniö and Lehtonen, 2005; Bocchetti and Regoli, 2006; Almeida et al., 2013). Thus, it is relevant to study season-dependent variations in mussel responses to Ag NPs as well as to other emerging pollutants.

In this context, the aim of this work was to assess differences in the expression profile of proteins in the digestive gland of female mussels fed with algae exposed to 10 µg Ag/L Ag NPs and to compare such expression profiles at two different seasons, in autumn and spring, in which mussels were at different developmental stages. In parallel, Ag accumulation was studied in mussel soft tissues and presence of Ag NPs was assessed in tissue sections using a hyperspectral imaging system. The selected dose of Ag NPs is above levels considered environmentally relevant (Gottschalk et al., 2009; Tiede et al., 2009; Giese et al., 2018) but it has been previously used in toxicological studies of waterborne exposed bivalves (Buffet et al., 2013; 2014; Gomes et al., 2013a; 2013b; 2014b). Also, in a previous study, we reported deleterious effects of dietary exposure to 10 µg Ag/L Ag NPs and to 1 µg Ag/L Ag NPs, a dose close to environmentally relevant concentrations, on spawning success of female mussels and on development of embryos descendant from exposed mussels (see Chapter 1).

2. MATERIALS AND METHODS

2.1. Characterization of NPs

Ag NPs coated with PVP/PEI (Poly N-vinyl-2-pyrrolidone + Polyethyleneimine; 77%:23% at a concentration of 104 g/L in the final dispersion) were purchased as a stable aqueous suspension from Nanogap (O Milladoiro, Galicia, Spain). According to the manufacturers' information, PVP/PEI coated Ag NPs showed an average size of 5.08 ± 2.03 nm (see Appendix) and a zeta potential of $+18.6 \pm 7.9$ mV in distilled water.

Particle size distribution and dissolution of PVP/PEI coated 5 nm Ag NPs in seawater (SW) were analyzed as reported in Chapter 1. Briefly, PVP/PEI coated 5 nm Ag NPs dispersed in SW immediately reached a mean size of roughly 97 nm according to Dynamic Light Scattering using a Zetasizer Nano Z (Malvern Instruments Ltd., Worcestershire, UK). After 24 hours, particle size remained stable around 94-96 nm

(see Chapter 1). Dissolution of PVP/PEI coated 5 nm Ag NPs was assessed in SW after 12, 24, 48 and 72 hours. For that, 10 mL samples of the Ag NP suspensions were prepared at a concentration of 10 mg/L and filled into dialyzer tubes (Spectra/ Por® Float-A-Lyzer; MWCO 0.1-0.5 kDa). The sample-filled dialyzers were then immersed in 1 L SW and samples (3 replicates of 1 mL) were extracted at 12, 24, 48 and 72 hours from the solution and analyzed for Ag ions using Inductively Coupled Plasma Mass Spectrometry (ICP-MS; Thermo X2 series) after 100-fold dilution using external calibration. Differences obtained for replicate samples were consistently lower than 5% (Relative Standard Deviation; R.S.D). Dissolution of Ag NPs in SW was detected along the 72 hours of experimentation. After 12 hours, Ag NPs released around 4% of Ag ions increasing the dissolution to around 14% at 24 hours. After 48 hours ~17% of Ag ions were released from Ag NPs and at 72 hours, dissolution increased to 20% (see Chapter 1).

2.2. Experimental design

Mussels *Mytilus galloprovincialis* 3.5-4.5 cm in shell length were collected in autumn (November 2013) and spring (March 2014) from San Felipe, Galicia (43° 27.599'N, 8° 17.904'W). Upon arrival to the laboratory, mussels were placed in an acclimation tank with natural filtered SW (temperature =15.6°C, salinity =28.7‰, conductivity =36.4 mS/cm, pH =7.7 at light regime 12 h/12 h L/D) for 10 days. Mussels were maintained 5 days without feeding and then mussels were fed with *Isochrysis galbana* microalgae (20 x 10⁶ cells/ mussel-day) for other 5 days. For that, microalgae were cultured with natural filtered (0.2 µm) and sterilized SW at 20°C under cool continuous white fluorescent light (GRO-LUX F58W) with constant aeration in reactors at a concentration of 6x10⁶ cells/mL. Commercial F2 algae medium (Fritz Aquatics, USA) was supplied according to manufacturer's instructions. Concentration of microalgae was checked every day before feeding mussels.

After the acclimation period, mussels were distributed in two high density polypropylene containers (250 L) containing 240 mussels per tank. Mussels in the control tank were fed for 21 days with the microalgae *Isochrysis galbana* (20 x 10⁶ cells/ mussel-day) and mussels in the treatment tank were fed for 21 days with the same ration of microalgae *I. galbana* (20 x 10⁶ cells/ mussel-day) previously exposed for 24 hours to 10 µg Ag/L Ag NPs. Microalgae exposure was performed in constantly aerated two beakers (control and exposed) that contained the same volume of 6x10⁶ cell/mL of microalgae. A stock suspension of PVP/PEI coated Ag NPs was daily diluted in MilliQ water, vortexed and spiked to microalgae at the selected nominal exposure

concentration. This concentration was lower than Ag NP concentrations causing growth inhibition (0.1 mg Ag/L Ag NPs) in 72 hours bioassays (Schiavo et al., 2017). As reported in Chapter 1, Ag was significantly accumulated in microalgae exposed to 10 µg Ag/L Ag NPs for 24 hours, reaching a mean value of 21.3 ± 2.1 µg Ag/g d.w. After 24 hours, the beaker content with non-exposed or exposed microalgae was transferred to the corresponding mussel tank. Water in the mussel tanks was renewed every day before animal feeding. No mussel mortality was recorded along the experimentation time.

After 21 days of exposure, whole soft tissues of 20 mussels per experimental group were collected for chemical analysis. For Ag NPs localization, whole soft tissues of 3 mussels were fixed in 10% neutral buffered formalin. A piece of gonad of 20 mussels per experimental group were dissected out and fixed in 10% neutral buffered formalin in order to select only female mussels for the proteomic study. Digestive glands of the same 20 mussels per group were stored at -80°C until processing. Then, digestive glands of 5 female mussels per experimental group were used for the proteomic analysis.

2.3. Accumulation of Ag in mussel soft tissues

Soft tissues of 20 mussels per experimental group were pooled in 4 groups (4 pools of 5 individuals each) and then lyophilized by a freeze-dryer (Telstar Cryodos) for 5 days. Afterwards, samples (20-150 mg) were mineralized using 1.4 ml of HNO₃ (14 M, PlasmaPur) and 2 ml of HCl (12 M, PlasmaPur), according to Daskalakis (1996). Briefly, closed tubes were digested for 3 hours on a hot plate at 90°C (DigiPREP MS; SCP SCIENCE). After cooling, digestates were diluted and analyzed for Ag concentrations by ICP-MS (Thermo, X Series II) using external calibration (made of commercially available standard solutions PLASMACAL, SCP Science). Accuracy (>90%) and precision (<5%, Relative Standard Deviation) were controlled during each analytical session by parallel analysis of international referenced certified materials (TORT 2, IAEA 407). Results are expressed as µg Ag/g d.w. Significant differences ($p < 0.05$) with respect to controls as well as among seasons were set based on the Kruskal-Wallis test followed by the Dunn's test using the statistical package SPSS v.22 (SPSS Inc., IBM Company, Chicago, USA).

2.4. Histology of samples

After 24 hours of fixation in 10% neutral buffered formalin, whole mussels and gonad samples were routinely processed for paraffin embedding using a Leica Tissue processor ASP 3000 (Leica Instruments, Wetzlar, Germany). Histological sections (5 μm in thickness) were cut in a Leica RM2255 microtome (Leica Instruments) and placed on microscope glass slides.

2.4.1. *Localization of Ag NPs*

Dewaxing of mussel samples was performed using either xylene or Roti-histol. After 3 washes in xylene or Roti-histol, samples were hydrated with decreasing concentrations of ethanol (100%, 95% and 70%) followed by a final wash in deionized water before being dehydrated with increasing concentrations of ethanol (70%, 95% and 100%). Then, slides were washed in xylene or Roti-histol and mounted on cover slips. Samples were let to dry for 48 hours at room temperature before CytoViva® analyses.

Slides were visualized using CytoViva® hyperspectral imaging system (CytoViva Inc., Auburn, Alabama, USA) mounted on an Olympus BX-43 optical microscope as described in Mehennaoui et al. (2018). Briefly, images of the digestive gland and gills of non-exposed and exposed mussels were captured at 60x oil immersion magnification using hyperspectral camera controlled by environment for visualization ENVI software (version 4.8 from Harris Corporation, Melbourne, FL, USA and modified by CytoViva, Inc.). Spectral libraries of exposed mussels were generated manually with the acquisition of about 200 spectra per individual mussel. Acquired libraries were filtered against non-exposed samples to filter out all spectra non-related to Ag NPs using a spectral angle mapper (SAM) algorithm with a 0.05 radians tolerance. Filtered libraries were mapped onto images of exposed samples using SAM with 0.1 radian tolerance which allows highlighting similarities between the spectra in the image and in the spectral library (Mehennaoui et al., 2018).

2.4.2. *Gonad histology*

Gonad sections from the same individuals used for proteomics were stained with hematoxylin-eosin (Gamble and Wilson, 2002) and examined under the light microscope (Nikon Eclipse Ni; Nikon Instruments, Tokyo, Japan) in order to identify and select female mussels. A gonad index (GI) value was assigned to each selected

female gonad as described by Kim et al. (2006). A mean GI was then calculated for controls and for mussels dietarily exposed to Ag NPs.

2.5. Proteomic analysis

2.5.1. *Cell-free extract preparation and protein assay*

A pool of five female digestive glands per experimental group was weighed, suspended in 20% (w/v) HEPES-saccharose buffer (10 mM HEPES and 250 mM saccharose) containing 1 mM DTT, 1 mM EDTA, 1 mM PMSF and 10% protease inhibitor mixture and homogenized at 4°C. Then, homogenates were centrifuged at 15000 g for 2 hours and cell free extracts of crude cytosolic fractions were collected. Protein content was determined following the Bradford method (Bradford, 1976) with bovine serum albumin (BSA) as standard. 100 µg of protein content of each sample was suspended in 9 volumes of a precipitation solution (20 mM DTT, 10% trichloroacetic in cold acetone) for 2 hours at -20°C, centrifuged at 10000 g for 30 minutes (4°C) and washed with cold acetone. The residual acetone was removed by air drying before rehydrating the samples for the separation of proteins by two-dimensional gel electrophoresis.

2.5.2. *Two-dimensional gel electrophoresis (2-DE)*

Proteins were first separated by isoelectric focusing (IEF) followed by SDS-PAGE. Each sample (containing 100 µg of protein) was incubated for 30 minutes in 300 µL of rehydration buffer (7 M urea, 2 M thiourea, 4% CHAPS, 0.8% pharmalyte, 65 mM DTT and bromophenol blue traces), centrifuged at 14000 g for 10 minutes (4°C) and loaded on 6 different Immobiline®DryStrip (pH 3-10; 18 cm). After 6 hours of passive and 6 hours of active (50 V) rehydration, IEF was carried out (20°C, 50 µA/strip) in a Ettan IPGphor II (GE Healthcare) using a four step program: 1000 V for 1 hour; 4000 V for 1 hour; 8000 V for 1 hour and 8000 V until 50000 V/h were reach. Before the second dimension protein separation, 6 strips per sample were equilibrated in SDS equilibration buffer (6 M urea, 75 mM Tris-HCl, 4% SDS, 29.3% glycerol, 0.1 mM EDTA and 0.25% bromophenol blue) first with 2% DTT and second with 2.5% iodoacetamide. After equilibration, SDS-PAGE was performed in 10% polyacrylamide gels using a Ettan Daltsix Electrophoresis Unit (GE Healthcare). The separation in 6 gels was run in two steps; first, at 120 V for 30 minutes and then at 500 V for 5 hours until separation was finished. Gels were silver stained using a protocol compatible with MS analysis (Blum et al., 1987). Four gel replicates out of 6 gels for each pool were analyzed to ensure the reproducibility of 2D electrophoresis.

2.5.3. Image acquisition and analysis

The four gels per experimental group were scanned using a GS-800 densitometer (BIORAD, Hercules, CA) and analyzed using the PDQuest Advanced 8.0 software (BIORAD, Hercules, CA). All the 2-DE maps were performed with identical background subtraction after spot detection. The normalized volume of each spot was used for quantitative analyses by dividing its volume by the total volume of detected spots on the image in order to reduce experimental errors related to protein loading and staining. The normalized volumes from the different spots obtained from exposed samples were matched against the corresponding spots from control gels. The protein intensity of each spot was normalized to the total intensity of each gel image. Significant differences in regulated protein spots between control and mussels dietarily exposed to Ag NPs were set based on the Mann–Whitney U-rank test. Only spots regulated at least in 3 of the 4 gels for each group were included in the statistical analysis. Significance level was set at 5% ($p < 0.05$). Principal Component Analysis (PCA) was conducted using the PRIMER-E v6 software after the normalization method described by Apraiz et al. (2009). Briefly, volume data (vol. %) was normalized according to the following equation:

$$\text{NVol \%} = \ln(\text{vol. \%} + 1)$$

where NVol.% is the normalized vol.% obtained for each spot. After normalization of volume data and to reduce the inter-replicate variability, only protein spots with a coefficient of variation smaller than 40% were considered for the PCA.

2.5.4. Digestion of proteins and protein identification

Protein spots from control and exposed mussels including spots with changes in protein expression above or below 4-fold were manually excised from silver stained gels. Digestion and analysis through mass spectrometry were performed in the Bioscope Bio-Analytcs and Proteomics Lab from the New University of Lisbon. Briefly, picked spots were digested with trypsin, as described in Shevchenko et al. (2007). Proteins were subjected to peptidmass fingerprint (PMF) and mass spectra were acquired using an Ultraflex II MALDI–TOF (Bruker Daltonics) operating with positive polarity in reflectron mode. Spectra were acquired in the range of m/z 900–3500. A total of 3000 spectra were acquired at each spot position at a laser frequency of 50 Hz. Data acquisition and processing was performed with Flex Analysis software 3.0 (Bruker Daltonics) with the SNAP peak detection algorithm. The obtained peptide mass list was sent to the MASCOT

search engine using the NCBI Database. Searches were performed using the following parameters: taxonomy: *M. galloprovincialis* or Bivalvia, proteolytic enzyme: trypsin, peptide tolerance: up to 100 ppm, fixed modifications: carbamidomethyl, variable modification: oxidation, peptide charge state: +1, missed cleavages allowed: up to 2. The significance threshold was set to a minimum of 95%.

Biological processes of proteins were identified according to UniProt database (UniProt Consortium, 2017). Then, the KEGG: Kyoto Encyclopedia of Genes and Genomes database (Kanehisa et al., 2017) was used to decipher the altered metabolic pathways. Briefly, identified sequences were annotated against the Ostreidae family using the BlastKOALA tool in order to get the KEGG identifiers. Then, assigned KEGG identifiers were introduced in the KEGG pathways mapping tool to identify the different metabolic pathways in which the identified protein spots were involved.

3. RESULTS

3.1. Accumulation of Ag in mussel soft tissues

Ag was significantly accumulated in mussel soft tissues after 21 days of dietary exposure to 10 µg Ag/L Ag NPs both in autumn and in spring (Table 1). Although microalgae and mussel exposure conditions were identical in both seasons, higher levels of Ag were accumulated in autumn (0.73 µg Ag/g d.w.) compared to spring (0.35 µg Ag/g d.w.) (Table 1).

Table 1. Bioaccumulation of Ag in mussel soft tissues after 21 days of dietary exposure to 10 µg /L of Ag NPs. Significant differences were set based on Dunn's test. Asterisks show significant differences with respect to controls ($p < 0.05$). Letters represent significant differences among seasons. Values are given as means \pm S.D. Mean values belong to 4 pools of 5 individuals each.

	µg Ag/g d.w.	
	AUTUMN	SPRING
Control	0.09 \pm 0.02 ^a	0.04 \pm 0.003 ^a
10 µg Ag/L Ag NPs	0.73 \pm 0.069 ^{*, b}	0.35 \pm 0.044 ^{*, c}

3.2. Localization of Ag NPs

CytoVIVA® analyses confirmed the presence of Ag NPs in the sections of the digestive gland of mussels dietarily exposed to 10 µg Ag/L Ag NPs both in autumn and in spring (Figure 2 A,B). Ag NPs were mainly located inside the digestive tubule cells and in the lumen in both seasons (Figure 2 A,B). Ag NPs were also found in the gills of mussels dietarily exposed both in autumn and in spring (Figure 2 C,D).

3.3. Gonad histology

All mussels selected for proteomic analysis were confirmed to be female. In autumn, female mussels showed gonads in early gametogenic stage (Figures 3 A,B). GI mean value was 2.2 ± 1.20 for non-exposed females and 1.9 ± 0.89 for dietarily exposed mussels. In spring, female gonads were in an advanced gametogenic stage or in a mature stage (Figures 3 C,D). Non-exposed females GI was 4.75 ± 0.67 and exposed females GI was 4.1 ± 0.82 .

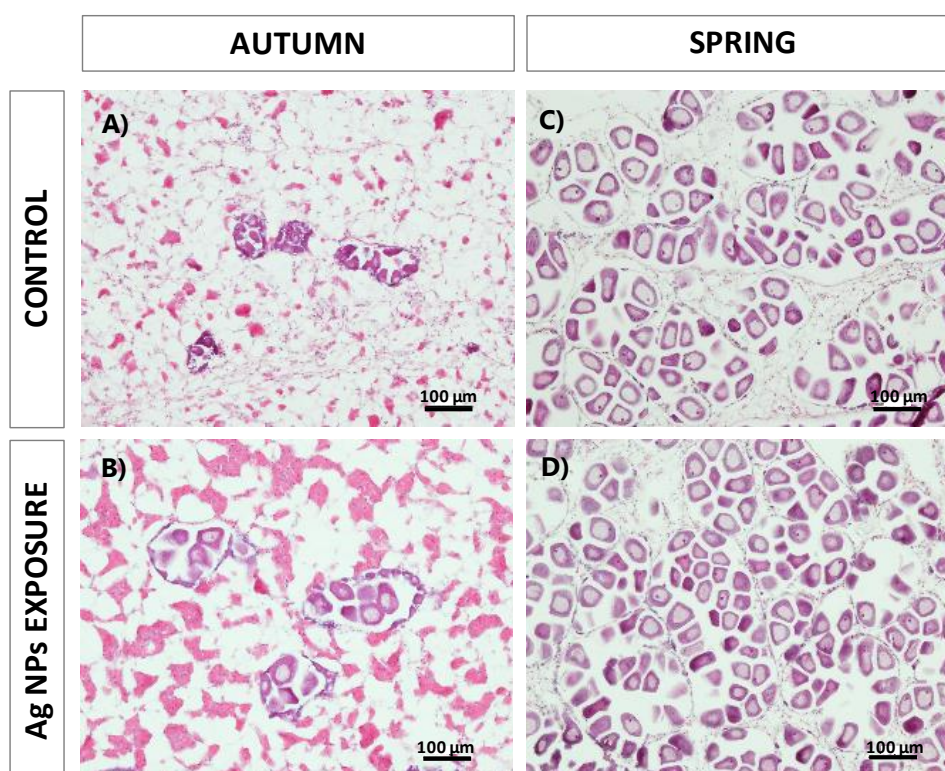


Figure 3. Representative micrographs showing the developmental stage of gametes of mussels belonging to **A)** non-exposed females in autumn, **B)** exposed females in autumn, **C)** non-exposed females in spring and **D)** exposed females in spring. Scale bars: 100 µm.

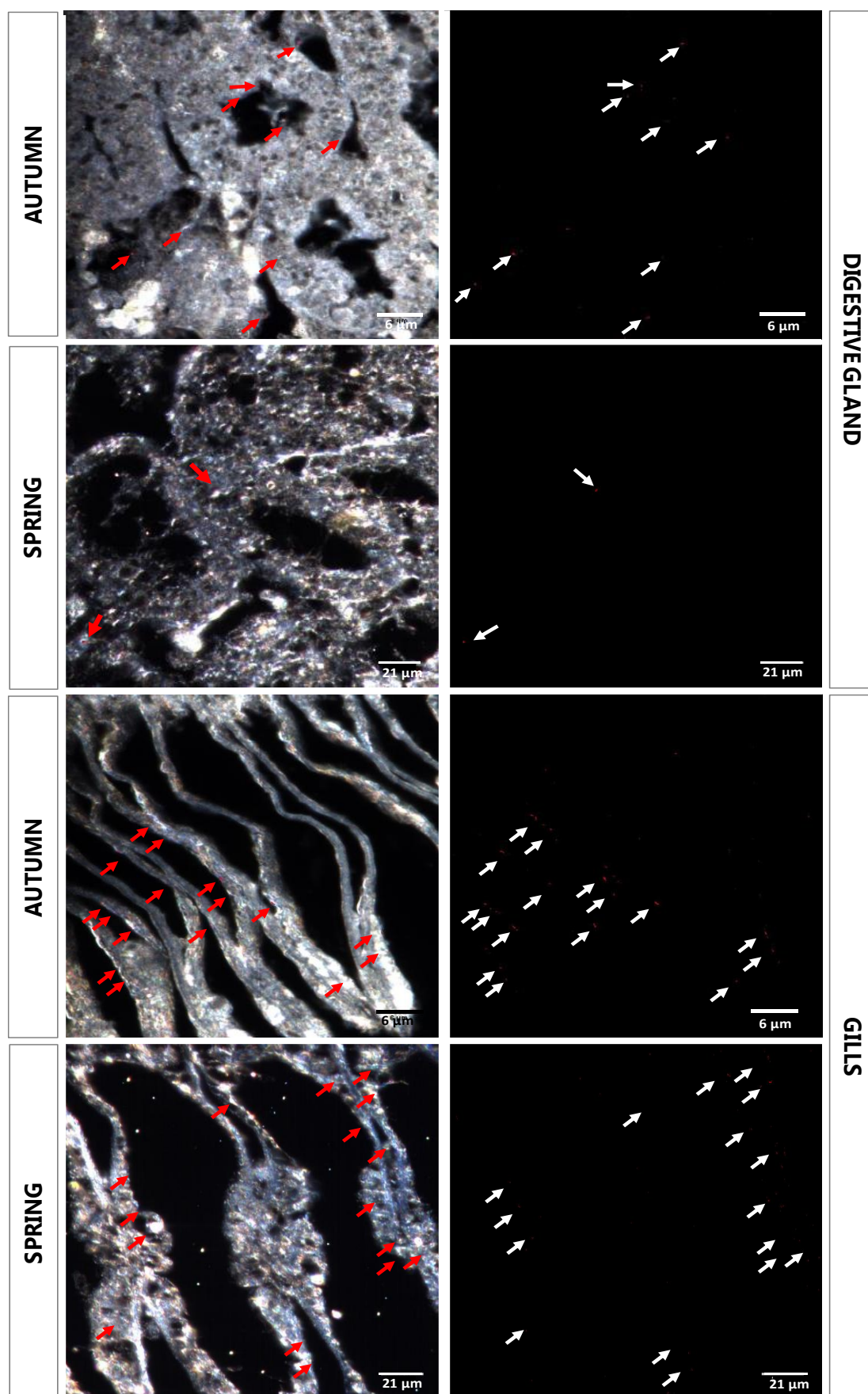


Figure 2. Hyperspectral images showing the presence of PVP/PEI coated 5 nm Ag NPs in the digestive gland tubule cells (A, B) and gills (C, D) of mussels dietarily exposed to 10 μg Ag/L of Ag NPs for 21 days in autumn (A, C) and spring (B, D). Micrographs in the left correspond to tissue sections observed under CytoViva® hyperspectral imaging system and micrographs in the right show the localization of Ag NPs. Red and white arrows indicate the presence of Ag NPs.

3.4. Proteomic analysis

3.4.1. *2-DE image analysis*

After 2-DE, different protein expression profiles were obtained in the digestive gland of unexposed mussels and in mussels dietarily exposed to 10 µg Ag /L Ag NPs for 21 days in two different seasons (Figure 4). Image analysis of the gels revealed 104 differentially expressed protein spots in autumn (Figure 5 A) and 142 differentially expressed protein spots in spring (Figure 5B).

In autumn, among the 104 protein spots differentially expressed, 46 were present only in control mussels and 36 protein spots were present only in exposed ones (Figure 5A). 22 protein spots differentially expressed were common for both groups and showed at least a 2-fold or a higher fold change in comparison to controls. 9 of them were overexpressed and 13 were underexpressed (Figure 5A).

Of the 142 protein spots differentially expressed in spring, 26 protein spots appeared significantly expressed only in non-exposed mussels, while 83 protein spots were significantly expressed only in exposed digestive glands (Figure 5B). 33 protein spots showing a fold change higher than 2 were expressed in both treatments. Among them, 11 protein spots were overexpressed and 22 protein spots were underexpressed (Figure 5B). Overall, more protein spots were differentially expressed in spring than in autumn (Figures 5 A,B).

Comparing control samples among seasons, 121 protein spots were differentially expressed (Figure 5C). 62 protein spots were only expressed in autumn while 22 protein spots were only expressed in spring (Figure 5C). 37 protein spots differentially expressed were common to both seasons being 19 of them overexpressed and 18 underexpressed (Figure 5C).

Finally, 156 protein spots were differentially expressed between seasons in the digestive gland of mussels dietarily exposed to 10 µg Ag/L Ag NPs (Figure 5D). Among them, 50 protein spots were only found in autumn and 63 protein spots were only found in spring (Figure 5D). 43 protein spots differentially expressed were common to both seasons; 9 of them were overexpressed and 34 were underexpressed (Figure 5D).

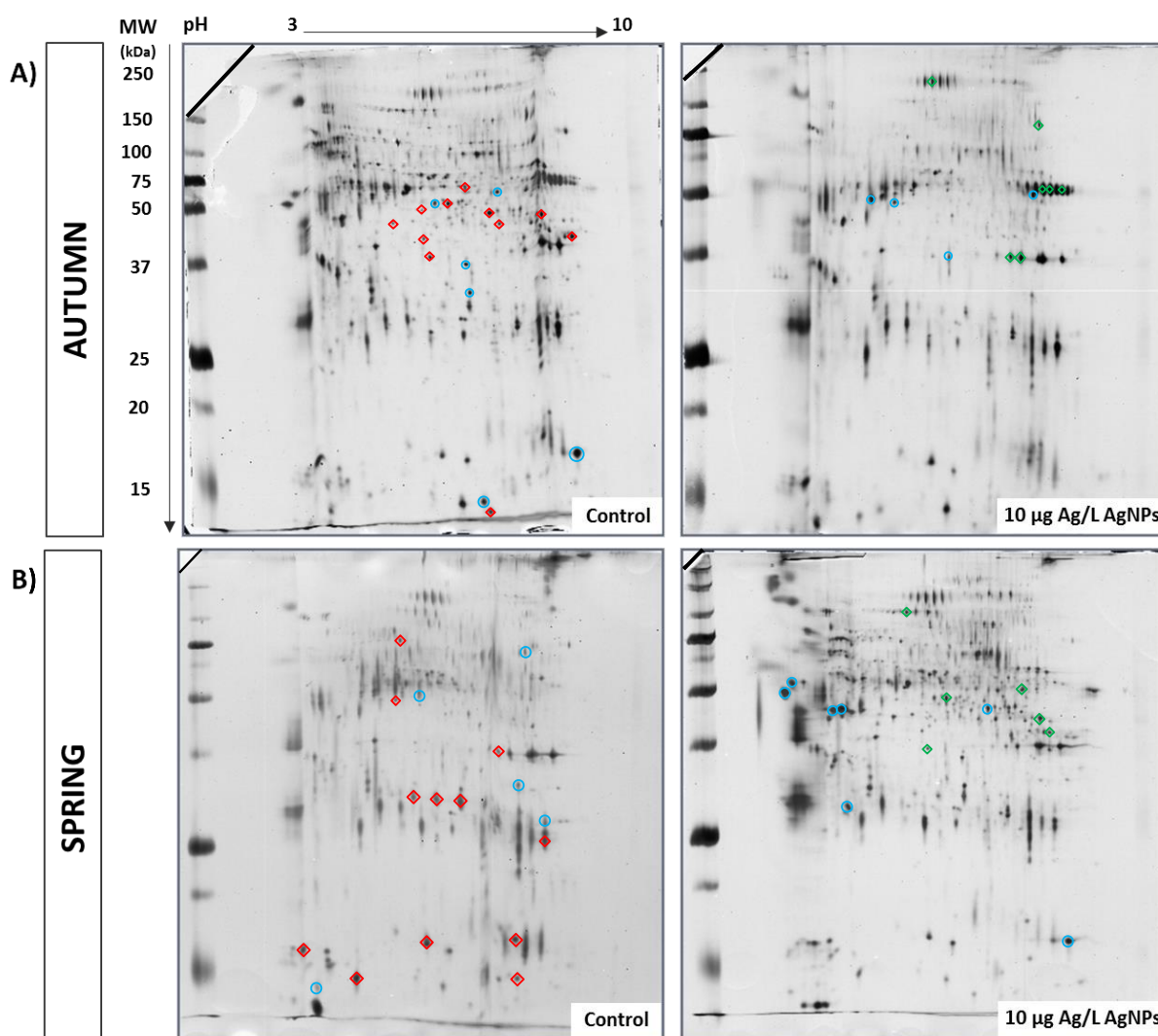


Figure 4. Representative 2-DE gels showing the expression profile of proteins observed in the digestive gland of mussels *M. galloprovincialis* in A) autumn and in B) spring. Gels on the left belong to non-exposed mussels and gels on the right correspond to mussels dietarily exposed to 10 µg Ag /L of Ag NPs for 21 days. pH gradient is represented in the x-axis and molecular weight (Mw) in kDa in the y-axis. Blue circles point out protein spots specific for each treatment that were picked for identification. Over and underexpressed protein spots picked for identification are pointed out by green and red rhombus, respectively.

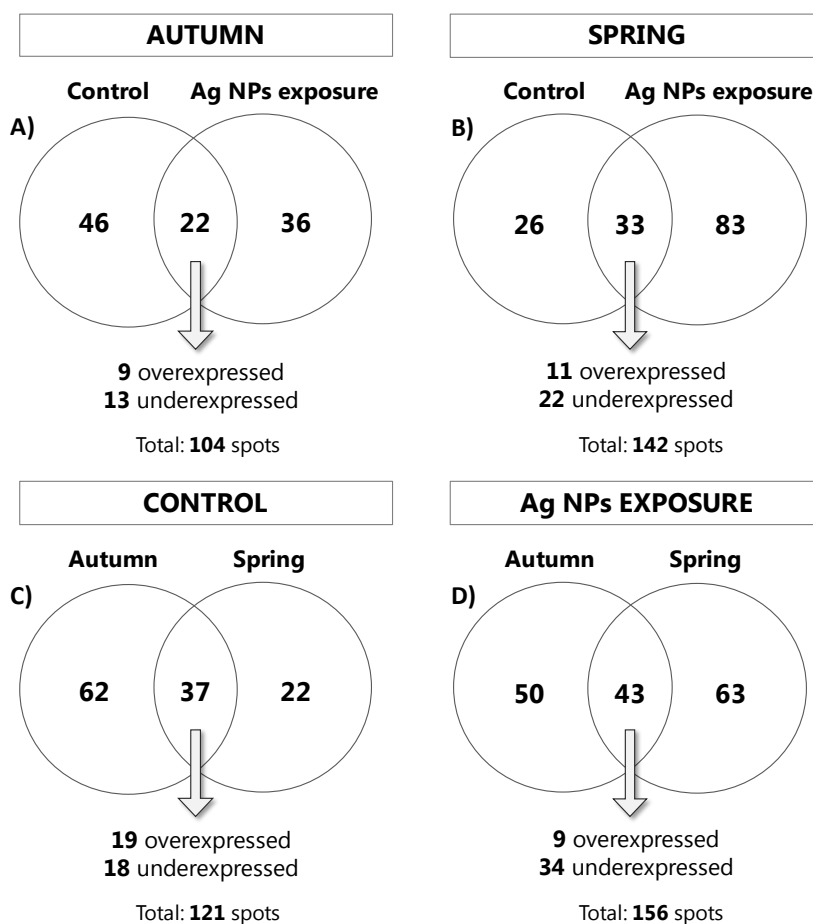


Figure 5. Venn diagrams showing the number of common and differentially expressed protein spots in **A)** autumn, **B)** spring **C)** controls and **D)** dietarily exposed mussels.

Therefore, the PCA showed differences in protein expression profiles based on the dietary exposure to Ag NPs and the season. PC1, which explained 36.8% of variation, clearly separated mussels exposed to 10 μg Ag/L Ag NPs in autumn from the rest of mussels (Figure 6). PC2 (34.6% of variation) discriminated the two seasons and PC3 (28.4% of variation) grouped non-exposed mussels belonging to both seasons together. The analysis revealed that the protein expression profiles were affected by the exposure treatment and that mussels showed differences in the response depending on the season (Figure 6).

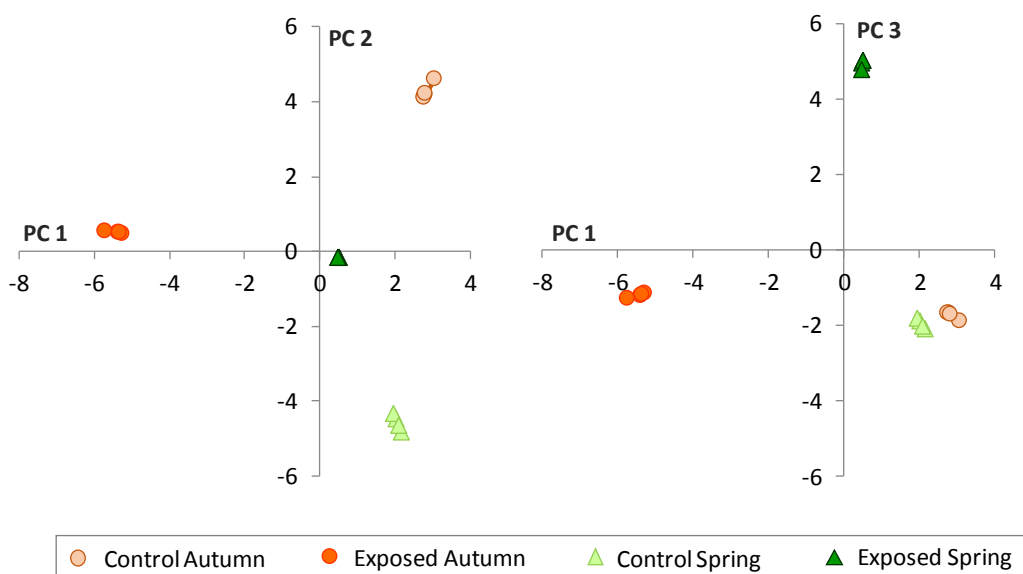


Figure 6. PCA plot based on the significantly expressed protein spots in all the treatments. PC1 was selected to be shown in both plots as it explained the highest percentage of variability. PC1= 36.8%; PC2= 34.6%; PC3= 28.4%. Each symbol point represents one gel (n=4 gels per treatment) and legend at the bottom of the graph shows symbols corresponding to each experimental group.

3.4.2. Protein identification by mass spectrometry

Based on the *Mytilus galloprovincialis* database (2666 sequences), 16 out of the 60 picked and differentially expressed protein spots were identified by MALDI-TOF. In autumn, 10 differentially expressed protein spots could be identified (Table 2). Among them, 4 different overexpressed protein spots (spots 7524, 8555, 8556, 8558) were identified as *chitinase like protein-3, partial* and 2 different overexpressed protein spots (spots 6325, 7304) as *glyceraldehyde-3-phosphate dehydrogenase, partial* (Table 2). The rest of protein spots were identified as *LKD-rich protein-1, nuclear receptor subfamily 1 DEF, partial, paramyosin* and *cytosolic malate dehydrogenase* (Table 2). In spring, 6 protein spots were identified based on the *M. galloprovincialis* database (Table 3). *Chitinase like protein-3, partial, superoxide dismutase* and *glyceraldehyde-3-phosphate dehydrogenase, partial* were significantly underexpressed, while *actin* (spots 3420, 2419) and *putative C1q domain containing protein MgC1q52* were significantly regulated only in dietarily exposed mussels (Table 3).

The identification search was extended to the Bivalvia database (120604 sequences) allowing the classification of 6 new protein spots in autumn and other

9 protein spots in spring (Tables 2, 3). In autumn, *matrix metalloproteinase-19*, two *hypothetical proteins* (CGI_10016468 and CGI_10001770, respectively) and *PREDICTED: inorganic pyrophosphatase-like isoform X2* were significantly underexpressed while *putative transcription factor PML* and *PREDICTED: vinculin-like isoform X7* were only significantly expressed in non-exposed and exposed mussels, respectively (Table 2). Among overexpressed protein spots in spring *putative transcription factor PML* (spots 8206, 5201) and *connector enhancer of kinase suppressor of ras 2* were identified (Table 3). *PREDICTED: GRIP and coiled-coil domain-containing protein 2-like* and *3-hydroxybutyryl-CoA dehydrogenase* were identified among underexpressed protein spots in spring (Table 3). *PREDICTED: lipoxygenase homology domain-containing protein 1-like isoform X3* appeared expressed only in control mussels and *selenoprotein H* only in dietarily exposed ones. *PREDICTED: centrosomal protein of 152 kDa-like* (spots 8602, 1506) was identified separately in control mussels as well as in dietarily exposed ones (Table 3).

KEGG pathway analysis successfully related some of the identified protein spots to different metabolic pathways in which they are involved (Tables 2, 3). Similar metabolic pathways such as *amino sugar and nucleotide sugar metabolism*, *carbon metabolism*, *glycolysis/gluconeogenesis* and the *biosynthesis of amino acids* in which *chitinase like protein-3, partial* and *glyceraldehyde-3-phosphate dehydrogenase* protein spots are involved in were altered in both seasons (Tables 2, 3). In addition, other specific pathways were altered in each season. In autumn, the *pyruvate metabolism*, *citrate cycle*, *cysteine and methionine metabolism* and *glyoxylate and dicarboxylate metabolism* were altered due to the under expression of the *cytosolic malate dehydrogenase* protein spot (Table 2). In spring, the overexpression of *actin* (2 protein spots) was associated to alterations in the *formation of phagosomes* and the under expression of *superoxide dismutase* to alterations in the *hydrogen peroxide metabolism of the antioxidant system of peroxisomes* (Table 3).

Table 2. Differentially expressed protein spots in autumn identified by MALDI-TOF. Spots present only in control samples, only in exposed samples and those common to control and exposed samples are shown.

AUTUMN	SPOT	NAME	ACCESSION NUMBER	SPECIES	P- value (<0.05) ^a	FOLD CHANGE	BIOLOGICAL PROCESS ^b	KEGG identifier	KEGG PATHWAY ^c
CONTROL	6111	<i>putative transcription factor PML</i>	EKC33587.1	<i>Crassostrea gigas</i>	0.002	-	localization, transport	crg:109618835	-
	8105	<i>LKD-rich protein-1</i>	AKS48185	<i>Mytilus galloprovincialis</i>	0.0034	-	-	crg:1053444531	-
	7524	<i>chitinase-like protein-3, partial</i>	AIK22450	<i>Mytilus galloprovincialis</i>	0.012	-	chitin catabolic process, carbohydrate metabolic process	crg:1053331570	metabolic pathways, amino sugar and nucleotide sugar metabolism
	4430	<i>PREDICTED: vinculin-like isoform X7</i>	XP_011426098	<i>Crassostrea gigas</i>	0.00085	-	cell adhesion	crg:105327367	-
EXPOSED	4407	<i>nuclear receptor subfamily 1 DEF, partial</i>	ABU89803	<i>Mytilus galloprovincialis</i>	0.027	-	regulation of transcription, DNA-templated; intracellular receptor signaling pathway; steroid hormone mediated signaling pathway	crg:105321080	-
	6325	<i>glyceraldhyde-3-phosphate dehydrogenase, partial</i>	AIK22450	<i>Mytilus galloprovincialis</i>	0.022	11.81	glucose metabolic process, glycolytic process, oxidation-reduction process	crg:105340512	metabolic pathways, carbon metabolism, glycolysis/ gluconeogenesis, biosynthesis of aminoacids
	7304				0.005	4.52			
	8555				0.0046	7.53			
	8556	<i>chitinase-like protein-3, partial</i>	AIK22450	<i>Mytilus galloprovincialis</i>	0.03	4.81	chitin catabolic process, carbohydrate metabolic process	crg:105345920	metabolic pathways, amino sugar and nucleotide sugar metabolism
	8558				0.05	4.73			
	8403	<i>paramyosin</i>	BAA36517	<i>Mytilus galloprovincialis</i>	0.029	-6.31	metabolic process	crg:105329634	-
	5312	<i>cytosolic malate dehydrogenase</i>	AAZ79367	<i>Mytilus galloprovincialis</i>	0.022	-5.8	carbohydrate metabolic process, tricarboxylic acid cycle, malate metabolic process, carboxylic acid metabolic process, oxidation- reduction process	crg:105343888	metabolic pathways, carbon metabolism, pyruvate metabolism, citrate cycle, cysteine and methionine metabolism, glyoxylate and dicarboxylate metabolism
	5317	<i>matrix metalloproteinase-19</i>	EKC37558	<i>Crassostrea gigas</i>	0.056	-10.67	proteolysis	crg:105338896	-
	5409	<i>hypothetical protein CGL_10016468</i>	EKC33615	<i>Crassostrea gigas</i>	0.024	-7.5	uncharacterized protein	crg:105330727	-
5415	<i>hypothetical protein CGL_10001770</i>	EKC26982	<i>Crassostrea gigas</i>	0.049	-6.87	uncharacterized protein	crg:105328562	-	
5401	<i>PREDICTED: inorganic pyrophosphatase-like isoform X2</i>	XP_011429567	<i>Crassostrea gigas</i>	0.054	-7.17	phosphate-containing compound metabolic process	crg:105329817	-	

^a Significance value of the matches obtained using MASCOT software for the protein identification using *M. galloprovincialis* or Bivalvia databases.

^b Biological process in which proteins are involved according to Uniprot database.

^c Metabolic pathways in which proteins are involved based on KEGG analysis.

Table 3. Differentially expressed protein spots in spring identified by MALDI-TOF. Spots present only in control samples, only in exposed samples and those common to control and exposed samples are shown.

SPRING	SPOT	NAME	ACCESSION NUMBER	SPECIES	p-value (<0.05) ^a	FOLD CHANGE	BIOLOGICAL PROCESS ^b	KEGG identifier	KEGG PATHWAY ^c
CONTROL	8602	PREDICTED: centrosomal protein of 152 kDa-like	XP_011436998	<i>Cassostrea gigas</i>	0.0063	-	centriole replication, de novo centriole assembly	crg:105335033	-
	5413	PREDICTED: lipoygenase homology domain-containing protein 1-like isoform X3	XP_011448787	<i>Cassostrea gigas</i>	0.065	-	-	crg:105343219	-
EXPOSED	1410	putative C1q domain containing protein Mgc1q52	CBX41701	<i>Mytilus galloprovincialis</i>	0.026	-	immune response	-	-
	3420	<i>actin</i>	AAD40314	<i>Mytilus galloprovincialis</i>	1.7 e ⁻⁵	-	-	crg:105326698	formation of phagosomes
	2419				0.0056	-		crg:105335713	
COMMON	1506	PREDICTED: centrosomal protein of 152 kDa-like	XP_011436998	<i>Cassostrea gigas</i>	0.026	-	centriole replication, de novo centriole assembly	crg:105335033	-
	7301	<i>Selenoprotein H</i>	EKC30285	<i>Cassostrea gigas</i>	0.045	-	-	crg:105317517	-
COMMON	8206	<i>putative transcription factor PML</i>	EKC33587	<i>Cassostrea gigas</i>	0.021	7.18	-	crg:109618835	-
	5201				0.0085	5.17			
COMMON	5423	<i>connector enhancer of kinase suppressor of ras 2</i>	XP_011420299	<i>Cassostrea gigas</i>	0.044	24.85	phosphorylation	crg:105323047	-
	5601	<i>chitinase-like protein-3, partial</i>	AKS48199	<i>Mytilus galloprovincialis</i>	0.029	-5.57	chitin catabolic process, carbohydrate metabolic process	crg:105345920	metabolic pathways, amino sugar and nucleotide sugar metabolism
	5110	<i>superoxide dismutase</i>	CAQ68509	<i>Mytilus galloprovincialis</i>	0.0045	-5.3	superoxide metabolic process, removal of superoxide radicals, oxidation - reduction process	crg:105327946	hydrogen peroxide metabolism in peroxisomes
COMMON	7202	<i>glyceraldehyde-3-phosphate dehydrogenase, partial</i>	AKK2450	<i>Mytilus galloprovincialis</i>	0.015	-5.3	glucose metabolic process, glycolytic process, oxidation-reduction process	crg:105340512	metabolic pathways, carbon metabolism, glycolysis/ gluconeogenesis, biosynthesis of aminoacids
	5307	PREDICTED: GRP and coiled-coil domain-containing protein 2-like	XP_011448370	<i>Cassostrea gigas</i>	0.0076	-12.12	protein targeting to Golgi	crg:105342939	-
	8220	<i>3-hydroxybutyryl-CoA dehydrogenase</i>	EKC26490	<i>Cassostrea gigas</i>	0.063	-6.05	fatty acid metabolic process, oxidation - reduction process	crg:105329039	-

^a Significance value of the matches obtained using MASCOT software for the protein identification using *M. galloprovincialis* or *Bivalvia* databases.

^b Biological process in which proteins are involved according to Uniprot database.

^c Metabolic pathways in which proteins are involved based on KEGG analysis.

4. DISCUSSION

Proteomic analysis has been already applied in mussels after the waterborne exposure to different metallic NPs (Tedesco et al., 2008; 2010a; 2010b; Gomes et al., 2014a; Hu et al., 2014), including Ag NPs (Gomes et al., 2013b; Bouallegui et al., 2018) in order to identify significant alterations in protein expression patterns. In the present study, differentially expressed protein signatures were investigated in the digestive gland of female mussels exposed to Ag NPs through the diet at two different seasons, autumn and spring.

In both seasons, mussel soft tissues significantly accumulated Ag after 21 days of dietary exposure to 10 µg Ag/L Ag NPs, but higher levels of Ag were accumulated in autumn than in spring. Differences in metal concentration in mussels can result from changes in the physiology of animals related to the season, rather than from changes in metal exposure conditions (Mubiana et al., 2005). For instance, gonadal growth decreased concentrations of Cu and Zn in oysters *Crassostrea iridiscensis* (Paéz-Osuna et al., 1995) and modified Ag and Cd concentrations in wild oysters of the Gironde estuary due to the weight losses and gains during the reproduction cycle (Lanceleur et al., 2011). In mussels collected from a metal polluted area during one year, the decrease in metal concentrations in the digestive gland was linked to the penetration of gonadic tissues into the digestive gland during gametogenesis, which biologically diluted metal concentrations (Regoli and Orlando, 1994). Thus, the lower concentration of Ag measured in mussel soft tissues in spring could be related to the increase of body weight caused by the development of gametes observed in spring. For future studies, the use of the metal/shell-weight index could be useful as it avoids variability in metal accumulation due to variations in soft-body weight related to the season (Fischer, 1983; Soto et al., 1995).

Silver has an unusually wide range of bioaccumulation as reviewed by Luoma and Rainbow (2005), but marine bivalves exposed to different types of Ag NPs usually accumulate low concentrations of Ag in their tissues, as observed in the present study (0.73 and 0.35 µg Ag/g d.w. in autumn and spring, respectively). Bivalves *Scrobicularia plana* waterborne exposed to 10 µg Ag/L of lactate-stabilized Ag NPs for 14 days accumulated around 0.753 µg/g w.w. of Ag in their tissues. When clams were exposed to the same dose of Ag NPs through the diet the concentration of accumulated Ag in their tissues was lower (0.4 µg/g w.w.) (Buffet et al., 2013). The same authors observed even a lower accumulation of Ag (0.25 µg/g w.w.) in clam tissues after waterborne exposure to 10 µg/L of maltose-Ag NPs for 21 days in comparison to their previous work (Buffet et al., 2014). Jimeno-Romero and colleagues (2017) also reported low values of Ag

accumulated in *M. galloprovincialis* mussel soft tissues after their exposure to 0.75 µg/L of different sized maltose-stabilized Ag NPs. After 1 day of exposure to 20 nm and 100 nm Ag NPs, around 0.101 ± 0.049 µg/g d.w. and 0.172 ± 0.112 µg/g d.w. of Ag were accumulated in mussel soft tissues, respectively, while accumulation of Ag significantly decreased at day 21 in both cases (Jimeno-Romero et al., 2017).

According to Ag NP dissolution results, most Ag (around 86%) remained in nanoparticulate form during the 24 hours exposure period (see Chapter 1). Thus, the main part of the Ag measured was in NP form and the presence of Ag NPs was confirmed in the digestive gland of mussels in both seasons, indicating a successful transfer of Ag NPs from microalgae to mussels. Ag NPs were mainly located inside the digestive tubules and in their lumen in both seasons, as previously observed by light and electron microscopy in mussels exposed to Ag NPs via water (Jimeno-Romero et al., 2017). In fact, the digestive gland of bivalves is considered the main organ for accumulation of NPs (Canesi and Corsi, 2016). However, Ag NPs were also localized in mussel gills, which are considered the first barrier to surrounding water and a vulnerable tissue to NP interactions (Corsi et al., 2014; Rocha et al., 2015a).

Even if accumulation of Ag was higher in autumn than in spring, the proteome level response was more marked in spring than in autumn. Season and exposure dependent alterations in the protein expression profile of mussels dietarily exposed to Ag NPs were shown by the PCA plots. These findings could be related to the sensitivity shown by mussels in some stages of their reproductive cycle such as the reproduction period (Leiniö and Lehtonen., 2005; Almeida et al., 2013) together with the effect of the treatment since other confounding factors such as gender and size of mussels can be discarded.

Based on the *M. galloprovincialis* and *Bivalvia* databases, out of 60 picked protein spots, 31 protein spots coding for 22 different proteins were identified. Peptide identification using MS spectra can be challenging and limiting in non-model organisms such as mussels, whose genomes are not yet fully sequenced or available to the public (Gomes et al., 2017). The identified sequences were set to KEGG pathway analysis in order to understand which metabolic pathways were affected after the dietary exposure of mussels to Ag NPs. *Chitinase like protein 3, partial* and *glyceraldehyde-3-phosphate dehydrogenase, partial* were involved in the same KEGG pathways that included the *amino sugar and nucleotide sugar metabolism*, *carbon metabolism*, *glycolysis/gluconeogenesis* and the *biosynthesis of amino acids* in both seasons. In mussels, chitinase enzymes are released by the crystalline style during digestion to break down glycoside bonds in chitin present in the exoskeleton of certain zooplankton species

and in the cell wall of some microalgae (Birkbeck and McHenry, 1984). Chitinases seem also to have immune functions (Gooday, 1999) and a role in the formation of the shell of molluscs (Weiss and Schönitzer, 2006). Alterations of the chitin metabolism in *Mytilus* spp. have been previously observed under hypoxic condition (Woo et al., 2011) and after the exposure to different contaminants such as metals, polycyclic aromatic hydrocarbons and fluorinated substances, among others (Díaz de Cerio et al., 2013; Dondero et al., 2006; 2010; 2011; Maria et al., 2013; Negri et al., 2013). On the other hand, Banni and colleagues (2011) proposed that alterations in chitinase-related activities should be considered as a typical response in bivalve molluscs during periods of intense feeding activity as consequence of higher food metabolism. In the present study, mussels were fed daily with microalgae during the experimental period, but *chitinase like protein 3, partial* was differentially expressed in exposed organisms suggesting that the exposure of mussels to Ag NPs through the diet could interfere in the metabolism of food.

Glyceraldehyde-3-phosphate dehydrogenase (G3PDH) is a glycolytic enzyme involved in glucose degradation and energy yield (Romero-Ruiz et al., 2006). Two protein spots (6325, 7304) of *glyceraldehyde-3-phosphate dehydrogenase, partial* were overexpressed in autumn while the same protein was underexpressed in spring (spot 7202) after the dietary exposure to Ag NPs. In *S. plana* clams inhabiting sites with high metal content, *G3PDH* was significantly more expressed and authors linked such overexpression with a heavy oxidative response (Romero-Ruiz et al., 2006). However, inactivation of *G3PDH* allows glucose metabolism to change temporally to the pentose phosphate pathway, enabling the cell to generate the antioxidant cofactor NADPH (Bernard et al., 2011). Underexpression of *G3PDH* was observed in mussels digestive gland after the exposure to diclofenac (Schmidt et al., 2014; Jaafar et al., 2015) and gemfibrozil (Schmidt et al., 2014), as a response to oxidative stress.

Oxidative stress has been described as one of the major modes of action of engineered metallic NPs, including Ag NPs, in bivalve tissues (reviewed in Baker et al., 2014; Rocha et al., 2015a; Canesi and Corsi, 2016). The burden of reactive oxygen species (ROS) production is largely counteracted by an antioxidant defense system that among others, includes enzymes such as superoxide dismutase (SOD), catalase and glutathione peroxidase (Finkel and Holbrook, 2000). Several studies have reported an increased activity of SOD in the digestive gland of mussels exposed to CuO NPs for 15 or 21 days (Gomes et al., 2012; Ruiz et al., 2015), to CdTe quantum dots for 14 days (Rocha et al., 2015b) or to Ag NPs for 15 days (Gomes et al., 2014b) as a response to ROS production. An increase in SOD activity was also described in *S. plana* clams exposed to Ag NPs or ionic Ag for 14 days through the diet (Buffet et al., 2013). In this work, the metabolism of

the antioxidant system of peroxisomes was affected in spring due to the under expression of the *superoxide dismutase* protein spot after the exposure of mussels to Ag NPs through the diet. Oxidative stress caused by the inhibition of enzymes such as SOD, catalase and peroxidases, after the exposure to Ag has been linked to the interaction of ionic Ag with the thiol groups found in such enzymes (Lapresta-Fernández et al., 2012). Thus, the under expression of *superoxide dismutase* suggests a situation of oxidative stress in mussels exposed in spring.

Oxidative stress has been observed to induce cytoskeleton disorganization in mussels hemocytes (Gómez-Mendikute et al., 2002; Gómez-Mendikute and Cajaraville, 2003) and clams (Rodríguez-Ortega et al., 2003) and this effect could be linked to increasing tubulin and actin levels (Clarkson et al., 2002). The integrity of actin cytoskeleton of mussel hemocytes can be disrupted by ionic Ag, Ag NPs and bulk Ag (Katsumiti et al., 2015) as well as by Cd and Cu (Gómez-Mendikute and Cajaraville, 2003). At proteome level, actin isoforms were under expressed in gills and digestive gland of mussels exposed to CuO NPs (Gomes et al., 2014a) or after the exposure to ionic Ag (Gomes et al., 2013b). Hu and colleagues (2014) also observed expression changes in four cytoskeletal components, including actin, after the exposure of mussels to CuO NPs. In this study, two protein spots identified as *actin* were overexpressed only in the digestive gland of mussels exposed to Ag NPs through the diet in spring, which was associated to alterations in phagosomes according to KEGG pathway analysis. Additionally, another cytoskeletal protein not classified by KEGG analysis but significantly under expressed in autumn was *paramyosin*. Previous studies have reported an induction of *paramyosin* after Ag NPs exposure in mussel gills (Gomes et al., 2013b) as well as an under expression of the same protein in mussels digestive gland after the exposure to CuO NPs (Gomes et al., 2014a). The disturbance of structural proteins of cytoskeleton such as *actin* and *paramyosin*, could be mediated by ROS formation (Gomes et al., 2013b; 2014a; Hu et al., 2014).

Further, the pyruvate metabolism, citrate cycle, cysteine and methionine metabolism, glyoxylate and dicarboxylate metabolism were altered in autumn associated to the under expression of the *cytosolic malate dehydrogenase* protein spot after the dietary exposure to Ag NPs. *Cytosolic malate dehydrogenase* is an enzyme that plays an important role in energy metabolism including the malate–aspartate (or NADH) shuttle, the acetate shuttle in lipogenesis and gluconeogenesis (Dahlhoff and Somero, 1993; Fields et al., 2006). Alteration in the expression of this protein has been already reported in juvenile mussels as well as in adult mussels *M. galloprovincialis* after the exposure to arsenate for 48 hours (Yu et al., 2016) and under acute heat stress (Tomanek and Zuzow,

2010), respectively, which was associated with the disturbance of energy metabolism in both cases. Thus, the exposure of mussels to Ag NPs through the diet seem to alter the energy metabolism in mussels digestive gland in autumn.

Moreover, the *nuclear receptor subfamily 1DEF* and *putative C1q domain containing protein MgC1q52* were also significantly altered after the dietary exposure of mussels to Ag NPs, although no KEGG pathway was associated in the analysis. The *nuclear receptor subfamily 1DEF, NR1DEF* was specifically expressed in exposed mussels in autumn. Gomes and co-authors (2013b) reported the overexpression of another nuclear receptor, the *nuclear receptor subfamily 1G*, in mussel gills after the exposure both to Ag NPs and to Ag⁺, suggesting that both Ag forms are able to interfere with the regulation of gene transcription.

In spring, the *putative C1q domain containing protein MgC1q52* was only expressed in exposed mussels, suggesting that the immune response of mussels was affected by the dietary exposure to Ag NPs. The large family of C1q domain containing proteins participates in several metabolic processes, such as tissue homeostasis, protein activation, immune response, apoptosis, phagocytosis, cell adhesion and cell growth modulation (Gestal et al., 2010; Gerdol et al., 2011; Gerdol and Venier, 2015). Under expression of one spot identified as *C1q domain protein* after the exposure to CuO NPs and Cu²⁺, as well as the overexpression of the *C1q domain containing protein 60* after the exposure to Ag⁺ were reported in mussel gills (Gomes et al., 2013b; Gomes et al., 2014a). In both cases, authors suggested that the immune capacity of exposed mussels was disrupted since cell-mediated immunity represents a significant target for NPs in bivalve molluscs (Canesi et al., 2012; Katsumiti et al., 2014; 2015; 2018).

5. CONCLUSIONS

Dietary exposure to PVP/PEI coated 5 nm Ag NPs significantly altered the proteome of digestive gland in mussels both in autumn and in spring. Treatment and season dependent protein signatures were found. Dietary exposure to Ag NPs altered common metabolic pathways such as amino sugar and nucleotide sugar metabolism, carbon metabolism, glycolysis/gluconeogenesis and the biosynthesis of amino acids in both seasons associated to the differential expression of *chitinase like protein-3*, *partial* and *glyceraldehyde-3-phosphate dehydrogenase*. The specific protein expression profile observed for each season showed that the dietary exposure to Ag NPs in autumn altered proteins related to the pyruvate metabolism, citrate cycle, cysteine and methionine

metabolism and glyoxylate and dicarboxylate metabolism, while in spring proteins involved in the formation of phagosomes and hydrogen peroxide metabolism of peroxisomes were differentially expressed. Other affected processes were the transcriptional regulation (*nuclear receptor subfamily 1DEF*) in autumn, the immune response (*putative C1q domain containing protein MgC1q52*) in spring and the organization of the cytoskeleton (*actin* and *paramyosin*) in both seasons. For future studies, season and related gamete developmental stage are factors that should be considered for assessing the potential effects caused by engineered NPs in marine bivalves since different protein expression profiles were found for autumn and spring after the dietary exposure to Ag NPs.

ACKNOWLEDGEMENTS

This work has been funded by the Spanish Ministry of Economy and Competitiveness (NanoSilverOmics project MAT2012-39372), Basque Government (SAIOTEK project S-PE13UN142 and Consolidated Research Group GIC IT810-13) and the University of the Basque Country UPV/EHU (UFI 11/37 and PhD fellowship to N.D.). This study had also the support of Fundação para a Ciência e Tecnologia (FCT) from Portugal through the Strategic Project UID/MAH00350/2013 granted to CIMA. The contribution of K. Mehennaoui was possible within the project NanoGAM (AFR-PhD-9229040) and M. Mikolaczyk was supported by a PhD fellowship from the French Ministry of Higher Education and Research.

REFERENCES

- ∴ Almeida C., Pereira C.G., Gomes T., Cardoso C., Bebianno M.J., Cravo A. 2013. Genotoxicity in two bivalve species from a coastal lagoon in the south of Portugal. *Marine Environmental Research* 89: 29-38.
- ∴ Apraiz I., Cajaraville M.P., Cristóbal S. 2009. Peroxisomal proteomics: Biomonitoring in mussels after the Prestige's oil spill. *Marine Pollution Bulletin* 58: 1815-1826.
- ∴ Baker T.J., Tyler C.R., Galloway T.S. 2014. Impacts of metal and metal oxide nanoparticles on marine organisms. *Environmental Pollution* 186: 257-271.
- ∴ Banni M., Negri A., Mignone F., Boussetta H., Viarengo A. and Dondero F. 2011. Gene expression rhythms in the mussel *Mytilus galloprovincialis* (Lam.) across an annual cycle. *PLoS ONE* 6 (5): e18904. doi:10.1371/journal.pone.0018904.
- ∴ Banni M., Attig H., Sforzini S., Oliveri C., Mignone F., Boussetta H., Viarengo A. 2014. Transcriptomic responses to heat stress and nickel in the mussel *Mytilus galloprovincialis*. *Aquatic Toxicology* 148: 104-112.
- ∴ Banni M., Sforzini S., Balbi T., Corsi I., Viarengo A., Canesi L. 2016. Combined effects of n-TiO₂ and 2,3,7,8-TCDD in *Mytilus galloprovincialis* digestive gland: A transcriptomic and immunohistochemical study. *Environmental Research* 145: 135-144.
- ∴ Banni M., Sforzini S., Arlt V.M., Barranguer A., Dallas L.J., Oliveri C., Aminot Y., Pacchioni B., Millino C., Lanfranchi G., Readman J.W., Moore M.N., Viarengo A., Jha A.N. 2017. Assessing the impact of benzo[a]pyrene on marine mussels: application of a novel targeted low density microarray complementing classical biomarker responses. *PLoS ONE* 12 (6): e0178460.
- ∴ Bayne B.L., Widdows J. 1978. The physiological ecology of two populations of *Mytilus edulis* L. *Oecologia* 37: 137-162.
- ∴ Bebianno M.J., Gonzalez-Rey M., Gomes T., Mattos J.J., Flores-Nunes F., Bainy A.C.D. 2015. Is gene transcription in mussel gills altered after exposure to Ag nanoparticles? *Environmental Science and Pollution Research* 22: 17425-17433.
- ∴ Bernard K.E., Parkes T.L., Merritt T.J.S. 2011. A Model of Oxidative Stress Management: Moderation of Carbohydrate Metabolizing Enzymes in SOD1-Null *Drosophila melanogaster*. *PLoS ONE* 6 (9): e24518.
- ∴ Bhuvaneshwari M., Thiagarajan V., Nemade P., Chandrasekaran N., Mukherjee A. 2018. Toxicity and trophic transfer of P25 TiO₂ NPs from *Dunaliella salina* to *Artemia salina*: Effect of dietary and waterborne exposure. *Environmental Research* 160: 39-46.
- ∴ Birkbeck T.H., McHenery J.G. 1984. Chitinases in the mussel (*Mytilus edulis*, L). *Comparative Biochemistry and Physiology, Part B* 77: 861-865.
- ∴ Blum H., Biere H., Gross H.J. 1987. Improved silver staining of plant proteins, RNA and DNA in polyacrylamide gels. *Electrophoresis* 8: 93-99.
- ∴ Bocchetti R., Regoli F. 2006. Seasonal variability of oxidative biomarkers, lysosomal parameters, metallothioneins and peroxisomal enzymes in the Mediterranean mussel *Mytilus galloprovincialis* from Adriatic Sea. *Chemosphere* 65: 913-921.

- .: Bouallegui Y., Ben Younes R., Oueslati R., Sheehan D. 2018. Role of endocytotic uptake routes in impacting the ROS-related toxicity of silver nanoparticles to *Mytilus galloprovincialis*: A redox proteomic investigation. *Aquatic Toxicology* 200: 21-27.
- .: Bradford M. 1976. A Rapid and Sensitive Method for the Quantitation of Microgram Quantities of Protein Utilizing the Principle of Protein-Dye Binding. *Analytical Biochemistry* 72: 248-254.
- .: Brown M., Davies I.M., Moffat C.F., Craft M.A. 2006. Application of SSH and microarray to investigate altered gene expression in *Mytilus edulis* in response to exposure to benzo[a]pyrene. *Marine Environmental Research* 62: S128-S135.
- .: Buffet P.E., Pan J.F., Poirier L., Amiard-Triquet C., Amiard J.C., Gaudin P., Risso. De Faverney C., Guibbolini M., Gilliland D., Valsami-Jones E. and Mouneyrac C. 2013. Biochemical and behavioural responses of the endobenthic bivalve *Scrobicularia plana* to silver nanoparticles in seawater and microalgal food. *Ecotoxicology and Environmental Safety* 89: 117-124.
- .: Buffet P.E., Zalouk-Vergnoux A., Châtel A., Berthet B., Métais I., Perrein-Ettajani H., Poirier L., Luna-Acosta A., Thomas-Guyon H., Risso-de Faverney C., Guibbolini M., Gilliland D., Valsami-Jones E., Mouneyrac C. 2014. A marine mesocosm study on the environmental fate of silver nanoparticles and toxicity effects on two endobenthic species: The ragworm *Hediste diversicolor* and the bivalve mollusc *Scrobicularia plana*. *Science of the Total Environment* 470-471: 1151-1159.
- .: Cancio I., Ibabe A., Cajaraville M.P. 1999. Seasonal variation of peroxisomal enzyme activities and peroxisomal structure in mussels *Mytilus galloprovincialis* and its relationship with the lipid content. *Comparative Biochemistry and Physiology, Part C* 123: 135-144.
- .: Canesi L., Ciacci C., Fabbri R., Marcomini A., Pojana G. and Gallo G. 2012. Bivalve molluscs as a unique target group for nanoparticle toxicity. *Marine Environmental Research* 76: 16-21.
- .: Canesi L. and Corsi I. 2016. Effects of nanomaterials on marine invertebrates. *Science of the Total Environment* 565: 933-940.
- .: Clarkson M.R., Murphy M., Gupta S., Lambe T., Mackenzie H. S., Godson C., Martin F., Brady H.R. 2002. High glucose-altered gene expression in mesangial cells. Actin regulatory protein gene expression is triggered by oxidative stress and cytoskeletal disassembly. *The Journal of Biological Chemistry* 277: 9707-9712.
- .: Corsi I., Cherr G.N., Lenihan H.S., Labille J., Hasselov M., Canesi L., Dondero F., Frenzilli G., Hristozov D., Puntès V., Della Torre C., Pinsino A., Libralato G., Marcomini A., Sabbioni E., Matranga V. 2014. Common Strategies and Technologies for the Ecosafety Assessment and Design of Nanomaterials Entering the Marine Environment. *ACS Nano* 8: 9694-9709.
- .: Dahlhoff E., Somero G.N. 1993. Kinetic and structural adaptations of cytoplasmic malate dehydrogenases of eastern Pacific abalone (genus *Haliotis*) from different thermal habitats: Biochemical correlates of biogeographical patterning. *The Journal of Experimental Biology* 185: 137-150.
- .: Daskalakis K.D. 1996. Variability of metal concentrations in oyster tissue and implications to biomonitoring. *Marine Pollution Bulletin* 32: 794-801.
- .: Díaz de Cerio O., Hands E., Humble J., Cajaraville M.P., Craft J.A., Cancio I. 2013. Construction and characterization of a forward subtracted library of blue mussels *Mytilus edulis* for the

- identification of gene transcription signatures and biomarkers of styrene exposure. *Marine Pollution Bulletin* 71: 230-239.
- ∴ Dondero F., Piacentini L., Marsano F., Rebelo M., Vergani L., Venier P., Viarengo A. 2006. Gene transcription profiling in pollutant exposed mussels (*Mytilus* spp.) using a new low-density oligonucleotide microarray. *Gene* 376: 24-36.
 - ∴ Dondero F., Negri A., Boatti L., Marsano F., Mignone F., Viarengo A. 2010. Transcriptomic and proteomic effects of a neonicotinoid insecticide mixture in the marine mussel (*Mytilus galloprovincialis*, Lam.). *Science of the Total Environment* 408: 3775-3786.
 - ∴ Dondero F., Banni M., Negri A., Boatti L., Dagnino A., Viarengo A. 2011. Interactions of a pesticide/heavy metal mixture in marine bivalves: a transcriptomic assessment. *BMC Genomics* 2011; 12: 195-212.
 - ∴ Dowling V.A., Sheehan D. 2006. Proteomics as a route to identification of toxicity targets in environmental toxicology. *Proteomics* 6: 5597-5604.
 - ∴ Fabrega J., Luoma S.N., Tyler C.R., Galloway T.S., Lead J.R. 2011. Silver nanoparticles: Behaviour and effects in the aquatic environment. *Environment International* 37: 517-531.
 - ∴ Fields P.A., Rudomin E.L., Somero G.N. 2006. Temperature sensitivities of cytosolic malate dehydrogenases from native and invasive species of marine mussels (genus *Mytilus*): sequence-function linkages and correlations with biogeographic distribution. *The Journal of Experimental Biology* 209: 656-667.
 - ∴ Finkel T., Holbrook N.J. 2000. Oxidants, oxidative stress and the biology of ageing. *Nature* 408: 239-247.
 - ∴ Fischer H. 1983. Shell weight as an independent variable in relation to cadmium content of molluscs. *Marine Ecology Progress Series* 12: 59-75.
 - ∴ Gambardella C., Costa E., Piazza V., Fabbrocini A., Magi E., Faimali M., Garaventa F. 2015. Effect of silver nanoparticles on marine organisms belonging to different trophic levels. *Marine Environmental Research* 111: 41-49.
 - ∴ Gamble M. and Wilson I. 2002. The hematoxylin and eosin. In: Brancfort J.D., Gamble M. (Eds.), *Theory and Practice of Histological Techniques*. Churchill Livingstone-Elsevier Science Ltd., London, UK. pp. 125.
 - ∴ Gerdol M., Manfrin C., De Moro G., Figueras A., Novoa B., Venier P., Pallavicini A. 2011. The C1q domain containing proteins of the Mediterranean mussel *Mytilus galloprovincialis*: A widespread and diverse family of immune-related molecules. *Developmental & Comparative Immunology* 35: 635-643.
 - ∴ Gerdol M., Venier P. 2015. An updated molecular basis for mussel immunity. *Fish and Shellfish Immunology* 46: 17-38.
 - ∴ Gestal C., Pallavicini A., Venier P., Novoa B., Figueras A. 2010. MgC1q, a novel C1q-domain-containing protein involved in the immune response of *Mytilus galloprovincialis*. *Developmental & Comparative Immunology* 34: 926-934.

- .: Giese B., Klaessig F., Park B., Kaegi R., Steinfeldt M., Wigger H., von Gleich A., Gottschalk F. 2018. Risks, release and concentrations of engineered nanomaterial in the environment. Scientific Reports 8: doi: 10.1038/s41598-018-19275-4.
- .: Gomes T., Pereira C.G., Cardoso C., Pinheiro J.P., Ibon Cancio I., Bebianno M.J. 2012. Accumulation and toxicity of copper oxide nanoparticles in the digestive gland of *Mytilus galloprovincialis*. Aquatic Toxicology 118-119: 72-79.
- .: Gomes T., Araújo O., Pereira R., Almeida A.C., Cravo A., Bebianno M.J. 2013a. Genotoxicity of copper oxide and silver nanoparticles in the mussel *Mytilus galloprovincialis*. Marine Environmental Research 84: 51-59.
- .: Gomes T., Pereira C.G., Cardoso C., Bebianno M.J. 2013b. Differential protein expression in mussels *Mytilus galloprovincialis* exposed to nano and ionic Ag. Aquatic Toxicology 136-137: 79-90.
- .: Gomes T., Chora S., Pereira C.G., Cardoso C., Bebianno M.J. 2014a. Proteomic response of mussels *Mytilus galloprovincialis* exposed to CuO NPs and Cu²⁺: An exploratory biomarker discovery. Aquatic Toxicology 155: 327-336.
- .: Gomes T., Pereira C.G., Cardoso C., Sousa V.S., Ribau Teixeira M., Pinheiro J.P., Bebianno M.J. 2014b. Effects of silver nanoparticles exposure in the mussel *Mytilus galloprovincialis*. Marine Environmental Research 101: 208-214.
- .: Gomes T., Albergamo A., Costa R., Mondello L., Dugo G. 2017. Potential use of proteomics in shellfish aquaculture: from assessment of environmental toxicity to evaluation of seafood quality and safety. Current Organic Chemistry 21: 1-24.
- .: Gómez-Mendikute A., Etxeberria A., Olabarrieta I., Cajaraville M.P. 2002. Oxygen radicals production and actin filament disruption in bivalve haemocytes treated with benzo(a)pyrene. Marine Environmental Research 54: 431-436.
- .: Gómez-Mendikute A., Cajaraville M.P. 2003. Comparative effects of cadmium, copper, paraquat and benzo[a]pyrene on the actin cytoskeleton and production of reactive oxygen species (ROS) in mussel haemocytes. Toxicology In Vitro 17: 539-546.
- .: Gooday G.W. 1999. Chitin and chitinases. Edited by: P. Jolles and R.A.A. Muzzarelli Birkhäuser Verlag. p.157.
- .: Gottschalk F., Sonderer T., Scholz R.W., Nowack B. 2009. Modeled environmental concentrations of engineered nanomaterials (TiO₂, ZnO, Ag, CNT, fullerenes) for different regions. Environmental Science and Technology 43: 9216-9222.
- .: Griffit R.J., Hyndman K., Denslow N.D., Barber D.S. 2009. Comparison of molecular and histological changes in zebrafish gills exposed to metallic nanoparticles. Toxicological Science 107: 404-415.
- .: Griffit R.J., Lavelle C.M., Kane A.S., Denslow N.D., Barber D.S. 2013. Chronic nanoparticulate silver exposure results in tissue accumulation and transcriptomic changes in zebrafish. Aquatic Toxicology 130-131: 192-200.
- .: Hu W., Culloty S., Darmody G., Lynch S., Davenport J., Ramirez-Garcia S., Dawson K.A., Lynch I., Blasco J., Sheehan D. 2014. Toxicity of copper oxide nanoparticles in the blue mussel, *Mytilus edulis*: a redox proteomic investigation. Chemosphere 108: 289-299.

- ∴ Jaafar S.N.T., Coelho A.V., Sheehan D. 2015. Redox proteomic analysis of *Mytilus edulis* gills: effects of the pharmaceutical diclofenac on a non-target organism. *Drug Testing and Analysis* 7: 957-966.
- ∴ Ji C., Li F., Wang Q., Zhao J., Sun Z., Wu H. 2016. An integrated proteomic and metabolomics study on the gender specific responses of mussels *Mytilus galloprovincialis* to tetrabromobisphenol A (TBBPA). *Chemosphere* 144: 527-539.
- ∴ Jimeno-Romero A., Bilbao E., Izagirre U., Cajaraville M.P., Marigómez I., Soto M. 2017. Digestive cell lysosomes as main targets for Ag accumulation and toxicity in marine mussels, *Mytilus galloprovincialis*, exposed to maltose- stabilized Ag nanoparticles of different sizes. *Nanotoxicology* 11: 168-183.
- ∴ Kanehisa M., Furumichi M., Tanabe M., Sato Y., Morishima K. 2017. KEGG: new perspectives on genomes, pathways, diseases and drugs. *Nucleic Acids Research* 45: D353-D361.
- ∴ Katsumiti A., Gilliland D., Arostegui I., Cajaraville M.P. 2014. Cytotoxicity and cellular mechanisms involved in the toxicity of CdS quantum dots in hemocytes and gill cells of the mussel *Mytilus galloprovincialis*. *Aquatic Toxicology* 153: 39-52.
- ∴ Katsumiti A., Gilliland D., Arostegui I., Cajaraville M.P. 2015. Mechanisms of toxicity of Ag nanoparticles in comparison to bulk and ionic Ag on mussel hemocytes and gill cells. *PLoS ONE* 10 (6): e0129039. doi:10.1371/journal.pone.0129039.
- ∴ Katsumiti A., Thorley A.J., Arostegui I., Reip P., Valsami-Jones E., Tetley T.D., Cajaraville M.P. 2018. Cytotoxicity and cellular mechanisms of toxicity of CuO NPs in mussel cells *in vitro* and comparative sensitivity with human cells. *Toxicology In Vitro* 48: 146-158.
- ∴ Khan F.R., Syberg K., Shashoua Y., Bury N.R. 2015. Influence of polyethylene microplastic beads on the uptake and localization of silver in zebrafish (*Danio rerio*). *Environmental Pollution* 206: 73-79.
- ∴ Kim Y., Ashton-Alcox K.A., Powell E.N. 2006. Gonadal analysis. NOAA histological techniques for marine bivalve mollusks: update. NOAA Technical Memories NOS NCCOS 27, Silver Spring (USA). pp. 1-18.
- ∴ Lacave J.M., Fanjul A., Bilbao E., Gutierrez N., Barrio I., Arostegui I., Cajaraville M.P., Orbea A. 2017. Acute toxicity, bioaccumulation and effects of dietary transfer of silver from brine shrimp exposed to PVP/PEI coated silver nanoparticles to zebrafish. *Comparative Biochemistry and Physiology, Part C* 199: 69-80.
- ∴ Lacave J.M., Vicario-Parés U., Bilbao E., Gilliland D., Mura F., Dini L., Cajaraville M.P., Orbea A. 2018. Waterborne exposure of adult zebrafish to silver nanoparticles and to ionic silver results in differential silver accumulation and effects at cellular and molecular levels. *Science of the Total Environment* 642: 1209-1220.
- ∴ Lancelleur L., Schäfer J., Chiffolleau J.F., Blanc G., Auger D., Renault S., Baudrimont M., Audry S. 2011. Long-term records of cadmium and silver contamination in sediments and oysters from the Gironde fluvial-estuarine continuum-Evidence of changing silver sources. *Chemosphere* 85: 1299-1305.
- ∴ Lapresta-Fernández A., Fernández A., Blasco J. 2012. Nanoecotoxicity effects of engineered silver and gold nanoparticles in aquatic organisms. *Trends in Analytical Chemistry* 32: 40-59.

- .: Larginho M., Correia D., Diniz M.S., Baptista P.V. 2014. Evidence of one-way flow bioaccumulation of gold nanoparticles across two trophic levels. *Journal of Nanoparticle Research* 16: 2549-2560.
- .: Leiniö S., Lehntonen K. 2005. Seasonal variability in biomarkers in the bivalves *Mytilus edulis* and *Macoma balthica* from the northern Baltic Sea. *Comparative Biochemistry and Physiology, Part C* 140: 408-421.
- .: Livingstone D.R., Farrar S.V. 1984. Tissue and subcellular distribution of enzyme activities of mixed function oxygenase and benzo[a]pyrene metabolism in the common mussel *Mytilus edulis*. *Science of the Total Environment* 39: 209-235.
- .: Luoma S.N., Rainbow P.S. 2005. Why Is Metal Bioaccumulation So Variable? *Biodynamics as a Unifying Concept. Environmental Science of Technology* 39: 1921-1931.
- .: Manzo S., Schiavo S., Oliviero M., Toscano A., Ciaravolo M., Cirino P. 2017. Immune and reproductive system impairment in adult sea urchin exposed to nanosized ZnO via food. *Science of the Total Environment* 599-600: 9-13.
- .: Maria V.L., Gomes T., Barreira L., Bebianno M.J. 2013. Impact of benzo(a)pyrene, Cu and their mixture on the proteomic response of *Mytilus galloprovincialis*. *Aquatic Toxicology* 144-145: 284-295.
- .: McCarthy M., Carroll D.L., Ringwood A.H. 2013. Tissue specific response of oysters, *Crassostrea virginica*, to silver nanoparticles. *Aquatic Toxicology* 138-139: 123-128.
- .: McGuillicuddy E., Murray I., Kavanagh S., Morrison L., Fogarty A., Cormican M., Dockery P., Prendergast M., Rowan N., Morris D. 2017. Silver nanoparticles in the environment: Sources, detection and ecotoxicology. *Science of the Total Environment* 575: 231-246.
- .: Mehennaoui K., Cambier S., Serchi T., Ziebel J., Lentzen E., Valle N., Guérold F., Thomann J.S., Giamberini L., Gutleb A.C. 2018. Do the pristine physico-chemical properties of silver and gold nanoparticles influence uptake and molecular effects on *Gammarus fossarum* (Crustacea Amphipoda)? *Science of the Total Environment* 643: 1200-1215.
- .: Moore M.N. 2006. Do nanoparticles present ecotoxicological risks for the health of the aquatic environment? *Environment International* 32: 967-976.
- .: Mubiana V.K., Qadah D., Meys J., Blust R. 2005. Temporal and spatial trends in heavy metal concentrations in the marine mussel *Mytilus edulis* from the Western Scheldt estuary (The Netherlands). *Hydrobiologia* 540: 169-180.
- .: Navarro E., Piccapietra F., Wagner B., Marconi F., Kaegi R., Odzak N., Sigg L., Behra R. 2008. Toxicity of silver nanoparticles to *Chlamydomonas reinhardtii*. *Environmental Science of Technology* 42: 8959-8964.
- .: Negri A., Oliveri C., Sforzini S., Mignione F., Viarengo A., Banni M. 2013. Transcriptional response of the mussel *Mytilus galloprovincialis* (Lam.) following exposure to heat stress and copper. *PLoS ONE* 2013; 8(6): e66802.
- .: Orbea A., González-Soto N., Lacave J.M., Barrio I., Cajaraville M.P. 2017. Developmental and reproductive toxicity of PVP/PEI-coated silver nanoparticles to zebrafish. *Comparative Biochemistry and Physiology, Part C* 199: 59-68.

- ∴ Páez-Osuna F., Frías-Espericueta M.G., Osuna-López J.I. 1995. Trace metal concentrations in relation to season and gonadal maturation in the oyster *Crassostrea iridescens*. *Marine Environmental Research* 40: 19-31.
- ∴ Pakrashi S., Tan C., Wang W.X. 2017. Bioaccumulation-based silver nanoparticle toxicity in *Daphnia magna* and maternal impacts. *Environmental Toxicology and Chemistry* 36: 3359-3366.
- ∴ Regoli F., Orlando E. 1994. Seasonal variation of trace metal concentrations in the digestive gland of the mediterranean mussel *Mytilus galloprovincialis*. Comparison between a polluted and a non-polluted site. *Archives of Environmental Contamination and Toxicology* 27: 36-43.
- ∴ Ribeiro F., Gallego-Urrea J.A., Jurkschat K., Crossley A., Hassellöv M., Taylor C., Soares A.M.V.M., Loureiro S. 2014. Silver nanoparticles and silver nitrate induce high toxicity to *Pseudokirchneriella subcapitata*, *Daphnia magna* and *Danio rerio*. *Science of the Total Environment* 466-467: 232-241.
- ∴ Ringwood A.H., McCarthy M., Bates T.C., Carrol D.L. 2010. The effects of silver nanoparticles on oyster embryos. *Marine Environmental Research* 69: S49-S51.
- ∴ Riva C., Binelli A., Rusconi F., Colombo G., Pedriali A., Zippel R., Provini A. 2011. A proteomic study using zebra mussels (*D. polymorpha*) exposed to benzo[a]pyrene: The role of gender and exposure concentrations. *Aquatic Toxicology* 104: 14-22.
- ∴ Rocha T.L., Gomes T., Sousa V.S., Mestre N.C., Bebianno M.J. 2015a. Ecotoxicological impact of engineered nanomaterials in bivalve molluscs: An overview. *Marine Environmental Research* 111: 74-88.
- ∴ Rocha T.L., Gomes T., Mestre N.C., Cardoso C., Bebianno M.J. 2015b. Tissue specific responses to cadmium-based quantum dots in the marine mussel *Mytilus galloprovincialis*. *Aquatic Toxicology* 169: 10-18.
- ∴ Rodríguez-Ortega M.J., Grøsvik B.E., Rodríguez-Ariza A., Goksøyr A., López-Barea J. 2003. Changes in protein expression profiles in bivalve molluscs (*Chamaelea gallina*) exposed to four model environmental pollutants. *Proteomics* 3: 1535-1543.
- ∴ Romero-Ruiz A., Carrascal M., Alhama J., Gómez-Ariza J.L., Abian J., López-Barea J. 2006. Utility of proteomics to assess pollutant response of clams from the Doñana bank of Guadalquivir Estuary (SW Spain). *Proteomics* 6: S245-S255.
- ∴ Ruiz P., Katsumiti A., Nieto J.A., Bori J., Reip P., Orbea A. and Cajaraville M.P. 2015. Short-term effects on antioxidant enzymes and long-term genotoxic and carcinogenic potential of CuO nanoparticles in mussels. *Marine Environmental Research* 111: 107-120.
- ∴ Schiavo S., Duroudier N., Bilbao E., Mikolaczyk M., Schäfer J., Cajaraville M.P., Manzo S. 2017. Effects of PVP/PEI coated and uncoated silver NPs and PVP/PEI coating agent on three species of marine microalgae. *Science of the Total Environment* 577: 45-53.
- ∴ Schmidt W., Rainville L.C., McEneff G., Sheehan D., Quinn B. 2014. A proteomic evaluation of the effects of the pharmaceuticals diclofenac and gemfibrozil on marine mussels (*Mytilus* spp.): evidence for chronic sublethal effects on stress-response proteins. *Drug Testing and Analysis* 6: 210-219.

- ∴ Sendra M., Yeste M.P., Gatica J.M., Moreno-Garrido I., Blasco J. 2017a. Direct and indirect effects of silver nanoparticles on freshwater and marine microalgae (*Chlamydomonas reinhardtii* and *Phaeodactylum tricorutum*). *Chemosphere* 179: 279-289.
- ∴ Sendra M., Blasco J., Araújo C.V.M. 2017b. Is the cell wall of marine phytoplankton a protective barrier or a nanoparticle interaction site? Toxicological responses of *Chlorella autotrophica* and *Dunaliella salina* to Ag and CeO₂ nanoparticles. *Ecological Indicators*. <http://dx.doi.org/10.1016/j.ecolind.2017.08.050>.
- ∴ Shevchenko A., Tomas H., Havlis J., Olsen J.V., Mann M. 2007. In-gel digestion for mass spectrometric characterization of proteins and proteomes. *Nature Protocols* 1: 2856-2860.
- ∴ Solé M., Porte C., Albaigés J. 1995. Seasonal variation in the mixed-function oxygenase system and antioxidant enzymes of the mussel *Mytilus galloprovincialis*. *Environmental Toxicology and Chemistry* 14: 157-164.
- ∴ Soto M., Kortabitarte M., Marigómez I. 1995. Bioavailable heavy metals in estuarine waters as assessed by metal/shell-weight indices in sentinel mussels *Mytilus galloprovincialis*. *Marine Ecology Progress Series* 125: 127-136.
- ∴ Tangaa S.R., Selck H., Winther-Nielsen M., Khan F.R. 2016. Trophic transfer of metal-based nanoparticles in aquatic environments: a review and recommendations for future research focus. *Environmental Science: Nano* 3: 966-981.
- ∴ Tedesco S., Doyle H., Redmond G., Sheehan D. 2008. Gold nanoparticles and oxidative stress in *Mytilus edulis*. *Marine Environmental Research* 66: 131-133.
- ∴ Tedesco S., Doyle H., Blasco J., Redmond G., Sheehan D. 2010a. Exposure of the blue mussel, *Mytilus edulis*, to gold nanoparticles and the pro-oxidant menadione. *Comparative Biochemistry and Physiology, Part C* 151: 167-174.
- ∴ Tedesco S., Doyle H., Blasco J., Redmond G., Sheehan D. 2010b. Oxidative stress and toxicity of gold nanoparticles in *Mytilus edulis*. *Aquatic Toxicology* 100: 178-186.
- ∴ Tiede K., Hassellöv M., Breitbarth E., Chaudhry Q., Boxall A.B.A. 2009. Considerations for environmental fate and ecotoxicity testing to support environmental risk assessments for engineered nanoparticles. *Journal of Chromatography A* 1216: 503-509.
- ∴ Tomanek L., Zuzow M.J. 2010. The proteomic response of the mussel congeners *Mytilus galloprovincialis* and *M. trossulus* to acute heat stress: implications for thermal tolerance limits and metabolic costs of thermal stress. *The Journal of Experimental Biology* 213: 3559-3574.
- ∴ UniProt Consortium. UniProt: the universal protein knowledgebase. 2017. *Nucleic Acids Research* 45: D158-D169.
- ∴ Vance M.E., Kuiken T., Vejerano E.P., McGinnis S.P., Hochella M. F. Jr., Rejeski D., Hull M.S. 2015. Nanotechnology in the real world: Redeveloping the nanomaterial consumer products inventory. *Beilstein Journal of Nanotechnology* 6: 1769-1780.
- ∴ Wang J., Wang W.X. 2014. Low bioavailability of silver nanoparticles presents trophic toxicity to marine medaka (*Orzyias melastigma*). *Environmental Science of Technology* 48: 8152-8161.

- ∴ Wang Z., Yin L., Zhao J., Xing B. 2016. Trophic transfer and accumulation of TiO₂ nanoparticles from clamworm (*Perinereis aibuhitensis*) to juvenile turbot (*Scophthalmus maximus*) along a marine benthic food chain. *Water Research* 95: 250-259.
- ∴ Weiss I.M., Schönitzer V. 2006. The distribution of chitin in larval shells of the bivalve mollusk *Mytilus galloprovincialis*. *Journal of Structural Biology* 153: 264-277.
- ∴ Woo S., Jeon H.Y., Kim S.R., Yum S. 2011. Differentially displayed genes with oxygen depletion stress and transcriptional responses in the marine mussel, *Mytilus galloprovincialis*. *Comparative Biochemistry and Physiology, Part D* 6: 348-356.
- ∴ Yu D., Ji C., Zhao J., Wu H. 2016. Proteomic and metabolomic analysis on the toxicological effects of As (III) and As (V) in juvenile mussel *Mytilus galloprovincialis*. *Chemosphere* 150: 194-201.
- ∴ Zhang C., Hu Z., Deng B. 2016. Silver nanoparticles in aquatic environments: Physicochemical behavior and antimicrobial mechanisms. *Water Research* 88: 403-427.



CHAPTER 4

Season influences the transcriptomic effects of dietary exposure to PVP/PEI coated Ag nanoparticles on mussels

Mytilus galloprovincialis

This chapter has been published as:

DUROUDIER N., MARKAIDE P., CAJARAVILLE M.P., BILBAO E. 2019. Season influences the transcriptomic effects of dietary exposure to PVP/PEI coated Ag nanoparticles on mussels *Mytilus galloprovincialis*. *Comparative Biochemistry and Physiology, Part C* 222: 19-30.

Parts of this chapter have been presented at:

19th INTERNATIONAL SYMPOSIUM ON POLLUTANT RESPONSES IN MARINE ORGANISMS (PRIMO), Matsuyama (Japan), 30 June- 3 July 2017.

DUROUDIER, N; MARKAIDE, P; BILBAO, E; CAJARAVILLE, MP. Effects of PVP/PEI coated Ag NPs on dietarily exposed mussels at different seasons: a transcriptomic study. Platform presentation.

31st CONGRESS OF THE NEW EUROPEAN SOCIETY FOR COMPARATIVE PHYSIOLOGY AND BIOCHEMISTRY ESCPB, Porto (Portugal), 9-12 September 2018.

DUROUDIER, N; MARKAIDE, P; BILBAO, E; CAJARAVILLE, MP. Alterations in transcription patterns in mussels *Mytilus galloprovincialis* dietarily exposed to PVP/PEI coated silver nanoparticles at different seasons. Platform presentation.

ABSTRACT

Toxicity of Ag NPs has been widely studied in waterborne exposed aquatic organisms. However, toxic effects caused by Ag NPs ingested through the diet and depending on the season are still unexplored. The first cell response after exposure to xenobiotics occurs at gene transcription level. Thus, the aim of this study was to assess transcription level effects in the digestive gland of female mussels after dietary exposure to Ag NPs both in autumn and in spring. Mussels were fed daily for 21 days with *Isochrysis galbana* microalgae previously exposed for 24 hours to a dose close to environmentally relevant concentrations of 1 µg Ag/L PVP/PEI coated 5 nm Ag NPs (in spring) and to a higher dose of 10 µg Ag/L of the same Ag NPs both in autumn and in spring. After 1 and 21 days, mussels RNA was hybridized in a custom microarray containing 7806 annotated genes. Mussels were more responsive to the high dose compared to the low dose of Ag NPs and a higher number of probes was altered in autumn than in spring. In both seasons, significantly regulated genes were involved in the *cytoskeleton* and *lipid transport and metabolism* COG categories, among others, while genes involved in *carbohydrate transport and metabolism* were specifically altered in autumn. Overall, transcription patterns were differently altered depending on the exposure time and season, indicating that season should be considered in ecotoxicological studies of metal nanoparticles in mussels.

Keywords: silver nanoparticles, dietary exposure, microarray, mussels *Mytilus galloprovincialis*, season.

RESUMEN

La toxicidad de las NPs de Ag ha sido ampliamente estudiada en organismos acuáticos expuestos a través del agua. Sin embargo, los posibles efectos tóxicos causados por las NPs de Ag ingeridas a través de la dieta y dependiendo de la estación del año siguen siendo desconocidos. La primera respuesta celular tras la exposición a xenobióticos ocurre a nivel transcripcional. Por ello, el objetivo de este estudio fue evaluar los efectos a niveles de transcripción en la glándula digestiva de mejillones hembra tras su exposición a NPs de Ag a través de la dieta tanto en otoño como en primavera. Los mejillones se alimentaron diariamente durante 21 días con microalgas *Isochrysis galbana* previamente expuestas durante 24 horas a una dosis cercana a las concentraciones ambientalmente relevantes de 1 µg Ag/L de NPs de Ag de 5 nm recubiertas de PVP/PEI (en primavera) y a una concentración mayor de 10 µg Ag/L de las mismas NPs de Ag tanto en otoño como en primavera. Tras 1 y 21 días, el RNA de los mejillones se hibridó en un microchip personalizado que contiene 7806 genes anotados. Los mejillones fueron más sensibles a la dosis alta que a la dosis baja y se alteró un mayor número de sondas en otoño en comparación con primavera. En ambas estaciones se regularon significativamente, entre otros, genes que forman parte del *citoesqueleto* y del *transporte y metabolismo de lípidos*, mientras que entre los genes específicamente alterados en otoño estaban los relacionados con el *metabolismo y transporte de carbohidratos*. En general, los patrones de transcripción se alteraron diferencialmente en función del tiempo de exposición y la estación del año, indicando que la estación de año debe considerarse en los estudios ecotoxicológicos con NPs metálicas en mejillones.

Palabras clave: nanopartículas de plata, exposición vía dieta, microchip, mejillones *Mytilus galloprovincialis*, estación del año.

1. INTRODUCTION

In living organisms, the first response to chemicals occurs at gene transcription level before the onset of physiological and biological changes (Snape et al., 2004; Fent and Sumpter, 2011). In fact, exposure related gene alterations are detectable within hours (Denslow et al., 2007). These alterations are measurable through the application of arrays or differential display methodologies, which have helped to increase the knowledge on transcriptomic profiles of sentinel species and to determine biological responses in organisms exposed to environmental pollutants (Veldhoen et al., 2012). Mussels *Mytilus* spp are widely used sentinel species (Goldberg, 1975; Cajaraville et al., 2000; Viarengo et al.; 2007; Beyer et al.; 2017) and high-throughput technologies, especially microarrays, have been applied in this marine organism in recent years. Different custom microarrays are available, such as the 1.7k cDNA MytArray platform (Dondero et al., 2010; 2011; Canesi et al., 2011; Varotto et al., 2013; Banni et al., 2014; 2016; Maria et al., 2016), an 8x60k oligo-DNA microarray (Mezzelani et al., 2016) or the low density "STressREsponse Microarray" (Banni et al., 2017), which have contributed to the identification of groups of genes involved in the early response and adaptation of mussels exposed to xenobiotics.

Due to the rapid development of nanotechnology during the last years, the release and input of nanoparticles (NPs) into freshwater and marine environments is expected to increase (Baker et al., 2014; Corsi et al., 2014). Ag NPs are among the most used metallic NPs due to their unique optical, catalytic and antimicrobial properties (Fabrega et al., 2011; Vance et al., 2015; Zhang et al., 2016; McGuillicuddy et al., 2017). As the use of Ag NPs in nano-enabled consumer products is increasing (Massarsky et al., 2014), environmental concentrations of Ag NPs are expected to rise. Different models have predicted that Ag NP concentrations in surface waters would range between 0.002 ng/L and 140 ng/L in European rivers (Blaser et al., 2008; Gottschalk et al., 2009; Tiede et al., 2009; Dumont et al., 2015; Giese et al., 2018) and would reach up to 40 µg/L in Taiwanese waters (Chio et al., 2012). NPs detection and quantification in environmental systems is challenging (Sikder et al., 2017) but for instance, Ag NP concentrations ranging from 0.7 to 11.1 ng/L have been measured in effluents of wastewater treatment plants over the seasons in Germany (Li et al., 2016).

Bivalves have been identified as an important target group to assess NPs toxicity in marine environments (Moore, 2006; Canesi et al., 2012; Corsi et al., 2014; Canesi and Corsi, 2016). Thus, mussels (Gomes et al., 2013a; 2013b; 2014b; Bebianno et al., 2015; Jimeno-Romero et al., 2017), clams (Buffet et al., 2013; 2014) and oysters (Ringwood et al., 2010; McCarthy et al., 2013) have been widely used to study toxic effects caused by waterborne exposure to Ag NPs. In general, bivalves exposed to Ag NPs accumulate silver

in their tissues and show different cell and tissue level responses, such as oxidative stress, DNA damage, lysosomal membrane destabilization and loss of digestive gland integrity (reviewed in Magesky and Pelletier, 2018). However, little is known about the potential effects of Ag NPs at gene transcription level. Ringwood et al. (2010) reported increased *metallothionein* mRNA levels both in embryos and adult oysters after exposure to 0.16 µg/L Ag NPs for 48 hours. On the other hand, longer exposures (15 days) to 10 µg/L Ag NPs did not alter transcription levels of the selected target genes (*superoxide dismutase*, *catalase*, *glutathione transferase*, *caspase 3/7-1*, *cathepsin L*, *heat shock protein 70*, *cytochrome P450 4YA*, *elongation factor*, *actin* and *α-tubulin*) in mussel gills (Bebiano et al., 2015). Microarrays applied in mussels exposed to NPs may help to identify molecular markers that indicate both exposure and subsequent biological effects (Rocha et al., 2015), as well as to determine adverse outcome pathways. However, few studies have investigated the effects of NPs on the transcriptome of mussels. Banni et al. (2016) found an upregulation of genes involved in microtubule-based movement and cellular component organization processes in mussels exposed to 100 µg/L TiO₂ NPs for 96 h. As far as we know, changes in the transcription pattern of bivalves exposed to Ag NPs through water or through the food web have not been reported yet.

Several investigations have reported gender-specific gene transcription patterns (Banni et al., 2011) and gender-dependent responses to contaminants (Livingstone and Farrar, 1984; Brown et al., 2006; Riva et al., 2011; Ji et al., 2016; Banni et al., 2017), suggesting that gender of mussels should be considered in ecotoxicological studies. In agreement, some studies have focused on female mussels only (Banni et al., 2014; 2016; 2017; Dondero et al., 2011; Negri et al., 2013). Thus, in the present study only female organisms were used in order to avoid biological variability related to gender. Moreover, mussels show season-dependent metabolic and enzymatic variations related to abiotic changes in the environment, such as temperature, food availability and oxygen levels and to their physiological state (Bayne and Widdows, 1978; Solé et al., 1995; Cancio et al., 1999; Sheehan and Power, 1999). In mussels from the northern coast of the Iberian Peninsula gametogenesis occurs along autumn and early winter and spawning takes place during spring (Villalba, 1995; Ortiz-Zarragoitia et al., 2011). Such season-dependent process can influence the response of mussels to pollutants (Bocchetti and Regoli, 2006).

The aim of the present study was to assess transcription level effects in the digestive gland of female mussels dietarily exposed to Ag NPs and to compare such transcription profiles in two different seasons, autumn and spring. Ag accumulation in mussel soft tissues and changes in protein expression profiles in the digestive gland of female mussels are reported in a separate study (see Chapter 3). Further, mussels dietarily

exposed to the same Ag NPs under the same experimental conditions showed altered reproduction and abnormal embryo development in offspring (see Chapter 1).

2. MATERIALS AND METHODS

2.1. Obtention and characterization of Ag NPs

Ag NPs coated with Poly N-vinyl-2-pyrrolidone/Polyethyleneimine (PVP/PEI; 77%:23% at a concentration of 104 g/L in the final dispersion) were purchased as a stable aqueous suspension from Nanogap (O Milladoiro, Galicia, Spain). According to the manufacturers' information, PVP/PEI coated Ag NPs showed an average size of 5.08 ± 2.03 nm (see Appendix) and a zeta potential of $+18.6 \pm 7.9$ mV in distilled water.

Particle size distribution and dissolution of these PVP/PEI coated 5 nm Ag NPs in seawater (SW) were analyzed as reported in Chapter 1. Briefly, PVP/PEI coated 5 nm Ag NPs dispersed in SW immediately reached a mean size of roughly 97 nm according to Dynamic Light Scattering measurements using a Zetasizer Nano Z (Malvern Instruments Ltd. Worcestershire, UK). After 24 hours, particle size remained stable around 94-96 nm. Dissolution of Ag NPs in SW was detected along the 72 hours of experimentation. After 12 hours, Ag NPs released around 4% of Ag ions and dissolution increased to around 14% at 24 hours. After 48 hours ~17% of Ag ions were released from Ag NPs and at 72 hours, dissolution increased to 20% (see Chapter 1).

2.2. Experimental design

Mussels *Mytilus galloprovincialis* 3.5-4.5 cm in shell length were collected in autumn (November 2013) and spring (March 2014) from San Felipe, Galicia (43° 27.599'N, 8° 17.904'W). Upon arrival to the laboratory, mussels were placed in an acclimation tank with natural filtered seawater (temperature =15.6°C, salinity =28.7 ‰, conductivity =36.4 mS/cm, pH =7.7 at light regime 12 h/12 h L/D) for 5 days without feeding. Then mussels were fed with *Isochrysis galbana* microalgae (20×10^6 cells/mussel-day) for additional 5 days. For that, microalgae were cultured with natural filtered (0.2 μ m) and sterilized seawater at 20°C under cool continuous white fluorescent light (GRO-LUX F58W) with constant aeration in reactors at a concentration of 6×10^6 cells/mL. Commercial F2 algae medium (Fritz Aquatics, USA) was supplied according to manufacturer's instructions. Before mussels feeding,

concentration of microalgae was checked every day and a volume corresponding to a final ration of 20×10^6 cells/mussel-day was added to the acclimation tank.

After the acclimation period, mussels were distributed in different high density polypropylene containers (250 L) containing 240 mussels per tank. Mussels in the control tank were fed for 21 days with *I. galbana* (20×10^6 cells/mussel-day) and mussels in the treatment tanks were fed for 21 days with the same ration of *I. galbana* (20×10^6 cells/mussel-day) previously exposed for 24 hours to $1 \mu\text{g Ag/L Ag NPs}$ in spring or to $10 \mu\text{g Ag/L Ag NPs}$ in autumn and in spring. The comparison between seasons only at the higher exposure dose was considered sufficient to study season-dependent transcription level effects. Water was renewed every day before animal feeding. No mortality was recorded along the experimentation time.

After 1 and 21 days of exposure, digestive gland of mussels was dissected out, immersed in RNA later, snap-frozen in liquid nitrogen and stored at -80°C until processing. A piece of gonad was also dissected out and fixed in 10% neutral buffered formalin in order to select female mussels and to determine their gonad index.

2.3. Gonad histology

After 24 hours of fixation in 10% neutral buffered formalin, gonad samples were routinely processed for paraffin embedding using a Leica Tissue processor ASP 3000 (Leica Instruments, Wetzlar, Germany). Histological sections ($5 \mu\text{m}$ in thickness) were cut in a Leica RM2255 microtome (Leica Instruments) and stained with hematoxylin-eosin (Gamble and Wilson, 2002). Gonad sections were examined under the light microscope (Nikon Eclipse Ni; Nikon Instruments, Tokyo, Japan) in order to identify and select female mussels. A gonad index (GI) value was also assigned to each gonad as described by Kim et al. (2006) and a mean GI was then calculated for each experimental group.

2.4. Sample processing for microarray hybridization

About 50-100 mg of digestive gland of 10 female mussels per experimental group were individually homogenized in TRIzol® Reagent (Invitrogen, Carlsbad, USA) using a Precellys®24 homogenizer (Bertin Technologies, France) at a shaking speed of 6000 rpm for 2 cycles of 25 seconds each. Total RNA was isolated following the manufacturer's recommendations and treated with the RNase-Free DNase Set (Qiagen, Venlo, The Netherlands) to digest contaminating DNA. Then, total RNA was

purified by using the RNeasy Mini Kit (Qiagen). The integrity and quality of purified RNA was checked both spectrophotometrically (A260/280; Epoch Biotek; Winooski, Vermont, USA) and by capillary electrophoresis (Agilent 2100 Bioanalyzer, Agilent Technologies). Samples of non-exposed and exposed individuals (n= 6 per experimental group) with a A260/280 ratio around 2.0 and showing a clear electropherogram were selected for microarray hybridizations.

2.5. Microarray design

A custom 8x60K SurePrint G3 Exon Microarray (Agilent Technologies, California, USA) was designed based on nucleotide sequences available in the MytiBase database (Venier et al., 2009) and on different *Mytilus* spp. nucleotide sequences published until February 2015 in the National Center for Biotechnology Information (NCBI). Briefly, obtained sequences were compared among them and those showing an identity higher than 99% were removed in order to avoid repetitions. Then, all sequences were aligned against Non Redundant (NR) protein database using BLASTx (E-value threshold $< 10e^{-10}$). Results were filtered to get the sequence that best represented a given unique protein in the NR database, based on the highest E-value and the longest sequence length. The annotation of each NR identifier was compared and the best sequence for a given loci was selected using the same criteria. At the end, the microarray contained 7806 annotated sequences representing unique proteins (5893 from *M. galloprovincialis*, 153 from *M. edulis*, 1658 from *M. californianus*, 3 from *M. trossolus*, 15 from *M. coruscus* and 1 from *M. chilensis*), placed as triplicate non-identical sense probes and 17941 non-annotated sequences, with a sense and antisense probe for each sequence. Positive and negative controls were included according to Agilent microarray design recommendations (eArray). The platform is available in the Gene Expression Omnibus (<https://www.ncbi.nlm.nih.gov/geo/>) with the following ID: GSE124126.

2.6. Microarray hybridization

Hybridizations were performed in the General Genomics Service, Sequencing and Genotyping Unit (SGIker) at the University of the Basque Country. RNA samples (100 ng) of 6 individuals per experimental group were retro-transcribed and labelled using the Low Input Quick Amp Labelling Kit, One Colour (Agilent Technologies, 5190-2305) following the manufacturer's instructions. Hybridized microarrays were scanned on a G2565CA DNA microarray scanner (Agilent Technologies) with ozone barrier slide

covers (Agilent Technologies P/N G2505-60550) and obtained images were processed using the Agilent Feature Extraction Software v10.7.3.1 (Agilent Technologies).

2.7. Differential gene transcription analysis

Obtained raw data files were analyzed using R (v.3.3.2, R Core Team (2017)) and the *limma* package (v.3.30.13; Ritchie et al., 2015). Probe signal was background corrected using the *normexp* method followed by a quantile normalization for inter array normalization. Based on *gIsPosAndSignif FE* flag, a filtering step was carried out to remove non-transcribed probes alongside with positive and negative controls. Non-annotated probes were also removed since they remained unknown at the time of data treatment. Only probes showing transcription levels above background transcription levels in all samples from at least one of the groups were considered as transcribed. These probes were used for downstream analyses, as described below.

Samples were clustered and outliers identified by a Principal Component Analysis (PCA; *scikit* v.0.19.1, Pedregosa et al., 2011) and by a Hierarchical Clustering. As this preliminary analysis demonstrated that seasonality was the main factor causing differences among samples, microarray datasets were analyzed separately for each season.

LIMMA analysis was used to determine differentially transcribed probes in each exposure group compared to each control group. Probes showing a not-adjusted p-value <0.001 and a Fold Change $-1.5 > FC > 1.5$ were considered differentially transcribed.

2.8. Functional analysis of differentially transcribed probes

Differentially transcribed sequences were functionally annotated against the eggNOG database (v.4.5.1, Huerta-Cepas et al., 2016) using the available web version of eggNOG-Mapper (<http://eggnogdb.embl.de/#/app/emapper>). Specifically, the HMMER mapping mode and the hidden Markov model (HMM) database optimized for Eukaryote were selected to functionally annotate each sequence in the corresponding Cluster of Orthologous Group (COG; Tatusov et al., 2003). Then, the Kyoto Encyclopedia of Genes and Genomes database (KEGG, Kanehisa et al., 2017) based on the Ostreidae family was used to decipher metabolic pathways in which regulated probes may be involved. Briefly, significantly regulated transcripts were blasted against the *Crassostrea* genome (taxid: 6564) using BLASTx. Obtained sequences were annotated against the Ostreidae family using the BlastKOALA tool in

order to get the KEGG identifiers. Finally, assigned KEGG identifiers were introduced in the KEGG pathways mapping tool to identify metabolic pathways.

3. RESULTS

3.1. Gonad histology

Gonad index (GI) of selected female mussels differed between autumn and spring (Table 1). In autumn, mussels gonads were in early gametogenic stage. In non-exposed females, GI mean value was 1.33 ± 0.25 at day 1 and 2 ± 1.18 at day 21 (Table 1). Similarly, females dietarily exposed to $10 \mu\text{g Ag/L Ag NPs}$ showed gonads in early gametogenic stage and GI values ranged from 1.41 ± 0.25 at day 1 to 2.16 ± 1.03 at day 21 (Table 1). In spring, female gonads were in advanced gametogenic stage. GI mean value in non-exposed females was 4 ± 0.77 at day 1 and 3.75 ± 0.61 at day 21 (Table 1). GI value of mussels dietarily exposed to both concentrations of Ag NPs at day 1 was also 4 ± 0.77 (Table 1). After 21 days of exposure, female gonads of mussels dietarily exposed to 1 or $10 \mu\text{g Ag/L Ag NPs}$ showed a GI mean value of 3.5 ± 0 and 3.66 ± 1.29 , respectively (Table 1).

Table 1. Gonad index values of female mussels selected for microarray hybridizations after 1 or 21 days of dietary exposure to Ag NPs both in autumn and in spring. Values are given as mean \pm S.D. (n= 6).

	AUTUMN		SPRING	
	1 DAY	21 DAYS	1 DAY	21 DAYS
Control	1.33 ± 0.25	2 ± 1.18	4 ± 0.77	3.75 ± 0.61
1 $\mu\text{g Ag/L Ag NPs}$	-	-	4 ± 0.77	3.5 ± 0
10 $\mu\text{g Ag/L Ag NPs}$	1.41 ± 0.25	2.16 ± 1.03	4 ± 0.77	3.66 ± 1.29

3.2. Differential gene transcription analysis

Based on annotated probes, the PCA grouped samples depending on the season and exposure time (Figure 1 A,B,C) being season the main factor explaining variability on the transcriptomic profile of female mussels (Figure 1A). Then, when samples were plotted separately according to their season, they were grouped

depending on the exposure time (1 or 21 days) both in autumn (Figure B) and in spring (Figure 1C).

According to the LIMMA statistical analysis (not-adjusted $p < 0.001$ and $-1.5 > FC > 1.5$), different number of probes were significantly regulated depending on the season, exposure time and dose (Table 2). In autumn, the dietary exposure of mussels to $10 \mu\text{g Ag/L Ag NPs}$ for 1 day significantly regulated 11 probes coding for 10 different genes, being 3 of them upregulated and 8 downregulated (Table 2). When the dietary exposure was extended to 21 days, 37 probes (coding for 27 different genes) were significantly altered. Among them, 25 probes were upregulated and 12 probes were downregulated (Table 2).

In spring, exposure to the same Ag NPs concentration significantly regulated 19 probes (coding for 12 genes) at day 1 and 22 (coding for 15 genes) at 21 days (Table 2). Among these significantly regulated probes, 15 were upregulated and 4 downregulated at day 1 while 12 were upregulated and 10 downregulated at 21 days. Exposure to the dose close to environmentally relevant concentrations ($1 \mu\text{g Ag/L Ag NPs}$) only altered 10 probes (coding for 8 genes) at day 1 and 6 probes (coding for 5 genes) at 21 days (Table 2). Out of the 10 significantly regulated probes, 9 were upregulated and 1 downregulated, while among the 6 significantly altered probes, 4 were upregulated and 2 downregulated (Table 2).

Table 2. Number of significantly regulated probes (in bold) after dietary exposure of mussels to different concentrations of PVP/PEI coated 5 nm Ag NPs for 1 and 21 days in autumn and in spring. Number of significantly upregulated and downregulated probes are shown by arrows (\uparrow and \downarrow , respectively). Number of differentially regulated genes are shown in brackets. Significant differences were set based on the LIMMA analysis (not-adjusted $p < 0.001$) and $-1.5 > \text{fold change} > 1.5$.

	AUTUMN		SPRING	
	1 DAY	21 DAYS	1 DAY	21 DAYS
Control vs $1 \mu\text{g Ag/L Ag NPs}$	-	-	10 9 \uparrow (8) 1 \downarrow	6 4 \uparrow (5) 2 \downarrow
Control vs $10 \mu\text{g Ag/L Ag NPs}$	11 3 \uparrow (10) 8 \downarrow	37 25 \uparrow (27) 12 \downarrow	19 15 \uparrow (12) 4 \downarrow	22 12 \uparrow (15) 10 \downarrow

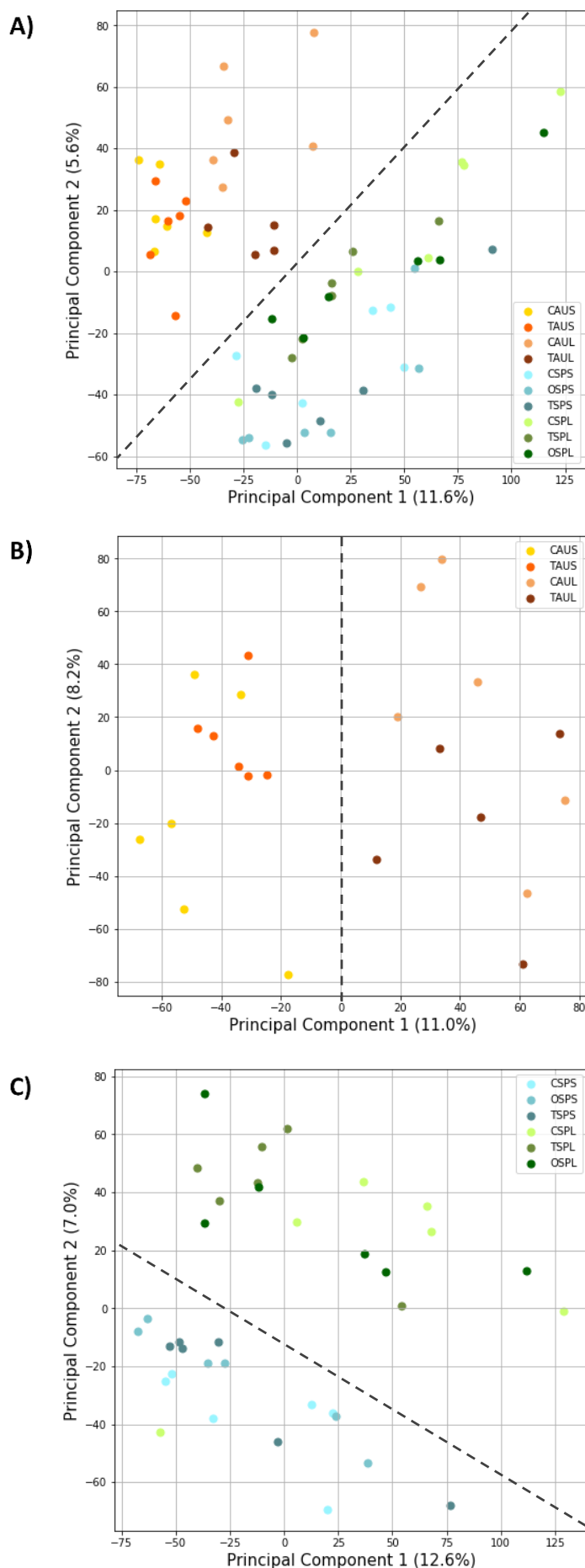


Figure 1. PCA plots based on all annotated probes included in the microarray. **A)** Distribution of samples after mussels dietary exposure for 1 and 21 days to 1 μg Ag/L Ag NPs in spring and 10 μg Ag/L Ag NPs in both seasons. **B)** Distribution of samples after mussels dietary exposure to 10 μg Ag/L Ag NPs for 1 and 21 days in autumn. **C)** Distribution of samples after mussels dietary exposure to 1 and 10 μg Ag/L Ag NPs for 1 and 21 days in spring. Each spot represents one female mussel ($n=6$ female mussels per experimental group). In the legends C stands for "control", O for "1 μg Ag/L Ag NPs", T for "10 μg Ag/L Ag NPs", AU for "Autumn", SP for "Spring", S for "1 day" and L for "21 days".

3.3. Functional analysis of differentially transcribed probes

Based on the eggNOG Mapper, significantly regulated transcripts were assigned to a functional category according to Clusters of Orthologous Groups (COG) annotation (Tables 3, 4, 5 and Supplementary material). The KEGG pathway analysis deciphered metabolic pathways in which significantly regulated probes may be involved. However, many of the significantly regulated transcripts were classified as *function unknown* COG category.

In autumn, after 1 day of dietary exposure to 10 µg Ag/L Ag NPs altered genes were classified in a number of COG functional categories: *chromatin structure and dynamics, cell cycle control, cell division and chromosome partitioning, nucleotide transport and metabolism, lipid transport and metabolism, translation, ribosomal structure and biogenesis* and *cell wall/membrane/envelope biogenesis*. A single gene was significantly regulated in each COG (Table 3A). *Elongation factor 1 alpha* that was grouped in the *translation, ribosomal structure and biogenesis* COG participates in *RNA transport* according to the KEGG analysis, which also revealed that *VPS10 domain-containing receptor 3* belongs to *lysosome* (Table 3A) although no COG was assigned.

After 21 days of exposure, out of the 27 significantly regulated genes, 4 were classified in the *posttranslational modification, protein turnover and chaperones* functional category. Among altered genes, *proteasome subunit alpha type-6* was found to be involved in the *proteasome* KEGG pathway (Table 3B). The *signal transduction mechanisms* COG category was also affected since *calcium calmodulin-dependent kinase type IV* was downregulated and *leucine-rich repeat-containing 15, CLN8 isoform X1* and *low affinity immunoglobulin epsilon Fc receptor* were upregulated (Table 3B). The latter was also classified in the *defense mechanisms* together with the downregulated *bactericidal permeability increasing* and *coiled-coil domain-containing mitochondrial* genes. In addition, 7 genes involved in different metabolic pathways and classified in *energy production and conversion* and *amino acid, carbohydrate and lipid transport and metabolism* were also altered (Table 3B). A single gene was significantly regulated in each following COG categories: *replication, recombination and repair, inorganic ion transport and metabolism, intracellular trafficking, secretion and vesicular transport, extracellular structures* and *cytoskeleton* (Table 3B). Among them, *Ras-related Rab-23* gene, which is involved in *endocytosis* processes, was significantly downregulated and classified in the *intracellular trafficking, secretion and vesicular transport* COG category (Table 3B).

After 1 day of dietary exposure to the same concentration of 10 µg Ag/L Ag NPs in spring, a single gene involved in each of the following functional categories was altered: *energy production and conversion, transcription, posttranslational modification, protein turnover and chaperones, secondary metabolites biosynthesis, transport and catabolism, signal transduction mechanisms, lipid transport and metabolism, translation, ribosomal structure and biogenesis, replication, recombination and repair* and *inorganic ion transport and metabolism* (Table 4A). These four latter COG categories were also altered after 21 days of exposure together with the *cytoskeleton* where *calponin-1* and *tropomyosin* were involved, *chromatin structure and dynamics* and the *intracellular trafficking, secretion and vesicular transport* COG categories (Table 4B). Among genes altered after 1 day of exposure, *39S ribosomal mitochondrial* and *serine threonine-kinase mitochondrial* were also classified in *ribosome* and *mitophagy-animal* KEGG pathways, respectively (Table 4A). After 21 days of exposure, *DNA-binding inhibitor ID-2* was classified in the *TGF-beta signaling pathway* KEGG pathway (Table 4B).

Finally, the dietary exposure to the dose close to environmentally relevant concentrations (1 µg Ag/L Ag NPs) for 1 day affected less genes than exposure to the higher concentration. However, regulated genes were involved in similar COG categories. Among them, 2 genes were upregulated in the *amino acid transport and metabolism* COG functional category (Table 5A). The *translation, ribosomal structure and biogenesis* as well as the *posttranslational modification, protein turnover and chaperones* functional categories appeared to be also affected since *39S ribosomal mitochondrial* and *disulfide-isomerase A4* were upregulated in each COG category, respectively. *39S ribosomal mitochondrial* may be involved in the KEGG pathway *ribosome* and *disulfide-isomerase A4* in the *protein processing in endoplasmic reticulum* KEGG pathway (Table 5A). *Arylacetamide deacetylase* classified in the *defense mechanism* was upregulated. Although no COG category was assigned for the *transport Sec61 subunit gamma* gene, it was classified in the *ubiquitin mediated proteolysis* KEGG pathway (Table 5A). After 21 days, *calponin-1* and *tropomyosin* classified in the *cytoskeleton* category were downregulated while the *intracellular trafficking, secretion and vesicular transport* functional category appeared altered due to the upregulation of *sorting nexin-14* (Table 5B).

Table 3. Significantly regulated transcripts (gene name) after **A**) 1 and **B**) 21 days of dietary exposure to 10 µg Ag/L Ag NPs in autumn. GenBank accession numbers (Accession No.) are shown followed by p-values (not-adjusted p<0.001) and transcripts fold change (-1.5>FC>1.5). Negative values indicate that transcripts were downregulated with respect to controls whereas positive values correspond to upregulated transcripts. COG summarizes functional categories based on the eggNOG database and KEGG pathway corresponds to the metabolic pathways in which significantly regulated transcripts may be involved according to the KEGG database. (-) symbol indicates that no hit was achieved in the analysis.

AUTUMN (CTRL vs 10 µg/L)						
TIME	GENE NAME	ACCESSION No.	Not-adjusted p-value <0.001	FC	COG	KEGG PATHWAY
1 DAY	<i>Histone acetyltransferase type B catalytic subunit-like</i>	XP_011428123.1	0.00086	-1.88	Chromatin structure and dynamics (B)	-
	<i>Cyclin-related FAM58A-like</i>	EKC32943.1	0.00048	-1.62	Cell cycle control, cell division and chromosome partitioning (D)	-
	<i>Probable uridine nucleosidase 2</i>	XP_019919249.1	0.00008	-3.61	Nucleotide transport and metabolism (F)	-
	<i>Very long-chain acyl-synthetase-like</i>	EKC20279.1	0.00080	-1.64	Lipid transport and metabolism (I)	-
	<i>Elongation factor 1 alpha</i>	BAD15289.1	0.00023	2.28	Translation, ribosomal structure and biogenesis (J)	RNA transport
	<i>Myoferlin isoform X14</i>	XP_022342091.1	0.00013	1.63	Cell wall/membrane/envelope biogenesis (M)	-
	<i>BTB POZ domain-containing 17 isoform X3</i>	XP_011421760.1	0.00081	-1.85	-	-
	<i>VPS10 domain-containing receptor 3</i>	EKC23554.1	0.00056	-1.78	-	Lysosome
	<i>Cyclin-D1-binding 1 homolog</i>	XP_022344126.1	0.00057	-1.63	-	-
	<i>Protogenin</i>	XP_019928882.1	0.00039	1.78	-	-

Table 3. Continuation

AUTUMN (CTRL vs 10 µg/L)						
TIME	GENE NAME	ACCESSION No.	Not-adjusted p-value <0.001	FC	COG	KEGG PATHWAY
	<i>Proteasome subunit alpha type-6</i>	EKC30164.1	0.00010	-3.97		Proteasome
	<i>Ribosomal RNA processing 36 homolog isoform X2</i>	XP_022334422.1	0.00033	-1.95	Posttranslational modification, protein turnover and chaperones (O)	-
	<i>Ubiquitin carboxyl-terminal hydrolase FAF-X</i>	EKC28083.1	0.00049	-1.60		-
	<i>Quinone oxidoreductase-like</i>	EKC35186.1	0.00016	2.10		-
	<i>Calcium calmodulin-dependent kinase type IV</i>	EKC30614.1	0.00022	-1.50		-
	<i>Low affinity immunoglobulin epsilon Fc receptor</i>	EKC39785.1	0.00058	1.70	Signal transduction mechanisms (T)	-
	<i>Leucine-rich repeat-containing 15</i>	EKC28269.1	0.00006	1.87		-
21 DAYS	<i>CLN8 isoform X1</i>	XP_022300210.1	0.00009	2.16		-
	<i>Bactericidal permeability increasing</i>	ACQ72925.1	0.00059	-2.62		-
	<i>Coiled-coil domain-containing mitochondrial</i>	EKC38504.1	0.00093	-1.54	Defense mechanisms (V)	-
	<i>Low affinity immunoglobulin epsilon Fc receptor</i>	EKC39785.1	0.00058	1.70		-
	<i>MOSC domain-containing mitochondrial</i>	XP_022330643.1	0.00034	1.67		-
	<i>Alcohol dehydrogenase [NADP(+)] A</i>	EKC26844.1	0.00093	1.94	Energy production and conversion (C)	Metabolic pathways, glycerolipid metabolism, folate biosynthesis, pentose and glucuronate interconversions, galactose metabolism, fructose and mannose metabolism

Table 3B. Continuation

TIME	GENE NAME	ACCESSION No.	Not-adjusted p-value <0.001	FC	COG	KEGG PATHWAY
	<i>Threonine synthase-like 2</i>	EKC19903.1	0.00040	1.90		-
	<i>Serine dehydratase-like</i>	EKC19408.1	0.00035	3.81	Amino acid transport and metabolism (E)	Metabolic pathways, carbon metabolism, valine, leucine and isoleucine biosynthesis, biosynthesis of aminoacids, cysteine and methionine metabolism; glycine, serine and threonine metabolism
	<i>Sulfotransferase family cytosolic 1B member 1-like</i>	EKC29613.1	0.00080	2.04	Carbohydrate transport and metabolism (G)	-
	<i>Endo-1,3(4)-beta-glucanase 1</i>	EKC37342.1	0.00052	2.09		-
	<i>Short-chain specific acyl-dehydrogenase mitochondrial</i>	EKC39792.1	0.00046	1.68	Lipid transport and metabolism (I)	Metabolic pathways, carbon metabolism, fatty acid metabolism, butanoate metabolism, valine, leucine and isoleucine degradation
21 DAYS	<i>Prostaglandin reductase 1</i>	EKC31524.1	0.00091	2.19	Replication, recombination and repair (L)	-
	<i>Deferochelatase peroxidase</i>	EKC43063.1	0.00015	1.55	Inorganic ion transport and metabolism (P)	-
	<i>Ras-related Rab-23</i>	EKC38762.1	0.00047	-1.55	Intracellular trafficking, secretion and vesicular transport (U)	Endocytosis
	<i>Galectin 2</i>	BAF75419.1	0.00032	1.81	Extracellular structures (W)	-
	<i>Centrosome-associated 350-like isoform X2</i>	XP_022320269.1	0.00009	-1.53	Cytoskeleton (Z)	-
	<i>Seleno T1b-like</i>	XP_011442224.1	0.00027	-1.67		-
	<i>Inactive carboxypeptidase X2</i>	EKC33118.1	0.00028	1.69		-
	<i>Leucine-rich repeat-containing 8D</i>	EKC20728.1	0.00016	1.78		-
	<i>PREDICTED: uncharacterized protein LOC105341287</i>	XP_011446028.1	0.00083	2.84		-
	<i>PREDICTED: uncharacterized protein LOC105324085</i>	XP_011421442.1	0.00090	3.11		-

Table 4. Significantly regulated transcripts (gene name) after **A)** 1 and **B)** 21 days of dietary exposure to 10 µg Ag/L Ag NPs in spring. GenBank accession numbers (Accession No.) are shown followed by p-values (not-adjusted p<0.001) and transcripts fold change (-1.5>FC>1.5). Negative values indicate that transcripts were downregulated with respect to controls whereas positive values correspond to upregulated transcripts. COG summarizes functional categories based on the eggNOG database and KEGG pathway corresponds to the metabolic pathways in which significantly regulated transcripts may be involved according to the KEGG database. (-) symbol indicates that no hit was achieved in the analysis.

SPRING (CTRL vs 10 µg/L)						
TIME	GENE NAME	ACCESSION No.	Not-adjusted p-value <0.001	FC	COG	KEGG PATHWAY
1 DAY	<i>ATP synthase subunit mitochondrial</i>	ABY27354.1	0.00026	2.23	Energy production and conversion (C)	Metabolic pathways, oxidative phosphorylation
	<i>Fatty acid synthase</i>	EKC30214.1	0.00085	1.51	Lipid transport and metabolism (I)	Metabolic pathways, fatty acid metabolism, fatty acid biosynthesis
	<i>39S ribosomal mitochondrial</i>	EKC33108.1	0.00094	2.43	Translation, ribosomal structure and biogenesis (J)	Ribosome
	<i>Opioid growth factor receptor 1</i>	XP_022325819.1	0.00099	2.34	Transcription (K)	-
	<i>DNA helicase B</i>	EKC24286.1	0.00070	-2.15	Replication, recombination and repair (L)	-
	<i>Peroxisredoxin 6</i>	XP_022328430.1	0.00089	1.58	Posttranslational modification, protein turnover and chaperones (O)	Metabolic pathways
	<i>Potassium channel subfamily T member 2</i>	EKC40703.1	0.00062	-1.83	Inorganic ion transport and metabolism (P)	-
	<i>2-oxoglutarate-Fe(II) type oxidoreductase-like</i>	XP_022311451.1	0.00028	2.09	Secondary metabolites biosynthesis, transport and catabolism (Q)	-
	<i>Serine threonine- kinase mitochondrial</i>	EKC25639.1	0.00097	2.87	Signal transduction mechanisms (T)	Mitophagy-animal
	<i>Chlorophyllase- chloroplastic</i>	XP_022337363.1	0.00099	-3.73	-	-
	<i>Oligosaccharyltransferase complex subunit OSTC</i>	XP_022327280.1	0.00014	1.78	-	-
	<i>Sarcoplasmic calcium-binding</i>	EKC29123.1	0.00016	1.92	-	-

Table 4. Continuation

SPRING (CTRL vs 10 µg/L)						
TIME	GENE NAME	ACCESSION No.	Not-adjusted p-value <0.001	FC	COG	KEGG PATHWAY
	<i>Calponin-1</i>	XP_011415482.1	0.00022	-1.93	Cytoskeleton (Z)	-
	<i>Tropomyosin</i>	ARX70262.1	0.00024	-1.55		-
	<i>SWI SNF-related matrix-associated actin-dependent regulator of chromatin subfamily A containing DEAD H box 1B isoform X1</i>	XP_022344572.1	0.00083	-1.51	Chromatin structure and dynamics (B)	-
	<i>2-acylglycerol O-acyltransferase 2-A</i>	EKC39954.1	0.00079	1.54	Lipid transport and metabolism (I)	-
	<i>Aspartate-tRNA cytoplasmic-like</i>	XP_022314406.1	0.00028	2.09	Translation, ribosomal structure and biogenesis (J)	-
	<i>Glutamate-cysteine ligase regulatory subunit</i>	XP_022320362.1	0.00059	1.68	Replication, recombination and repair (L)	Metabolic pathways, glyoxylate and dicarboxylate metabolism, cysteine and methionine metabolism, glutathione metabolism
21 DAYS	<i>Solute carrier family 13 member 2-like</i>	EKC42539.1	0.00026	2.15	Inorganic ion transport and metabolism (P)	-
	<i>Protein YIPF5-like</i>	EKC39619.1	0.00083	1.58	Intracellular trafficking, secretion and vesicular transport (U)	-
	<i>Tetraspanin-31-like isoform X1</i>	XP_022326247.1	0.00010	-3.97		-
	<i>Uncharacterized protein C4orf22 homolog</i>	XP_022318512.1	0.00005	-3.24		-
	<i>DNA-binding inhibitor ID-2</i>	EKC35853.1	0.00010	-1.67		TGF-beta signaling pathway
	<i>X-ray radiation resistance-associated 1</i>	XP_022287824.1	0.00024	-1.50		-
	<i>Protein LCHN-like</i>	XP_022338022.1	0.00002	1.51		-
	<i>Insoluble matrix shell 5</i>	XP_022323531.1	0.00047	1.96		-
	<i>PREDICTED: uncharacterized protein LOC105339560</i>	XP_011443440.1	0.00000	2.90		-

Table 5. Significantly regulated transcripts (gene name) after **A)** 1 and **B)** 21 days of dietary exposure to 1 µg Ag/L Ag NPs in spring. GenBank accession numbers (Accession No.) are shown followed by p-values (not-adjusted p<0.001) and transcripts fold change (-1.5>FC>1.5). Negative values indicate that transcripts were downregulated with respect to controls whereas positive values correspond to upregulated transcripts. COG summarizes functional categories based on the eggNOG database and KEGG pathway corresponds to the metabolic pathways in which significantly regulated transcripts may be involved according to the KEGG database. (-) symbol indicates that no hit was achieved in the analysis.

SPRING (CTRL vs 1 µg/L)						
TIME	GENE NAME	ACCESSION No.	Not-adjusted p-value <0.001	FC	COG	KEGG PATHWAY
1 DAY	<i>Ornithine decarboxylase antizyme 1</i>	EKC32251.1	0.00094	1.51	Amino acid transport and metabolism (E)	-
	<i>DBH-like monoxygenase 1</i>	EKC40694.1	0.00079	1.84		-
	<i>39S ribosomal mitochondrial</i>	EKC33108.1	0.00022	2.75	Translation, ribosomal structure and biogenesis (J)	Ribosome
	<i>Disulfide-isomerase A4</i>	EKC22564.1	0.00071	4.76	Posttranslational modification, protein turnover and chaperones (O)	Protein processing in endoplasmic reticulum
	<i>Arylacetamide deacetylase</i>	EKC19968.1	0.00094	1.80	Defense mechanisms (V)	-
	<i>Doublecortin domain-containing 5</i>	EKC26279.1	0.00099	-1.71		-
	<i>Transport Sec61 subunit gamma</i>	EKC33064.1	0.00077	1.55		Ubiquitin mediated proteolysis
	<i>Prolyl 4-hydroxylase subunit alpha-1-like</i>	EKC30309.1	0.00028	1.73		Metabolic pathway, arginine and proline metabolism

Table 5. Continuation

B)						
SPRING (CTRL vs 1 µg/L)						
TIME	GENE NAME	ACCESSION No.	Not-adjusted p-value <0.001	FC	COG	KEGG PATHWAY
21 DAYS	<i>Calponin-1</i>	<u>XP_011415482.1</u>	0.00043	-1.69		-
	<i>Tropomyosin</i>	<u>ARX70262.1</u>	0.00046	-1.51	Cytoskeleton (Z)	-
	<i>Sorting nexin-14</i>	<u>EKC18113.1</u>	0.00032	1.51	Intracellular trafficking, secretion and vesicular transport (U)	-
	<i>PREDICTED: uncharacterized protein LOC105339560</i>	<u>XP_011443440.1</u>	0.00036	2.09	-	-
	<i>Apolipoprotein D</i>	<u>XP_022327499.1</u>	0.00060	3.12	-	-

4. DISCUSSION

In order to compare the transcriptomic pattern of the digestive gland of female mussels dietarily exposed to different concentrations of PVP/PEI coated 5 nm Ag NPs both in autumn and in spring, a custom-made microarray (containing 7806 annotated and 17941 non-annotated sequences) was developed and hybridized. Due to the reported differences in gene expression patterns between male and female mussels (Banni et al., 2011), female mussels were selected based on histological analysis, which also showed that mussels collected in autumn were in early gametogenic stage whereas those collected in spring were in advanced gametogenic stage. Consequently, GI values varied depending on the season in agreement with previous works (Villalba, 1995; Ortiz-Zarragoitia et al., 2011; Cuevas et al., 2015; Azpeitia et al., 2017). Otherwise, exposure conditions including food ration, salinity and temperature were similar in the two seasons.

Mytilus spp. mussels are widely used in ecotoxicology (Cajaraville et al., 2000; Viarengo et al., 2007; Beyer et al., 2017) and nanotoxicology (Rocha et al., 2015; Canesi and Corsi, 2016) but unfortunately, information on the sequence of their genomes has not been thoroughly investigated yet (Piña and Barata, 2011; Banni et al., 2017). Thus, in the present study, annotation and assignment of biological functions of non-annotated transcripts was not successful enough even a couple of years after the development of the microarray. In addition, many of the known sequences could not be grouped in any functional category or KEGG pathway. Consequently, significantly regulated probes whose functional category remained unknown reached up to 60% in the group exposed to the dose close to environmentally relevant concentrations for 21 days, clearly indicating that further transcriptomic studies are still needed in mussels.

After 1 day of exposure to 10 μg Ag /L Ag NPs, a similar number of significantly regulated transcripts was found both in autumn and in spring (10 and 12 genes, respectively), while exposure for a longer period of time (21 days) altered more transcripts in autumn than in spring (27 and 15 genes, respectively). In fact, the PCA revealed that the main factors affecting transcription patterns in the digestive gland of mussels were exposure time and season. This season related difference could be due to the higher accumulation of Ag previously reported in mussels exposed in autumn compared to spring (see Chapter 3), which could be associated to the increase of body weight caused by the development of gametes in spring. Using the same experimental conditions as in the present work, in Chapter 3 a successful transfer of Ag NPs from microalgae to mussels was reported and the presence of Ag NPs was demonstrated in the digestive gland of exposed mussels. On the other hand, exposure to the dose close

to environmentally relevant concentrations of Ag NPs (1 µg Ag /L Ag NPs) in spring altered a low and similar number of transcripts after 1 or 21 days (8 and 5 genes, respectively), suggesting that low concentrations of Ag NPs ingested through the food web did not alter the transcription pattern of adaptive or compensative genes at the studied exposure conditions. Even though, in a previous work mussels dietarily exposed to the same dose of Ag NPs accumulated Ag, especially in digestive gland and gills, and showed a significantly reduced release of eggs by exposed female mussels and a significantly higher percentage of abnormal embryos descendant from exposed adults (see Chapter 1).

Cytoskeleton was amongst common biological functions that appeared regulated in both seasons and even after exposure to the dose close to environmentally relevant concentrations. Previous proteomic and transcriptomic studies have suggested that reorganization of the cytoskeleton is a general potential mechanism to cope with metallic NPs such as Ag NPs (Gomes et al., 2013b), CuO NPs (Gomes et al., 2014a; Hu et al., 2014) and TiO₂ NPs (Banni et al., 2016). In the present work, exposure to Ag NPs provoked significant alterations in the transcription levels of genes involved in the cytoskeleton. In autumn the *centrosome-associated 350-like isoform X2* was significantly downregulated after 21 days of exposure while in spring, *calponin-1* and *tropomyosin* were significantly downregulated after 21 days of exposure to both concentrations of Ag NPs. Similarly, a proteomic study performed using mussels exposed in the same experimental conditions as those presented here, revealed that the cytoskeletal proteins *paramyosin* and *actin* were significantly altered in the digestive gland of female mussels after 21 days of exposure to 10 µg Ag/L Ag NPs both in autumn and in spring (see Chapter 3). In agreement, maltose-stabilized 20 nm Ag NPs disrupted the integrity of the actin cytoskeleton in mussel hemocytes (Katsumiti et al., 2015). Further, cytoskeletal proteins such as *actin* and *tubulin* were found to readily interact with Ag NPs through hydrogen bonding, electrostatic, van der Waals and hydrophobic interactions, inducing changes in secondary structures (Wen et al., 2013). Thus, the *cytoskeleton* can be considered a main target for Ag NP toxicity in mussels at both protein and transcription levels, even after the exposure to a dose close to environmentally relevant concentrations.

Interactions of actin filaments with the motor protein *myosin V* have a significant role in vesicle and organelle transport along the filament tracks (Alberts et al., 2008). In consequence, the above reported disruption of the actin cytoskeleton could affect the intracellular trafficking pathways. In fact, genes involved in the *intracellular trafficking, secretion and vesicular transport* COG category were altered after the dietary exposure of mussels to 10 µg/L Ag NPs for 21 days both in autumn and in spring. Among genes

significantly altered in such category, *Ras-related Rab related 23* plays an important role in endosomal membrane trafficking (Evans et al., 2003). Even if this gene was downregulated, the internalization of Ag NPs and their agglomerates into digestive cells of mussels is known to occur through the endolysosomal system (Jimeno-Romero et al., 2017). In bivalve species, the endolysosomal pathway is considered as the major subcellular route for entry and handling of metallic NPs (Katsumiti et al., 2014; Rocha et al., 2015; Jimeno-Romero et al., 2019). According to the conceptual model proposed by Katsumiti et al. (2014) for mussel gill cells and hemocytes, metallic NPs could then be eliminated from cells by exocytosis. Direct or indirect damage to lysosomal membranes could lead to the release of ions or NPs from the lysosomal compartment into the cytosol (Katsumiti et al., 2014) and then, the multidrug resistance (MDR) transport activity could be activated as a mechanism of detoxification (Katsumiti et al., 2014; 2018), as shown in mussels gill cells after *in vitro* exposure to Ag NPs (Katsumiti et al., 2015). In the present work, dietary exposure of mussels to 10 µg/L Ag NPs for 21 days upregulated genes involved in the *inorganic ion transport and metabolism* COG category in both seasons, probably in order to prevent intracellular accumulation of Ag and to protect the cells from Ag toxicity.

The functional category *lipid transport and metabolism* appeared altered in both seasons after mussels dietary exposure to 10 µg Ag/L Ag NPs for 1 and 21 days. In autumn, the *very long-chain acyl-synthase-like* and *short-chain specific acyl-dehydrogenase mitochondrial* transcripts were significantly down- and upregulated after 1 and 21 days of exposure, respectively, while in spring, the *fatty acid synthase* and *2-acylglycerol O-acyltransferase 2-A* were significantly upregulated after 1 and 21 days of exposure, respectively. Previous microarray studies in zebrafish revealed a significant downregulation of transcripts related to *lipid transport and localization* pathways after zebrafish waterborne and dietary exposure to 10 µg/L of maltose-coated 20 nm Ag NPs and 100 µg/L of PVP/PEI coated 5 nm Ag NPs, respectively (Lacave et al., 2017; 2018). In addition, Lacave et al. (2018) reported that hepatocytes of zebrafish waterborne exposed to Ag NPs showed more glycogen and lipid droplets than unexposed zebrafish. Thus, the significant regulation of transcripts reported in the present work after the dietary exposure to Ag NPs in both seasons could imply impairment of lipid metabolism at cell or tissue level, especially at the highest concentration of 10 µg Ag/L Ag NPs.

The COG category *carbohydrate transport and metabolism* was altered after 21 days of dietary exposure to Ag NPs only in autumn. Interestingly, among genes involved in such category, *sulfotransferase family cytosolic 1B member 1-like* catalyzes sulfation of compounds containing hydroxyl or amino groups to both detoxify dietary and

environmental xenobiotics and regulates the level and activity of endogenous molecules such as steroid hormones (Sugahara et al., 2003; Fernandes et al., 2011) involved in the reproduction cycle of mussels. *Endo-1,3-beta-glucanase* catalyzes the depolymerization of dietary polysaccharides in order to provide carbon and energy sources in molluscs (Zakharenko et al., 2011; Sova et al., 2013). A similar disruption of carbohydrate metabolism of mussels was also reported at proteome level in organisms exposed to Ag NPs through water (Gomes et al., 2013b) or diet, especially in autumn (see Chapter 3). Further, such changes, together with the disorganization of the cytoskeleton, may promote physical changes in cell membranes, altering the respiratory, oxidative and Ca^{2+} buffering capacity of mitochondria (Gomes et al., 2013b).

Also in autumn after 21 days of exposure to 10 μg Ag/L Ag NPs, the upregulated *leucine-rich repeat-containing 15* and *low affinity immunoglobulin epsilon Fc receptor* transcripts and the downregulated *calcium calmodulin-dependent kinase type IV* were classified in the *signal transduction* COG functional category. The gene *serine threonine-kinase mitochondrial*, upregulated after 1 day exposure to the same Ag NP concentration in spring, was also classified in the same category. Interestingly, the upregulated transcripts have been related to the immune system cell signaling pathway. In bivalves, the innate immune system is under the control of a complex network of evolutionarily conserved signaling pathways such as Toll like receptors (TLR), which play a key role in initiating and activating the immune system (Song et al., 2010; Gerdol and Venier, 2015). TLR-mediated mechanisms directly interact with *immunoglobulin E (IgE)* synthesis which together with the signal input from different receptors promote the immune response in vertebrates (Novak et al., 2010). Thus, regulation of such transcripts in mussels dietarily exposed to Ag NPs could indicate alterations of the immune response. Alterations in the immune cells of mussels, the hemocytes, have been already associated with the exposure to different metallic NPs both *in vitro* (Canesi et al., 2008; 2010; Ciacci et al., 2012; Katsumiti et al., 2014; 2018) and *in vivo* (Balbi et al., 2014; Barmo et al., 2013); including Ag NPs (Katsumiti et al., 2015).

Further, after just 1 day of dietary exposure to the high concentration of Ag NPs in autumn, genes involved in the *translation, ribosomal structure and biogenesis* COG functional category were altered, while after 21 days of dietary exposure, the *posttranslational modification, protein turnover, chaperones* category seemed to be affected, suggesting that synthesis of ribosomes and general metabolism of proteins could be affected after the exposure to Ag NPs. In spring, 1 day of exposure to even the dose close to environmentally relevant concentrations, was enough to alter the transcription level of genes involved in such categories. Ribosomal genes are

constitutively expressed since their products are necessary for the synthesis of all cell proteins. Thus, regulation of ribosome biogenesis can be considered a key element of cell biology (Laferté et al., 2006). Several transcriptomic studies reported alterations in the transcription level of genes involved in ribosomal processes and translation after mussel exposure to different pollutants including insecticides, metals, pharmaceuticals and polycyclic aromatic hydrocarbons (Dondero et al., 2010; Negri et al., 2013; Mezzelani et al., 2016; Banni et al., 2017) and linked such alterations to the increased rate of ribosome biogenesis (Dondero et al., 2010; Negri et al., 2013) necessary to support basic cellular activities (Negri et al., 2013). Similarly, exposure to different metallic NPs such as iron oxide NPs or Ag NPs was found to induce changes in transcription levels of genes related to ribosome biogenesis and translation in aquatic organisms (Nair and Choi, 2011; Nair et al., 2011; Villacis et al., 2017).

Synthesized proteins are posttranslationally modified through hydroxylation and ubiquitination which influence enzyme activities, protein turnover and localization, protein-protein interactions, modulation of signaling cascades, DNA repair and cell division (Karve and Cheema, 2011). Therefore, ubiquitin labeling serves as a degradation signal for numerous target proteins in the proteasome and ubiquitin hydrolases are required to control the degree of modification as well as to regenerate functional ubiquitin molecules (Rose, 1988). In the present work, the *proteasome subunit alpha type-6* and *ubiquitin carboxyl-terminal hydrolase FAF-X* were significantly downregulated, suggesting that the dietary exposure of mussels to Ag NPs could affect degradation of misfolded or damaged proteins, which could finally lead to alterations in cell protein homeostasis. It is known that trace metals such as Cd or Cu disrupt the ubiquitin-proteasome system and inhibit proteasome activity in mammals (Yu et al., 2011; Neslund-Dudas et al., 2012) however, mechanisms are not well understood in bivalves (Götze et al., 2014). In oysters, exposure to Cu decreased *ubiquitin* mRNA levels, suggesting suppression of the ubiquitin-proteasome system, although transcription of proteasome-related genes was not affected in clams exposed to Cu or Cd (Götze et al., 2014). On the contrary, exposure of mussels to a mixture of Cu, Cd and Hg overexpressed proteasome subunits and ubiquitin transcripts, suggesting a boost of protein synthesis, folding and degradation (Varotto et al., 2013).

5. CONCLUSIONS

Dietary exposure to PVP/PEI coated 5 nm Ag NPs significantly altered the transcription profile of the digestive gland in female mussels both in autumn and in spring. The main factors explaining observed transcription patterns were season and exposure time. Overall, a higher number of probes was significantly regulated after 21 days of dietary exposure to Ag NPs in autumn compared to spring, probably due to a higher accumulation of Ag in mussel soft tissues in autumn. Transcripts involved in biological processes related to *carbohydrate transport and metabolism* were significantly regulated only in autumn and *signal transduction mechanisms* were more affected in autumn than in spring. Transcripts altered in both seasons affected general cell processes including *cytoskeleton, intracellular trafficking, secretion and vesicular transport; inorganic ion transport and metabolism; lipid transport and metabolism; translation, ribosomal structure and biogenesis and posttranslational modification, protein turnover and chaperones*, among others. The dietary exposure of mussels to 1 µg Ag /L Ag NPs altered a lower number of transcripts compared to 10 µg Ag /L Ag NPs but affecting similar pathways, suggesting that environmentally relevant concentrations of Ag NPs show similar mechanisms of action compared to higher concentrations. For future studies, season should be considered for assessing the potential effects caused by engineered NPs in marine bivalves since different transcription profiles were found in autumn and spring after dietary exposure to Ag NPs.

ACKNOWLEDGEMENTS

This work has been funded by the Spanish Ministry of Economy and Competitiveness (NanoSilverOmics project MAT2012-39372), Basque Government (SAIOTEK project S-PE13UN142 and Consolidated Research Group GIC12/IT-810-13) and the University of the Basque Country UPV/EHU (UFI 11/37 and PhD fellowships to N.D. and P.M.). Technical and human support provided by SGIker (UPV/EHU, ERDF and ESF) is gratefully acknowledged.

REFERENCES

- ∴ Alberts B., Johnson A., Lewis J., Morgan D., Raff M., Roberts K., Walter P. 2008. The Cytoskeleton. In: Molecular Biology of the Cell. 6th Edition. Garland Science, New York.
- ∴ Azpeitia K., Ortiz-Zarragoitia M., Revilla M., Mendiola D. 2017. Variability of the reproductive cycle on the estuarine and coastal populations of the mussel *Mytilus galloprovincialis* Lmk. from the SE Bay of Biscay (Basque Country). International Aquatic Research: DOI 10.1007/s40071-017-0180-3.
- ∴ Baker T.J., Tyler C.R., Galloway T.S. 2014. Impacts of metal and metal oxide nanoparticles on marine organisms. Environmental Pollution 186: 257-271.
- ∴ Balbi T., Smerilli A., Fabbri E., Ciacci C., Montagna M., Graselli E., Brunelli A., Pojana G., Marcomimi A., Gallo G., Canesi L. 2014. Co-exposure to n-TiO₂ and Cd²⁺ results in interactive effects on biomarker responses but not in increased toxicity in the marine bivalve *M. galloprovincialis*. Science of the total Environment 493: 355- 364.
- ∴ Banni M., Negri A., Mignone F., Boussetta H., Viarengo A. and Dondero F. 2011. Gene expression rhythms in the mussel *Mytilus galloprovincialis* (Lam.) across an annual cycle. PLoS ONE 6 (5): e18904. doi:10.1371/journal.pone.0018904.
- ∴ Banni M., Attig H., Sforzini S., Oliveri C., Mignone F., Boussetta H., Viarengo A. 2014. Transcriptomic responses to heat stress and nickel in the mussel *Mytilus galloprovincialis*. Aquatic Toxicology 148: 104-112.
- ∴ Banni M., Sforzini S., Balbi T., Corsi I., Viarengo A., Canesi L. 2016. Combined effects of n-TiO₂ and 2,3,7,8-TCDD in *Mytilus galloprovincialis* digestive gland: A transcriptomic and immunohistochemical study. Environmental Research 145: 135-144.
- ∴ Banni M., Sforzini S., Arlt V.M., Barranguer A., Dallas L.J., Oliveri C., Aminot Y., Pacchioni B., Millino C., Lanfranchi G., Readman J.W., Moore M.N., Viarengo A., Jha A.N. 2017. Assessing the impact of benzo[a]pyrene on marine mussels: application of a novel targeted low density microarray complementing classical biomarker responses. PLoS ONE 12 (6): e0178460.
- ∴ Barmo C., Ciacci C., Canonico B., Fabbri R., Cortesec K., Balbi T., Marcomini A., Pojana G., Gallo G., Canesi L. 2013. *In vivo* effects of n-TiO₂ on digestive gland and immune function of the marine bivalve *Mytilus galloprovincialis*. Aquatic Toxicology 132-133: 9-18.
- ∴ Bayne B.L., Widdows J. 1978. The physiological ecology of two populations of *Mytilus edulis* L. Oecologia 37: 137-162.
- ∴ Bebianno M.J., Gonzalez-Rey M., Gomes T., Mattos J.J., Flores-Nunes F., Bairy A.C.D. 2015. Is gene transcription in mussel gills altered after exposure to Ag nanoparticles? Environmental Science and Pollution Research 22: 17425-17433.
- ∴ Beyer J., Green N.W., Brooks S., Allan I.J., Ruus A., Gomes T., Bråte I.L.N., Schøyen M. 2017. Blue mussels (*Mytilus edulis* spp.) as sentinel organisms in coastal pollution monitoring: A review. Marine Environmental Research 130: 338-365.
- ∴ Blaser S.A., Scheringer M., Macleod M., Hungerbühler K. (2008). Estimation of cumulative aquatic exposure and risk due to silver: contribution of nano-functionalized plastics and textiles. Science of the Total Environment 390: 396-409.

- ∴ Bocchetti R., Regoli F. 2006. Seasonal variability of oxidative biomarkers, lysosomal parameters, metallothioneins and peroxisomal enzymes in the Mediterranean mussel *Mytilus galloprovincialis* from Adriatic Sea. *Chemosphere* 65: 913-921.
- ∴ Brown M., Davies I.M., Moffat C.F., Craft M.A. 2006. Application of SSH and macroarray to investigate altered gene expression in *Mytilus edulis* in response to exposure to benzo[a]pyrene. *Marine Environmental Research* 62: S128-S135.
- ∴ Buffet P.E., Pan J.F., Poirier L., Amiard-Triquet C., Amiard J.C., Gaudin P., Risso. De Faverney C., Guibbolini M., Gilliland D., Valsami-Jones E. and Mouneyrac C. 2013. Biochemical and behavioural responses of the endobenthic bivalve *Scrobicularia plana* to silver nanoparticles in seawater and microalgal food. *Ecotoxicology and Environmental Safety* 89: 117-124.
- ∴ Buffet P.E., Zalouk-Vergnoux A., Châtel A., Berthet B., Métais I., Perrein-Ettajani H., Poirier L., Luna-Acosta A., Thomas-Guyon H., Risso-de Faverney C., Guibbolini M., Gilliland D., Valsami-Jones E., Mouneyrac C. 2014. A marine mesocosm study on the environmental fate of silver nanoparticles and toxicity effects on two endobenthic species: The ragworm *Hediste diversicolor* and the bivalve mollusc *Scrobicularia plana*. *Science of the Total Environment* 470-471: 1151-1159.
- ∴ Cajaraville M.P., Bebianno M.J., Blasco J., Porte C., Sarasquete C., Viarengo A. 2000. The use of biomarkers to assess the impact of pollution in coastal environments of the Iberian Peninsula: a practical approach. *Science of the Total Environment* 247: 295-311.
- ∴ Cancio I., Ibabe A., Cajaraville M.P. 1999. Seasonal variation of peroxisomal enzyme activities and peroxisomal structure in mussels *Mytilus galloprovincialis* and its relationship with the lipid content. *Comparative Biochemistry and Physiology, Part C* 123: 135-144.
- ∴ Canesi L., Ciacci C., Betti M., Fabbri R., Canonico B., Fantinati A., Marcomini A., Pojana G. 2008. Immunotoxicity of carbon black nanoparticles to blue mussel hemocytes. *Environment International* 34: 1114-1119.
- ∴ Canesi L., Ciacci C., Vallotto D., Gallo G., Marcomini A., Pojana G. 2010. *In vitro* effects of suspensions of selected nanoparticles (C60 fullerene, TiO₂, SiO₂) on *Mytilus* hemocytes. *Aquatic Toxicology* 96: 151-158.
- ∴ Canesi L., Negri A., Barmo C., Banni M., Gallo G., Viarengo A., Dondero F. 2011. The organophosphate chlorpyrifos interferes with the responses to 17β-estradiol in the digestive gland of the marine mussel *Mytilus galloprovincialis*. *PLoS ONE* 6 (5): e19803. doi:10.1371/journal.pone.0019803.
- ∴ Canesi L., Ciacci C., Fabbri R., Marcomini A., Pojana G. and Gallo G. 2012. Bivalve molluscs as a unique target group for nanoparticle toxicity. *Marine Environmental Research* 76: 16-21.
- ∴ Canesi L. and Corsi I. 2016. Effects of nanomaterials on marine invertebrates. *Science of the Total Environment* 565: 933-940.
- ∴ Chio C.P., Chen W.Y., Chou W.W., Hsieh N.H., Ling M.P., Liao C.M. 2012. Assessing the potential risks to zebrafish posed by environmentally relevant copper and silver nanoparticles. *Science of the Total Environment* 420: 111-118.
- ∴ Ciacci C., Canonico B., Bilaničová D., Fabbri R., Cortese K., Gallo G., Marcomini A., Pojana G., Canesi L. 2012. Immunomodulation by different types of N-oxides in the hemocytes of the

marine bivalve *Mytilus galloprovincialis*. PLoS ONE 7 (5): e36937. doi:10.1371/journal.pone.0036937.

- ∴ Corsi I., Cherr G.N., Lenihan H.S., Labille J., Hasselov M., Canesi L., Dondero F., Frenzilli G., Hristozov D., Punes V., Della Torre C., Pinsino A., Libralato G., Marcomini A., Sabbioni E., Matranga V. 2014. Common Strategies and Technologies for the Ecosafety Assessment and Design of Nanomaterials Entering the Marine Environment. *ACS Nano* 8: 9694-709.
- ∴ Cuevas N., Zorita I., Costa P.M., Franco J., Larreta J. 2015. Development of histopathological indices in the digestive gland and gonad of mussels: integration with contamination levels and effects of confounding factors. *Aquatic Toxicology* 162: 152-164.
- ∴ Denslow N.D., Garcia-Reyero N., Barber D.S. 2007. Fish 'n' chips: the use of microarrays for aquatic toxicology. *Molecular BioSystems* 3: 172-177.
- ∴ Dondero F., Negri A., Boatti L., Marsano F., Mignone F., Viarengo A. 2010. Transcriptomic and proteomic effects of a neonicotinoid insecticide mixture in the marine mussel (*Mytilus galloprovincialis*, Lam.). *Science of the Total Environment* 408: 3775-3786.
- ∴ Dondero F., Banni M., Negri A., Boatti L., Dagnino A., Viarengo A. 2011. Interactions of a pesticide/heavy metal mixture in marine bivalves: a transcriptomic assessment. *BMC Genomics* 12: 195-212.
- ∴ Dumont E., Johnson A.C., Keller V.D.J., Williams R.J. 2015. Nano silver and nano zinc-oxide in surface waters-Exposure estimation for Europe at high spatial and temporal resolution. *Environmental Pollution* 196: 341-349.
- ∴ Evans T.M., Ferguson C., Wainwright B.J., Parton R.G., Wicking C. 2003. Rab23, a Negative Regulator of Hedgehog Signaling, Localizes to the Plasma Membrane and the Endocytic Pathway. *Traffic* 4: 869-884.
- ∴ Fabrega J., Luoma S.N., Tyler C.R., Galloway T.S., Lead J.R. 2011. Silver nanoparticles: Behaviour and effects in the aquatic environment. *Environmental International* 37: 517-531.
- ∴ Fent K., Sumpter J.P. 2011. Progress and promises in toxicogenomics in aquatic toxicology: Is technical innovation driving scientific innovation? *Aquatic Toxicology* 105S: 25-39.
- ∴ Fernandes D., Loi B., Porte C. 2011. Biosynthesis and metabolism of steroids in molluscs. *Journal of Steroid Biochemistry & Molecular Biology* 127: 189-195.
- ∴ Gamble M., Wilson I. 2002. The hematoxylin and eosin. In: Bancroft J.D., Gamble M. (Eds.), *Theory and Practice of Histological Techniques*. Churchill Livingstone-Elsevier Science Ltd., London, UK, pp. 125.
- ∴ Gerdol M., Venier P. 2015. An updated molecular basis for mussel immunity. *Fish & Shellfish Immunology* 46: 17-38.
- ∴ Giese B., Klaessig F., Park B., Kaegi R., Steinfeldt M., Wigger H., von Gleich A., Gottschalk F. 2018. Risks, release and concentrations of engineered nanomaterial in the environment. *Scientific Reports* 8: doi: 10.1038/s41598-018-19275-4.
- ∴ Goldberg E.D. 1975. The mussel watch- a first step in global marine monitoring. *Marine Pollution Bulletin* 6: 111.

- .: Gomes T., Araújo O., Pereira R., Almeida A.C., Cravo A., Bebianno M.J. 2013a. Genotoxicity of copper oxide and silver nanoparticles in the mussel *Mytilus galloprovincialis*. *Marine Environmental Research* 84: 51-59.
- .: Gomes T., Pereira C.G., Cardoso C., Bebianno M.J. 2013b. Differential protein expression in mussels *Mytilus galloprovincialis* exposed to nano and ionic Ag. *Aquatic Toxicology* 136-137: 79-90.
- .: Gomes T., Chora S., Pereira C.G., Cardoso C., Bebianno M.J. 2014a. Proteomic response of mussels *Mytilus galloprovincialis* exposed to CuO NPs and Cu²⁺: An exploratory biomarker discovery. *Aquatic Toxicology* 155: 327-336.
- .: Gomes T., Pereira C.G., Cardoso C., Sousa V.S., Ribau Teixeira M., Pinheiro J.P., Bebianno M.J. 2014b. Effects of silver nanoparticles exposure in the mussel *Mytilus galloprovincialis*. *Marine Environmental Research* 101: 208-214.
- .: Gottschalk F., Sonderer T., Scholz R.W., Nowack B. 2009. Modeled environmental concentrations of engineered nanomaterials (TiO₂, ZnO, Ag, CNT, fullerenes) for different regions. *Environmental Science and Technology* 43: 9216-9222.
- .: Götz S., Matoo O.B., Beniash E., Saborowski R., Sokolova I.M. 2014. Interactive effects of CO₂ and trace metals on the proteasome activity and cellular stress response of marine bivalves *Crassostrea virginica* and *Mercenaria mercenaria*. *Aquatic Toxicology* 149: 65-82.
- .: Hu W., Culloty S., Darmody G., Lynch S., Davenport J., Ramirez-Garcia S., Dawson K.A., Lynch I., Blasco J., Sheehan D. 2014. Toxicity of copper oxide nanoparticles in the blue mussel, *Mytilus edulis*: a redox proteomic investigation. *Chemosphere* 108: 289-299.
- .: Huerta-Cepas J., Szklarczyk D., Forslund K., Cook H., Heller D., Walter M.C., Rattei T., Mende D.R., Sunagawa S., Kuhn M., Jensen L.J., von Mering C., Bork P. 2016. eggNOG 4.5: a hierarchical orthology framework with improved functional annotations for eukaryotic, prokaryotic and viral sequences. *Nucleic Acids Research* 44: D286-D293.
- .: Ji C., Li F., Wang Q., Zhao J., Sun Z., Wu H. 2016. An integrated proteomic and metabolomics study on the gender specific responses of mussels *Mytilus galloprovincialis* to tetrabromobisphenol A (TBBPA). *Chemosphere* 144: 527-539.
- .: Jimeno-Romero A., Bilbao E., Izagirre U., Cajaraville M.P., Marigómez I., Soto M. 2017. Digestive cell lysosomes as main targets for Ag accumulation and toxicity in marine mussels, *Mytilus galloprovincialis*, exposed to maltose-stabilized Ag nanoparticles of different sizes. *Nanotoxicology* 11: 168-183.
- .: Jimeno-Romero A., Bilbao E., Valsami-Jones E., Cajaraville M.P., Soto M., Marigómez I. 2019. Bioaccumulation, tissue and cell distribution, biomarkers and toxicopathic effects of CdS quantum dots in mussels, *Mytilus galloprovincialis*. *Ecotoxicology and Environmental Safety* 167: 288-300.
- .: Kanehisa M., Furumichi M., Tanabe M., Sato Y., Morishima K. 2017. KEGG: new perspectives on genomes, pathways, diseases and drugs. *Nucleic Acid Research* 45: D353-D361.
- .: Karve T.M., Cheema A.V. 2011. Small Changes Huge Impact: The Role of Protein Posttranslational Modifications in Cellular Homeostasis and Disease. *Journal of Amino Acids* 2011: doi:10.4061/2011/207691.

- ∴ Katsumiti A., Gilliland D., Arostegui I., Cajaraville M.P. 2014. Cytotoxicity and cellular mechanisms involved in the toxicity of CdS quantum dots in hemocytes and gill cells of the mussel *Mytilus galloprovincialis*. *Aquatic Toxicology* 153: 39-52.
- ∴ Katsumiti A., Gilliland D., Arostegui I., Cajaraville M.P. 2015. Mechanisms of toxicity of Ag nanoparticles in comparison to bulk and ionic Ag on mussel hemocytes and gill cells. *PLoS ONE* 10 (6): e0129039. doi:10.1371/journal.pone.0129039.
- ∴ Katsumiti A., Thorley A.J., Arostegui I., Reip P., Valsami-Jones E., Tetley T.D., Cajaraville M.P. 2018. Cytotoxicity and cellular mechanisms of toxicity of CuO NPs in mussel cells *in vitro* and comparative sensitivity with human cells. *Toxicology In Vitro* 48: 146-158.
- ∴ Kim Y., Ashton-Alcox K.A., Powell E.N. 2006. Gonadal analysis. NOAA histological techniques for marine bivalve mollusks: update. NOAA Technical Memories NOS NCCOS 27, Silver Spring (USA): 1–18.
- ∴ Lacave J.M., Fanjul A., Bilbao E., Gutierrez N., Barrio I., Arostegui I., Cajaraville M.P., Orbea A. 2017. Acute toxicity, bioaccumulation and effects of dietary transfer of silver from brine shrimp exposed to PVP/PEI coated silver nanoparticles to zebrafish. *Comparative Biochemistry and Physiology, Part C* 199: 69-80.
- ∴ Lacave J.M., Vicario-Parés U., Bilbao E., Gilliland D., Mura F., Dini L., Cajaraville M.P., Orbea A. 2018. Waterborne exposure of adult zebrafish to silver nanoparticles and to ionic silver results in differential silver accumulation and effects at cellular and molecular levels. *Science of the Total Environment* 642: 1209-1220.
- ∴ Laferté A., Favry E., Sentenac A., Riva M., Carles C., Chédin S. 2006. The transcriptional activity of RNA polymerase I is a key determinant for the level of all ribosome components. *Genes and Development* 20: 2030-2040.
- ∴ Li L., Stoiber M., Wimmer A., Xu Z., Lindenblatt C., Helmreich B., Schuster M. 2016. To what extent can full-scale wastewater treatment plant effluent influence the occurrence of silver-based nanoparticles in surface waters? *Environmental Science and Technology* 50: 6327-6333.
- ∴ Livingstone D.R., Farrar S.V. 1984. Tissue and subcellular distribution of enzyme activities of mixed function oxygenase and benzo[a]pyrene metabolism in the common mussel *Mytilus edulis*. *Science of the Total Environment* 39: 209-235.
- ∴ Maria V.L., Amorim M.J., Bebianno M.J., Dondero F. 2016. Transcriptomic effects of the non-steroidal anti-inflammatory drug Ibuprofen in the marine bivalve *Mytilus galloprovincialis* Lam. *Marine Environmental Research* 119: 31-39.
- ∴ Magesky A., Pelletier E. 2018. Cytotoxicity and physiological effects of silver nanoparticles on marine invertebrates, in: Saquib, Q., Faisal, M., Al-Khedhairy, A.A., Alatar, A.A. (Eds.), *Cellular and Molecular Toxicology of Nanoparticles*. Springer International Publishing, pp.285-309.
- ∴ Massarsky A., Trudeau V.L., Moon T.W. 2014. Predicting the environmental impact of nanosilver. *Environmental Toxicology and Pharmacology* 38: 861-873.
- ∴ McCarthy M., Carroll D.L., Ringwood A.H. 2013. Tissue specific response of oysters, *Crassostrea virginica*, to silver nanoparticles. *Aquatic Toxicology* 138-139: 123-128.

- ∴ McGillicuddy E., Murray I., Kavanagh S., Morrison L., Fogarty A., Cormican M., Dockery P., Prendergast M., Rowan N., Morris D. 2017. Silver nanoparticles in the environment: Sources, detection and ecotoxicology. *Science of the Total Environment* 575: 231-246.
- ∴ Mezzelani M., Gorbi S., Fattorini D., d'Errico G., Benedetti M., Milan M., Bargelloni L., Regoli F. 2016. Transcriptional and cellular effects of Non-Steroidal Anti-Inflammatory Drugs (NSAIDs) in experimentally exposed mussels, *Mytilus galloprovincialis*. *Aquatic Toxicology* 180: 306-319.
- ∴ Moore M.N. 2006. Do nanoparticles present ecotoxicological risks for the health of the aquatic environment? *Environment International* 32: 967-976.
- ∴ Nair P.M.G., Choi J. 2011. Characterization of a ribosomal protein L15 cDNA from *Chironomus riparius* (Diptera; Chironomidae): Transcriptional regulation by cadmium and silver nanoparticles. *Comparative Biochemistry and Physiology, Part B* 159: 157-162.
- ∴ Nair P.M.G., Park S.Y., Lee S.W., Choi J. 2011. Differential expression of ribosomal protein gene, gonadotrophin releasing hormone gene and Balbiani ring protein gene in silver nanoparticles exposed *Chironomus riparius*. *Aquatic Toxicology* 101: 31-37.
- ∴ Negri A., Oliveri C., Sforzini S., Mignione F., Viarengo A., Banni M. 2013. Transcriptional response of the mussel *Mytilus galloprovincialis* (Lam.) following exposure to heat stress and copper. *PLoS ONE* 8(6): e66802.
- ∴ Neslund-Dudas C., Mitra B., Kandegedara A., Chen D., Schmitt S., Shen M., Cui Q., Rybicki B.A., Dou P.Q. 2012. Association of metals and proteasome activity in erythrocytes of prostate cancer patients and controls. *Biological Trace Element Research* 149: 5-9.
- ∴ Novak N., Bieber T., Peng W.M. 2010. The Immunoglobulin E-Toll-Like Receptor Network. *International Archives of Allergy and Immunology* 151: 1-7.
- ∴ Ortiz-Zarragoitia M., Garmendia L., Barbero M.C., Serrano T., Marigómez I., Cajarville M.P. 2011. Effects of the fuel oil spilled by the Prestige tanker on reproduction parameters of wild mussel populations. *Journal of Environmental Monitoring* 13: 84-94.
- ∴ Pedregosa F., Varoquaux G., Gramfort A., Michel V., Thirion B., Grisel O., Blondel M., Prettenhofer P., Weiss R., Dubourg V., Vanderplas J., Passos A., Cournapeau D., Brucher M., Duchesnay M.P.E. 2011. Scikit-learn: Machine Learning in Python. *Journal of Machine Learning Research* 12: 2825-2830.
- ∴ Piña B., Barata C. 2011. A genomic and ecotoxicological perspective of DNA array studies in aquatic environmental risk assessment. *Aquatic Toxicology* 105S: 40-49.
- ∴ R Core Team, 2017. R: A Language and Environment for Statistical Computing. <https://www.R-project.org>.
- ∴ Ringwood A.H., McCarthy M., Bates T.C., Carrol D.L. 2010. The effects of silver nanoparticles on oyster embryos. *Marine Environmental Research* 69: S49-S51.
- ∴ Ritchie M.E., Phipson B., Wu D., Hu Y., Law C.W., Shi W., Smyth G.K. 2015. limma powers differential expression analyses for RNA-sequencing and microarray studies. *Nucleic Acids Research* 20: e47.

- ∴ Riva C., Binelli A., Rusconi F., Colombo G., Pedriali A., Zippel R., Provini A. 2011. A proteomic study using zebra mussels (*D. polymorpha*) exposed to benzo[a]pyrene: The role of gender and exposure concentrations. *Aquatic Toxicology* 104: 14-22.
- ∴ Rocha T.L., Gomes T., Sousa V.S., Mestre N.C., Bebianno M.J. 2015. Ecotoxicological impact of engineered nanomaterials in bivalve molluscs: An overview. *Marine Environmental Research* 111: 74-88.
- ∴ Rose I.A. 1988. Chapter 5: Ubiquitin Carboxyl-Terminal Hydrolases. In: Rechsteiner M. (Ed.) *Ubiquitin*. Springer Science+Business Media, New York. pp.135-153.
- ∴ Sheehan D., Power A. 1999. Effects of seasonality on xenobiotic and antioxidant defence mechanisms of bivalve molluscs. *Comparative Biochemistry and Physiology, Part C* 123: 193-199.
- ∴ Sikder M., Lead J.R., Chandler G.T., Baalousha M. 2017. A rapid approach for measuring silver nanoparticle concentration and dissolution in seawater by UV-Vis. *Science of the Total Environment* 618: 597-607.
- ∴ Snape J.R., Maund S.J., Pickford D.B., Hutchinson T.H. 2004. Ecotoxicogenomics: the challenge of integrating genomics into aquatic and terrestrial ecotoxicology. *Aquatic Toxicology* 67: 143-154.
- ∴ Solé M., Porte C., Albaigés J. 1995. Seasonal variation in the mixed-function oxygenase system and antioxidant enzymes of the mussel *Mytilus galloprovincialis*. *Environmental Toxicology and Chemistry* 14: 157-164.
- ∴ Song L., Wang L., Qiu L., Zhang H. 2010. Bivalve immunity. In: Söderhall K. (Ed.) *Invertebrate Immunity*. Springer Science + Business Media, LCC. New York. pp: 44-60.
- ∴ Sova V.V., Pesentseva M.S., Zakharenko A.M., Kovalchuk S.N., Zvyagintseva T.N. 2013. Glycosidases of Marine Organisms. *Biochemistry (Moscow)* 78: 746-759.
- ∴ Sugahara T., Liu C.C., Pai T.G., Liu M.C. 2003. Molecular cloning, expression, and functional characterization of a novel zebrafish cytosolic sulfotransferase. *Biochemical and Biophysical Research Communications* 300: 725-730.
- ∴ Tatusov R.L., Fedorova N.D., Jackson J.D., Jacobs A.R., Kiryutin B., Koonin E.V., Krylov D.M., Mazumder R., Mekhedov S.L., Nikolskaya A.N., Rao B.S., Smirnov S., Sverdlov A.V., Vasudevan S., Wolf Y.I., Yin J.J., Natale D.A. 2003. The COG database: an updated version includes eukaryotes. *BMC Bioinformatics* 4: 41-55.
- ∴ Tiede K., Hassellöv M., Breitbarth E., Chaudhry Q., Boxall A.B.A. 2009. Considerations for environmental fate and ecotoxicity testing to support environmental risk assessments for engineered nanoparticles. *Journal of Chromatography A* 1216: 503-509.
- ∴ Varotto L., Domeneghetti S., Rosani U., Cajaraville M.P., Raccanelli S., Pallavicini A., Venier P. 2013. DNA damage and transcriptional changes in the gills of *Mytilus galloprovincialis* exposed to nanomolar doses of combined metal salts (Cd, Cu, Hg). *PLoS ONE* 8 (1): e54602. doi:10.1371/journal.pone.0054602.
- ∴ Vance M.E., Kuiken T., Vejerano E.P., McGinnis S.P., Hochella M. F. Jr., Rejeski D., Hull M.S. 2015. Nanotechnology in the real world: Redeveloping the nanomaterial consumer products inventory. *Beilstein Journal of Nanotechnology* 6: 1769-1780.

- ∴ Veldhoen N., Ikonomidou M.G., Hlebing C.C. 2012. Molecular profiling of marine fauna: Integration of omics with environmental assessment of the world's oceans. *Ecotoxicology and Environmental Safety* 76: 23-38.
- ∴ Venier P., De Pittà C., Bernante F., Varotto L., De Nardi B., Bovo G., Roch P., Novoa B., Figueras A., Pallavicini A., Lanfranchi G. 2009. MytiBase: a knowledgebase of mussel (*M. galloprovincialis*) transcribed sequences. *BMC Genomics* 10: 72-87.
- ∴ Viarengo A., Lowe D., Bolognesi C., Fabbri E., Koehler A. 2007. The use of biomarkers in biomonitoring: a 2-tier approach assessing the level of pollutant-induced stress syndrome in sentinel organisms. *Comparative Biochemistry and Physiology, Part C* 146: 281-300.
- ∴ Villacis R.A.R., Filho J.S., Piña B., Azevedo R.B., Pic-Taylor A., Mazzeu J.F., Grisolia C.K. 2017. Integrated assessment of toxic effects of maghemite (γ -Fe₂O₃) nanoparticles in zebrafish. *Aquatic Toxicology* 191: 219-225.
- ∴ Villalba A. 1995. Gametogenic cycle of cultured mussel, *Mytilus galloprovincialis*, in the bays of Galicia (N.W. Spain). *Aquaculture* 130: 269-277.
- ∴ Wen Y., Geitner N.K., Chen R., Ding F., Chen P., Andorfer R.E., Govindanb P.N., Ke P.C. 2013. Binding of cytoskeletal proteins with silver nanoparticles. *RSC Advances* 3: 22002-22007.
- ∴ Yu X., Ponce R.A., Faustman E.M. 2011. Metals induced disruption of ubiquitin proteasome system, activation of stress signaling and apoptosis. In: Banfalvi G. (eds) *Cellular Effects of Heavy Metals*. Springer, Dordrecht, pp 291-311.
- ∴ Zakharenko A.M., Kusaykin M.I., Kovalchuk S.N., Anastyuk S.D., Ly B.M., Sova V.V., Rasskazov V.A., Zvyagintseva T.N. 2011. Enzymatic and molecular characterization of an endo-1,3- β -d-glucanase from the crystalline styles of the mussel *Perna viridis*. *Carbohydrate Research* 346: 243-252.
- ∴ Zhang C., Hu Z., Deng B. 2016. Silver nanoparticles in aquatic environments: Physicochemical behavior and antimicrobial mechanisms. *Water Research* 88: 403-427.

SUPPLEMENTARY MATERIAL

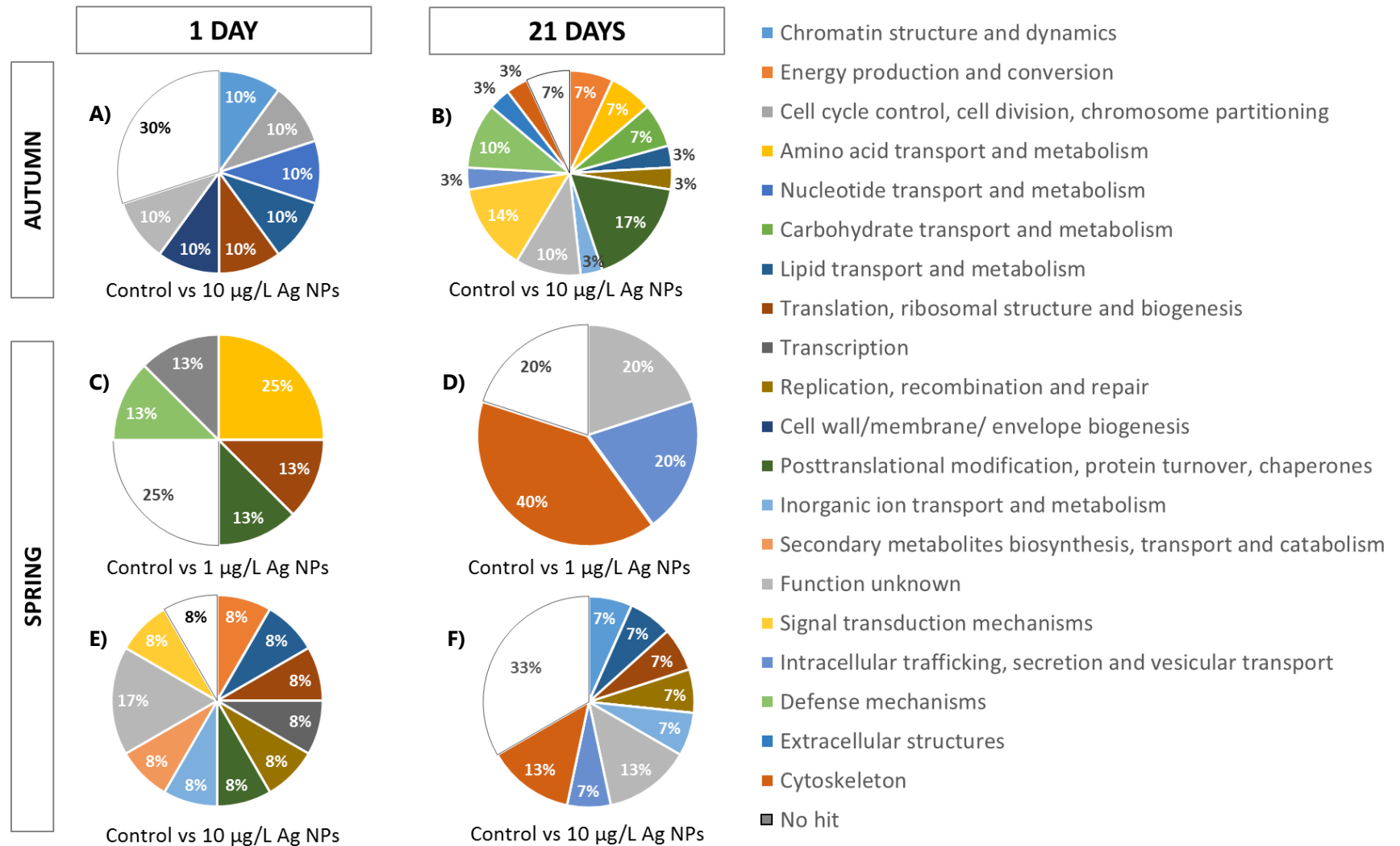


Figure S1. Multilevel pie graphs showing distribution of COG functional categories in which significantly regulated genes were classified after dietary exposure to **A)** 10 µg Ag/L Ag NPs for 1 day in autumn, **B)** 10 µg Ag/L Ag NPs for 21 days in autumn, **C)** 10 µg Ag/L Ag NPs for 1 day in spring, **D)** 10 µg Ag/L Ag NPs for 21 days in spring, **E)** 1 µg Ag/L Ag NPs for 1 day in spring and **F)** 1 µg Ag/L Ag NPs for 21 days in spring.



IV. GENERAL DISCUSSION

Silver NPs (Ag NPs) have gained high commercial and scientific interest due to their unique optical, catalytical and antimicrobial properties (Fabrega et al., 2011; Zhang et al., 2016; McGuillicuddy et al., 2017). Applications for Ag NPs are increasing and the global use and end-of-life of Ag NPs containing products may provoke Ag NPs release into the marine environment via wastewater streams and effluents (António et al., 2015; McGuillicuddy et al., 2017; Magesky and Pelletier, 2018). Predictions based on modelling studies estimated Ag NP concentrations ranging between 0.17 ng/L and 9 µg/L in sewage treatment effluents and 0.002-140 ng/L in surface waters (Blaser et al., 2008; Gottschalk et al., 2009; Tiede et al., 2009; Dumont et al., 2015; Giese et al., 2018). For marine waters, predictions revealed that concentrations of Ag NPs will reach up to 1 pg/L at the highest extremes in 2050 (Giese et al., 2018), but bioturbation and resuspension processes in the sediments could lead to Ag NPs exchange between the sediment and water column, thereby making Ag NPs available to marine organisms (Baker et al., 2014; Rocha et al., 2015a).

Thermodynamically, Ag NPs are unstable in complex physiological or natural environments and tend to transform to other dominant silver species such as AgCl_2^- and Ag^0 under certain conditions (Levard et al., 2012; Zhang et al., 2018). Environmental conditions such as pH, ionic strength and dissolved organic matter play an important role in the final behavior of Ag NPs (Levard et al., 2012; Zhang et al., 2018). Marine waters are saline and high ionic strength media (~700 mM) where intense aggregation and dissolution of Ag NPs takes place (Klaine et al., 2008; Lapresta-Fernández et al., 2012; Levard et al., 2012; Sikder et al., 2017). In fact, small increases in salinity can dramatically decrease colloid concentrations by aggregation and precipitation processes (Klaine et al., 2008). Even if coating agents such as citrate or PVP are used in the synthesis of Ag NPs to prevent or reduce their aggregation and/or dissolution (El Badawy et al., 2010), in the present work PVP/PEI coated 5 nm Ag NPs aggregated and released Ag ions in seawater as already reported in previous studies (Angel et al., 2013; Buffet et al., 2014; Katsumiti et al., 2015a; Odzak et al., 2014; Schiavo et al., 2017; Sikder et al., 2017). In consequence, in the present work *Isochrysis galbana* microalgae were exposed to 94-97 nm aggregates of Ag NPs (>80% of the nominal Ag concentration) and also to dissolved Ag (14-18% of the nominal Ag concentration in 24-48 hours, respectively).

I. galbana is one of the most common marine microalgae species used in aquaculture (Heimann and Huerlimann, 2015). Cells are typically round (3-7.5 µm in diameter), biflagellate and covered with several layers of organic oval scales (Parke, 1949; Bendif et al., 2013). In this work, although it remains unclear whether Ag NPs were internalized in the microalgae or not, Ag was accumulated in microalgae *I. galbana* exposed to PVP/PEI

coated 5 nm Ag NPs for 24 hours. Microalgae cell wall is considered as a potential barrier against NP entry into the cells, only NPs smaller than the diameter of cell wall pores (5-20 nm) being internalized (Navarro et al., 2008; Yue et al., 2017). Thus, in the present work Ag accumulated in microalgae cells could derive partly from dissolved Ag and single Ag particles internalized through the spaces between the oval scales and partly from Ag NP aggregates attached to the microalgae cell surface, as observed by Schiavo et al. (2017).

The uptake and accumulation of ENPs by microalgae could lead to a widespread transfer of ENPs across other trophic levels since microalgae are primary producers that constitute the base of marine aquatic food chains (Matranga and Corsi, 2012; Baker et al., 2014; Moreno-Garrido et al., 2015). In fact, trophic transfer of different metallic NPs has already been reported from marine microalgae to bivalves or brine shrimps (Buffet et al., 2013; Larginho et al., 2014; Bhuvaneshwari et al., 2018) as well as from brine shrimps to marine medaka (Wang and Wang, 2014). Whether internalized or attached to the surface of microalgae, under the present experimental conditions a successful transfer of Ag NPs occurred from microalgae to mussels. Both in autumn and in spring, mussel soft tissues significantly accumulated Ag after 21 days of dietary exposure to 10 μg Ag/L Ag NPs. Although concentrations of accumulated Ag were low, values were in accordance to those usually reported in waterborne exposure studies of bivalves to Ag NPs (Buffet et al., 2013; 2014; Jimeno-Romero et al., 2017a). Higher levels of Ag were significantly accumulated after 21 days of dietary exposure to PVP/PEI coated 5 nm Ag NPs in autumn compared to spring. These differences in metal concentration in mussels can result from changes in the physiology of animals related to the season, rather than from changes in metal exposure conditions (Mubiana et al., 2005), since food ration, salinity and temperature were similar along the experimental period in the two seasons. For instance, the effect of seasonal development of gonadic tissues on whole body weight in bivalves has been shown to biologically dilute the total burden of different metals such as Cu, Zn, Ag, Cd, Cu and Pb, thus resulting in lower concentrations of metals during the gametogenesis period (Regoli and Orlando, 1994; Paéz-Osuna et al., 1995; Fattorini et al., 2008; Lanceleur et al., 2011). In this sense, mussels collected in autumn were in early gametogenic stage whereas those collected in spring were in advanced gametogenic stage, suggesting that the increase of body weight caused by the development of gametes observed in spring could influence the Ag accumulation pattern observed in the present work. For future studies, the use of the metal/shell-weight index could be useful as it avoids variability in metal accumulation due to variations in soft-body weight related to the season (Fischer, 1983; Soto et al., 1995).

In mussels, NPs are trapped by gills which are the first organ in contact to surrounding water vulnerable to particle interactions (Corsi et al., 2014; Rocha et al., 2015a), but digestive gland is considered the main organ for NP accumulation, due to the role of digestive cells in intracellular digestion of food particles (Moore, 2006; Canesi et al., 2012; Rocha et al., 2015a). In accordance, mussels fed for 21 days with microalgae exposed to Ag NPs, accumulated Ag mainly in the digestive gland and gills. The presence of Ag in NP form was confirmed in such tissues by hyperspectral imaging analysis in both seasons. Additionally, autometallographic BSDs were mainly located in gills and digestive gland of mussels dietarily exposed to both doses of Ag NPs, with the highest values of intralysosomal metal accumulation occurring in digestive cells of mussels exposed to 10 µg Ag/L Ag NPs for 21 days in both seasons. At the dose close to environmentally relevant concentrations of 1 µg Ag/L Ag NPs a significant intralysosomal metal accumulation was also observed after 21 days of exposure in spring. The low pH inside lysosomes could enhance the dissolution of Ag NPs, releasing Ag ions that could produce reactive oxygen species (ROS) and provoke damage in lysosomal membranes (Jimeno-Romero et al., 2017a).

In mussels, lysosomal perturbations such as the destabilization of the lysosomal membrane are considered early indicators of adverse effects (Lowe et al., 1995; Cajarville et al., 2000; Moore et al.; 2006). Damage to lysosomal membranes can cause the release of acid hydrolases to the cytosol, possibly leading to a more severe damage and to cell death (Viarengo et al., 2007). Destabilization of the lysosomal membrane has been widely reported in digestive cells of mussels exposed through water to metal-containing NPs such as TiO₂ NPs (Barmo et al., 2013; Balbi et al., 2014; Jimeno-Romero et al., 2016), Au NPs (Jimeno-Romero et al., 2017b), CdS QDs (Jimeno-Romero et al., 2019) as well as Ag NPs (Jimeno-Romero et al., 2017a). In accordance with the reported studies, the dietary exposure of mussels to PVP/PEI coated 5 nm Ag NPs provoked a dose- and time-dependent decrease in lysosomal membrane stability in both seasons that could lead into cytosolic acidification and necrosis of cells (Stern et al., 2012).

The immune system of marine invertebrates represents also an important target for the effects of NPs due to the specialized systems of hemocytes for endocytosis and phagocytosis of particles of different size (Canesi and Corsi, 2016, Manzo et al., 2017). Additionally, NPs can be potentially translocated from the digestive system to the hemolymph and to circulating hemocytes (Canesi and Corsi, 2016). *In vitro* studies in *M. galloprovincialis* mussel hemocytes showed that different types of metal-bearing NPs affected lysosomal function, phagocytic activity, actin cytoskeleton as well as pro-apoptotic processes and induced genotoxicity and oxidative stress (Canesi et al., 2010;

Ciacci et al., 2012; Katsumiti et al., 2014, 2015b, 2018; reviewed in Katsumiti and Cajaraville, 2019). Even if in the present work the phagocytic activity of hemocytes was not significantly affected in mussels dietarily exposed to Ag NPs, immunotoxic effects in terms of reduction of cell viability and increased DNA damage occurred in mussel hemocytes, including at the dose close to environmentally relevant concentrations at all exposure times. Cytotoxic effects measured as a reduction in cell viability are a common response that has been previously observed after *in vitro* exposure of mussel hemocytes to a wide concentration range of different types of metallic NPs (CdS QDs, TiO₂ NPs, Au NPs, ZnO NPs, SiO₂ NPs, CuO NPs) for 24 hours (Katsumiti et al., 2014, 2015a; 2015b, 2016; 2018; reviewed in Katsumiti and Cajaraville, 2019). Additionally, DNA damage has also been observed after the *in vitro* exposure of mussel hemocytes to CdS QDs, Ag NPs or CuO NPs (Katsumiti et al., 2014; 2015b; 2018) and the waterborne exposure of mussels to CuO NPs, Ag NPs or CdTe QDs (Gomes et al., 2013a; Rocha et al., 2014; Ruiz et al., 2015). When levels of DNA strand breaks exceed the repair capacity of dividing cells micronuclei are formed (Luzhna et al., 2013) and chromosomal DNA damage occurs as a result of either chromosome breakage or chromosome mis-segregation during mitosis (Bolognesi and Fenech, 2012). In the present work, the increasing trend in micronuclei frequency observed after 1 and 7 days of dietary exposure to 10 µg Ag/L Ag NPs both in autumn and in spring suggests that the DNA repair capacity was overwhelmed. However, after 21 days of exposure these repair mechanisms could be activated or damaged cells could be eliminated by apoptosis (Luzhna et al., 2013) since a decrease in micronuclei frequencies was measured in both seasons. As previously reported for a number of different NPs, the toxicity of Ag NPs to mussel cells appeared to be driven by their capacity to promote oxidative stress which then could cause genotoxic and cytotoxic damages (reviewed in Katsumiti and Cajaraville, 2019), but direct interaction with DNA could also take place (Singh et al., 2009).

The increase in atretic oocyte prevalences has been linked to the impairment of reproduction ability of female mussels and a possible decrease in gamete quality (Ortiz-Zarragoitia and Cajaraville, 2010; Ortiz-Zarragoitia et al., 2011). Although no differences in prevalence of atretic oocytes occurred among groups after the dietary exposure to Ag NPs, spawning success in females was significantly reduced indicating that the reproduction ability of female mussels at the two doses tested was affected. Further, a significantly higher percentage of abnormal embryos was observed after parental exposure to both doses of Ag NPs that could be related to the quality of eggs since sperm motility and fertilization success were not altered. In fact, eggs released from stressed females can show less lipid and protein content affecting their quality (Bayne et

al., 1978). From an ecotoxicological perspective, data on embryo development is important to address the consequences for the early life stages of the organisms (Balbi et al., 2014). Different studies have assessed the effects on mussels larval development after the exposure of sperm or fertilized eggs to different types of metallic NPs (Kadar et al., 2010; 2013; Libralato et al., 2013; Balbi et al., 2014; Auguste et al., 2018), but to the best of our knowledge, this is the first work reporting the effects on mussel embryos after the exposure of parentals to Ag NPs.

Identifying initial molecular markers that are key factors of direct molecular initiating events is crucial in order to decipher adverse outcome pathways (AOPs). For that, the application of omic tools such as transcriptomics, genomics, proteomics and metabolomics could be helpful (Hook et al., 2014; Vinken et al., 2014; Lee et al., 2015). In this sense, proteomic analysis has been already applied in mussels after the waterborne exposure to different metallic NPs (Gomes et al., 2014a; Hu et al., 2014), including Ag NPs (Gomes et al., 2013b) in order to identify significant alterations in protein expression patterns. However, few studies have focused on the effects of NPs on the transcriptome of mussels (Banni et al., 2016). Moreover, the identification of molecular markers in *Mytilus* spp. is challenging since information on the sequence of their genomes has not been thoroughly investigated yet (Piña and Barata, 2011; Banni et al., 2017; Gomes et al., 2017) even if mussels are widely used in ecotoxicology (Cajaraville et al., 2000; Viarengo et al., 2007; Beyer et al., 2017) and nanotoxicology (Rocha et al., 2015; Canesi and Corsi, 2016).

While the transcriptome gives rise to proteins that contribute to cell or tissue fate, the proteome complement is also influenced by protein turnover, post-translational modifications and protein compartmentalization. Thus, proteome-associated profiling can provide greater insight into the mechanistic nature of responses to chemical contaminant exposure or to other diverse environmental stressors (Veldhoen et al., 2012). In the present work, the integration of both transcriptomic and proteomic approaches revealed that the cytoskeleton can be considered a main target for Ag NP toxicity in mussels at both transcription and protein levels, even after the exposure to a dose close to environmentally relevant concentrations. In agreement, previous proteomic and transcriptomic studies have suggested that reorganization of the cytoskeleton is a general potential mechanism to cope with metallic NPs such as Ag NPs (Gomes et al., 2013b), CuO NPs (Gomes et al., 2014a; Hu et al., 2014) and TiO₂ NPs (Banni et al., 2016). Specifically, alterations in *actin* could be considered as an initial molecular marker for AOPs since as reported in previous studies (Gomes et al., 2014a; Hu et al., 2014), the expression of this protein was significantly altered after 21 days of exposure to 10 µg

Ag/L Ag NPs both in autumn and in spring. The disturbance of structural proteins of cytoskeleton such as actin could affect the endocytic processes as well as the intracellular movement of the endocytic vesicles towards the interior of the cells since actin polymerization plays a key role in those processes (Canton and Battaglia, 2012; Kafshgari et al., 2015). This hypothesis is also supported by the alteration of genes involved in the intracellular trafficking, secretion and vesicular transport after the dietary exposure of mussels to 10 µg/L Ag NPs for 21 days both in autumn and in spring. Transcription changes in genes such as *ras-related Rab-23* and *sorting nexin-1* may probably affect the endolysosomal pathway, which is considered as the major subcellular route for entry and handling of metallic NPs in bivalves (Katsumiti et al., 2014; Rocha et al., 2015; Jimeno-Romero et al., 2019).

The disruption of actin integrity could be mediated by ROS formation (Gomes et al., 2013b; 2014a; Hu et al., 2014). Oxidative stress has been described as one of the major modes of action of engineered metallic NPs, including Ag NPs, in bivalve tissues (reviewed in Baker et al., 2014; Rocha et al., 2015a; Canesi and Corsi, 2016). The antioxidant defense system counteracts the burden of ROS production modulating the activity of enzymes such as superoxide dismutase (SOD), catalase and glutathione peroxidase (Finkel and Holbrook, 2000). For instance, SOD activity increased in the digestive gland of mussels exposed through water to CuO NPs for 15 or 21 days (Gomes et al., 2012; Ruiz et al., 2015), to CdTe quantum dots for 14 days (Rocha et al., 2015b) or to Ag NPs for 15 days (Gomes et al., 2014b) as a response to ROS production. In this work, SOD was underexpressed after dietary exposure of mussels to 10 µg/L Ag NPs for 21 days in spring, suggesting a situation of oxidative stress. This contrasting result in comparison to previous studies could be related to multiple factors such as spatial and temporal regulation of expression of enzymes and posttranslational modifications that regulate enzyme activities (Baruch et al., 2004; Karve and Cheema, 2011).

Enzyme activities as well as protein turnover and localization, protein-protein interactions, modulation of signaling cascades, DNA repair and cell division are influenced by posttranslational modifications related to phosphorylation, hydroxylation and ubiquitination, among others (Karve and Cheema, 2011). Therefore, ubiquitin labeling serves as a degradation signal for numerous target proteins in the proteasome and ubiquitin hydrolases are required to control the degree of modification as well as to regenerate functional ubiquitin molecules (Rose, 1988). In the present work, the *proteasome subunit alpha type-6* and *ubiquitin carboxyl-terminal hydrolase FAF-X* transcripts among others, as well as the *matrix metalloproteinase-19* and *connector enhancer of kinase suppressor of ras 2* proteins were significantly altered, suggesting

that the dietary exposure of mussels to Ag NPs could affect degradation of misfolded or damaged proteins, which could finally lead to alterations in cell protein homeostasis.

Exposure to metals may disturb mussels lipid metabolism, which is reflected as changes in lipid and fatty acid composition (Fokina et al., 2013). In the present work, lipid transport and metabolism appeared altered in both seasons after mussels dietary exposure to 10 µg Ag/L Ag NPs for 1 and 21 days. Previous microarray studies in zebrafish revealed a significant downregulation of transcripts related to lipid transport and localization pathways after zebrafish waterborne and dietary exposure to 10 µg/L of maltose-coated 20 nm Ag NPs and 100 µg/L of PVP/PEI coated 5 nm Ag NPs, respectively (Lacave et al., 2017; 2018). In addition, Lacave et al. (2018) reported that hepatocytes of zebrafish waterborne exposed to Ag NPs showed more glycogen and lipid droplets than unexposed zebrafish. Thus, the significant regulation of transcripts and proteins reported in the present work after the dietary exposure to Ag NPs in both seasons could imply impairment of lipid metabolism at cell or tissue level, especially at the highest concentration of 10 µg Ag/L Ag NPs.

Summarizing, PVP/PEI coated 5 nm Ag NPs were successfully transferred from microalgae to mussels. The dietary exposure provoked Ag accumulation in mussel soft tissues and caused adverse effects at different levels of biological organization, including molecular, cellular and transgenerational effects. All the common results to the two studied seasons have been used to propose an AOP, which is illustrated in Figure 1.

In the environment, due to abiotic factors such as temperature, food availability and oxygen level, as well as biotic factors, as the physiological state, mussels present seasonal variations in biomarker responses including lysosomal parameters, metallothionein levels, antioxidant enzyme activities and DNA damage (Cancio et al., 1999; Orbea et al., 1999; Leiniö and Lehtonen, 2005; Pisanelli et al., 2009; Hagger et al., 2010; Nahrgang et al., 2013; Schmidt et al., 2013; Lekube et al., 2014; González-Fernández et al., 2016; Balbi et al., 2017). Additionally, other confounding factors such as age and gender could influence the response of biomarkers (Hylland et al., 2009; Ji et al., 2016). In the present work, dietary exposure experiments were performed with mussels of same size. Food ration as well as other abiotic parameters were also similar in both seasons. Consequently, similar cellular effects in intralysosomal metal accumulation, lysosomal membrane stability and micronuclei frequency were observed in mussels dietarily exposed to PVP/PEI coated 5 nm Ag NPs both in autumn and in spring. But, when only females were considered, season significantly influenced the responses observed at

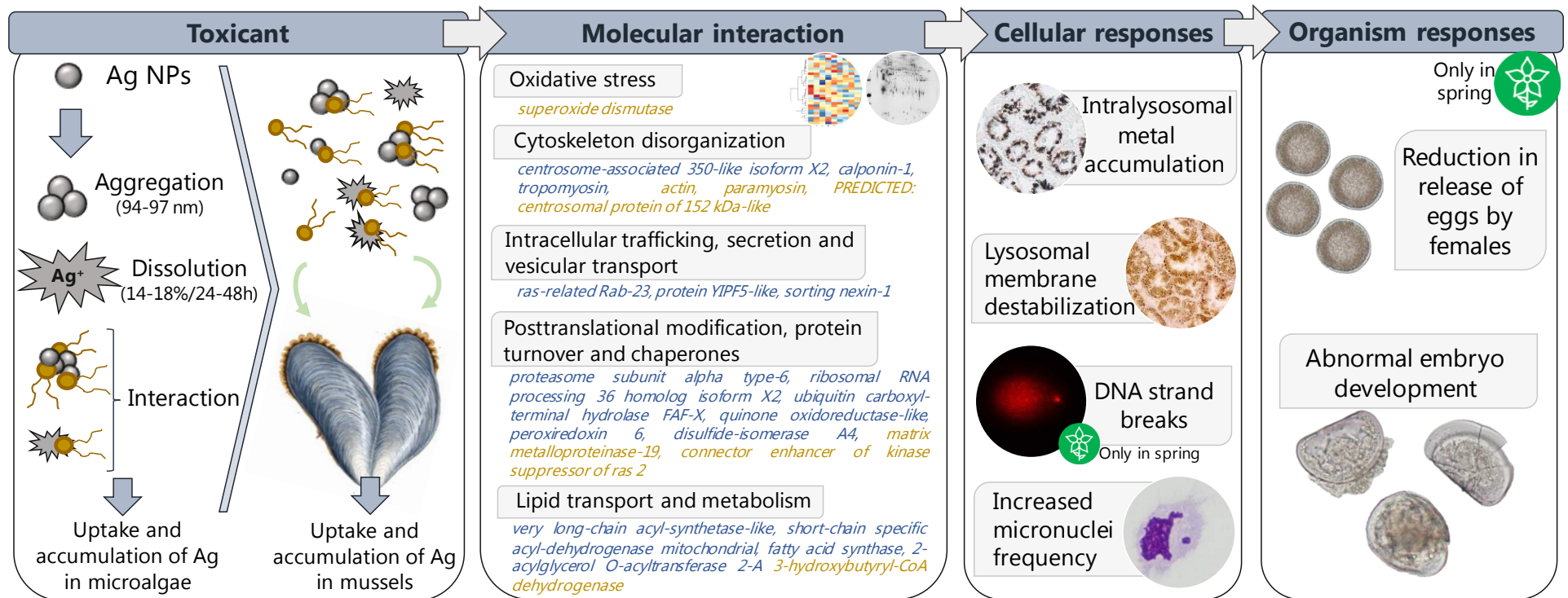


Figure 1. Conceptual diagram of key features of an adverse outcome pathway in mussels after the exposure to Ag NPs through the diet in the two studied seasons. Molecular interactions determined after transcriptomic and proteomic analysis are represented as pathways in which involved genes or proteins are colored in blue or dark yellow, respectively. Even if not directly measured, ROS overproduction could be one of the molecular initiating events after the dietary exposure of mussels to PVP/PEI coated 5 nm Ag NPs aggregates and Ag ions released from Ag NPs. ROS could interact with different components of the cytoskeleton, as observed by transcriptomic and proteomic analysis. Further, the disturbance of the cytoskeleton could affect the endocytic processes at cellular level as well as the movement of the endocytic vesicles and lysosomes. This hypothesis is also supported by the alteration of genes involved in the intracellular trafficking, secretion and vesicular transport. Ag NPs are delivered into lysosomes, where they are accumulated according to intralysosomal metal accumulation results. The low intralysosomal pH could promote the dissolution of Ag NPs, releasing Ag ions that could produce ROS, and finally induce destabilization of lysosomal membranes and DNA strand breaks. Due to the damage in lysosomal membranes Ag NPs and Ag ions could be released into the cytosol, further increasing ROS production and DNA damage, the latter measured in hemocytes. Although tissue level damage was not observed neither in the digestive gland nor in gonads, at organism level spawning success in females was affected and the development of abnormal embryos increased, triggering reproductive impairment that could impact on population fitness of mussels.

transcriptomic and proteomic levels. In an attempt to integrate bioaccumulation data and all the biomarker responses and to assess the relative contribution of season, exposure concentration and exposure time on the overall variability, the average value of each studied endpoint for each experimental group both in autumn and spring was plotted together in a Principal Component Analysis (PCA). Genotoxic effects measured by comet assay as well as endpoints assessed in Chapter 1 were excluded from the analysis because measurements were performed only in spring. The variation explained by the two main components (PC1 and PC2) reached 81.7% (Figure 2). Lysosomal membrane stability (LP) and intralysosomal metal accumulation (VvBSD) were the biomarkers that presented higher weight (0.449 and -0.436, respectively) with the first component (PC1), while the distribution of experimental groups along the second component (PC2) was explained mainly by changes in lysosomal membrane stability (0.211) and bioaccumulation of Ag (-0.650) (Figure 2).

Overall, PC1 discriminated experimental groups according to the exposure time and PC2 according to the exposure concentration of Ag NPs (Figure 2). Control mussels both from autumn and spring, as well as mussels dietarily exposed to 1 µg Ag/L Ag NPs or 10 µg Ag/L Ag NPs in both seasons for 1 day were clustered together, indicating that season and exposure concentration did not influence mussels short-term (1 day) response (Figure 2). Mussels dietarily exposed to 1 µg Ag/L Ag NPs for 7 days in spring were grouped with control mussels from the same exposure time and two studied seasons, suggesting that the dose close to environmentally relevant concentrations was not toxic enough to affect mussels at that exposure time (7 days). However, mussels dietarily exposed to 10 µg Ag/L Ag NPs for 7 days both in autumn and spring were clustered together and separated from the previous cluster, showing a concentration-dependent response independent from season (Figure 2). Similarly, exposure concentration affected to mussels response after 21 days of exposure, since control mussels from both seasons were clustered together but discriminated from mussels dietarily exposed to 1 µg Ag/L Ag NPs in spring or to 10 µg Ag/L Ag NPs both in autumn and in spring. Additionally, mussels exposed dietarily to 10 µg Ag/L Ag NPs in both seasons were not grouped together at this exposure time, suggesting that mussels responded differently depending on the season (Figure 2).

Overall, toxic effects observed in mussels dietarily exposed to Ag NPs depended on exposure time, exposure concentration and season. In long exposure periods (21 days), the response of exposed mussels was different in comparison to non-exposed ones, suggesting that even doses close to environmentally relevant concentrations provoked toxic effects. At the same time, mussels dietarily exposed to 10 µg Ag/L Ag NPs were

discriminated according to the season, revealing that season is a factor that should be considered for assessing the potential effects caused by long-term exposures to engineered NPs in marine bivalves.

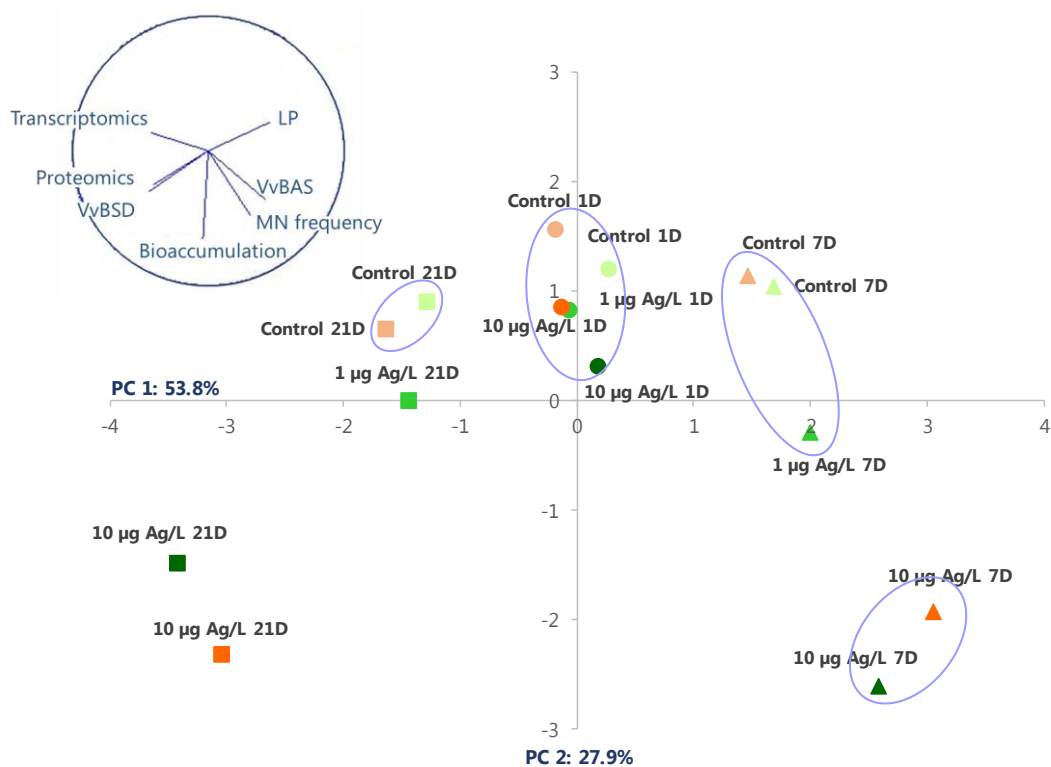


Figure 2. PCA plot based on the bioaccumulation data and biomarker responses of mussels after the dietary exposure to Ag NPs both in autumn and in spring. Variables were standardized and normalized and then plotted based on Euclidean distances using PRIMER-6 software. For transcriptomic and proteomic data, a mean value of the expression of each experimental group was calculated as in Chapter 3. Ellipses cluster different experimental groups based on Euclidean distances. Circles, triangles and squares stand for experimental groups exposed to Ag NPs for 1, 7 and 21 days respectively, both in autumn and in spring. Symbols colored in light orange and dark orange correspond to non-exposed and mussels exposed dietarily to 10 µg Ag/L Ag NPs in autumn, respectively. Symbols colored in green gradient (from light to dark) correspond to non-exposed and mussels exposed dietarily to 1 or 10 µg Ag/L Ag NPs in spring, respectively.

REFERENCES

- ∴ Angel B.M., Batley G.E., Jarolimek C.V., Rogers N.J. 2013. The impact of size on the fate of nanoparticulate silver in aquatic systems. *Chemosphere* 93: 359-365.
- ∴ António D.C., Cascio C., Jakšić Ž., Jurašin D., Lyons D.M., Nogueira A.J., Rossi F., Calzolari L. 2015. Assessing silver nanoparticles behaviour in artificial seawater by mean of AF4 and spICP-MS. *Marine Environmental Research* 111: 162-169.
- ∴ Auguste M., Ciacci C., Balbi T., Brunelli A., Caratto V., Marcomini A., Cuppini R., Canesi L. 2018. Effects of nanosilver on *Mytilus galloprovincialis* hemocytes and early embryo development. *Aquatic Toxicology* 203: 107-116.
- ∴ Baker T.J., Tyler C.R., Galloway T.S. 2014. Impacts of metal and metal oxide nanoparticles on marine organisms. *Environmental Pollution* 186: 257-271.
- ∴ Balbi T., Smerilli A., Fabbri E., Ciacci C., Montagna M., Graselli E., Brunelli A., Pojana G., Marcomini A., Gallo G., Canesi L. 2014. Co-exposure to n-TiO₂ and Cd²⁺ results in interactive effects on biomarker responses but not in increased toxicity in the marine bivalve *M. galloprovincialis*. *Science of the Total Environment* 493: 355-364.
- ∴ Balbi T., Fabbri R., Montagna M., Camisassi G., Canesi L. 2017. Seasonal variability of different biomarkers in mussels (*Mytilus galloprovincialis*) farmed at different sites of the Gulf of La Spezia, Ligurian sea, Italy. *Marine Pollution Bulletin* 116: 348-356.
- ∴ Banni M., Sforzini S., Balbi T., Corsi I., Viarengo A., Canesi L. 2016. Combined effects of n-TiO₂ and 2,3,7,8-TCDD in *Mytilus galloprovincialis* digestive gland: A transcriptomic and immunohistochemical study. *Environmental Research* 145: 135-144.
- ∴ Banni M., Sforzini S., Arlt V.M., Barranguer A., Dallas L.J., Oliveri C., Aminot Y., Pacchioni B., Millino C., Lanfranchi G., Readman J.W., Moore M.N., Viarengo A., Jha A.N. 2017. Assessing the impact of benzo[a]pyrene on marine mussels: application of a novel targeted low density microarray complementing classical biomarker responses. *PLoS ONE* 12 (6): e0178460.
- ∴ Barmo C., Ciacci C., Canonico B., Fabbri R., Cortesec K., Balbi T., Marcomini A., Pojana G., Gallo G., Canesi L. 2013. *In vivo* effects of n-TiO₂ on digestive gland and immune function of the marine bivalve *Mytilus galloprovincialis*. *Aquatic Toxicology* 132-133: 9-18.
- ∴ Baruch A., Jeffery D.A., Bogoy M. 2004. Enzyme activity-it's all about image. *TRENDS in Cell Biology* 14: 29-35.
- ∴ Bayne B., Holland D., Moore M., Lowe D., Widdows, J. 1978. Further studies on the effects of stress in the adult on the eggs of *Mytilus edulis*. *Journal of the Marine Biological Association of the United Kingdom* 58: 825-841.
- ∴ Bendif E.M., Porbert I., Schroeder D.C., Vargas C. 2013. On the description of *Tisochrysis lutea* gen. nov. sp. nov. and *Isochrysis nuda* sp. nov. in the Isochrysidales, and the transfer of *Dicrateria* to the Prymnesiales (Haptophyta). *Journal of Applied Phycology* 25: 1763-1776.
- ∴ Beyer J., Green N.W., Brooks S., Allan I.J., Ruus A., Gomes T., Bråte I.L.N., Schøyen M. 2017. Blue mussels (*Mytilus edulis* spp.) as sentinel organisms in coastal pollution monitoring: A review. *Marine Environmental Research* 130: 338-365.

- ∴ Bhuvaneshwari M., Thiagarajan V., Nemade P., Chandrasekaran N., Mukherjee A. 2018. Toxicity and trophic transfer of P25 TiO₂ NPs from *Dunaliella salina* to *Artemia salina*: Effect of dietary and waterborne exposure. *Environmental Research* 160: 39-46.
- ∴ Bolognesi C., Fenech M. 2012. Mussel micronucleus cytome assay. *Nature Protocols* 7: 1125-1137.
- ∴ Buffet P.E., Pan J.F., Poirier L., Amiard-Triquet C., Amiard J.C., Gaudin P., Risso. De Faverney C., Guibbolini M., Gilliland D., Valsami-Jones E. and Mouneyrac C. 2013. Biochemical and behavioural responses of the endobenthic bivalve *Scrobicularia plana* to silver nanoparticles in seawater and microalgal food. *Ecotoxicology and Environmental Safety* 89: 117-124.
- ∴ Buffet P.E., Zalouk-Vergnoux A., Châtel A., Berthet B., Métais I., Perrein-Ettajani H., Poirier L., Luna-Acosta A., Thomas-Guyon H., Risso-de Faverney C., Guibbolini M., Gilliland D., Valsami-Jones E., Mouneyrac C. 2014. A marine mesocosm study on the environmental fate of silver nanoparticles and toxicity effects on two endobenthic species: The ragworm *Hediste diversicolor* and the bivalve mollusc *Scrobicularia plana*. *Science of the Total Environment* 470-471: 1151-1159.
- ∴ Cajaraville M.P., Bebianno M.J., Blasco J., Porte C., Sarasquete C., Viarengo A. 2000. The use of biomarkers to assess the impact of pollution in coastal environments of the Iberian Peninsula: a practical approach. *Science of the Total Environment* 247: 295-311.
- ∴ Cancio I., Ibabe A., Cajaraville M.P. 1999. Seasonal variation of peroxisomal enzyme activities and peroxisomal structure in mussels *Mytilus galloprovincialis* and its relationship with the lipid content. *Comparative Biochemistry and Physiology, Part C* 123: 135-144.
- ∴ Canesi L., Barmo C., Fabbri R., Ciacci C., Vergani L., Roch P., Gallo G. 2010. *In vitro* effects of suspensions of selected nanoparticles (C60 fullerene, TiO₂, SiO₂) on *Mytilus* hemocytes. *Aquatic Toxicology* 96: 151-158.
- ∴ Canesi L., Ciacci C., Fabbri R., Marcomini A., Pojana G. and Gallo G. 2012. Bivalve molluscs as a unique target group for nanoparticle toxicity. *Marine Environmental Research* 76: 16-21.
- ∴ Canesi L., Corsi I. 2016. Effects of nanomaterials on marine invertebrates. *Science of the Total Environment* 565: 933-940.
- ∴ Canton I., Battaglia G. 2012. Endocytosis at the nanoscale. *Chemical Society Reviews* 41: 2718-2739.
- ∴ Ciacci C., Canonico B., Bilaničovă D., Fabbri R., Cortese K., Gallo G., Marcomini A., Pojana G., Canesi L. 2012. Immunomodulation by different types of N-oxides in the hemocytes of the marine bivalve *Mytilus galloprovincialis*. *PLoS ONE* 7 (5): e36937. doi:10.1371/journal.pone.0036937.
- ∴ Corsi I., Cherr G.N., Lenihan H.S., Labille J., Hasselov M., Canesi L., Dondero F., Frenzilli G., Hristozov D., Punes V., Della Torre C., Pinsino A., Libralato G., Marcomini A., Sabbioni E., Matranga V. 2014. Common Strategies and Technologies for the Ecosafety Assessment and Design of Nanomaterials Entering the Marine Environment. *ACS Nano* 8: 9694-9709.
- ∴ El Badawy A.M., Luxton T.P., Silva R.G., Scheckel K.G., Suidan M.T., Tolaymat T.M. 2010. Impact of environmental condition (pH, ionic strength and electrolyte type) on the surface charge and

- aggregation of silver nanoparticles suspensions. *Environmental Science and Technology* 44: 1260-1266.
- ∴ Fabrega J., Luoma S.N., Tyler C.R., Galloway T.S., Lead J.R. 2011. Silver nanoparticles: behaviour and effects in the aquatic environment. *Environmental International* 37: 517-531.
 - ∴ Fattorini D., Notti A., Di Mento R., Cicero A.M., Gabellini M., Russo A., Regoli F. 2008. Seasonal, spatial and inter-annual variations of trace metals in mussels from the Adriatic sea: a regional gradient for arsenic and implications for monitoring the impact of off-shore activities. *Chemosphere* 72: 1524-1533.
 - ∴ Finkel T., Holbrook N.J. 2000. Oxidants, oxidative stress and the biology of ageing. *Nature* 408: 239-247.
 - ∴ Fischer H. 1983. Shell weight as an independent variable in relation to cadmium content of molluscs. *Marine Ecology Progress Series* 12: 59-75.
 - ∴ Fokina N.N., Ruokolainen T.R., Nemova N.N., Bakhmet I.N. 2013. Changes of blue mussels *Mytilus edulis* L. lipid composition under cadmium and copper toxic effect. *Biological Trace Element Research* 154: 217-225.
 - ∴ Gomes T., Araújo O., Pereira R., Almeida A.C., Cravo A., Bebianno M.J. 2013a. Genotoxicity of copper oxide and silver nanoparticles in the mussel *Mytilus galloprovincialis*. *Marine Environmental Research* 84: 51-59.
 - ∴ Gomes T., Pereira C.G., Cardoso C., Bebianno M.J. 2013b. Differential protein expression in mussels *Mytilus galloprovincialis* exposed to nano and ionic Ag. *Aquatic Toxicology* 136-137: 79-90.
 - ∴ Gomes T., Chora S., Pereira C.G., Cardoso C., Bebianno M.J. 2014a. Proteomic response of mussels *Mytilus galloprovincialis* exposed to CuO NPs and Cu²⁺: An exploratory biomarker discovery. *Aquatic Toxicology* 155: 327-336.
 - ∴ Gomes T., Pereira C.G., Cardoso C., Sousa V.S., Ribau Teixeira M., Pinheiro J.P., Bebianno M.J. 2014b. Effects of silver nanoparticles exposure in the mussel *Mytilus galloprovincialis*. *Marine Environmental Research* 101: 208-214.
 - ∴ Gomes T., Albergamo A., Costa R., Mondello L., Dugo G. 2017. Potential use of proteomics in shellfish aquaculture: from assessment of environmental toxicity to evaluation of seafood quality and safety. *Current Organic Chemistry* 21: 1-24.
 - ∴ González-Fernández C., Albentosa M., Campillo J.A., Viñas L., Franco A., Beiras J. 2016. Effect of mussel reproductive status on biomarker responses to PAHs: Implications for large-scale monitoring programs. *Aquatic Toxicology* 177: 380-394.
 - ∴ Hagger J.A., Lowe D., Dissanayake A., Jones M.B. 2010. The influence of seasonality on biomarker responses in *Mytilus edulis*. *Ecotoxicology* 19: 953-962.
 - ∴ Heimann K., Huerlimann R. 2015. Microalgal classification: major classes and genera of commercial microalgal species. In: Kim S.K. (Ed.) *Handbook of Marine Microalgae: Biotechnology Advances*. Academic Press, London, UK, pp. 25-41.
 - ∴ Hook S.E., Gallagher E.P., Batley G.E. 2014. The role of biomarkers in the assessment of aquatic ecosystem health. *Integrated Environmental Assessment and Management* 10: 327-341.

- ∴ Hu W., Culloty S., Darmody G., Lynch S., Davenport J., Ramirez-Garcia S., Dawson K.A., Lynch I., Blasco J., Sheehan D. 2014. Toxicity of copper oxide nanoparticles in the blue mussel, *Mytilus edulis*: a redox proteomic investigation. *Chemosphere* 108: 289-299.
- ∴ Hylland K., Ruus A., Grung M., Green N. 2009. Relationships between physiology, tissue contaminants, and biomarker responses in Atlantic cod (*Gadus morhua* L.). *Journal of Toxicology and Environmental Health, A* 72: 226-233.
- ∴ Ji C., Li F., Wang Q., Zhao J., Sun Z., Wu H. 2016. An integrated proteomic and metabolomics study on the gender specific responses of mussels *Mytilus galloprovincialis* to tetrabromobisphenol A (TBBPA). *Chemosphere* 144: 527-539.
- ∴ Jimeno-Romero A., Oron M., Cajaraville M.P., Soto M., Marigómez I. 2016. Nanoparticle size and combined toxicity of TiO₂ and DSLS (surfactant) contribute to lysosomal responses in digestive cells of mussels exposed to TiO₂ nanoparticles. *Nanotoxicology* 10: 1168-1176.
- ∴ Jimeno-Romero A., Bilbao E., Izagirre U., Cajaraville M.P., Marigómez I., Soto M. 2017a. Digestive cell lysosomes as main targets for Ag accumulation and toxicity in marine mussels, *Mytilus galloprovincialis*, exposed to maltose-stabilized Ag nanoparticles of different sizes. *Nanotoxicology* 11: 168-183.
- ∴ Jimeno-Romero A., Izagirre U., Gilliland D., Warley A., Cajaraville M.P., Marigómez I., Soto M. 2017b. Lysosomal responses to different gold forms (nanoparticles, aqueous, bulk) in mussel digestive cells: a trade-off between the toxicity of the capping agent and form, size and exposure concentration. *Nanotoxicology* 11: 658-670.
- ∴ Jimeno-Romero A., Bilbao E., Valsami-Jones E., Cajaraville M.P., Soto M., Marigómez I. 2019. Bioaccumulation, tissue and cell distribution, biomarkers and toxicopathic effects of CdS quantum dots in mussels, *Mytilus galloprovincialis*. *Ecotoxicology and Environmental Safety* 167: 288-300.
- ∴ Kadar E., Lowe D.M., Solé M., Fisher A.S., Jha A., Readman J.W., Hutchinson T.H. 2010. Uptake and biological responses to nano-Fe versus soluble Fe-Cl₃ in excised mussel gills. *Analytical and Bioanalytical Chemistry* 396: 657-666.
- ∴ Kadar E., Dyson O., Handy R.D., Al-Subiai S.N. 2013. Are reproduction impairments of free spawning marine invertebrates exposed to zero-valent nano-iron associated with dissolution of nanoparticles? *Nanotoxicology* 7: 135-143.
- ∴ Kafshgari M.H., Harding F.J., Voelcker N.H. 2015. Insights into cellular uptake of nanoparticles. *Current Drug Delivery* 12: 63-77.
- ∴ Karve T.M., Cheema A.V. 2011. Small changes huge impact: the role of protein posttranslational modifications in cellular homeostasis and disease. *Journal of Amino Acids* 2011: doi:10.4061/2011/207691.
- ∴ Katsumiti A., Gilliland D., Arostegui I., Cajaraville M.P. 2014. Cytotoxicity and cellular mechanisms involved in the toxicity of CdS quantum dots in hemocytes and gill cells of the mussel *Mytilus galloprovincialis*. *Aquatic Toxicology* 153: 39-52.
- ∴ Katsumiti A., Gilliland D., Arostegui I., Cajaraville M.P. 2015a. Mechanisms of toxicity of Ag nanoparticles in comparison to bulk and ionic Ag on mussel hemocytes and gill cells. *PLoS ONE* 10 (6): e0129039. doi:10.1371/journal.pone.0129039

- ∴ Katsumiti A., Berhanu D., Howard K.T., Arostegui I., Oron M., Reip P., Valsami-Jones E., Cajaraville M.P. 2015b. Cytotoxicity of TiO₂ nanoparticles to mussel hemocytes and gill cells *in vitro*: influence of synthesis method, crystalline structure, size and additive. *Nanotoxicology* 9: 543-553.
- ∴ Katsumiti A., Arostegui I., Oron M., Gilliland D., Valsami-Jones E., Cajaraville M.P. 2016. Cytotoxicity of Au, ZnO and SiO₂ NPs using *in vitro* assays with mussels hemocytes and gill cells: Relevance of size, shape and additives. *Nanotoxicology* 10: 185-193.
- ∴ Katsumiti A., Thorley A.J., Arostegui I., Reip P., Valsami-Jones E., Tetley T.D., Cajaraville M.P. 2018. Cytotoxicity and cellular mechanisms of toxicity of CuO NPs in mussel cells *in vitro* and comparative sensitivity with human cells. *Toxicology In Vitro* 48: 146-158.
- ∴ Katsumiti A., Cajaraville M.P. 2019. *In vitro* toxicity testing with bivalve molluscs and fish cells for the risk assessment of nanoparticles in the aquatic environment. In: Corsi I., Blasco J. (Eds.) *Ecotoxicology of nanoparticles in aquatic systems*. CRC Press Taylor & Francis Group. pp. 62-98.
- ∴ Klaine J.K., Alvarez P.J.J., Batley G.E., Fernandes T.F., Handy R.D., Lyon D.Y., Mahendra S., McLaughlin M.J., Lead, J.R. 2008. Nanomaterials in the environment: behaviour, fate, bioavailability and effects. *Environmental Toxicology and Chemistry* 27: 1825-1851.
- ∴ Lacave J.M., Fanjul A., Bilbao E., Gutierrez N., Barrio I., Arostegui I., Cajaraville M.P., Orbea A. 2017. Acute toxicity, bioaccumulation and effects of dietary transfer of silver from brine shrimp exposed to PVP/PEI coated silver nanoparticles to zebrafish. *Comparative Biochemistry and Physiology, Part C* 199: 69-80.
- ∴ Lacave J.M., Vicario-Parés U., Bilbao E., Gilliland D., Mura F., Dini L., Cajaraville M.P., Orbea A. 2018. Waterborne exposure of adult zebrafish to silver nanoparticles and to ionic silver results in differential silver accumulation and effects at cellular and molecular levels. *Science of the Total Environment* 642: 1209-1220.
- ∴ Lancelleur L., Schäfer J., Chiffolleau J.F., Blanc G., Auger D., Renault S., Baudrimont M., Audry S. 2011. Long-term records of cadmium and silver contamination in sediments and oysters from the Gironde fluvial-estuarine continuum-Evidence of changing silver sources. *Chemosphere* 85: 1299-1305.
- ∴ Lapresta-Fernández A., Fernández A., Blasco J. 2012. Nanoecotoxicity effects of engineered silver and gold nanoparticles in aquatic organisms. *Trends in Analytical Chemistry* 32: 40-59.
- ∴ Larginho M., Correia D., Diniz M.S., Baptista P.V. 2014. Evidence of one-way flow bioaccumulation of gold nanoparticles across two trophic levels. *Journal of Nanoparticle Research* 16: 2549-2560.
- ∴ Lee J.W., Won E.J., Raisuddin S., Lee J.S. 2015. Significance of adverse outcome pathways in biomarker-based environmental risk assessment in aquatic organisms. *Journal of Environmental Science* 35: 115-127.
- ∴ Leiniö S., Lehntonen K. 2005. Seasonal variability in biomarkers in the bivalves *Mytilus edulis* and *Macoma balthica* from the northern Baltic Sea. *Comparative Biochemistry and Physiology, Part C* 140: 408-421.

- .: Lekube X., Izagirre U., Soto M., Marigómez I. 2014. Lysosomal and tissue-level biomarkers in mussels cross-transplanted among four estuaries with different pollution levels. *Science of the Total Environment* 472: 36-48.
- .: Levard C., Hotze E.M., Lowry G.V., Brown Jr. G.E. 2012. Environmental transformations of silver nanoparticles: impact on stability and toxicity. *Environmental Science and Technology* 46: 6900-69
- .: Libralato G., Minetto D., Totaro S., Micetic I., Pigozzo A., Sabbioni E., Marcomini A., Ghirardini A.V. 2013. Embryotoxicity of TiO₂ nanoparticles to *Mytilus galloprovincialis* (Lmk). *Marine Environmental Research* 92: 71-78.
- .: Lowe D.M., Soverchia C., Moore M.N. 1995. Lysosomal membrane responses in the blood and digestive cells of mussels experimentally exposed to fluoranthene. *Aquatic Toxicology* 33: 105-112.
- .: Luzhna L., Kathiria P., Kovalchuk O. 2013. Micronuclei in genotoxicity assessment: from genetics to epigenetics and beyond. *Frontiers in Genetics* 4: 131-147.
- .: Magesky A., Pelletier E. 2018. Cytotoxicity and physiological effects of silver nanoparticles on marine invertebrates, In: Saquib Q., Faisal M., Al-Khedhairi A.A., Alatar A.A. (Eds.), *Cellular and Molecular Toxicology of Nanoparticles*. Springer International Publishing, pp. 285-309.
- .: Manzo S., Schiavo S., Oliviero M., Toscano A., Ciaravolo M., Cirino P. 2017. Immune and reproductive system impairment in adult sea urchin exposed to nanosized ZnO via food. *Science of the Total Environment* 599-600: 9-13.
- .: Matranga V., Corsi I. 2012. Toxic effects of engineered nanoparticles in the marine environment: Model organisms and molecular approaches. *Marine Environmental Research* 76: 32-40.
- .: McGuillicuddy E., Murray I., Kavanagh S., Morrison L., Fogarty A., Cormican M., Dockery P., Prendergast M., Rowan N., Morris D. 2017. Silver nanoparticles in the environment: sources, detection and ecotoxicology. *Science of the Total Environment* 575: 231-246.
- .: Moore M.N. 2006. Do nanoparticles present ecotoxicological risks for the health of the aquatic environment? *Environment International* 32: 967-976.
- .: Moore M.N., Allen J.I., McVeigh A. 2006. Environmental prognostics: An integrated model supporting lysosomal stress responses as predictive biomarkers of animal health status. *Marine Environmental Research* 61: 278-304.
- .: Moreno-Garrido I., Pérez S., Blasco J. 2015. Toxicity of silver and gold nanoparticles on marine microalgae. *Marine Environmental Research* 111: 60-73.
- .: Mubiana V.K., Qadah D., Meys J., Blust R. 2005. Temporal and spatial trends in heavy metal concentrations in the marine mussel *Mytilus edulis* from the Western Scheldt estuary (The Netherlands). *Hydrobiologia* 540: 169-180.
- .: Nahrgang J., Brooks S.J., Evenset A., Camus L., Jonsson M., Smith T.J., Lukina J., Frantzen M., Giarratano E., Renaud P.E. 2013. Seasonal variation in biomarkers in blue mussel (*Mytilus edulis*), Icelandic scallop (*Chlamys islandica*) and Atlantic cod (*Gadus morhua*): implications for environmental monitoring in the Barents Sea. *Aquatic Toxicology* 127: 21-35.

- .: Navarro E., Baun A., Behra R., Hartmann N.B., Filser J., Miao A.J., Quigg A., Santschi P.H., Sigg L. 2008. Environmental behavior and ecotoxicity of engineered nanoparticles to algae, plants, and fungi. *Ecotoxicology* 17: 372-386.
- .: Odzak N., Kistler D., Behra R., Sigg L. 2014. Dissolution of metal and metal oxide nanoparticles in aqueous media. *Environmental Pollution* 191: 132-138.
- .: Orbea A., Marigómez I., Fernández C., Tarazona J.V., Cancio I., Cajaraville M.P. 1999. Structure of peroxisomes and activity of the marker enzyme catalase in digestive epithelial cells in relation to PAH content of mussels from two Basque estuaries (Bay of Biscay): seasonal and site-specific variations. *Archives of Environmental Contamination and Toxicology* 36: 158-166.
- .: Ortiz-Zarragoitia M., Cajaraville M.P. 2010. Intersex and oocyte atresia in a mussel population from the Biosphere's Reserve of Urdaibai (Bay of Biscay). *Ecotoxicology and Environmental Safety* 73: 693-701.
- .: Ortiz-Zarragoitia M., Garmendia L., Barbero M.C., Serrano T., Marigómez I., Cajaraville M.P. 2011. Effects of the fuel oil spilled by the *Prestige* tanker on reproduction parameters of wild mussel populations. *Journal of Environmental Monitoring* 13: 84-94.
- .: Páez-Osuna F., Frías-Espéricueta M.G., Osuna-López J.I. 1995. Trace metal concentrations in relation to season and gonadal maturation in the oyster *Crassostrea iridescens*. *Marine Environmental Research* 40: 19-31.
- .: Parke M. 1949. Studies on marine flagellates. *Journal of the Marine Biological Association UK* 28: 255-288.
- .: Piña B., Barata C. 2011. A genomic and ecotoxicological perspective of DNA array studies in aquatic environmental risk assessment. *Aquatic Toxicology* 105S: 40-49.
- .: Pisanelli B., Benedetti M., Fattorini D., Regoli F. 2009. Seasonal and inter-annual variability of DNA integrity in mussels *Mytilus galloprovincialis*: a possible role for natural fluctuations of trace metal concentrations and oxidative biomarkers. *Chemosphere* 77: 1551-1557.
- .: Regoli F., Orlando E. 1994. Seasonal variation of trace metal concentrations in the digestive gland of the mediterranean mussel *Mytilus galloprovincialis*: Comparison between a polluted and a non-polluted site. *Archives of Environmental Contamination and Toxicology* 27: 36-43.
- .: Rocha T.L., Gomes T., Cardoso C., Letendre J., Pinheiro J.P., Sousa V.S., Teixeira M.R., Bebianno M.J. 2014. Immunocytotoxicity, cytogenotoxicity and genotoxicity of cadmium-based quantum dots in the marine mussel *Mytilus galloprovincialis*. *Marine Environmental Research* 101: 29-37.
- .: Rocha T.L., Gomes T., Sousa V.S., Mestre N.C., Bebianno M.J. 2015a. Ecotoxicological impact of engineered nanomaterials in bivalve molluscs: An overview. *Marine Environmental Research* 111: 74-88.
- .: Rocha T.L., Gomes T., Mestre N.C., Cardoso C., Bebianno M.J. 2015b. Tissue specific responses to cadmium-based quantum dots in the marine mussel *Mytilus galloprovincialis*. *Aquatic Toxicology* 69: 10-18.
- .: Ruiz P., Katsumiti A., Nieto J.A., Bori J., Reip P., Orbea A., Cajaraville M.P. 2015. Short-term effects on antioxidant enzymes and long-term genotoxic and carcinogenic potential of CuO nanoparticles in mussels. *Marine Environmental Research* 111: 107-120.

- ∴ Schiavo S., Duroudier N., Bilbao E., Mikolaczyk M., Schäfer J., Cajaraville M.P., Manzo S. 2017. Effects of PVP/PEI coated and uncoated silver NPs and PVP/PEI coating agent on three species of marine microalgae. *Science of the Total Environment* 577: 45-53.
- ∴ Schmidt W., Power E., Quinn B. 2013. Seasonal variations of biomarker responses in the marine blue mussel (*Mytilus* spp.). *Marine Pollution Bulletin* 74: 50-55.
- ∴ Sikder M., Lead J.R., Chandler G.T., Baalousha M. 2017. A rapid approach for measuring silver nanoparticle concentration and dissolution in seawater by UV-Vis. *Science of the Total Environment* 618: 597-607.
- ∴ Singh N., Manshian B., Jenkins G.J., Griffiths S.M., Williams P.M., Maffei T.G., Wright C.J., Doak S.H. 2009. NanoGenotoxicology: the DNA damaging potential of engineered nanomaterials. *Biomaterials* 30: 3891-3914.
- ∴ Soto M., Kortabitarte M., Marigómez I. 1995. Bioavailable heavy metals in estuarine waters as assessed by metal/shell-weight indices in sentinel mussels *Mytilus galloprovincialis*. *Marine Ecology Progress Series* 125: 127-136.
- ∴ Stern S., Adiseshaiah P., Crist R. 2012. Autophagy and lysosomal dysfunction as emerging mechanisms of nanomaterial toxicity. *Particle and Fibre Toxicology* 9: 20-35.
- ∴ Veldhoen N., Ikonomou M.G., Hlebing C.C. 2012. Molecular profiling of marine fauna: Integration of omics with environmental assessment of the world's oceans. *Ecotoxicology and Environmental Safety* 76: 23-38.
- ∴ Viarengo A., Lowe D., Bolognesi C., Fabbri E., Koehler A. 2007. The use of biomarkers in biomonitoring: a 2-tier approach assessing the level of pollutant-induced stress syndrome in sentinel organisms. *Comparative Biochemistry and Physiology, Part C* 146: 281-300.
- ∴ Vinken M., Whelan M., Rogiers V. 2014. Adverse outcome pathways: hype or hope? *Archives of Toxicology* 88: 1-2.
- ∴ Wang J., Wang W.X. 2014. Low bioavailability of silver nanoparticles presents trophic toxicity to marine medaka (*Orzias melastigma*). *Environmental Science of Technology* 48: 8152-8161.
- ∴ Yue Y., Li X., Sigg L., Suter M.J.F., Pillai S., Behra R., Schirmer K. 2017. Interaction of silver nanoparticles with algae and fish cells: a side-by-side comparison. *Journal of Nanobiotechnology* 15: 16-26.
- ∴ Zhang C., Hu Z., Deng B. 2016. Silver nanoparticles in aquatic environments: physicochemical behavior and antimicrobial mechanisms. *Water Research* 88: 403-427.
- ∴ Zhang W., Xiao B., Fang T. 2018. Chemical transformation of silver nanoparticles in aquatic environments: mechanism, morphology and toxicity. *Chemosphere* 191: 324-334.



V. CONCLUSIONS AND THESIS

CONCLUSIONS

- I. PVP/PEI coated 5 nm Ag NPs aggregated and released Ag ions both in seawater and in Basal Medium Eagle culture media. As a consequence, mussel hemocytes *in vitro* and microalgae were exposed to mainly 94-97 nm aggregates of Ag NPs and also to ~14-18% dissolved Ag.
- II. Ag was significantly accumulated in microalgae exposed for 24 hours to a dose close to environmentally relevant concentrations of 1 µg Ag /L Ag NPs and to 10 µg Ag /L Ag NPs. Whether internalized or attached to the surface of microalgae, accumulated Ag was successfully transferred to mussels exposed for 21 days to contaminated algae both in autumn and in spring. Although higher levels of Ag were accumulated in autumn in comparison to spring, intralysosomal metal accumulation in digestive cells in comparison to controls was similar in both seasons. Ag accumulation was highest in the digestive gland and gills, where Ag NPs were mainly detected in the epithelium of digestive tubules and in their lumen.
- III. Although no changes occurred in mussel growth and prevalence of atretic oocytes in females after the dietary exposure to Ag NPs, spawning success was significantly reduced indicating that their reproduction ability was affected at the two studied doses. Sperm motility and fertilization success were not altered, but a significantly higher percentage of abnormal embryos was observed after parental dietary exposure to both doses of Ag NPs, suggesting that low doses of Ag NPs in aquatic environments could have an impact on the health of individuals as well as on population fitness of mussels and other sensitive organisms.
- IV. PVP/PEI coated 5 nm Ag NPs were cytotoxic to mussel hemocytes exposed *in vitro*, whereas hemocytes phagocytic activity was slightly reduced after *in vivo* dietary exposure of mussels. Ag NPs ingested through the diet caused genotoxic effects by increasing DNA strand breaks in mussel hemocytes even at the dose close to environmentally relevant concentrations. On the other hand, the increase in micronuclei frequency was transitory in both seasons, suggesting the activation of DNA repair mechanisms.
- V. The dietary exposure of mussels to PVP/PEI coated 5 nm Ag NPs caused significant cellular responses in mussels which were comparable to those reported in waterborne exposure studies to Ag NPs. Lysosomal membrane stability decreased in a dose- and time-dependent manner showing a general

stress response in mussels, even if cell type composition of the digestive tubules was not altered. Similar effects were observed in mussels both in autumn and in spring, suggesting that selected cell and tissue biomarkers are stable enough to be applied in sentinel mussels at different seasons.

- VI. Dietary exposure to PVP/PEI coated 5 nm Ag NPs significantly altered the proteome of digestive gland in female mussels both in autumn and in spring. Treatment- and season-dependent protein signatures were found. In both seasons, common metabolic pathways such as amino sugar and nucleotide sugar metabolism, carbon metabolism, glycolysis/gluconeogenesis and the biosynthesis of amino acids associated to the differential expression of *chitinase like protein-3*, *partial* and *glyceraldehyde-3-phosphate dehydrogenase* were altered. The specific protein expression profile observed for each season showed that the dietary exposure to Ag NPs in autumn altered proteins related to the pyruvate metabolism, citrate cycle, cysteine and methionine metabolism and glyoxylate and dicarboxylate metabolism, while in spring proteins involved in the formation of phagosomes and hydrogen peroxide metabolism of peroxisomes were differentially expressed. Other affected processes were the transcriptional regulation (*nuclear receptor subfamily 1DEF*) in autumn, the immune response (*putative C1q domain containing protein MgC1q52*) in spring and the organization of the cytoskeleton (*actin* and *paramyosin*) in both seasons.
- VII. Transcription profile of the digestive gland in female mussels was significantly altered after the dietary exposure to PVP/PEI coated 5 nm Ag NPs both in autumn and in spring, being season and exposure time the main factors explaining observed transcription patterns. Overall, a higher number of probes was significantly regulated after 21 days of dietary exposure to Ag NPs in autumn compared to spring, probably related to the higher accumulation of Ag in mussels soft tissues in autumn. Transcripts involved in biological processes related to *carbohydrate transport and metabolism* were significantly regulated only in autumn and *signal transduction* mechanisms were more affected in autumn than in spring. Transcripts altered in both seasons affected general cell processes including *cytoskeleton, intracellular trafficking, secretion and vesicular transport; inorganic ion transport and metabolism; lipid transport and metabolism; translation, ribosomal structure and biogenesis* and *posttranslational modification, protein turnover and chaperones*, among others. The dietary exposure of mussels to 1 µg Ag /L Ag NPs altered a lower number of transcripts compared to 10 µg Ag /L Ag NPs but affected similar pathways.

- VIII. Overall, taking into account all the different responses measured at different levels of biological organization both in autumn and in spring, toxic effects observed in mussels depended on the exposure time, exposure concentration and season. For future studies, season should be considered when assessing the potential effects caused by engineered NPs in marine bivalves, especially in females at gene and protein expression levels.

THESIS

Dietary exposure of *Mytilus galloprovincialis* mussels to Ag nanoparticles caused significant accumulation of Ag and deleterious effects at different levels of biological organization including molecular, cellular and transgenerational effects, even at a dose close to environmentally relevant concentrations. Effects at the molecular level such as changes in transcriptome and proteome of female mussels are modulated depending on the season.



VI. APPENDIX



CERTIFICATE OF ANALYSIS

NGAP NP Ag-2106-W Silver nanoparticles

Chemist: Noelia Durán

Product: Aqueous dispersion of silver nanoparticles stabilized with PEI and PVP.

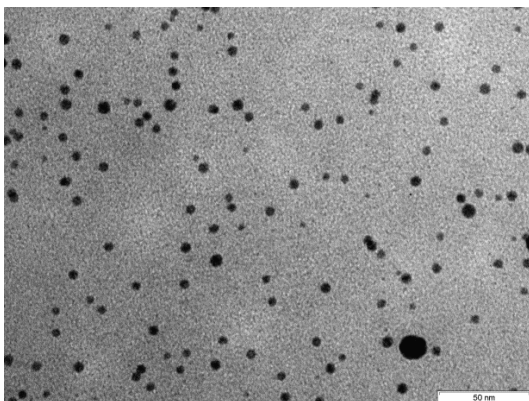
Batch: 08.02.11

Date: 19.04.2013

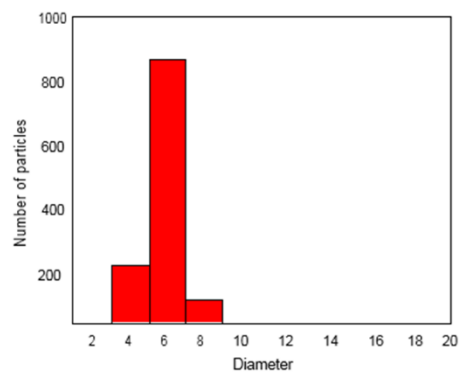
2106-W	Size distribution 4,9 ± 1,4 nm	Product Form Aqueous solution	Concentration 10 g/L Ag	Colour Black, Yellow (when diluted)
	Volume 1L	Density 1,031 g/ml	Density of particles ≈ 8,7·10 ¹⁸ part/l	Storage At room temperature

Characterization:

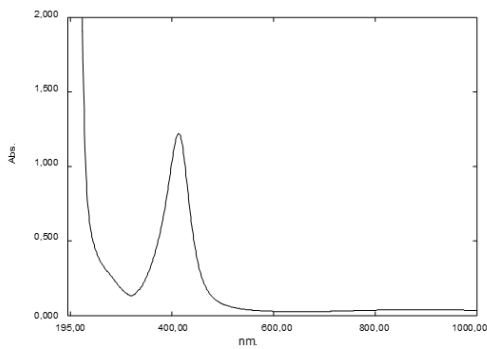
TEM



Size distribution



UV-Visible



PROTOCOLS

∴ CHAPTER 1.

- Phagocytic activity
- Histology
- Autometallography
- Spawning and embryo development

∴ CHAPTER 2.

- Lysosomal membrane stability
- Micronuclei test
- Comet assay

∴ CHAPTER 3.

- Proteomic analysis
 1. Cell-free extract preparation
 2. Protein quantification
 3. Isoelectric Focusing
 4. Second dimension SDS-PAGE
 5. Silver staining of gels

∴ CHAPTER 4.

- ∴ Transcriptomic analysis
 1. RNA extraction
 2. DNase digestion of RNA
 3. RNA cleanup and concentration
 4. RNA quality assessment
 5. First-strand cDNA synthesis

PHAGOCYTTIC ACTIVITY

∴ EQUIPMENT AND REAGENTS

Equipment

- Micropipette set and tips
- Microscope slides
- Falcon-type tubes (VWR 21008-178)
- 96-well microplates (Sarstedt Ref. 82.1581.001)
- V bottom 96-wells microplate (Sarstedt Ref. 82.1583)

Reagents

- $\text{Na}_2\text{HPO}_4 \cdot 12\text{H}_2\text{O}$ (Panreac 131678)
- KH_2PO_4 (Sigma-Aldrich P5379)
- KCl (Sigma-Aldrich P3911)
- NaCl (Scharlau SO02271000)
- TRIS Buffer Solution (TBS) 50mM NaCl 2.5% pH 7.6
- 1% (w/v) Neutral Red (Sigma-Aldrich N7005)
- 1.8% (w/v) Phosphomolybdic acid hydrate (VWR Pbi International 1.00532.0100)
- 6% (w/v) Ammonium heptamolybdate (Fluka 09880)
- Zymosan A (Sigma Aldrich Z4250)
- Baker's Formol Solution (formaldehyde 4% (v/v), NaCl 2% (w/v), calcium acetate 1% (w/v))
- Glycerol (Sigma-Aldrich G9012)
- Artificial seawater (ASW)

∴ PROCEDURE

a. Preparation of solutions

▪ Phosphate buffered saline (PBS)

- $\text{Na}_2\text{HPO}_4 \cdot 12\text{H}_2\text{O}$ 2.037 g
- KH_2PO_4 200 mg
- KCl..... 200 mg
- NaCl..... 32 g
- dH_2O complete to 1L

▪ Extraction solution

- Acetic acid..... 1 mL
- 50% ethanol..... complete to 100 mL

b. Staining of zymosan particles with neutral red solution

1. Mix 15 mg of zymosan particles with 10-15 mL of distilled water and stir well.
2. Centrifuge at 1000 rpm for 5 minutes and resuspend the pellet in PBS
3. Centrifuge at 1000 rpm for 5 minutes and resuspend the pellet in 1% aqueous neutral red solution.
4. Heat fix by boiling the suspension for 1 hour.
5. After cooling, centrifuge at 1000 rpm and resuspend the pellet in PBS (repeat this step several times to eliminate remaining neutral red).
6. Resuspend the pellet in 1.8% phosphomolybdic acid for 30 minutes at 4°C.
7. Centrifuge and wash in distilled water.
8. Centrifuge and resuspend in 6% ammonium heptamolybdate for 1 hour at 4°C.
9. Centrifuge and wash in distilled water.
10. Centrifuge and resuspend in PBS to give a final concentration of 10^7 zymosan particles/mL and store at -20°C.

*Note: in order to avoid clumps of zymosan particles, it is very important to stir the zymosan suspension gently at all steps after centrifugation.

c. Evaluation of phagocytosis

1. Add 100 μ L of hemolymph in each well (8 wells per mussel).
2. Allow the attachment of hemocytes to the well for 30 minutes.
3. Remove the excess of hemolymph.
4. Pre fix some wells with methanol for 20 minutes as blanks.
5. Incubate cells with 50 μ L zymosan stained with neutral red for 30 minutes at 18°C.
6. Wash wells several times until no stained zymosan is visible in the negative control.
7. Pipette 50 μ L of a standard concentrations of stained zymosan (5×10^6 zymosan/mL) down to 0.313×10^6 zymosan/mL in duplicate
8. Incubate wells with extraction solution for 20 minutes at 18°C.
9. Transfer samples to a V bottom 96-wells microplate
10. Mix or shake the plate and read at 550 nm.

HISTOLOGICAL PROCESSING OF TISSUES

∴ EQUIPMENT AND REAGENTS

Equipment

- Disposable tissue cassettes
- Tissue processor (Leica ASP 3000)
- Wax dispenser (Leica EG 1150H)
- Plastic moulds
- Microtome (Leica RM2125 RTS)
- Cold plate (Bio Optica PF100)
- pHmeter (Crison Basic 20)
- Disposable microtome blades
- Thermostatic water bath
- Microscope slides and cover slips
- Drying oven
- Robotic stainer (Leica Autostainer XL) and coverslipper (Leica CV5030)
- Light microscope (Nikon Eclipse E200)

Reagents

- Formaldehyde 37% (Panreac 141328)
- $\text{Na}_2\text{HPO}_4 \cdot 12\text{H}_2\text{O}$ (Panreac 131678)
- $\text{Na}_2\text{HPO}_4 \cdot \text{H}_2\text{O}$ (Panreac 13965)
- Ethanol (Panreac 131086)
- Xylene (Technical 28973.363)
- Paraffin (Panreac 253211)
- Albumin (Fluka 05461)
- Timol (Probus 12278)
- Harris hematoxylin solution (Sigma-Aldrich HHS32)
- Eosin yellowfish hydroalcoholic solution 1% (Panreac 251301.1611)
- DPX mounting media (Sigma-Aldrich 06522)

∴ PROCEDURE

a. Preparation of solutions

▪ *Formaldehyde 4% pH 7.2 (for 1L; 20 samples per liter)*

- Formaldehyde 37%100 mL
- $\text{Na}_2\text{HPO}_4 \cdot 12\text{H}_2\text{O}$28.92 g
- $\text{Na}_2\text{HPO}_4 \cdot \text{H}_2\text{O}$2.56 g
- dH_2O900 mL

▪ **Albumin solution 1% (for 100 mL)**

- Egg albumin1 g
- Timol1 g
- dH₂O100 mL

A dilution 1:20 in dH₂O is made at the moment of use.

b. Histological processing of the tissue

1. Immediately after sampling, immerse mussel tissues in fixative (formaldehyde 4%).
2. Maintain samples in fixative for 24 hours and then, replace the fixative by 70% ethanol for storage at 4°C until processing.
3. Dehydrate and embed individual tissue samples in paraffin using an automatic tissue processor with the following sequence under vacuum conditions.

<u>Reagent</u>	<u>Conditions</u>
70 ^o ethanol	60 min at 40 ^o C
96 ^o ethanol	60 min at 40 ^o C
96 ^o ethanol	60 min at 40 ^o C
100 ^o ethanol (absolute)	60 min at 40 ^o C
100 ^o ethanol (absolute)	60 min at 40 ^o C
50 ^o ethanol: xylene (1:1)	60 min at 40 ^o C
Xylene	60 min at 40 ^o C
Xylene	60 min at 40 ^o C
96 ^o ethanol	60 min at 40 ^o C
100 ^o ethanol	60 min at 40 ^o C
Paraffin	120 min at 60 ^o C
Paraffin	120 min at 60 ^o C
Paraffin	120 min at 60 ^o C

4. After embedding in paraffin, place tissues in a plastic mould oriented and cover them totally with melted paraffin. Use the tissue cassette as holder. Leave the mould at room temperature for paraffin to harden for at least one day before the mould is removed.
5. Cut paraffin blocks in sections of 5 µm thickness using a microtome. Place sections on the surface of distilled warm water and allowed to expand. Then, pick up the sections on a slide covered with albumin.
6. Place slides are placed in a drying oven at 37^oC. After drying overnight, the slides are ready to stain.
7. For staining, dewax sections in xylene and hydrate them using an ethanol series. Following hydration, stain slides with hematoxylin and eosin, dehydrate in ethanol

and clear in xylene. The whole staining protocol is performed in an automatic stainer with the following program:

<u>Reagent</u>	<u>Time</u>
Xylene	10 min x 2 steps
100 ⁰ ethanol (absolute)	2 min x 2 steps
96 ⁰ ethanol	2 min
70 ⁰ ethanol	2 min
dH ₂ O	5 min
Harris hematoxylin	4 min
Tap water	4 min
Acid ethanol	10 s
Tap water	5 min
Lithium carbonate	10 s
Tap water	1 min
Eosin yellowfish	1min 30s
Tap water	1 s
Tap water	1min 30s
70 ⁰ ethanol	5s (2 min-5s)*
96 ⁰ ethanol	10s (2 min-10s)*
100 ⁰ ethanol (absolute)	15s (2 min-10s)*
100 ⁰ ethanol (absolute)	20s (2 min-10s)*
Xylene	1 min x 2 steps

*Time depends on the number of staining uses of the eosin yellowfish reagent.

8. Mount coverslips with DPX mounting media using a coverslipper.

∴ **HISTOLOGICAL ANALYSIS**

Stained slides are examined individually under the light microscope using a x10 or x20 magnification. If any tissue needs, a x40 or x100 magnification may be used for closer examination.

AUTOMETALLOGRAPHY

∴ EQUIPMENT AND REAGENTS

Equipment

- Disposable tissue cassettes
- Tissue processor (Leica ASP 3000)
- Wax dispenser
- Plastic moulds
- Microtome (Leica RM2125 RTS)
- Cold plate (Bio Optica PF100)
- pHmeter (Crison Basic 20)
- Disposable microtome blades
- Thermostatic water bath
- Microscope slides and cover slips
- Drying oven
- Robotic stainer (Leica Autostainer XL) and coverslipper (Leica CV5030)

Reagents

- Formaldehyde 37% (Panreac 141328)
- $\text{Na}_2\text{HPO}_4 \cdot 12\text{H}_2\text{O}$ (Panreac 131678)
- $\text{Na}_2\text{HPO}_4 \cdot \text{H}_2\text{O}$ (Panreac 13965)
- Ethanol (Panreac 131086)
- Xylene (Technical 28973.363)
- Paraffin (Panreac 253211)
- Albumin (Fluka 05461)
- Timol (Probus 12278)
- Kaiser glycerine gelatine (Merck 109242)
- BBIInternational Silver Enhancing Kit for Light and Electron Microscopy (Agar Scientific Ltd.)

∴ PROCEDURE

1. Follow steps 1-6 for conventional histological processing of tissues.
2. Dewax sections in xylene and hydrate them using an ethanol series. The whole staining protocol is performed in an automatic stainer with the following program:

Reagent	Time
Xylene	10 min x 2 steps
100 ⁰ ethanol (absolute)	2 min x 2 steps
96 ⁰ ethanol	2 min
70 ⁰ ethanol	2 min
dH ₂ O	5 min

3. Dry samples at room temperature.
4. Prepare the emulsion following manufacturer's instruction (initiator and enhancer, 1:1).
5. Add the emulsion as drops into each tissue section and incubate samples in a moisture chamber in darkness.
6. Check the reaction in control and treated samples and stop it when visible (after 20-25 minutes).
7. Stop the reaction washing immediately the slides in tap water for 2 minutes.
8. Wash samples in dH₂O.
9. Mount slides in glycerin.

SPAWNING OF MUSSELS AND EMBRYO TOXICITY TEST

∴ EQUIPMENT AND REAGENTS

Equipment

- Micropipette set and tips
- Microscope slides
- Light microscope (Nikon Eclipse *M*)
- Sterilized glass beakers
- Sieves (30 µm; 100 µm)
- Falcon-type tubes (VWR 21008-178)
- Shaker

Reagents

- Natural and sterilized seawater (SW)
- Formaldehyde 37% (Panreac 141328)

∴ PROCEDURE

1. Keep mussels for 2 hours at 4°C.
2. Induce mussels spawning by thermal stimulation alternating immersion in seawater of 18°C and 28°C.
3. Transfer spawners individually to beakers with 100 mL of sterilized SW.
4. Male spawners produce a dense milky sperm solution. Sieve the solution through a 30 µm mesh to remove debris. Sperm motility is checked visually and sperm of 4 males per experimental group is pooled.
5. Sieve eggs from 4 females spawners through a 100 µm sieve to remove tissue debris. Number of eggs are counted under the light microscope.
6. Add 5 mL of the pooled sperm solution to each beaker containing eggs.
7. Verify eggs fertilization by microscopic examination (round eggs with expelled polar bodies) and calculate fertilization success as number of fertilized eggs/ number of total eggs x 100.
8. After fertilization, transfer volumes corresponding to 600 eggs to sterile Falcons containing 25 mL of sterilized SW (3 replicates per female).
9. Incubate fertilized eggs were incubated at 18°C for 48 hours in a shaker (lowest speed).
10. After the incubation period (48 hours), add 100 µL of 4% buffered formalin to each.

∴ SCORING

Percentage of abnormal larvae is determined by direct observation of the individuals. 100 of the 600 individuals are randomly selected and observed in each of the 3 replicates under the light microscope. The categories of abnormal larvae include: (a) segmented eggs, normal or malformed embryos that have not reached the D-larval stage; and (b) D larvae, with either convex hinge, indented shell margins, incomplete shell or protruded mantle (Figure 1).

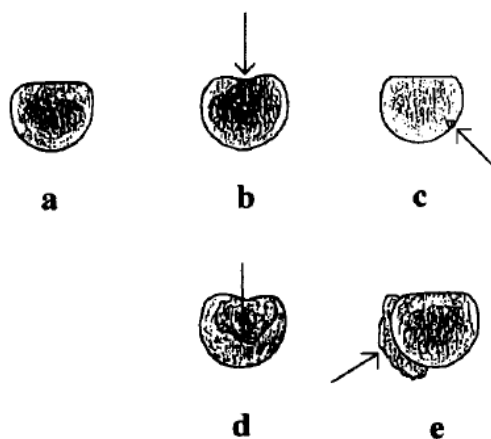


Figure 1. Different abnormalities observed in bivalves larvae that reached D-shell stage. a) normal larvae, b) convex hinge, c) incomplete shell, e) protruding mantle (Taken from His et al., 1997).

LYSOSOMAL MEMBRANE STABILITY TEST

∴ EQUIPMENT AND REAGENTS

Equipment

- Slides
- Coverslips
- Coupling jars
- Cryostat (Leica Microsystems CM3050S)
- Shaking thermostatic water-bath (Mettler)
- Freezer (-80°C)
- Fridge or cold store (4°C)
- pHmeter (Crison Basic 20)
- Light microscope (Nikon Eclipse Ni)

Reagents

- $C_6H_5NaO_7 \cdot 2H_2O$ (Fluka 71406)
- NaCl (Scharlau SO02271000)
- Naphtol AS-BI N-acetyl-β-D-glucosaminide (Sigma-Aldrich N4006)
- 2-methoxyethanol (Sigma 64719)
- Polypep® (Sigma-Aldrich P5115)
- $Na_2HPO_4 \cdot 12 H_2O$ (Panreac 131678)
- $NaH_2PO_4 \cdot H_2O$ (Panreac 13965)
- Fast Violet (Sigma-Aldrich F1631)
- $Ca(C_2H_3O_2)_2$ (Sigma-Aldrich C4705)
- Formaldehyde 37% (Panreac 141328)
- Kaiser glycerine gelatine (Merck 109242)

∴ PROCEDURE

a. Preparation of solutions

- **Solution A: Lysosomal membrane labilizing buffer pH 4.5 (for 100 mL)**
 - $C_6H_5NaO_7 \cdot 2H_2O$ 2.94 g
 - NaCl..... 2.5 g
 - dH₂O..... 90 mL
 - Adjust pH to 4.5 and add dH₂O up to 100 mL
- **Solution B: Substrate incubation medium (for 50 mL)** (freshly prepared)
 - Naphtol AS-BI N-acetyl-β-D-glucosaminide..... 20 mg
 - 2-metoxyethanol..... 2.5 mL
 - Polypep®..... 3.5 g
 - Solution A..... up to 50 mL

- **Solution C: Saline solution (for 100 mL)**
 - NaCl..... 3g
 - dH₂O..... 100 mL

- **Solution D: Diazonium dye pH 7.4 (for 100 mL)**
 - Na₂HPO₄·12 H₂O..... 2.892 g
 - NaH₂PO₄·H₂O..... 0.265 g
 - dH₂O..... 90 mL
 - Adjust pH to 7.4 and add dH₂O up to 100 mL
 - NaCl..... 2.5 g
 - Fast Violet..... 100 mg

- **Solution E: Fixative Baker's calcium formaldehyde (for 100 mL)**
 - Ca(C₂H₃O₂)₂..... 2 g
 - 37% Formaldehyde..... 10 mL
 - dH₂O..... 90 mL

b. Histochemical procedure

1. Cut five digestive glands samples of each chuck in 10 µm thick serial sections using a 15° knife angle using a cryostat at a cabinet temperature below -25°C.
2. Transfer each section to a warm slide (at room temperature) to get them stuck. At least, 8 serial sections are required from each chuck, to obtain 8 slides in the end.
3. Store slides at -40°C until required for staining, but no longer than 24 hour to avoid artifact formation.
4. Take out the slides of the -40°C freezer to warm them at room temperature 10 minutes before staining.
5. Place in a coupling jar containing solution A. One slide per chuck will be kept in the jar from 3 min up to 40 min (completing the serial of 0, 3, 5, 10, 15, 20, 30 and 40 min within the labilizing buffer). This first step sets up the difference between groups, regarding the time needed to completely labilize the lysosomal membrane (labilization period, LP).
6. After 40 minutes, transfer slides solution B and incubate for 20 minutes.
7. Wash slides in saline solution C for 2 to 3 minutes. Steps with solutions A and B and also the washing step with saline solution must be done at 37°C in a shaking bath.
8. Transfer slides to solution D containing the diazonium dye for 10 minutes at room temperature.
9. Rinse slides in running tap water for 5 minutes.
10. Fix sections for 10 minutes in solution E at 4°C.
11. Finally, rinse sections in dH₂O and mount in aqueous mounting medium.

∴ MEASUREMENT

Slides are examined under a light microscope. Using the minimum amplification (4x), each digestive gland per slide is divided into four areas (quarters) (see Figure 1).

Increasing microscope magnification, lysosomes will be recognized as reddish- purple rounded bodies due to the reactivity of the substrate with N-acetyl- β -D-glucosaminide. The LP for the first quarter of the digestive gland will be assigned to the time of incubation in acid buffer that produces maximal staining reactivity. This procedure must be repeated for the remaining quarters of the same digestive gland. The mean of the results obtained in the four quarters represents the LP value for the first individual. The same procedure is adopted for the other sections present on the slides derived from the other four remaining individuals (n =5). Finally, a mean value of LP for the sample will be calculated utilizing the 5 data obtained from the 5 animals analyzed. If there are two peaks of staining intensity, only the main staining peak should be considered as the LP. "0" time will be utilized only to verify the correct lysosomal enzyme activity staining and it will not be considered in the evaluation of the maximal staining intensity peak.

As stated by Viarengo et al. (2007), four categories of lysosomal membrane stability are established:

Labilization period (LP)

- LP \geq 20 min
- 10 min < LP < 20 min
- 5 min < LP < 10 min
- LP < 5 min

Status

- Healthy
- Minor disease
- Reversible
- Irreversible, degenerative

MICRONUCLEI FREQUENCY

∴ EQUIPMENT AND REAGENTS

Equipment

- Slides
- Coverslips
- Micropipette set and tips
- Coupling jars
- Scalpel
- Syringe (1 mL) and needles
- Falcon-type tubes (VWR 21008-178)
- Single Chambers (Cytopro, ELItech Biomedical Systems Ref. SS-113)
- Cytospin (Cytopro Cyto centrifuge, ELItech Biomedical Systems)
- Inverted microscope (Nikon Eclipse *Ti*)
- Light microscope (Nikon Eclipse *Mi*)

Reagents

- NaCl (Scharlau SO02271000)
- EDTA tetrasodium salt dihydrate (Sigma-Aldrich E6511)
- Microscopy Hemacolor staining kit (Merck 1.11661.)
- DPX mounting medium (Fluka 44581)

∴ PROCEDURE

a. Preparation of solution

▪ ***Saline water- EDTA 10 mM (for 1 L)***

- NaCl 25 g
- EDTA..... 0.292 g
- dH₂O..... 1 L

b. Mussel hemolymph extraction and preparation

1. The mussel shell valves are carefully prised apart by the insertion of a fixed scalpel blade. Once opened, keep the blade in position to maintain the valves open. Seawater is drained out using absorbent paper toweling.
2. Using a 1 mL syringe, fitted with a needle, the posterior adductor muscle is located. Insert the needle towards the posterior end of the shell close to the valve opening. Drawn down the needle horizontally until it meets resistance by touching the muscle.
3. Withdrawn slightly the needle and then push gently into the muscle to extract the hemolymph slowly.

4. Transfer the hemolymph to a Falcon-type tube containing 1 mL of saline-water EDTA.

c. Staining

1. Spread several μL of the hemolymph solution on a slide to check cell density under a microscope. If many hemocytes are observed, the sample is diluted with saline-water EDTA.
2. Centrifuge 200 μL of the hemolymph solution in the cytospin at 700 rpm for 2 minutes.
3. Air dry the slides for 20 minutes and transfer them to a coupling jar containing Hemacolor solution A for 1 minute.
4. Then, transfer the slides to Hemacolor solution B for 2 minutes.
5. Finally, transfer the slides to Hemacolor solution C for 2 minutes.
6. Rinse the slides with abundant dH_2O and air dry overnight.
7. Rinse the slides in xylene and mount in DPX.

∴ SCORING

Identification of micronuclei and other nuclear abnormalities

Slides are scored blind under the microscope. Hemolymph cells are examined under x100 magnification and micronuclei (MN), binucleated cells and mitotic figures are identified (Figure 1).

MN are identified following the generally accepted criteria (Venier et al., 1997):

- (1) Similar staining as the main nucleus
- (2) Spherical or rounded body with well-preserved cytoplasm
- (3) Diameter smaller than one-third of the main nucleus
- (4) No contact with nucleus (absence of chromatin bridge)

At least 1000 hyalinocytes per mussel and 8 mussels per group are analyzed. Results from individual mussels are reported in ‰ frequency.

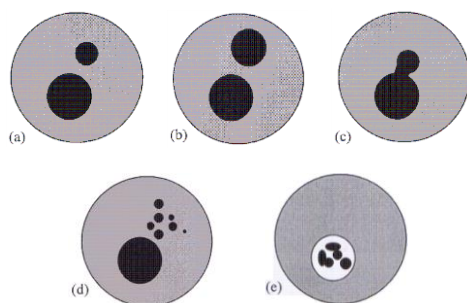


Figure 1. Criteria adopted to analyse for structures that are not micronuclei. **a)** micronucleus larger than one-third, **b)** binucleated cell, **c)** micronucleus touching the main nucleus showing a bridge-like appearance, **d)** small fragments of the main nucleus showing micronucleus-like structures, **e)** micronucleus-like structure formed during apoptosis (Picture taken from the Procedural Guidelines of the laboratory of T. Galloway in the University of Plymouth).

COMET ASSAY

∴ EQUIPMENT AND REAGENTS

Equipment

- Micropipette set and tips
- Microscope slides
- Electrophoresis tank (BIORAD)
- Coupling jars
- Eppendorf tubes
- Centrifuge (Beckman Coulter Microfuge 20 Centrifuge)

Reagents

- Agarose (Sigma-Aldrich A4679)
- Low melting point agarose (Sigma-Aldrich A9414)
- Tris base (Sigma-Aldrich T4661)
- NaCl (Scharlau SO02271000)
- EDTA tetrasodium salt dehydrate (Sigma-Aldrich E6511)
- Triton X-100 (Sigma-Aldrich X100)
- N-lauroyl-sarcosine sodium salt (Sigma-Aldrich L9150)
- Dimethylsulfoxide, DMSO (Sigma-Aldrich D5879)
- NaOH (Scharlau SO041801000)
- Tris-HCl (Sigma-Aldrich T3253)
- Methanol (Scharlau ME0316000)
- Distilled water
- Ethidium bromide (Sigma E1385)

∴ PROCEDURE

a. Preparation of solutions

▪ **Phosphate buffered saline (PBS)**

- $\text{Na}_2\text{HPO}_4 \cdot 12\text{H}_2\text{O}$ 2.037 g
- KH_2PO_4 200 mg
- KCl..... 200 mg
- NaCl..... 32 g
- dH_2O complete to 1L

▪ **Normal agarose**

- Agarose 1%..... 1 g
- PBS..... complete to 100 mL

- **Low melting point agarose**
 - Low melting point agarose 0.5%..... 100 mg
 - PBS..... complete to 20 mL

- **Lysis solution (pH 10)**
 - Tris base 10 mM.....363.42 mg
 - NaCl 2.5 mM.....43.83 g
 - EDTA tetrasodium salt dihydrate 100 mM.....12.48 g
 - Triton X-100 1%.....3 mL
 - N-lauroyl-sarcosine sodium salt 1%.....3 g
 - DMSO 10%.....30 mL
 - Distilled water.....complete to 300 mL

- **Electrophoresis buffer (pH 13)**
 - NaOH 150 mM..... 17.991 g
 - EDTA tetrasodium salt dihydrate 300 mM..... 374.58 g
 - Distilled water..... complete to 3 L

- **Neutralization buffer (pH 7.5)**
 - Tris-HCl 400 mM..... 18.912 g
 - Distilled water..... complete to 300 mL

b. Steps

1. Coat slides with 1% normal melting agarose and leave overnight to dry (1 day before).
2. Centrifuge 100 μ L of hemolymph at 300 g for 10 minutes.
3. Mix 200 μ L of 0.5% low melting point agarose with the pellet.
4. Place 100 μ L suspensions on the coated microscope slides.
5. Extend the drops along the slides with a coverslip.
6. Chill slides at 4°C for 10 minutes in darkness.
7. Immerse slides into 4°C lysis solution for 1 hour in darkness.
8. Wash slides with distilled water and transfer slides to an electrophoresis tank containing electrophoresis buffer.
9. Incubate slides for 20 minutes to allow alkaline DNA unwinding (kept on dark).
10. Run the electrophoresis (1 V/cm, 30 min) in the same electrophoresis buffer (kept on dark).
11. Neutralize slides with neutralization buffer for 10 minutes.
12. Fix cells for 3 min in -20°C methanol.
13. Dry slides.

NOTE

- All buffers should be kept at 4°C.

∴ SCORING

1. Stain slides adding one drop of diluted ethidium bromide (2 µg/ mL) in each slide. Extend the drop with a coverslip.
2. Slides are scored blind under the fluorescence microscope under x40 magnification. Pictures of 100 nuclei (50 per slide) are taken per organism and then then analyzed by using the Komet 5.5 software.

PROTEOMICS

1. CELL-FREE EXTRACTION

∴ EQUIPMENT AND REAGENTS

Equipment

- Volumetric balloons
- Precision weight (AG 245, Metter Toledo)
- Homogenizer IKA (Ultra-Turrax T-25)
- Eppendorf tubes

Reagents

- HEPES
- Sacarose
- DTT
- PMSF
- Ethanol
- Na₂EDTA
- Sodium hydroxide
- Protease inhibitor
- Milli Q H₂O

∴ PROCEDURE

a. Preparation of solutions

▪ **HEPES-sacarose solution**

- HEPES..... 5 mL
- Sacarose..... 42.79 g
- Milli Q H₂O..... 500 mL

▪ **DTT solution**

- DTT..... 154.2 mg
- Milli Q H₂O..... 10 mL

▪ **PMSF solution**

- PMSF..... 87.1 mg
- Ethanol..... 10 mL

▪ **EDTA solution**

- Na₂EDTA..... 74.44 g
- Sodium hydroxide..... 10 g
- Milli Q H₂O..... 500 mL

▪ **Homogenization buffer (1L, pH 7.6-7.8)**

- HEPES-sacarose solution..... 967 mL
- DTT solution..... 10 mL
- EDTA solution..... 2 mL
- PMSF..... 20 mL
- Protease inhibitor..... 1 mL

b. Steps

2.1 Protein extraction

1. Weight each tissue.
2. Add 3 mL of homogenization buffer per initial gram of tissue.
3. Homogenate the tissue on ice for 1 minute using the homogenizer.
4. Centrifuge samples at 15000 g for 2 hours.
5. Remove the supernatant and keep it in clean Eppendorf tubes.
6. Determine protein content following the Bradford Assay and store samples at -80°C.

2. BRADFORD PROTEIN ASSAY

∴ EQUIPMENT AND REAGENTS

Equipment

- Micropipettes and tips
- Eppendorf tubes
- 96-well microplates
- Precision weight (AG245, Metter Toledo)
- Multimode microplate reader Infinite® 200 PRO (Tecan)

Reagents

- Bovine Serum Albumin (BSA) standard solution (1mg/mL)
- Milli Q H₂O

∴ PROCEDURE

a. Preparation of solutions

▪ **BSA standard**

- BSA..... 500 mg
- Milli Q H₂O..... 500 mL

▪ **Bradford solution**

- Dilute 1 part of Dye Reagent Concentrate (Bradford) with 4 parts of Milli Q H₂O.

b. Steps

1. Prepare a standard curve as follows:

Concentration (mg/mL)	0	0.005	0.01	0.025	0.05	0.1	0.5	1
BSA solution (mL)	0	0.025	0.05	0.125	0.25	0.5	2.5	5
Milli Q H₂O	5	4.975	4.95	4.875	4.75	4.5	2.5	0

2. Dilute samples (1:20) and vortex gently.
3. Add 5 µL of Milli Q H₂O (as blank) and 5 µL of sample in each well (5 replicates per each)
4. Add 200 µL of Bradford solution in each well (including in standard curve).
5. Incubate for 20 minutes.
6. Read absorbance at 595 nm.

∴ DATA ANALYSIS

1. Create a standard curve by plotting the absorbance values (y-axis) against the concentration in mg/mL (x-axis).
2. Calculate the absorbance average of the five replicates for each sample.
3. Determine the unknown sample concentration using the standard curve $y = ax + b$

$$\text{Concentration} \left(\frac{\text{mg}}{\text{mL}} \right) = \frac{(\text{Absorb. average} \times b)}{a}$$

4. Consider the dilution factor of samples

$$\text{Dilution factor} = \frac{\text{Total volume}}{\text{Sample volume}}$$

5. Adapt the concentration to the amount of tissue and buffer used in the initial procedure.

$$\text{PROT} \left(\frac{\text{mg}}{\text{g}} \right) = \text{Conc.} \left(\frac{\text{mg}}{\text{ml}} \right) \times \frac{\text{Vol. Tris (mL)}}{\text{W tissue (g)}}$$

Where:

PROT = Total protein content

Conc. = Concentration

Vol. Tris = Volume of buffer used to dilute the sample before homogenization

W tissue = Weight of tissue before homogenization

3. ISOELECTRIC FOCUSING

∴ EQUIPMENT AND REAGENTS

Equipment

- Immobiline DryStrip ph 3-10, 18 cm (GE Healthcare, 17-231-01)
- Strip holder
- Ettan IPGphor II platform (GE Healthcare)

Reagents

- Trichloroacetic acid
- DTT
- Acetone
- Urea
- Thiourea
- CHAPS
- Amberlite
- Pharmalyte
- Bromophenol blue
- Immobiline DryStrip Cover Fluid

∴ PROCEDURE

a. Preparation of solutions

▪ Precipitation solution

- Trichloroacetic acid..... 1 mL
- DTT..... 30.84 mg
- Acetone..... 9 mL

▪ Lysis solution

- Urea..... 4.2 g
 - Thiourea..... 1.52 g
 - CHAPS..... 400 mg
 - Amberlite..... 50 mg
 - Pharmalyte..... 80 µL
 - DTT..... 100.23 mg
 - Bromophenol blue..... <25 mg
- Store the solution at -80°C in aliquots of 600 µL

b. Steps

3.1 Protein precipitation

1. Calculate the volume of sample necessary to get 100 µg of protein.
2. Add 9 times the volume of the protein sample of precipitation solution.
3. Incubate samples for 2 hours at -20°C.

4. Centrifuge samples for 30 minutes at 10000 g.
5. Remove the supernatant.
6. Wash the pellet with acetone (3 times) and dry the pellet at room temperature for 3 minutes.

3.2. Protein solubilization

1. Add 300 μ L of lysis solution to each sample.
2. Resuspend the pellet by vortexing and pipetting. Incubate samples at room temperature for 30 minutes to increase protein solubility.

3.3. Preparation of strips

1. Centrifuge samples for 10 minutes at 14000 g.
2. Add carefully each sample in the corresponding strip holder. Distribute the sample over the channel length and remove bubbles.
3. Carefully remove the cover foil from the Immobiline DryStrip, starting from the anodic end (+ end).
4. Place the Immobiline DryStrip into the holder channel with the gel-side down. Avoid the formation of bubbles.
5. Cover the strips with 2.5 mL Immobiline DryStrip Cover Fluid to minimize evaporation and prevent urea crystallization.
6. Ensure that the Strip Holders are properly positioned on the Ettan IPGphor II platform. Use the guide marks along the sides of the platform to position each strip holder and check that the pointed end of the Strip Holder is over the anode (pointing to the back of the unit) and the blunt end is over the cathode. Check that both external electrode contacts on the underside of each Strip Holder make metal-to-metal contact with the platform.
7. Program the Ettan IPGphor as follows:

<u>Step</u>	<u>Voltage (V)</u>	<u>Time (h)</u>
1	0	6.00
2	50	6.00
3	1000	1.00
4	4000	1.00
5	8000	1.00
6	8000	1.00

4. SECOND DIMENSION SDS-PAGE

∴ EQUIPMENT AND REAGENTS

Equipment

- Micropipette set and tips
- Precision weight (AG245, Metter Toledo)
- Ettan Daltsix Electrophoresis Unit (GE Healthcare)
- Shaker

Reagents

- Tris
- Urea
- Glycerol
- SDS
- Bromofenol blue
- Glycine
- Agarose
- Acrylamide
- APS
- TEMED
- Ethanol
- Acetic acid
- Milli Q H₂O
- DTT
- EDTA
- Iodoacetamide
- Precision Plus Protein Standard Ladder (BIORAD, Cat No. 161-0374)

∴ PROCEDURE

a. Preparation of solutions

▪ **Tris-HCl solution**

- Tris..... 90.85 g
 - Milli Q H₂O..... 500 mL
- Adjust pH to 8.8 with HCl

▪ **Equilibration buffer**

- Urea..... 72.1 g
- Tris-HCl solution..... 10 mL
- Glycerol..... 69 mL
- SDS..... 8 g
- Milli Q H₂O..... 200 mL

- **Bromophenol blue solution**
 - Bromophenol blue..... 25 mg
 - Tris-HCl solution..... 10 mL

- **Electrophoresis buffer**
 - SDS..... 10 g
 - Glycine..... 144.1 g
 - Tris..... 30.3 g
 - Milli Q H₂O..... 1000 mL

- **Agarose solution (0.5%)**
 - Electrophoresis buffer..... 50 mL
 - Agarose..... 0.5 g

- **SDS solution (10%)**
 - SDS..... 5 g
 - Milli Q H₂O..... 50 mL

- **Acrylamide gels (30%)**
 - Acrylamide..... 18 mL
 - Tris-HCl solution..... 15 mL
 - SDS solution..... 600 µL
 - Milli Q H₂O..... 26.1 mL
 - APS..... 300 µL
 - TEMED..... 30 µL
 - *Proportions corresponding for one gel.

- **Fixation solution**
 - Ethanol..... 200 mL
 - Acetic acid..... 50 mL
 - Milli Q H₂O..... 250 mL

- **DTT-equilibration solution**
 - Equilibration solution..... 10 mL
 - DTT..... 100 mg
 - EDTA..... .2 µL
 - Bromophenol blue..... 50 µL
 - *Proportions corresponding for two strips

- **Equilibration solution**
 - Equilibration solution..... 10 mL
 - Iodoacetamide..... 400 mg
 - EDTA..... .2 µL
 - Bromophenol blue..... 50 µL
 - *Proportions corresponding for two strips.

b. Steps

4.1. Equilibration of Immobiline DryStrip gels

1. Immerse each strip in 5 mL of DTT-equilibration solution
2. Cover the strips and place them in a shaker for 15 minutes at room temperature.
3. Remove the DTT-equilibration solution.
4. Immerse each strip in 5 mL of equilibration solution.
5. Cover the strips and place them in a shaker for 15 minutes at room temperature.
6. Wash the strips with dH₂O and dry at room temperature.

4.2. Electrophoresis

1. Place the strip with the acidic end to the left, gel surface up onto the protruding edge of the longer glass plate.
2. With a thin plastic ruler, gently push the Immobiline DryStrip gel down so that the entire lower edge of the Immobiline DryStrip gel is in contact with the top surface of the gel. Avoid the formation of bubbles.
3. Place the molecular marker in contact with the gel at the positive end of the strip.
4. Seal the Immobiline DryStrip gel in place with the agarose sealing solution.
5. Insert the cassettes into the tank and pour the electrophoresis buffer to the fill line.
6. Run the electrophoresis at 120 V for 30 minutes and then at 500 V for 5 hours.
7. After the electrophoresis, fix gels in the fixation solution at room temperature.

5. SILVER STAINING OF GELS

∴ EQUIPMENT AND REAGENTS

Equipment

- Volumetric balloons
- Nalgene® staining boxes
- Micropipette set and tips
- Precision weight (AG245, Metter Toledo)
- GS-800 densitometer (BIORAD)
- PDQuest v8.0 software (BIORAD)

Reagents

- Ethanol
- Sodium thiosulfate
- Silver nitrate
- Formaldehyde (37%)

- Sodium carbonate
- Glycine
- Milli Q H₂O

∴ **PROCEDURE**

a. Preparation of solutions

▪ **Washing solution (30% ethanol)**

- Ethanol (96%)..... 150 mL
- Milli Q H₂O 350 mL

▪ **Reduction solution**

- Sodium thiosulfate 50 mg
- Milli Q H₂O 250 mL

▪ **Incubation solution**

- Silver nitrate..... 500 mg
- Formaldehyde..... 50 µL
- Milli Q H₂O..... 250 mL

*Keep the solution in dark

▪ **Developing solution**

- Sodium carbonate..... 7.5 g
- Formaldehyde..... 125 µL
- Sodium thiosulfate..... A grain
- Milli Q H₂O..... 250 mL

▪ **Stopping solution**

- Glycine..... 1.25 g
- Milli Q H₂O..... 250 mL

b. Steps

1. Prepare freshly all the working solutions.
2. Follow the incubation steps using staining boxes as detailed below:

Step	Reagent	Time
Washing	30% ethanol	3 x 20 minutes
Reduction	Thiosulfate solution	1 minute
Washing	dH ₂ O	3 x 20 seconds
Incubation	Silver nitrate solution (in darkness)	20 minutes
Washing	dH ₂ O	3 x 20 seconds
Developing	Developing solution	3-5 minutes (depends on each gel)
Stop	Stopping solution	5 minutes
Washing	dH ₂ O	30 minutes
Washing	5% ethanol	>30 minutes

3. Scan gels in the GS-800 densitometer.

∴ SCORING

Protein spots are analyzed using the PDQuest v8.0 software.

TRANSCRIPTOMICS

1. RNA EXTRACTION (TRIzol® METHOD)

∴ EQUIPMENT AND REAGENTS

Equipment

- Micropipette set and tips
- Vortex
- Mini-centrifuge
- Precision weight (Ohaus)
- RNase free polypropylene Eppendorf tubes (AMBION AM12400)
- Tissue homogenizer (Precellys®24, Bertin Technologies)
- Refrigerated centrifuge (Beckman Coulter Microfuge 22R Centrifuge)

Reagents

- RNA later® (Sigma-Aldrich R0901)
- TRIzol® (Invitrogen Life Technologies, Ref 15596018)
- 1 mm Zirconia/ Silica beads (BioSpec products, Inc, Cat No. 11079110)
- Ethanol (Panreac 131086)
- RNase free water (Thermo Scientific, HyClone SH30538.02)
- Chloroform (Scharlau CL01982500)
- Isopropyl alcohol (Scharlau AL 03101000)

∴ PROCEDURE

1. Dissect tissues and keep them in 1 mL RNA later® for at least 30 minutes. Then, freeze samples in liquid nitrogen and store at -80°C until processing.
2. Homogenize 50-100 mg of tissue in 1 mL of TRIzol® reagent using a Precellys®24 cell disrupter at 6000 rpm for 2 cycles of 25 seconds each.
3. Incubate homogenized samples at room temperature for 5 minutes to allow complete dissociation of nucleoprotein complexes.
4. Add 0.2 mL of chloroform and hand-shake tubes vigorously for 15 seconds.
5. Incubate tubes at room temperature for 2 minutes.
6. Centrifuge samples at 12000 g for 15 minutes at 4°C. After centrifugation, the mixture separates into a lower red phenol-chloroform phase, an interphase and a colorless upper aqueous phase. RNA remains exclusively in the aqueous phase. Transfer the aqueous phase to a new tube.
7. Mix samples with 0.5 mL of isopropyl alcohol (stored at -40°C) in order to precipitate RNA.
8. Incubate samples at room temperature for 10 minutes.

9. Centrifuge samples at 12000 g for 10 minutes at 4⁰C. RNA precipitates, often invisible before centrifugation, forms a gel-like pellet on the bottom of the tube.
10. Remove the supernatant and wash the RNA pellet with 1 mL of cold 75% ethanol.
11. Mix samples vortexing and centrifuge at 7500 g for 5 minutes at 4⁰C.
12. Dry the RNA pellet for 5 minutes, but not completely since complete drying would decrease its solubility.
13. Dissolve RNA with 100 µL RNase free water.
14. Incubate samples for 5 minutes at 55⁰C and vortex well.
15. Store samples at -80⁰C.

2. DNase DIGESTION OF RNA

∴ EQUIPMENT AND REAGENTS

Equipment

- Micropipettes set and tips
- Vortex
- DNase-RNase polypropylene free microtubes (Ref. 4095.9N)

Reagents

- RNase-Free DNase Set (Qiagen, Cat No. 79254) which contains:
 - Buffer RDD
 - DNase I stock solution
 - RNase-free water

∴ PROCEDURE

1. DNase I stock solution is prepared before using the RNase-Free DNase Set for the first time. Dissolve the lyophilized DNase I (1500 Kunitz units) in 550 µL of the RNase-free water provided.
2. Mix the following reagents in a microcentrifuge tube:
 - ≤ 87.5 µL RNA sample (contaminated with genomic DNA)
 - 10 µL Buffer RDD
 - 2.5 µL DNase I stock solution
 - Make the volume up to 100 µL with RNase-free water
3. Incubate samples at room temperature (25⁰C) for 10 minutes.

3. RNA CLEANUP AND CONCENTRATION

∴ EQUIPMENT AND REAGENTS

Equipment

- Micropipette set and tips
- RNase free polypropylene Eppendorf tubes (AMBION AM12400)
- Centrifuge (Beckman Coulter Microfuge 22R Centrifuge)
- Microplate spectrophotometer (Epoch Biotek)
- Vortex

Reagents

- RNeasy® MinElute® Cleanup Kit (Qiagen, Cat No. 74106) which contains:
 - Buffer RTL
 - Buffer RPE
 - RNase free water
- Ethanol (Panreac 131086)

∴ PROCEDURE

1. Adjust samples to a volume of 100 µL with RNase-free water. Add 350 µL of Buffer RLT and mix well.
2. Add 250 µL of 100% ethanol to the diluted RNA and mix well by pipetting.
3. Immediately, transfer samples to an RNeasy MinElute spin column placed in a 2 mL collection tube. Close gently the lid and centrifuge samples for 20 seconds at 10000 rpm. After centrifugation, the flow-through is discarded.
4. Place the RNeasy MinElute spin column in a new 2 mL collection tube. Add 500 µL of Buffer RPE to the RNeasy spin column. Close gently the lid and centrifuge samples at 10000 rpm for 20 seconds to wash the spin column membrane. The flow-through is discarded.
5. Add 500 µL of 80% ethanol to the RNeasy MinElute spin column. Close gently the lid and centrifuge samples for 2 minutes at 10000 rpm to wash the spin column membrane. The flow-through is discarded.
6. Centrifuge the RNeasy MinElute spin columns at maximum speed for 5 minutes. The flow-through and the collection tubes are discarded.
7. Place the RNeasy MinElute spin column in a new 1.5 mL collection tube. Add 10 µL of RNase free water directly to the center of the spin column membrane. Close gently the lid and centrifuge samples for 1 minute at 10000 rpm.
8. Repeat step 7 to obtain 20 µL of purified RNA.
9. Measure RNA concentration.

4. RNA QUALITY ASSESSMENT

∴ EQUIPMENT AND REAGENTS

Equipment

- Micropipette set and tips
- Vortex
- Heating block
- Chip Priming Station
- Syringe
- IKA MS3 vortexer
- RNA Nano Chips
- Electrode cleaners
- Agilent 2100 Bioanalyzer

Reagents

- RNase ZAP® (AMBION, AM9780)
- RNase free water
- Agilent RNA 6000 Nano Reagents Part I (Ref. 5067-1511) that contains:
 - Agilent RNA 6000 Ladder
 - RNA Nano Dye Concentrate
 - Agilent RNA 6000 Nano Marker
 - Agilent RNA 6000 Nano Gel Matrix

∴ PROCEDURE

a. Preparing the RNA ladder after arrival

1. Ladder (●) is pipetted in a RNase-free vial.
2. Heat denature it for 2 minutes at 70°C.
3. Cool immediately the vial on ice.
4. Prepare aliquots in RNase-free vials with the required amount for a typical daily use.
5. Store aliquots at -70°C. After initial heat denaturing, frozen aliquots do not need to be heat denatured again.
6. Thaw ladder aliquots on ice before use (avoid extensive warming).

b. Decontaminating the electrodes

1. Slowly fill one of the wells of an electrode cleaner with 350 µL RNase ZAP®.
2. Open the lid and place the electrode cleaner in the 2100 Bioanalyzer.
3. Close the lid and leave it closed for 1 minute.
4. Open the lid and remove the electrode cleaner.

5. Slowly fill one of the wells of another electrode cleaner with 350 μL RNase free water.
6. Place electrode cleaner in the Agilent 2100 Bioanalyzer.
7. Close the lid and leave it closed for about 10 seconds.
8. Open the lid and remove the electrode cleaner.
9. Wait another 10 seconds for the water on the electrodes to evaporate before closing the lid.

c. Preparing the Gel

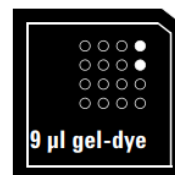
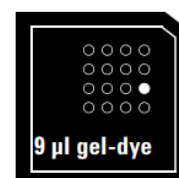
1. Pipette 500 μL of RNA 6000 Nano gel matrix (●) into a spin filter.
2. Centrifuge at 1500 g for 10 minutes at room temperature.
3. Aliquot 65 μL filtered gel into 0.5 mL RNase free microfuge tubes. Use filtered gels within 4 weeks.

d. Preparing the Gel-Dye Mix


1. Allow RNA 6000 Nano Dye concentrate (●) to equilibrate to room temperature for 30 minutes.
2. Vortex RNA 6000 Nano dye concentrate for 10 seconds, spin down and add 1 μL of dye into a 65 μL aliquot filtered gel.
3. Vortex solution well. Spin the tube at 13000 g for 10 minutes at room temperature. Use prepared gel-dye mix within one day.

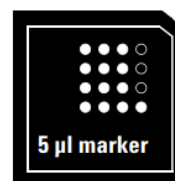
e. Loading the Gel- Dye Mix


1. Put a new RNA 6000 Nano chip on the chip priming station.
2. Pipette 9 μL of gel-dye mix in the well marked as **G**.
3. Make sure that the plunger is positioned at 1 mL and then close the chip priming station.
4. Press the plunger until it is held by the clip.
5. Wait for exactly 30 seconds and then release the clip.
6. Wait for 5 seconds. Slowly pull back the plunger to 1 mL position.
7. Open the chip priming station and pipette 9 μL of gel-dye mix in the wells marked as **G**.
8. Discard the remaining gel-dye mix.

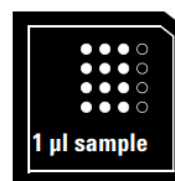
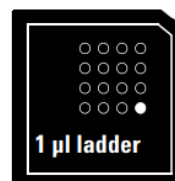


f. Loading the Agilent RNA 6000 Nano Marker

1. Pipette 5 μL of RNA 6000 Nano marker (●) in all 12 samples wells and in the well marked 

**g. Loading the Ladder and Samples**

1. Pipette 1 μL of prepared ladder in well marked 
2. Pipette 1 μL of sample in each of the 12 sample wells. Pipette 1 μL of RNA 6000 Nano Marker in each unused sample well.
3. Put the chip horizontally in the adapter of the IKA vortexer and vortex for 1 minute at 2400 rpm.
4. Run the chip in the Agilent 2100 Bioanalyzer within 5 minutes.

***NOTES**

- Freeze the unused RNA 6000 Nano ladder at -20°C and keep all other reagents and reagent mixes refrigerated at 4°C when not in used to avoid poor results caused by reagent decomposition.
- Protect dye and dye mixtures from light. Remove light covers only when pipetting. Dye decomposes when exposed to light.

5. FIRST-STRAND cDNA SYNTHESIS

∴ EQUIPMENT AND REAGENTS

Equipment

- Micropipette set and tips
- DNase-RNase polypropylene free microtubes (Ref. 4095.9N)
- Vortex
- Thermocycler (BIORAD C1000 Touch Thermal Cycler)

Reagents

- AffinityScript Multiple Temperature cDNA Synthesis Kit (Agilent Technologies, Cat No. 200436) which contains:
 - AffinityScript Multiple Temperature Reverse Transcriptase
 - 10× AffinityScript RT buffer
 - RNase Block Ribonuclease Inhibitor (40 U/μL)
 - Oligo(dT) primer (0.5 μg/μL)
 - Random primers (0.1 μg/μL)
 - 100 mM dNTPs (25 mM each dNTP)
 - RNase free water

∴ PROCEDURE

1. Prepare the first-strand cDNA synthesis reaction in a microcentrifuge tube by adding the following components in order:

2 μg total RNA
3 μL random primers
RNase free water up to 15.7 μL

Final volume: 15.7 μL per sample

2. Incubate the reaction at 65°C for 5 minutes and then at 25°C for 10 minutes.



3. Add the following components to each reaction, in order, for a final reaction volume of 20 μ L:

2 μ L 10 \times AffinityScript RT buffer
0.8 μ L dNTP mix
0.5 μ L RNase Block Ribonuclease Inhibitor
1 μ L AffinityScript Multiple Temperature RT

Final volume: 4.3 μ L per sample

4. Mix the reaction components gently, incubate the reaction at 25°C for 10 minutes to extend the primers and then place the tubes in a temperature-controlled thermal block at 42-55°C. Incubate the reaction for 60 minutes. Terminate the reaction by incubating at 70°C for 15 minutes.

